Towards Interlocked Structures

based on H-bonded barbiturate complexes

by Mathias Rocher

A thesis submitted to The University of Birmingham for the degree of

DOCTOR OF PHILOSOPHY

Volume 1 - Thesis

School of Chemistry

The University of Birmingham

1st version: August 2009 - Corrections: May 2010

Abstract

Despite the privileged position of Hamilton's barbiturate binding system in supramolecular chemistry, this motif has never been used in generating interlocked structures, such as rotaxanes or catenanes. This thesis demonstrates the feasibility of such structures. A series of Hamilton-like receptors has been synthesised. Their conversion from "open" to "closed" forms by metathesis and their binding with barbital was studied, demonstrating the importance of the macrocycle size. Barbiturates disubstituted with flexible chains terminated either by reacting groups (anthracenes, olefins) or stoppers (trityl) were also synthesised. The fluorescence properties of anthracene-tagged barbiturates and their kinetics of intramolecular anthracene photodimerisation and thermal return were studied, demonstrating remarkable differences depending on the chain length. Binding studies of these barbiturates with the receptors were then undertaken, revealing smaller binding constants compared with barbital. A series of ring-closing experiments involving the barbiturate complexes was then undertaken, either by anthracene photodimerisation or olefin metathesis. In one metathesis experiment, indirect evidence for the formation of a low amount of catenane was obtained by mass spectrometry, where the smallest ring is formed by a chain of only 19 carbon atoms, which is unprecedented. Finally, different synthetic pathways for the synthesis of barbiturates substituted with large rigid substituents were investigated. Models of their complexes with the receptors and IR studies are presented that suggest that their structure would facilitate the formation of interlocked complexes.

Acknowledgements

No scientific work has ever been carried out alone. This thesis is not an exception to the rule, and will not have existed without the work, interest or support of many people. I would like to thank them all.

First, I would like to thank my supervisor Dr. James H. R. Tucker for giving me the opportunity to do this work in his group. I am grateful for his discrete but strong guidance, his support, his availability when needed and unbreakable confidence both in this project and in me, which all made this thesis possible.

I would like also to thank Dr. Nathan D. McClenaghan who welcomed me at the University of Bordeaux where all the work related with fluorescence and photochemistry presented in this thesis was done, for his enthusiasm, availability and care that were vital for this thesis.

I must also acknowledge the excellent work done here in Birmingham by the Analytical staff, especially Peter Ashton (mass spec.) and Dr. Neil Spencer (NMR), and to thank Dr. Louise Malle (XRD), as well as Prof. Baz Jackson (School of Biosciences, for letting me use his ITC apparatus). I would also like to acknowledge the work done at the *Université Bordeaux 1* by Isabelle Pianet (NMR), Christelle Absalon and Christiane Vitry (mass spec.), Thierry Buffeteau and Dominique Cavagnat (*ab initio* models and IR), Brice Kaufmann and Jean-Pierre Desvergne (crystal structures). I would like to thank also Jean-Pierre, as well as Dario Bassani, for their help with the photochemistry.

This work is only a part of a wider project which started before my arrival in Birmingham and my first stay in Bordeaux. Therefore, I must thank Dr. Yann Molard, who was previously a post-doc on a related subject in the Tucker Group, and Christophe Lincheneau, who worked

on this project for his Master's thesis in Bordeaux, and has shown a constant interest when we have met again at different conferences.

I also helped different undergraduate students of the University of Birmingham who did their research project in the Tucker Group. I would like to thank those who worked on this "barbiturate" project, Jack Manchester and Abhinav Saraswat, as well as those who worked on the "templated metathesis" project, Stuart Wickson, Chris McGuire and Khatija Bhayat.

I would like also to thank all the present and past members of the groups working on the 4th floor, and also the rest of the School of Chemistry, for maintaining the best atmosphere and spirit, which has mase working here a real pleasure.

I would also like also to thank my friends from France who kept in contact with me, Stéphane, Tung, Marie-Aimée, and the new friends from here, especially Po-wei, and the wonderful people he presented to me, Peter, Miklos, Puvan, Kitty... And in Bordeaux, I would like to thank very specially all the Go players of the *Ze zem*.

And at last, I would like to thank my family, especially my Mum and Dad and my twin brother Jérémie (who also checked the mathematical correctness of some parts of this thesis), as well as Muriel, François, Clément, Charlie, Élisa, Benoît, Laurence, Mélusine, Solange and Éloise.

Abbreviations, units and symbols

Unless otherwise stated, the units and prefixes used in this thesis are SI units. Other units are indicated in the following table.

A	Absorption (dimensionless).
AU	Arbitrary unit.
cal	Calorie (*1 cal = 4.1868 J*).
br.	In NMR spectra: broad peak (for example: br. s: broad singlet).
d	In NMR spectra: doublet.
ddt	In NMR spectra: doublet of doublet of triplets.
$\delta(\ )$	In IR spectra: deformation band.
δ	Chemical shift (in *ppm*) in NMR spectra.
$\Delta G°$	Standard molar free enthalpy of complexation (in $kcal.mol^{-1}$).
$\Delta H°$	Standard molar enthalpy of complexation (in $kcal.mol^{-1}$).
DBU	1,8-Diazabicyclo[5.4.0]undec-7-ene.
DCM	Dichloromethane.
DMF	Dimethylformamide.
DMSO	Dimethyl sulfoxide.
DMSO-d_6	Deuteriated dimethyl sulfoxide.
$\Delta S°$	Standard molar entropy of complexation (in $cal.mol^{-1}.K^{-1}$).
ε	Molar extinction coefficient.
EI	Electronic ionisation mass spectrometry.
ES	Electrospray mass spectrometry.
ES^+	Electrospray, positive ions mode.
ES^-	Electrospray, negative ions mode.
exp( )	Exponential.
Φ	Quantum yield (dimensionless).
FTIR	Fourier transform infrared spectrometry.

hh	head to head (anthracene dimer).
HSAB	Hard and Soft Acids and Bases theory.
ht	head to tail (anthracene dimer).
I_F	Intensity of fluorescence (in *AU*).
IR	Infrared spectrometry; infrared spectrum.
J	Coupling constant (in Hz).
K	Binding constant (dimensionless).
k	Rate constant (in s^{-1}).
l	Optical path (in *cm*).
L	Litter ($1\ L = 10^{-3}\ m^3$).
λ	Wavelength (in *nm*).
$\lambda_{em.}$	Wavelength of emission (in *nm*).
$\lambda_{exc.}$	Wavelength of excitation (in *nm*).
log( )	Decimal logarithm.
ln( )	Natural logarithm.
m	In NMR spectra: multiplet. In IR spectra: medium band.
M	Molar ($1\ M = 1\ mol.L^{-1}$).
MALDI	Matrix assisted laser desorption ionisation mass spectrometry.
MS	Mass spectrometry.
Me	Methyl.
ν	Wave number (in cm^{-1}).
ν( )	In IR spectra: vibration band.
$\mathcal{N}_A$	Avogadro constant ($\mathcal{N}_A = 6.02214179(30) \times 10^{23}\ mol^{-1}$).
NMR	Nuclear magnetic resonance spectrometry; NMR spectrum.
P	Photonic flux.
pK_a	$pK_a = -\ log(K_a)$ where K_a is the acid dissociation constant.

ppm	Part per million.
q	In NMR spectra: quadruplet.
quint.	In NMR spectra: quintuplet.
R	Molar gas constant ($R = 8.314472(15)\ J.mol^{-1}.K^{-1}$).
rt.	Room temperature.
s	In NMR spectra: singlet. In IR spectra: strong band.
t	In NMR spectra: triplet.
THF	Tetrahydrofuran.
UV-Vis	UV-Visible spectrometry; electronic absorption.
w	In IR spectra: weak band.
(**C**)	Activity of chemical species **C** in solution (dimensionless). $(\boldsymbol{C}) = [\boldsymbol{C}] / C_0$ where $C_0 = 1\ M$.
[**C**]	Concentration of chemical species **C** (in *M*).

1) INTRODUCTION

1.1) Background

1.1.1) Supramolecular and Dynamic Covalent Chemistries

1.1.1.1) Introduction to the field

According to *The Concise Oxford Dictionary*, [1] the first meaning of "chemistry" is "*the branch of science concerned with the properties and interactions of the substances of which matter is composed*". The second is "*the chemical properties of a substance or body*", and the third is "*the emotional or psychological interaction between two people, especially when experienced as a powerful mutual attraction*". Even if this last metaphorical meaning is very far from the subject of this thesis, it is interesting to notice that even in this common meaning, chemistry deals with interaction and especially attraction. Therefore, it can seem surprising that "classical" organic chemistry, as it has developed since the ninetieth century, has been mainly concerned with only one type of interaction: the *covalent bond*. By contrast with this molecular chemistry, *supramolecular chemistry*[2] is concerned with the synthesis and the study of supermolecules, which can be defined as entities resulting from the association of at least two chemical species (molecules or ions) held together by *intermolecular bonds weaker than covalent*.

This thesis is written in the context of supramolecular chemistry. This concept started to emerge as a new field of study in the late 1960's, and was acknowledged for the wider audience by the Nobel Prize awarded in 1987 to three of its pioneers, Donald J. Cram, J.-M. Lehn and Charles J. Pedersen, "*for their development and use of molecules with structure-specific interactions of high selectivity, awarded for syntheses of molecules that mimic important biological processes*". [3] Indeed some of the most important concepts of

supramolecular chemistry come from biochemistry. Many biological processes involve the *recognition* and fixation of a guest molecule or substrate by a host or receptor: The recognition of antigens by antibodies is the basis of the immune system, and the catalysis of biological reactions by enzymes depends on the complexation and stabilization of transition states in the enzyme's active site.[4] For this reason, supramolecular chemistry has sometimes been described as *host-guest chemistry*. The molecular recognition of a guest molecule by a host implies a *complementarity* between the host and the guest, which is both a shape or steric complementarity (illustrated by Emil Fischer[5] as "lock and key") and a complementarity of interaction, in the sense that functional groups that will interact together have to be facing each other.

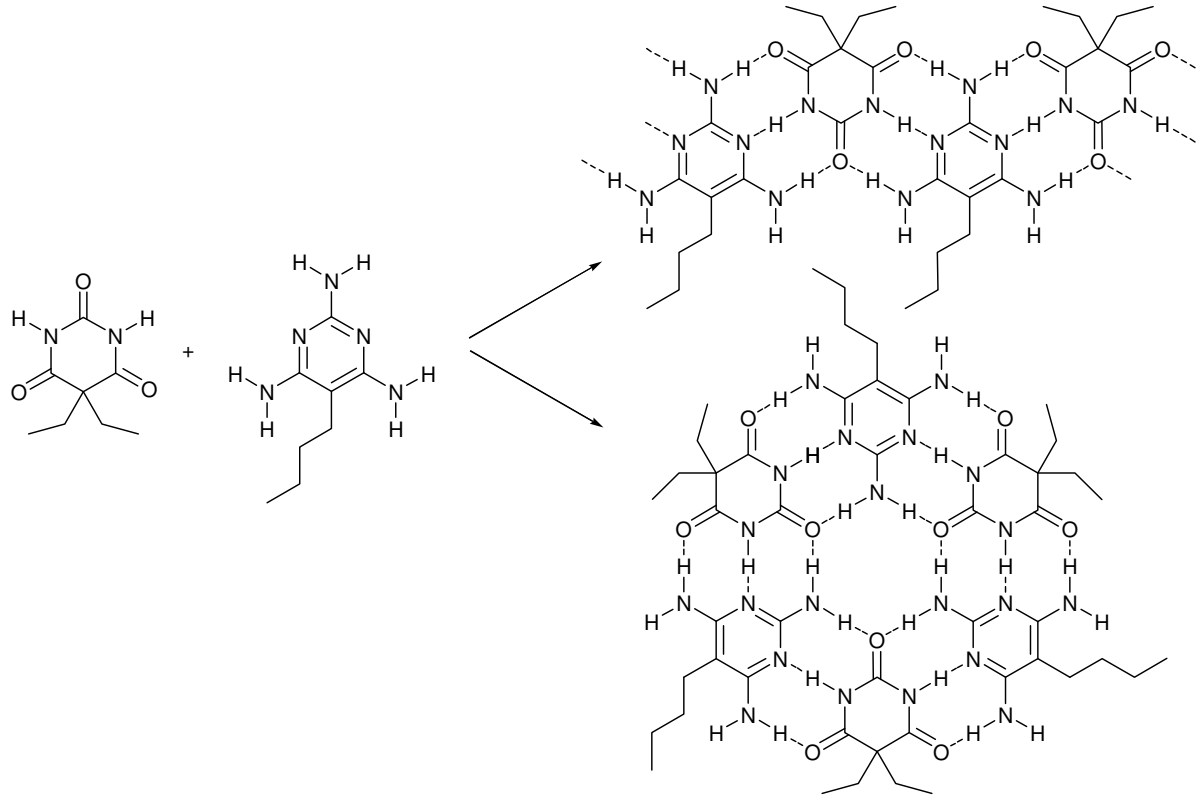

Scheme 1.1. An exemple of self-assembly: barbital and 2,4,6-diamino-5-butyl-pyrimidine forming supramolecular ribbons or supramolecular macrocycles.[6a]

The spontaneous recognition of molecules in solution by the formation of reversible bonds can be used strategically to access complex molecular and supramolecular structures. The terms *pre-organisation* and *template effect* come into play when it is the structure and

binding properties of one of the molecules or ions forming the supermolecule that determine its overall geometry. When the molecular recognition and assembly tends to form a complex structure by itself, the process is described as *self-assembly*. When self-assembly leads to the apparition of a new entity which involves several self-assembly processes, then it is possible to describe it as *self-organisation*. This is illustrated by the self assembly of barbital and triaminopyrimidine derivatives (**Scheme 1.1**).[6a]

The bonds used in supramolecular chemistry are weaker than typical covalent bonds and are formed reversibly, which implies that their formation remains under thermodynamic control. This is another difference compared to classical "synthetic" chemistry, where covalent bonds are usually formed under kinetic control, which makes their formation practically irreversible. This is because the aim of synthetic chemistry is to maximise the yield of reaction in a definite direction as a purpose for synthesis, but there are many reactions well known in organic chemistry that form covalent bonds under thermodynamic control. The emergence of supramolecular chemistry, and its ability to form complex supramolecular architectures via molecular recognition, pre-formation and self-assembly has revived the interest in a branch of chemistry where covalent bonds are formed, broken and re-arranged under thermodynamic equilibrium control: this branch is called *dynamic covalent chemistry*.[7]

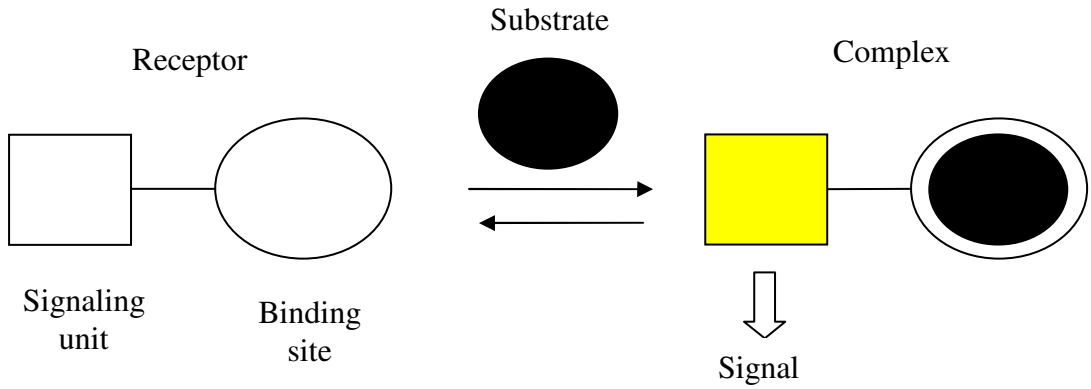

Figure 1.1. A supramolecular device where the input is a guest species.

Another field that has been revived by the development of supramolecular and dynamic covalent chemistries is the synthesis, study and use of *molecular* and *supramolecular devices* (see **Figure 1.1**). They can be defined as molecular or supramolecular systems whose physicochemical properties are reversibly changed or altered by an external input. This input can be light (photochemical input), applied potential (electrochemical input) or the binding of a guest species (chemical input), and the physicochemical property that is affected can also be the photochemical or electrochemical properties of the device or its binding affinities, but it can also be its shape or position in space: in this case the input gives rise to *chemical motion*. Depending on the function that they perform, these devices can also be designed as *sensors*, *switches* or *molecular machines*. It has to be noted that such systems can be considered as devices that are able to receive and/or transfer *information* beyond their molecular scale, or in other words that they are dealing with *signals.*

1.1.1.2) Interactions

The definition of supramolecular chemistry given above makes it necessary to explain the different kinds of interactions used in "covalent" and supramolecular chemistry. The first thing to note is that they are all a different expression of the same fundamental interaction, the *electromagnetic interaction* between electrically charged particles, which at the scale of chemistry are the nuclei of atoms and their electronic clouds.

Covalent bonds are bonds between atoms characterized by the *sharing of electron pairs*. It is possible to describe these bonds with the theory of *molecular orbitals*. Covalent bonds are strong, with an energy ranging between *150* and *1000 kJ.mol*$^{-1}$. Another interaction approximately as strong as covalent bond is the *ionic bond*, encountered in ionic solids, the classical example being sodium chloride. In solids, ionic bonds are usually not localised between two precise atoms but give rise to lattice structures. It is the *electrostatic interaction* between charged species that defines the ionic bond.

If molecules, in contrast to ions, have a global electric charge of zero, the difference of electronegativity between atoms, and the effects of exterior electric and magnetic field on the shape of the electronic cloud, give rise to a distribution of the electric charge in a molecule. It affects the nature of the bonds in the molecule, which shift from the pure covalent bond to ionic bond when the difference of electronegativity of the atoms gets higher, as the sharing of electron pair becomes less important compared to the electrostatic interaction between the partly charged atoms. Some bonds can be described as having both ionic and covalent character: *Polar covalent bonds* are covalent bonds between atoms of different electronegativities, which confers them some ionic character. *Dative bonds*, also known as *coordinate covalent bonds,* created between a metal ion and a ligand, are encountered in coordination chemistry. As covalent bonds, they can in fact be described in terms of molecular orbitals.

These different kinds of covalent bonds are what define molecules or ions as separate species, therefore their creation and breaking belong to the domain of classical chemistry, not supramolecular. Ionic bonds, on the contrary, are already supramolecular in nature in the sense that they act beyond the limit of the separate species they involve, but their strong energies, poor localisation and absence of selectivity puts them in a different category than other supramolecular bonds.

The distribution of charges inside neutral molecules also gives rise to *intramolecular interactions*, that are the specific domain of supramolecular chemistry. As for the ionic bond, they can be described as electrostatic interactions between the charge distributions, often simplified as *dipoles* by considering the *dipole moment* of the molecules. There is a distinction to be made between *permanent dipoles*, that is molecules that possess a permanent dipole moment because of the difference of electronegativity of their constituting atoms, and *instantaneous dipoles*, which appear by induction even in practically non-polar molecules

because of their surrounding electromagnetic field. However the interactions between non-permanent dipoles (sometimes referred to as repulsion, induction and dispersion interactions, or Van der Waals interactions) are much weaker than electrostatic interactions between permanent distributions of charges, which are usually sufficient to quantify intermolecular interactions.[8]

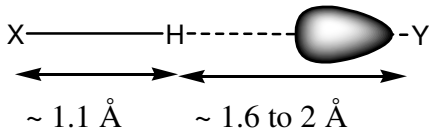

Figure 1.2. General description of a hydrogen bond

One of the most frequently employed interactions is the *hydrogen bond*. As represented in **Figure 1.2**, it is described as a bond involving a hydrogen atom bonded covalently to a relatively electronegative atom X, and another electronegative atom Y of the same or another molecule, bearing a lone pair, and in the direction of the X-H bond. Also as they are usually considered as a particular kind of electrostatic interaction between dipoles, it has been demonstrated that they are better described as partly covalent.[9] Hydrogen bonds are involved in many biological supramolecular systems; in particular, they play a major role in determining the 3D structure of proteins and nucleic acids. Supramolecular assemblies based on H-bonds often have a well-defined 3D structure, and this geometric precision makes H-bonding useful for controlling reactivity and stereoselectivity in a reversible manner.[10]

1.1.1.3) On the thermodynamics of binding

Some concepts coming from thermodynamics will be used later in this thesis; in order to introduce them now, a simple equilibrium will be considered:

$$A + B \rightleftarrows C$$

The direction in which this equilibrium will evolve is determined by the value of the *standard molar free enthalpy* of the equilibrium, noted ΔG°: spontaneous chemical reactions

have a negative $\Delta G°$. But the value of $\Delta G°$ also indicates where the reaction is going to stop: it can be demonstrated,[11] by considering the chemical potential of each species involved in the equilibrium, that the following equation will be verified at equilibrium:

$$\Delta G° = -R.T.ln\left(\frac{\gamma_C}{\gamma_A.\gamma_B}.\frac{C°.C_C}{C_A.C_B}\right)_{eq}$$

where γ_i is the activity coefficient of the species i, C_i its concentration and $C°$ the standard concentration. If the standard concentration is *1 M*, and if the concentrations are small enough to have all $\gamma_i = 1$, then the equation above can be re-written with the concentrations *(i)* of the species i, expressed in M, but dimensionless (as the activity):

$$\Delta G° = -R.T.ln\left(\frac{(C)}{(A).(B)}\right)_{eq}$$

We can now introduce the *binding constant K*:

$$K = e^{-\frac{\Delta G°}{R.T}}$$

This leads immediately to the following equation:

$$\left(\frac{(C)}{(A).(B)}\right)_{eq} = K$$

This last equation indicates that at a given temperature, and whatever the quantity of starting materials are, the quotient of reaction will be equal to the binding constant at equilibrium. It has to be noted that this last equation can also be obtained by *kinetic* considerations: if we can define a speed of complexation k_C and a speed of dissociation k_D, then it can be demonstrated that the expression of the concentrations will tend for an infinite time to a limit where the equation above is verified, provided that $K = k_C / k_D$. So if these speeds are fast enough, we can consider that the limit is reached in the time of the experiment and the reaction or binding is said to be *under thermodynamic control*. Nearly all the non-covalent binding equilibria encountered in supramolecular chemistry and biochemistry are under thermodynamic control. By contrast, reactions that involve the creation or breaking or

sigma bonds are usually not under thermodynamic control, and when they are the equilibration processes are usually much slower because of the slower kinetics associated with dynamic covalent bond formation. For this reason, most of the reactions encountered in dynamic covalent chemistry require a *catalyst* to reach equilibrium in a reasonable time scale.[7]

The binding constant K can be evaluated by any method allowing to measure the concentration of all species A, B and C in solution. It is theoretically dimensionless but often expressed with the dimensions implied by its calculation from concentrations (in $L.mol^{-1}$ or M^{-1} for a 1:1 binding), or expressed as its decimal logarithm $log(K)$. Using the following reaction, we can see that $\Delta G°$ is proportional to $log(K)$ at a given temperature T:

$$\Delta G° = -R.T.ln(K) = -R.T.ln(10).log(K)$$

For reactions or binding in solution at atmospheric pressure, $\Delta G°$ and K will vary with the temperature. The definition of G as $G = H - T.S$ leads immediately to the following equation:

$$\Delta G° = \Delta H° - T.\Delta S°$$

where $\Delta H°$ is the *standard molar enthalpy* of the equilibrium, or *enthalpic term* of $\Delta G°$, and $\Delta S°$ its *standard molar entropy*, and $- T.\Delta S°$ the *entropic term* of $\Delta G°$. Both $\Delta H°$ and $\Delta S°$ vary with temperature:

$$\Delta H°(T) = \Delta H°(T_{ref}) + \int_{T_{ref}}^{T} \Delta C_P°(T).dT$$

$$\Delta S°(T) = \Delta S°(T_{ref}) + \int_{T_{ref}}^{T} \frac{\Delta C_P°(T)}{T}.dT$$

where $\Delta C_P°$ is the *standard molar heat capacity at constant pressure*.[12] It is reasonable to consider that $\Delta C_P°$ is independant of temperature in a given limited range. Then if we

integrate the equations above and consider that $T - T_{ref} \ll T_{ref}$ we obtain the following expression for $\Delta G°(T)$ where all terms containing $\Delta C_P°$ have disappeared:

$$\Delta G°(T) \simeq \Delta H°(T_{ref}) - T.\Delta S°(T_{ref})$$

This can give an idea of the dependance of $\Delta G°$ with temperature, and allows us to evaluate $\Delta H°(T_{ref})$ and by difference $\Delta S°(T_{ref})$ from a set of measures of $\Delta G°$ at different temperatures through what is often referred to as a *Van't Hoff plot*. However, this method requires a large number of titrations in a limited range of temperature, it can often give results with a poor precision. $\Delta H°$ measures the *exothermicity* of the reaction or binding, whereas $\Delta S°$ measures the amount of disorder generated by the reaction. For a binding equilibrium, which obviously implies an increase of order, $\Delta S°$ is very often negative. In this case, as $\Delta G°$ has to be negative, it implies that $\Delta H°$ is also negative if the binding is efficient. $\Delta H°$ can be measured by measuring the heat change (a method called *calorimetry*), which gives a direct measure of $\Delta H°$ provided that the advancement of the reaction under the measurement conditions is known. The measure of the heat change during a titration at a given temperature is called *isothermal titration calorimetry* (*ITC*) and has become an established method to measure biological interactions in the last 15 years.[13] $\Delta S°$ cannot be measured directly, so it is evaluated by difference, using the equation $\Delta S° = (\Delta G° - \Delta H°) / T$.

It has been observed that many supramolecular systems present a phenomenon known as *entropy-enthalpy compensation*:[14] In the formation of complexes of similar guests binding to similar receptors, it can be observed that the individual entropic and enthalpic terms in the expression of the free enthalpy vary from one complex to another in a compensatory way, so that large variations of $\Delta H°$ and $\Delta S°$ are often associated with smaller variations of $\Delta G°$. For this reason, the interpretation of variations of binding affinity in terms of $\Delta H°$ and $\Delta S°$ is often difficult and some models consider directly the effects of different factors as terms of free

enthalpy.[8] Moreover, a plot of $\Delta H°$ vs. $\Delta S°$ often shows that the plots corresponding to each complex are often roughly aligned, as if there was a linear relationship between $\Delta H°$ and $\Delta S°$, where the slope can be defined as the *compensation temperature* T_C*:*

$$\Delta H° = \alpha + T_C.\Delta S°$$

Both the fact in itself and its interpretation are subject to important controversies. It has been argued that this may be a consequence of the narrow range of $\Delta G°$ that can be measured experimentally compared to the wide range of $\Delta H°$, leading to an illusion of relative constancy of $\Delta G°$ due to this small *free energy window*, which reflects into an artificial linear relationship between $\Delta H°$ and $\Delta S°$.[12] However this does not explain why for many series of complexes $\Delta G°$ actually remains in the accessible free energy window. It was also proved that the experimental errors induced by the calculation of $\Delta S°$ by difference between $\Delta H°$ and $\Delta G°$ could lead to an artificial linear relationship between $\Delta H°$ and $\Delta S°$, and a statistical test on the value of T_C has been developed to reject these cases:[14b] if the temperature of measure T verifies the following relationship where σ is the standard deviation on the value of T_C obtained from the model, then the compensation observed is not distinguishable from an artificial relationship:

$$T_C - 2.\sigma < T < T_C + 2.\sigma$$

Applying this test shows that in some cases, such a relationship between $\Delta H°$ and $\Delta S°$ is genuine in the sense that it cannot be due to the experimental error, but that very frequently the series of measures reported in the literature as presenting entropy-enthalpy compensation fail this test. However even in the rejected cases, it cannot be assumed that no relationship is present, as the value of the compensation temperature T_C may be close to the measurement temperature. A qualitative explanation for this phenomenon is that when the bonds created upon complexation are stronger (which is reflected in $\Delta H°$), the freedom of motion is

restrained (which is reflected in $\Delta S°$), and on the contrary if the bonds created upon complexation are weaker or less numerous, then the freedom of motion is relatively bigger. Some models, both at a very general and theoretical level[15a] and on specific complexes[15b] suggest that this may give a correct explanation for the entropy-enthalpy compensation.

1.1.1.4) Olefin metathesis and its role in this field

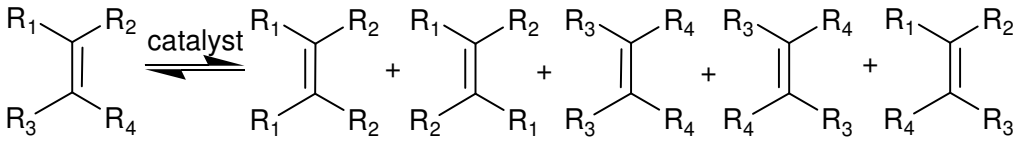

Scheme 1.2. General case of metathesis.

This thesis makes use of a particular reaction, *olefin metathesis*, which therefore needs to be introduced. This reaction has become one of the most important reactions in many fields of organic chemistry, including synthesis, polymer science and supramolecular and dynamic chemistries, a success that has been acknowledged by the Nobel Prize awarded to Y. Chauvin, R. R. Schrock and R. H. Grubbs in 2005. The name of this reaction comes from Greek *metathesis*, which means transposition or exchange. In this reaction, two olefins will formally exchange their carbenes. It is a catalytic equilibrium and often not very selective, so in the general case an olefin in the presence of a metathesis catalyst would lead to a complex mixture as illustrated on **Scheme 1.2**.

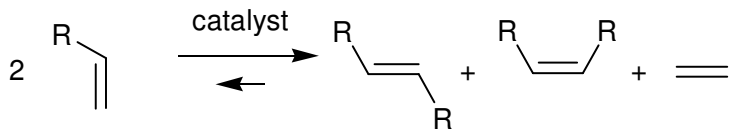

Scheme 1.3. Homodimerisation by metathesis of a terminal alkene.

Depending on the nature of the substituents of the olefin and the context of this reaction, it can become a very interesting tool for synthesis. A classical application is illustrated in **Scheme 1.3**: When the starting material is a terminal alkene, then one of the by-products is ethylene which will be eliminated from the reacting mixture by evaporation,

displacing the equilibrium in the direction of the coupling product, which will be obtained as a mixture of *cis* and *trans* isomers. The same reaction can occur on a molecule with two terminal olefins, which will lead, depending on the concentration and on steric considerations, either to polymerisation or *ring closure metathesis* (RCM). Another classical application is the opening of a cyclic olefin leading to polymerisation (*ring opening polymerisation*, ROMP).

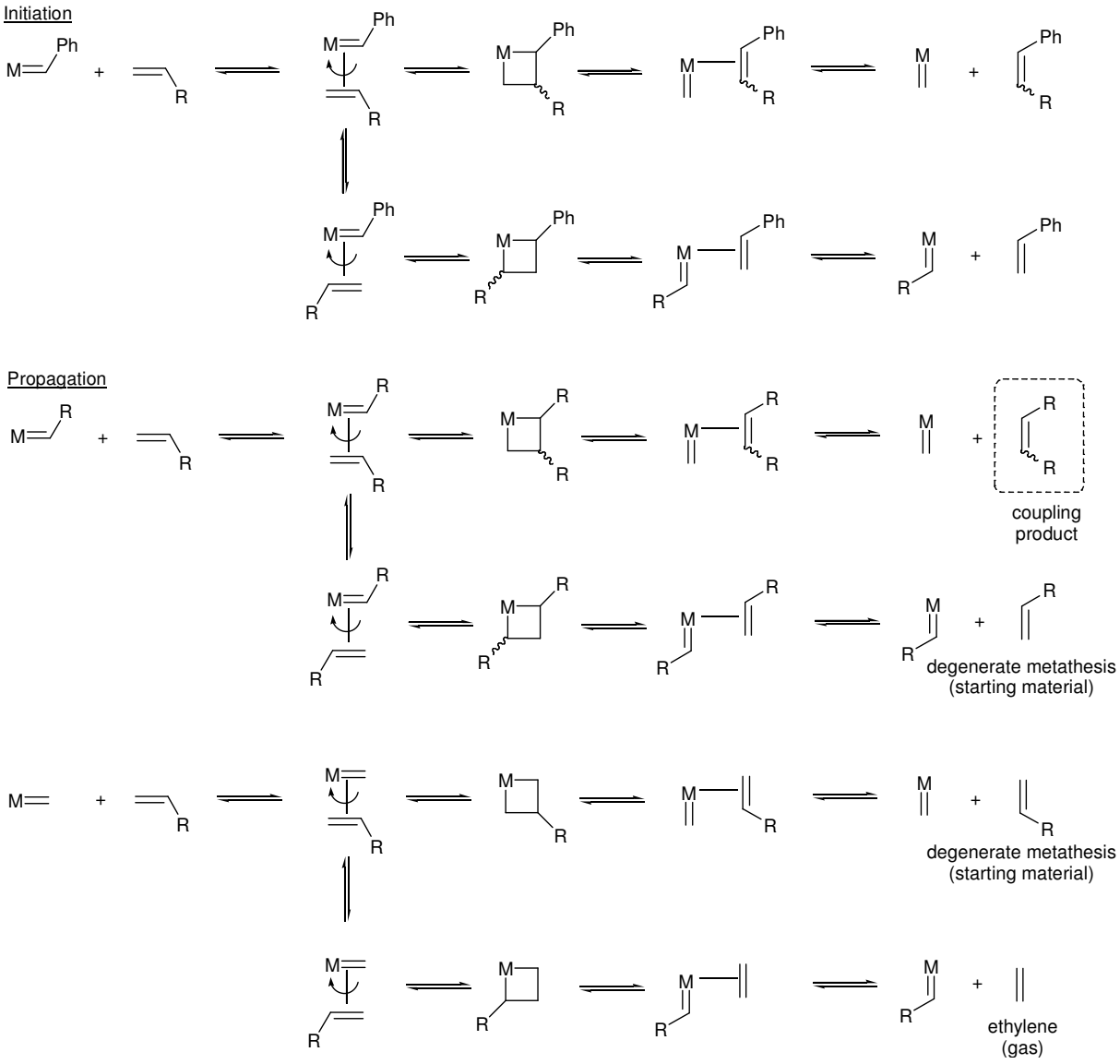

Scheme 1.4. Chauvin's mechanism for olefin metathesis.

The first metathesis reactions reported were observed with simple catalysts such as molybdenum metal, or oxide, or $[Mo(CO)_6]$ on alumina $WCl_6/AlEt_2Cl$ and the mechanism

was not known.[16] It was Yves Chauvin who proposed for the first time in 1974 a mechanism[17] (see **Scheme 1.4**) for this reaction involving metallocarbenes as catalytic species and metallacyclobutane intermediates. This mechanism is now considered as the main mechanism for all olefin metathesis reactions. Many other organometallic reactions that involve square intermediates comprising a metal atom have been discovered, and new catalysts for this reaction have been developed that wouldn't have been conceived without this mechanism.[18] The two main families of catalysts used today derive from the works of Schrock[19] and Grubbs[20]. Some of these catalysts are represented on **Figure 1.3**.

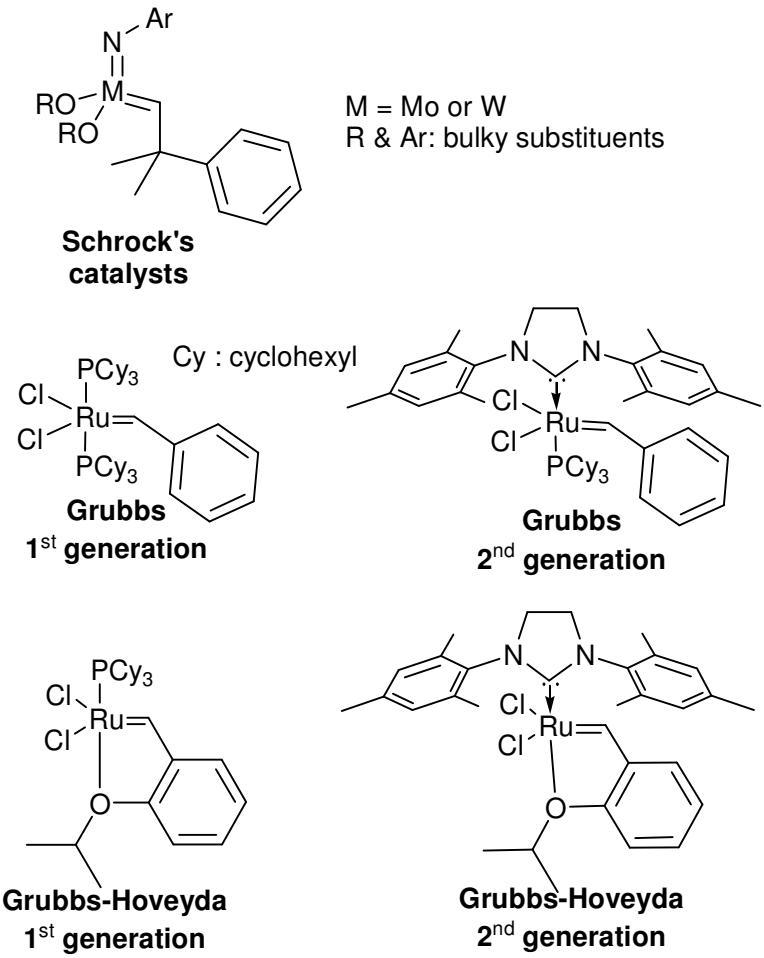

Figure 1.3. Some catalysts for metathesis.

As it is a reaction under thermodynamic control, it falls into the category of reactions that can be studied in the context of dynamic covalent chemistry. The ring closure metathesis for macrocycles, in particular, has been applied several times to the synthesis of *interlocked*

structures both as a synthetic step[21] and making use of its dynamic nature in the context of dynamic covalent chemistry[22f-h].

1.1.2) Interlocked structures

1.1.2.1) Definitions

As mentioned in the title, this thesis is about *interlocked structures*. It is a general term used for a large array of molecules and supermolecules which can be either molecules with unusually complex topologies, or supermolecules where two or more independent molecular fragments are "mechanically" linked. The nature of this *mechanical bond* is that the molecular components are not bonded by any of the "classical" forces described above, but because of *steric interaction* (repulsion of the electron clouds) they have no way to be separated without breaking one of the bonds that define their structure. The most classical interlocked structures are called *catenanes* and *rotaxanes* (see **Figure 1.4**). Other less classical examples of interlocked structures are often described by a name describing their topology: Trefoil knot, Borromean rings, Solomon rings, etc...

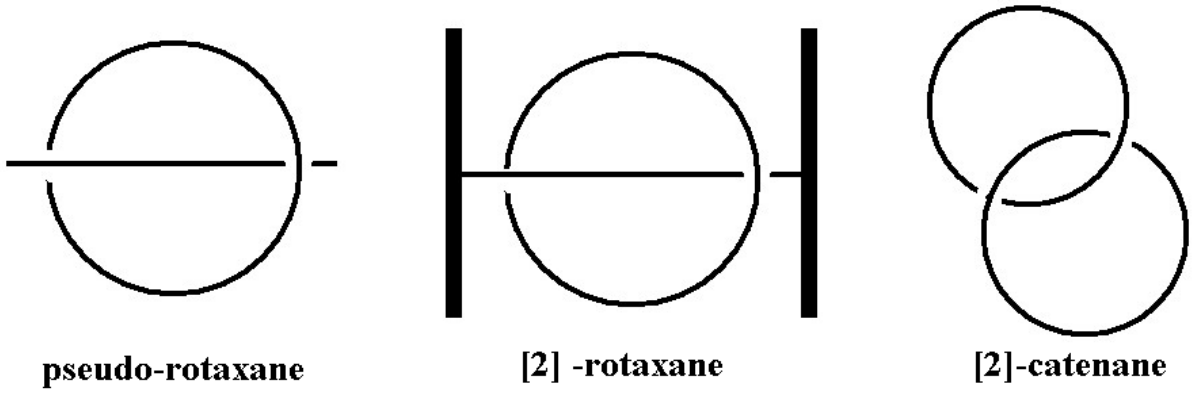

Figure 1.4. Interlocked structures.

In rotaxanes and *pseudo-rotaxanes*, the two molecules that are linked mechanically can be called "wheel" and "axle" by an evident analogy. Pseudo-rotaxanes are not fully in compliance with the definition of interlocked structures given above as the wheel and axle

parts are not irreversibly linked. It is the presence of bulky stoppers at both ends of the axle in rotaxanes or the topology of catenanes that forces the two parts to remain linked.

Concepts borrowed from the field of mathematics called topology are often used in order to describe interlocked structures. For example, two molecules or supermolecules that have the same crude formula, but cannot be represented by the same graph, are called *topological isomers*, and if one of these isomers cannot be represented by a planar graph, this isomer is an interlocked structure. However, it is important to note that the concepts borrowed from topology are not sufficient to define interlocked structures in chemistry: in mathematics, two objects have the same topology if there is a continuous transformation from one to the other, which transformation has a continuous inverse. With actual chemical structures, which are not conceptual mathematical objects but actual material ones, such transformations are not always possible because the covalent bonds cannot be stretched infinitely. It is because the transformation of a rotaxane to two separated components is impossible using only possible chemical motion and without breaking any bond, that rotaxanes belong to the field of interlocked structures.

The synthesis of interlocked structures is only possible with macrocycles which have an inner diameter large enough to accommodate the thinner part of the molecular fragment that will be interlocked. Most of the time, this means that the inner diameter of the macrocycle should be large enough to accommodate an alkyl chain. In the case of an alkyl chain threaded inside an cycloalkane ring, different models indicate that the smallest ring size possible is between 18 and 22 CH_2.[23, 24] Experimentally, rotaxanes of this type have been detected with rings as small as 21 CH_2.[25] More recently, high-yielding syntheses of rotaxanes with a 21-membered ring have been described where the macrocycle is of crown or benzo-crown ether type.[26] Indirect evidence have also been provided for the threading of an alkyl chain in a 20-membered ring.[27] It has also been postulated[23] that the size of the smallest ring

that can be used for making interlocked structures is likely to depend on the strategy used to obtain this structure, and that rotaxanes and catenanes with small ring sizes should be more easily obtained using ring-closing reactions rather than threading.

1.1.2.2) Brief history of interlocked structures

The possibility of the existence of interlocked structures was admitted in informal discussions and seminars but only rarely mentioned in the literature,[24] but the first time the presence of a catenane was demonstrated, as well as the first occurrence of the word "catenane" in the literature, was is an article by E. Wasserman and M. Hill in the *Journal of the American Chemical Society* in 1960.[28a] Although Wasserman recognised two years later that his yield was overestimated,[28b] this article kindled the interest in these species and the exploration of what was called at this time *chemical topology*.[24] However the way these interlocked structures were obtained, which is now referred to as the *statistical approach*, was rather inefficient: the catenanes were obtained as byproducts in polymerisation reactions. This statistical approach to catenanes and rotaxanes have been the basis of the first works studying these new compounds, in particular by G. Schill.[23,25]

The first review on chemical topology cited above[24] also mentioned some ideas of strategies to direct the synthesis of catenanes instead of obtaining them statistically. These proposed strategies all involved a temporary binding of the future parts of the catenane, which at this time (prior to the development of supramolecular chemistry) meant implicitly covalent binding. This kind of "covalent strategy" was applied successfully as early as 1964 by G. Schill and A. Lüttringhaus,[29] using a phenyl ring as a central core to which the future components of the second ring were successively attached, displaced inside the first ring, cyclised and cleaved to yield a catenane (**Scheme 1.4**).

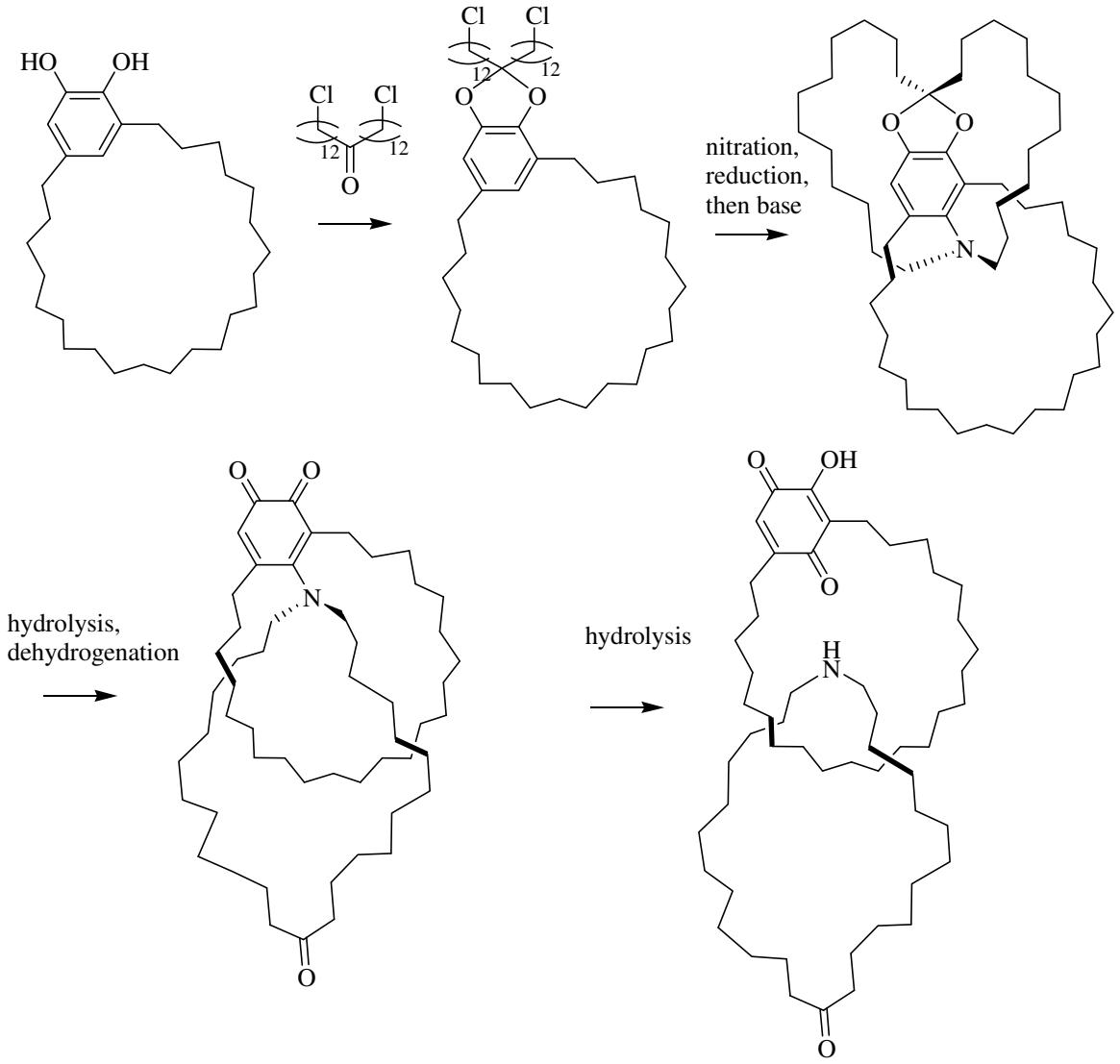

Scheme 1.4. Catenanes obtained by covalent strategy.[29]

It was also in the 60's that the first naturally occurring interlocked structures were discovered, with the first observation of catenated DNA.[30a] It was discovered later that these structures were associated with different stages in the replication of DNA, and that catenation and decatenation of DNA was catalysed by a family of enzymes known as DNA topoisomerases.[30b]

The development of supramolecular chemistry in the 1980's and 1990's offered new possibilities to make interlocked structures: instead of using temporary bonds that have to be cleaved, bonds weaker than covalent were used to pre-form the future interlocked structure before cyclisation or stoppering. There are now numerous examples of such an approach, but

two research teams have dominated this field of research during this period, those of J.-P. Sauvage[21,31] and of J. F. Stoddart.[32]

The work of J.-P. Sauvage used the template effect of copper I ions in the pre-formation of a complex with two 2,9-disubsitituted 1,10-phenanthrolines. By using a classical ring-closing reaction, he was able to obtain an interesting interlocked structure that he called a *catenate* (see **Scheme 1.5**): it is a complex with a metallic ion, where the ligand (a *catenand*) has the topology of a catenane once it is demetalated.[31] Using the same template effect of copper with phenanthroline-based ligands, many interlocked structures with different topologies were obtained, such as [3]-catenanes,[31] doubly interlocked [2]-catenanes,[32a] rotaxanes,[32a] molecular knots,[32a,21a] handcuff-like supermolecules, etc.[21b]

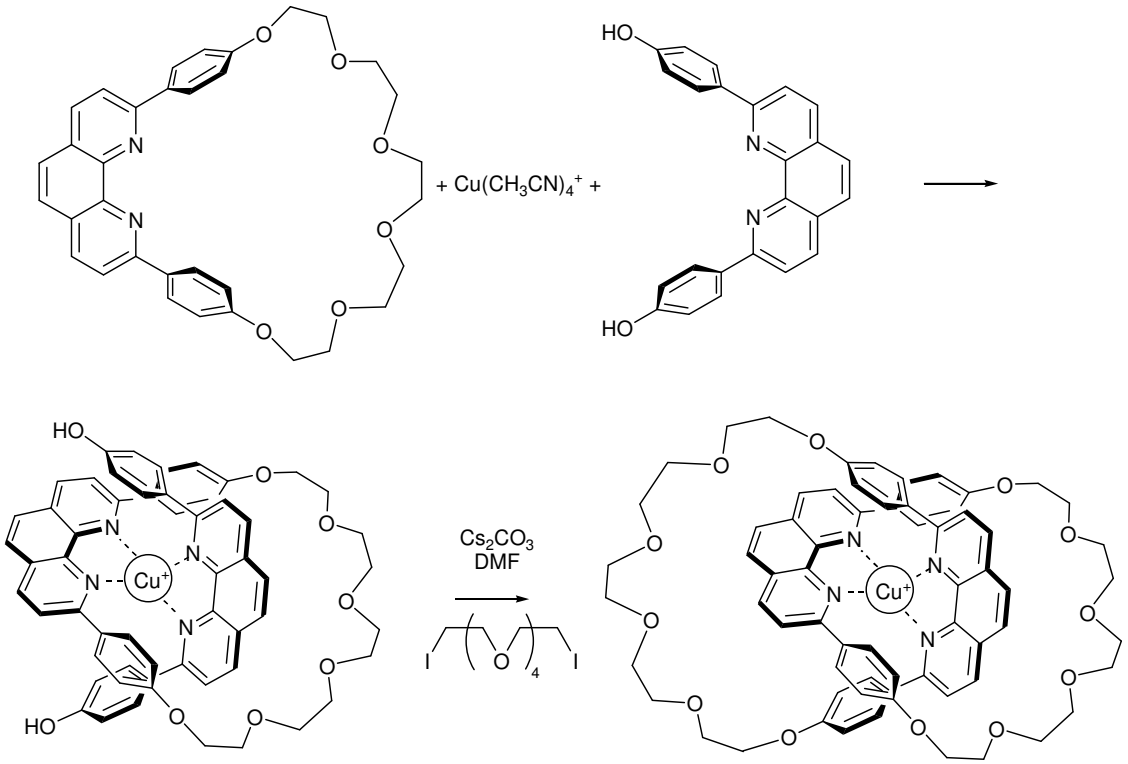

Scheme 1.5. Copper-based catenates designed by J.-P. Sauvage and C. Dietrich-Buchecker.[31]

The work of the Stoddart group[32] evolved from the study of the binding of an organic cation, diquat, by benzo-crown ethers in sandwich-like charge-transfer complex,[33] to pseudorotaxanes and then naturally to interlocked structures. In a series of 60 articles called

molecular meccano and published between 1992[32d] and 2000,[32e] this team developed a range of simple building blocks that constituted a molecular meccano kit, aimed to be used in the construction of supramolecular devices and machines using the possibilities offered by mechanical bond. It is important to notice that the intention to develop molecular devices from interlocked structures was already mentioned in his first article of the *molecular meccano* series.[32d]

Interlocked structures were seen for thirty years as pure academic curiosity, and the interest of their synthesis was mainly aesthetical, as can be clearly seen by reading the review of Sauvage[31] cited above. By comparison, the review of Stoddart,[32a] if it also insists on this beauty of interlocked structures, mentioned already "*the potential applications that might be addressed by incorporating the aspect of entanglement into chemical systems*" and evokes in its conclusion "*the possibility of constructing molecular computers*" by using "*"devices" at the molecular scale*". The work of Stoddart's group and a few others opened the way to the conception of dynamic, informed systems containing mechanical bonds in the last two decades.

The conception of dynamic interlocked systems has developed from two ideas: controlling the rotational and translational motion of mechanically bonded molecules, and making the formation of this mechanical bond itself reversible. The study of molecular motion in catenanes was initiated by the Stoddart group, as illustrated with the *molecular shuttle*[34] of **Scheme 1.6**. Leigh's group, who previously entered in the world of catenanes with what was probably the first high-yielding serendipitous synthesis of a catenane,[35a,b] have also designed and studied molecular devices presenting the possibility of directed motion inside catenanes[35b-e] and rotaxanes.[22h ,35f,g]

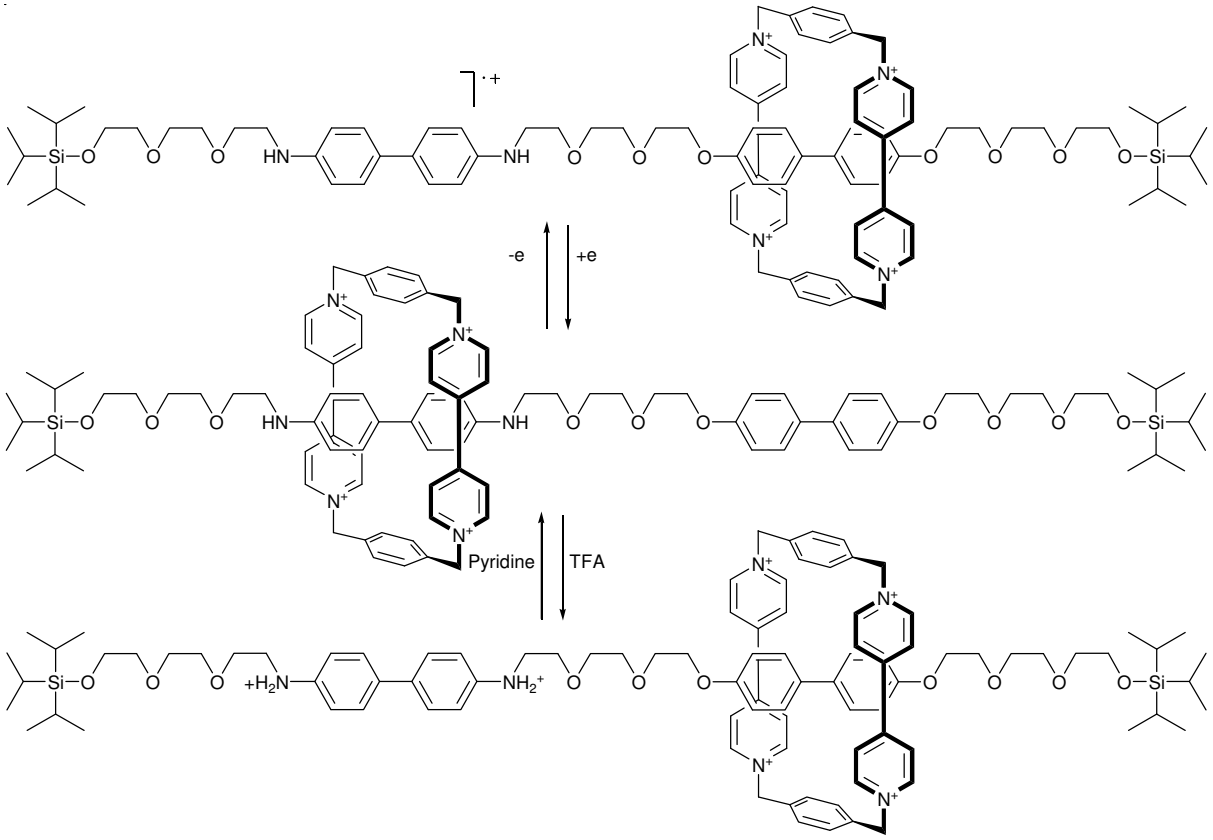

Scheme 1.6. Stoddart's electrochemically and chemically driven molecular shuttle.[34]

Fujita's name, although he was not the first to obtain a catenane under thermodynamic control,[22a] remains associated with what he first called *magic ring catenanes*,[22b-e] as the interlocking of separate rings may remind one of the conjurors trick of interlocking "magic" rings. These first examples used the reversible formation of weak metal-ligand bonds. Other magic ring catenanes and rotaxanes were subsequently developed by the Leigh group using olefin metathesis.[22f-h] It was also by using ring-closure reactions under thermodynamic control that the Stoddart group finally synthesised Borromean rings (see **Scheme 1.7**).[36]

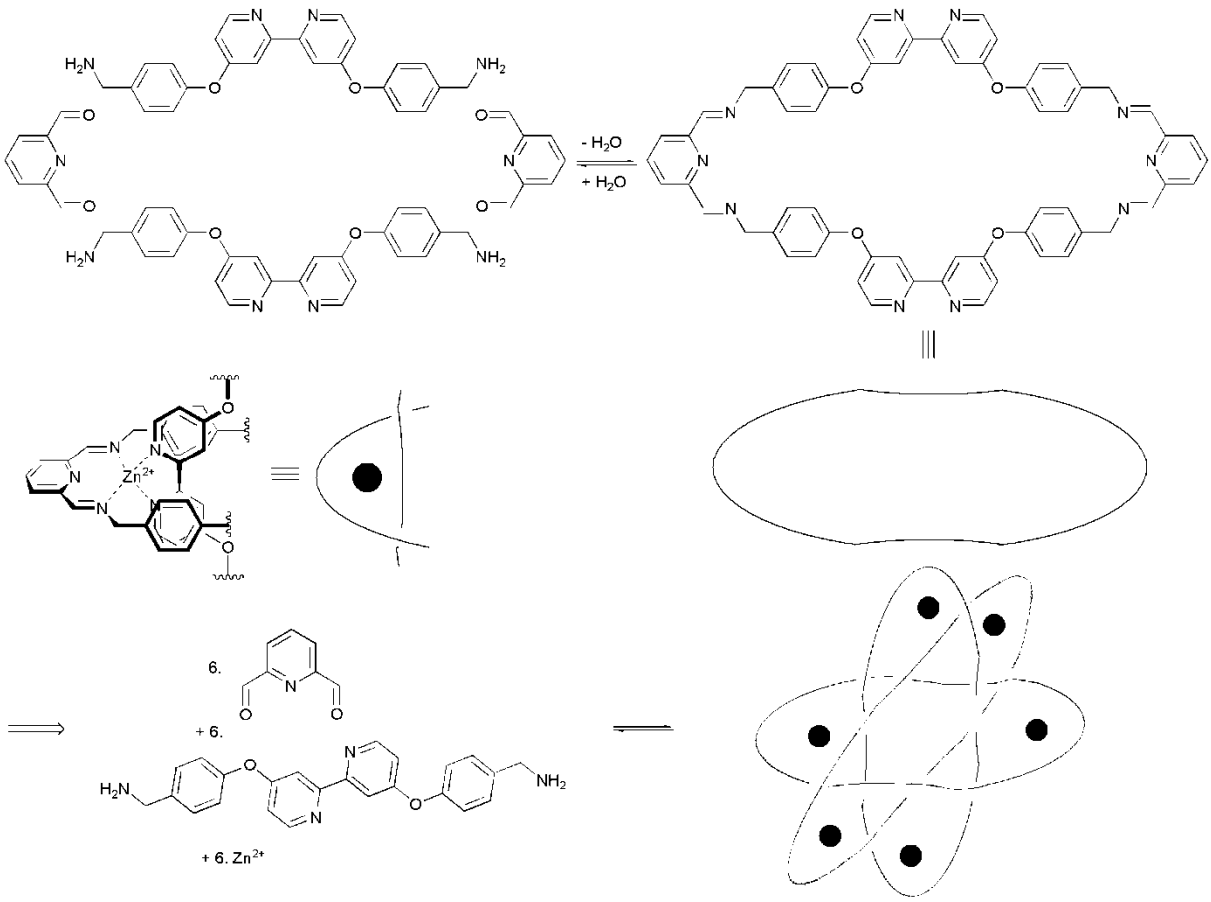

Scheme 1.7. Stoddart's dynamic synthesis of Borromean rings.[36]

The future of research in interlocked structures will probably involve more practical applications. A few recent results show how the particular molecular-scale properties of interlocked structures can be used for applications at a macroscopic level. The first will be an example, given by Leigh's group, of how molecular machines based on rotaxanes can be used for macroscopic transport.[37] By attaching specially designed photochemically driven rotaxane-based molecular shuttles to a surface, it was shown that upon irradiation of these rotaxanes, the surface tension was changed, which was then used to move a droplet of iodomethane on the surface. The second example is the concept of mechanised nanoparticles by Stoddart's group.[38] Pseudorotaxanes and bistable rotaxanes can be used as actual *nanovalves* allowing the controlled release of molecules imprisoned in hollow nanoparticles equipped with these valves. Obviously, one of the possible applications of this technology is

in drug delivery. The last example is also given by Stoddart's group[39a] and uses molecular shuttles in the concept of a 160 kilobit molecular electronic memory. This is probably one of the most promising application of rotaxanes as it may give in the future an alternative to silicon electronics. Other work carried out today in the field of rotaxanes are clearly aimed at being used for the establishment of alternative "bottom-up" technologies in the field of computing.[39b]

1.1.3) Fluorescence and photochemistry

1.1.3.1) Overview of fluorescence and photochemistry[40]

The work in this thesis makes it necessary to introduce the notions of fluorescence, photochemistry and in particular the photochemical and fluorescence properties of anthracene derivatives. Photochemistry is the study of the changes in matter induced by light. In a more general perspective, it is the study of the interaction of light with matter. In modern physics, light is understood as a flux of elementary particles, photons, which are the force carriers of the electromagnetic interaction. As a result, photochemical processes can be understood at the molecular level using quantum physics. The *absorption* of a UV photon by a molecule leads to an *electronic transition*, as one of the electrons of the molecule will be promoted from its occupied orbital to an unoccupied orbital of higher energy. As a consequence, the overall energy of the molecule will be higher: it is said to be in an *excited state*. It is for this reason that the *UV-Vis spectrum* of a molecule is sometimes referred to as *electronic absorption spectrum*, in contrast with *IR spectrum* which corresponds to *vibrational spectrum*.

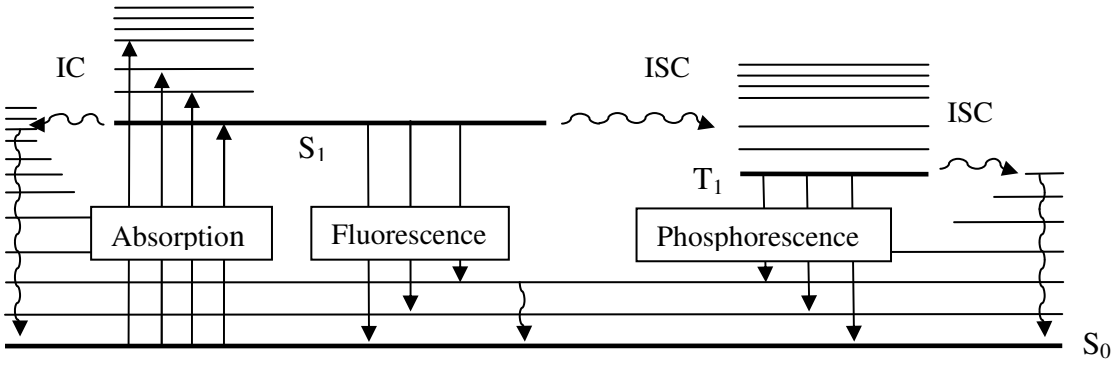

Figure 1.6. Perrin-Jablonski diagram.

The different processes that excited states can follow without chemical transformation are illustrated in **Figure 1.6**, which is an example of *Perrin-Jablonski diagram*. When an electron is promoted from the ground state to a higher energy level, its spin remains generally unchanged. A state where the total spin number is zero is called a *singlet state*, and as for most molecules the ground state is a singlet state (S_0), therefore the excited state formed initially by photon absorption is also a singlet state (S_1). On the diagram in **Figure 1.6** they are represented by bold lines, whereas the fine lines above them represent the different vibrational states of these electronic states. A molecule in the singlet excited state can *relax*, which means go back to the ground state, by emitting a photon: this phenomenon gives rise to *fluorescence emission*. It can also relax without light emission: in this case, it will first undergo an *internal conversion* (IC) to a higher vibrational state of the ground state followed by a *vibrational relaxation*. But it can also be converted to a state where the spin of the electron has changed: this process is called *intersystem crossing* (ISC) and gives rise to a new excited state which is called *triplet state* (T_1). It can relax either by another intersystem crossing followed by vibrational relaxation, or less frequently by emission of a photon, which in this case is called *phosphorescence*.

Apart from these intrinsic relaxation processes, there are other processes[40] that an excited state can undergo that can happen in the presence of another molecule. It can also transfer its charge through either intra- or inter-molecular proton or electron transfer. This last

case, known as *photoinduced electron transfer* (*PET*), has a role in natural *photosynthesis* and is used in applications using solar energy such as photocells. It can also transfer the energy of its excited state to another molecule, either by emission and reabsorption of a photon, which is known as *radiative energy transfer*, or without emission of a photon, a process known as *non-radiative energy transfer*, which can occur either through dipole-dipole interaction (which can allow to determine the distance between donor and acceptor) or, at close distance only, through recovery of molecular orbitals of the donor and acceptor. It has to be noted that this last mechanism is the only one that can happen when the excited state that transfers its energy is a triplet state. And finally, the molecules in the excited state can be involved in chemical transformations. Such chemical reactions that follow the absorption of a photon are called *photochemical reactions*.

As the molecules in the excited state are highly reactive and/or have a tendency to go back to the ground state, the excited states are usually short lived. In the simpler cases, for an impulsional irradiation and when there is no equilibrium between different excited states, it is possible to define this lifetime. In the case described in the Perrin-Jablonski diagram of **Figure 1.6**, the singlet excited state S_1 can relax either by fluorescence, with a rate constant k_F, or by internal conversion with a rate constant k_{nr}, or by intersystem crossing with a rate constant k_{ISC}. A rate constant for non-radiative relaxation can be defined as $k_{nr} = k_{IC} + k_{ISC}$. If the concentration of the molecule in this excited state is noted (M^*), then it will follow this equation as in classical kinetics:

$$-\frac{d(M^*)}{dt} = (k_F + k_{nr}).(M^*)$$

The integration of this equation leads to:

$$(M^*) = (M^*)_0.e^{-\frac{t}{\tau}}$$

In this equation, $(M^*)_0$ is the initial concentration of this excited state after the impulsional excitation, and τ is the lifetime of this excited state, given by the following equation:

$$\tau = \frac{1}{k_F + k_{nr}}$$

The fluorescence intensity $i_F(t)$ is then given by the following equation:

$$i_F(t) = k_F.(M^*) = k_F.(M^*)_0.e^{-\frac{t}{\tau}}$$

For this reason, it is possible to evaluate the lifetime of the excited state by fitting the fluorescence decay with a monoexponential model. In a more general case, the fluorescence decay at a given wavelength can be a sum of exponential terms with as many terms as different excited states in equilibrium that emit fluorescence at this wavelength, and the expression of the lifetime can contain terms other than rate constants of radiative or non-radiative relaxations, such as rate constants of photochemical reactions.

The *quantum yield* of a process (fluorescence, photochemical reaction...) is defined as the fraction of molecules in the excited state that follow this process. For example, in the simple case described above the quantum yield of fluorescence Φ_F, which measures the efficiency of the fluorescence as relaxation process, is given by the following equation:

$$\Phi_F = \frac{k_F}{k_F + k_{nr}} = k_F.\tau$$

In the general case, it is given by the following equation:

$$\Phi_F = \frac{1}{(M^*)_0}\int_0^\infty i_F(t).dt$$

However, it is usually measured by calculating the integral of the whole emission spectrum at a wavelength of excitation λ_{exc} and comparing it to a known compound, according to the following formula:[41]

$$\Phi_{F,A} = \Phi_{F,B} \cdot \frac{I_A}{A_A} \cdot \frac{A_B}{I_B} \cdot \left(\frac{n_{s,A}}{n_{s,B}}\right)^2$$

Where $\Phi_{F,M}$ is the quantum yield of fluorescence of the compound M, I_M the integral of the fluorescence signal of the solution of M between λ_{exc} and $+\infty$, A_M is its absorbance at λ_{exc}, and $n_{s,M}$ is the refractive index of the solvent used for making the solution of M.

1.1.3.2) Interface with supramolecular chemistry

As suggested above in the definition of supramolecular devices, a change in the fluorescence or photochemical properties of a molecule or supermolecule upon a specific input can be considered as a *signal*. For example, a molecule whose fluorescence spectrum is changed upon binding to a specific guest can be defined as a *fluorescent sensor* for this guest species. This is illustrated with anthracene-tagged azacrown ethers (**Scheme 1.8**) .[42]

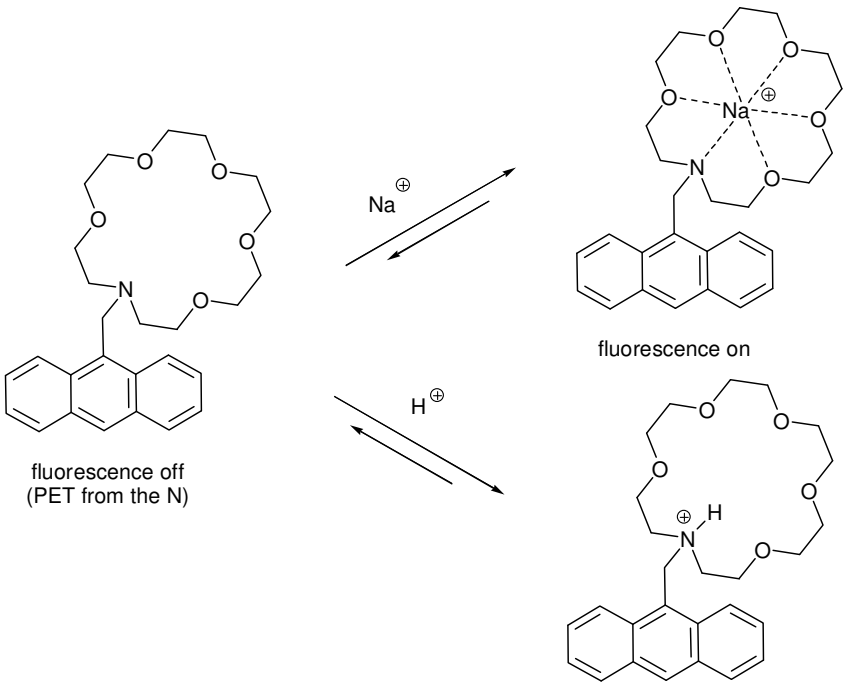

Scheme 1.8. Anthracene-tagged azacrown ether as fluorescent sensor. The fluorescence of the anthracene is quenched by electron transfer from the nitrogen when no guest is bound, but switched on by the binding of an alkali metal cation[42a,b] or a proton.[42c]

The input itself can also be irradiation: molecules which see their binding affinities to a specific guest reversibly modified upon irradiation can be defined as *photochromic switched*

receptors. This is illustrated with a spirobenzopyran derivative used to transport ion pairs across membranes (**Scheme 1.9**). [43]

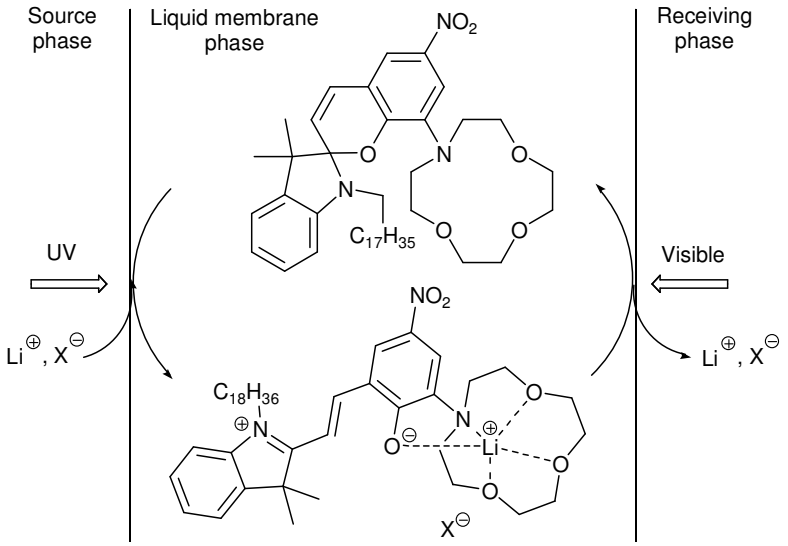

Scheme 1.9. A photochromic transporter.[43] Upon irradiation in UV of the source phase, the spirobenzopyran is opened and its binding affinity with lithium cation is switched on, whereas upon irradiation in visible light of the receiving phase, the binding with lithium is switched off and the ion pair released in the receiving phase.

Some other examples of such photochemical devices and others are given above in the short review on interlocked structures, and others will be given below in the review on "Hamilton-like" receptors.

1.1.3.3) Photochemical properties of anthracene derivatives

The second excited singlet state (S_2) of anthracene is situated at an energy difference of *114 kcal.mol*$^{-1}$ above the electronic ground state (S_0), which corresponds to an intense absorption band near *254 nm* in its UV-visible spectrum (band labelled $S_0 \rightarrow S_2$ in **Figure 1.7**).[44b] Despite its very high absorption coefficient (close to *200 000* $M^{-1}.cm^{-1}$) this band is not usually used in photochemical experiments because this region of the UV spectrum normally also contains absorption bands of the photoproducts, whose excitation is undesirable.[44b] The first excited singlet state, (S_1) lies at *76 kcal.mol*$^{-1}$ above S_0, corresponds to a series of vibrationally spaced bands below *380 nm* (bands labelled $S_0 \rightarrow S_1$ in

Figure 1.7).[44b] Its absorption coefficient is much weaker, close to *9 000* $M^{-1}.cm^{-1}$, but this part of the spectrum is characteristic of anthracene and it is usually at a wavelength corresponding to one of these bands that anthracene derivatives are irradiated in photochemical experiments.[44b] In anthracene derivatives, the substituents will affect the level of these energy levels. For example, with an electron donating group such as -OR, the absorption band will be displaced to higher wavelength and the different bands will be broader and less structured.

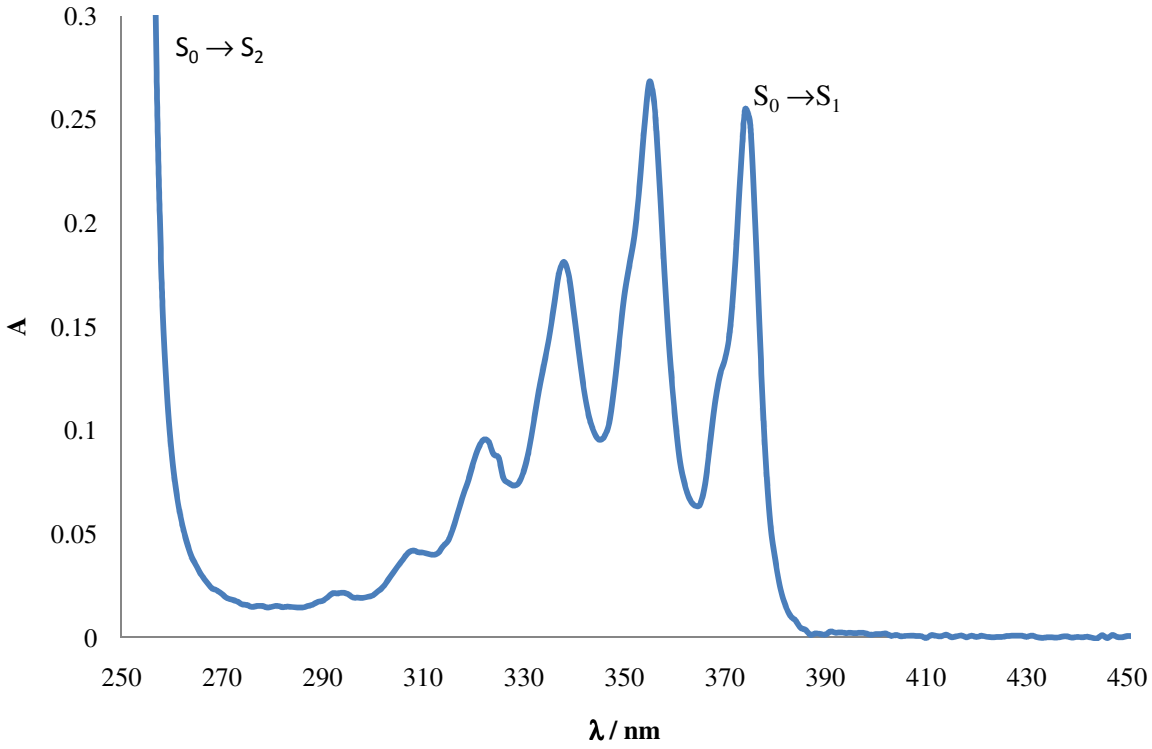

Figure 1.7. UV-visible spectrum of anthracene, *2.9* $\times$ 10^{-5} *M* in ethanol, at room temperature.

When a solution of anthracene is irradiated in one of these bands around *350 nm*, the excited state S_1 is obtained. Fluorescence is then observed, with a quantum yield close to *0.3* (*0.27* in ethanol at room temperature).[44a] The second triplet state (T_2) of anthracene lies at *74 kcal.mol*$^{-1}$ above S_0 (*2 kcal.mol*$^{-1}$ below S_1), and the lowest triplet state (T_1) at *42 kcal.mol*$^{-1}$ above S_0.[44b] The proximity of S_1 and T_2 means that intersystem crossing from the S_1 state to T_2 is efficient, with a quantum yield of *0.7*.[44b] Furthermore, for many other substituted anthracenes it has been established that the sum of quantum yields of fluorescence and of

intersystem crossing to the triplet state is close to *1*.[44b] Thus, for many anthracene derivatives, the main deactivation process is intersystem crossing and not internal conversion.

In concentrated solutions of anthracene derivatives, or in solutions of molecules or complexes containing two anthracene units, an anthracene in its excited state can come in close contact to another anthracene in its ground state, which can give rise to an *excimer*.[40] It is a 1:1 complex of two anthracene units, stable in the excited state but not in the ground state. It also emits fluorescence, also at higher wavelength (close to *550 nm* in a bis-9-anthracene)[45a] than monomeric anthracene (which emits around *430 nm* in the same molecule), and with a featureless band. It has been shown that the excited state that gives rise to excimer when binding to a ground-state anthracene is the S_1 singlet state.[46b] The geometry of this excimer in intermolecular formation is a slightly staggered sandwich configuration, but it has been shown that when the excimer is formed intramolecularily, different orientations of the anthracene subunits can lead to different excimers.[46b, 47]

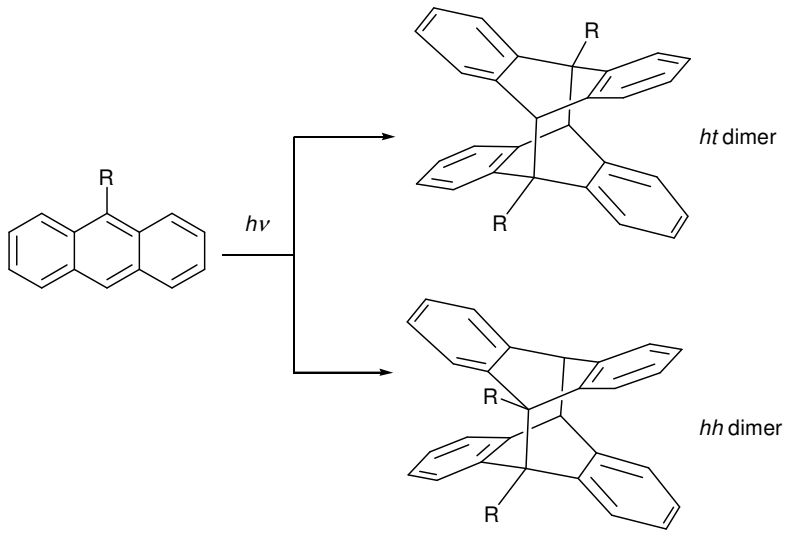

Scheme 1.10. Photodimerisation of 9-substituted anthracenes.

As well as excimers, that return to the ground state in a similar way to other excited states, anthracene is known to form *photodimers*, as illustrated on **Scheme 1.10**.[46] It has been demonstrated that as for excimer formation, it is the S_1 state which is involved in this photoreaction.[45] There are also good evidences that the photodimer forms from the excimer

rather than in competition with it.[45] The photodimer can then be reverted to the anthracene monomer either by irradiation (typically at *270 nm*) or by heating.[45] Different substituents on the anthracene can lead to different dimers; when the anthracene is substituted on the 9 position, then two different dimers can theoretically be formed, the *head to head* dimer (*hh*) and the *head to tail* dimer (*ht*).[45] These two dimers however have usually very different thermal stabilities; with intermolecular dimers, the half-life of *ht* dimers are usually between a few years and thousands of years, whereas the half-life of *hh* dimers are usually expressed in hours.[45] However these times of thermal return are usually much more varied in intramolecular dimers and can be affected by other chemicals.[45]

Anthracenes can also be involved in other photoreactions that will not be mentioned here,[44b] but it has to be mentioned that they are often oxidised to anthraquinone in non-degased solutions or even in air when not kept in the dark. This is in fact the result of a photochemical reaction of the triplet state of anthracene with singlet oxygen, that leads to an endoperoxide which later decomposes partly to anthraquinone.[44c]

Because of these interesting fluorescence and photochemical properties, anthracene groups have been used in the conception of different kinds of supramolecular devices. A few examples of theses applications can be given. Anthracene has been used as signalling unit in fluorescence probes, for example in the conception of DNA probes[48] in order to detect SNPs.* On the other hand, anthracene dimerisation has been used to design photocrown ethers[45] and other cryptands and coronands.[49] It has also been used in the synthesis of polyrotaxanes.[50] And as will be explained later, it has also been used in photoswitchable artificial receptors for barbiturates (cf. **Scheme 1.13**).[51]

* SNPs stands for "single-nucleotide polymorphisms", which designs a variation of a single nucleotide in a DNA sequence.

1.1.4) Hydrogen-bonded receptors for Barbiturates

1.1.4.1) Receptors in supramolecular chemistry[2]

A *receptor* can be defined as a molecule that can selectively bind to an ionic or molecular *substrate* by the mean of diverse intermolecular interactions, leading to the assembly of at least two species, a supermolecule. This concept is central in supramolecular chemistry and a complete overview of the different kinds of receptors would be out of the scope of this thesis.

Supramolecular chemistry emerged from the study of the selective fixation of alkali and alkaline earth metal cations. Crown ethers and cryptates were studied for their ability to bind these positively charged, spherical substrates by electrostatic interactions and to select them by their size. The binding of spherical anions was later performed in a similar way by using polyammonium macrocycles and polymacrocycles. But the binding of non-spherical substrates required to develop shape-specific receptors. Hydrogen bonds, with their particularity of being directional, became an interesting choice. Their use also made possible the binding of neutral molecules by multiple hydrogen bonds. One of the most classical receptors for neutral molecules is A. D. Hamilton's receptor for barbiturates,[52] which will be described here.

1.1.4.2) Barbiturates

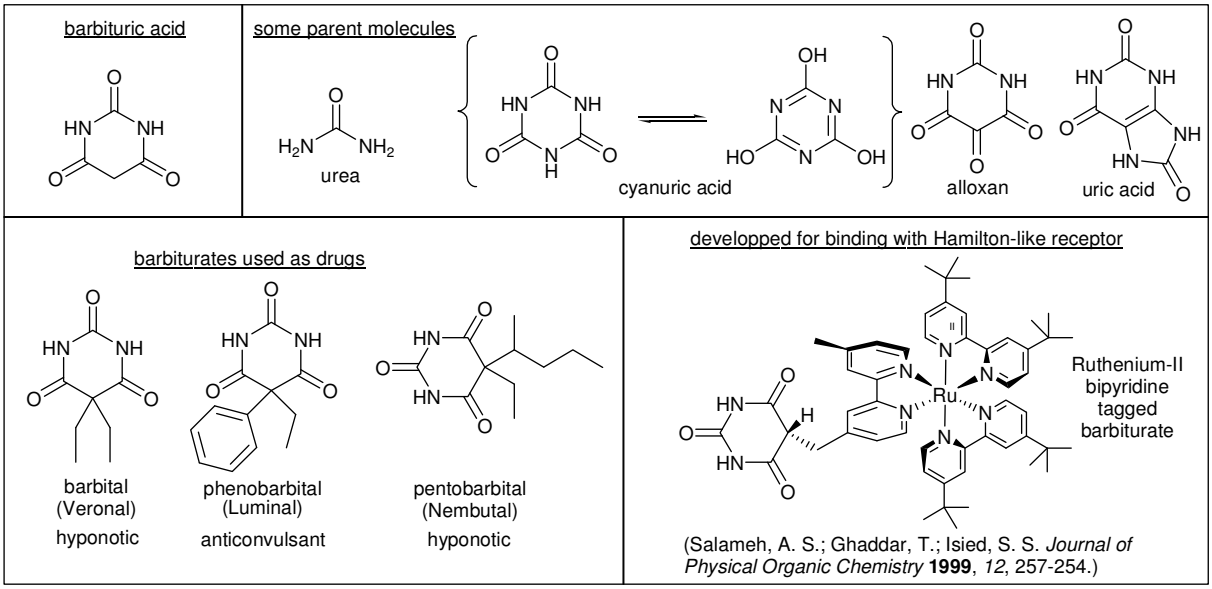

Figure 1.8. Examples of barbiturates and parent molecules.

Barbituric acid was first named by Adolf von Baeyer in 1863 and synthesised in 1864 by condensation of urea and diethyl malonate.[53] Its oxidised parent alloxan was known since 1818, when it was obtained by oxidation of the natural uric acid using nitric acid.[54] Also barbituric acid on its own has no effect on the central nervous system, Emil Fischer and Joseph von Mering discovered in 1903[55] that 5,5-diethylbarbiturate (also known as veronal, its first commercial name, or barbital as it will be called in this thesis) was a very powerful central nervous system depressant. This drug, as well as other barbiturates, was then used for applications ranging from mild sedation to anaesthesia, but they were also used as anxiolytics, hypnotics and as anticonvulsants. The story of barbiturates from this point is the story of psychotropic drug use... and abuse. Also most of their medical use belongs to history as they have been replaced by benzodiazepines, they are still drugs of abuse, and most infamously used in lethal injections.

Besides this use, following the publication by A. D. Hamilton of the first synthesis and binding studies of a series of new artificial receptor for barbital,[52] the synthesis of barbiturates has seen a revival for their applications in supramolecular chemistry.

There are different ways to synthesise C-substituted or disubstituted barbiturates described in the literature. Also some of the more reactive alkyl halides react directly with barbituric acid,[56] most do not, and the classical method derives from the historical synthesis of barbituric acid[53b] as it consists in synthesising first a substituted malonate, which is then reacted with urea to form the barbiturate (see **Scheme 1.11**).[57] The conditions of this reaction were historically using sodium ethoxide in ethanol,[57a-c] but since then it has been proved that the reaction was faster and gave better yields in DMSO, because the side reaction of decarbethoxylation[57d] was either less important or avoided depending on the base used (alkoxide or hydroxide). However, side reactions such as saponification and decarboxylation could still take place when using these bases.[57e] The modern syntheses of barbiturates are now often performed in DMSO using sodium hydride as a base.[57f]

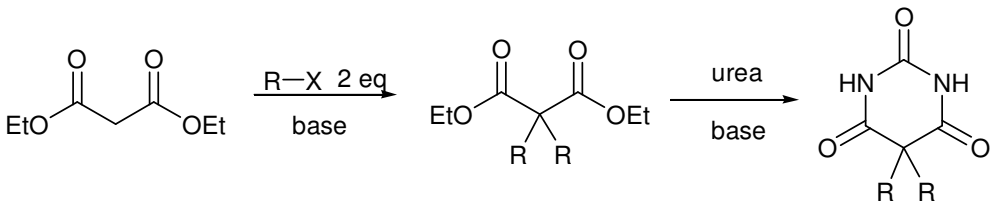

Scheme 1.11. Synthesis of disubstituted barbiturates by the classical method, only efficient when RX is an alkyl halide.

There are some drawbacks to this strategy: first introduction on the malonate of another substituent than an alkyl, for example an aryl group, can usually not be done by nucleophilic substitution. The introduction of aryl groups on the malonate was made possible using Friedel-Crafts reactions from diethyl ketomalonate,[58a] but it was then observed that the yields of cyclisation with urea of malonates with bulky substituents were often low,[58b] supposedly because of the side reactions mentioned above.[57d] The direct introduction of the aryl substituents by Friedel-Crafts reaction on alloxan was attempted as early as 1935,[58c-d] and greatly improved in 1999,[58e] but due to the poor physiological effects of diaryl barbiturates compared to their alkyl parents, the synthesis of diarylbarbituric acids remained a rare curiosity. This thesis will show that they may have another unexpected practical interest.

Some other ways to obtain C-substituted barbituric acids have also been developed, that start from barbituric acid. To mention only two, diarylbarbituric acids were also obtained by reacting barbituric acid with different aryllead triacetates,[59a] and dialkyl barbituric acids where also obtained by reductive C-alkylation using aldehydes and ketones in the presence of platinum and palladium catalysts.[59b]

1.1.4.3) Hamilton's receptors

Hamilton's receptors mentioned above[52] bind barbital and other barbituric acids by forming six complementary H-bonds (see **Figure 1.9**). Because of the complementarity of their structure with the structure of barbituric acids, the binding constants obtained in these systems were remarkably high (see **Table 1.1**) by comparison to other H-bonded systems.

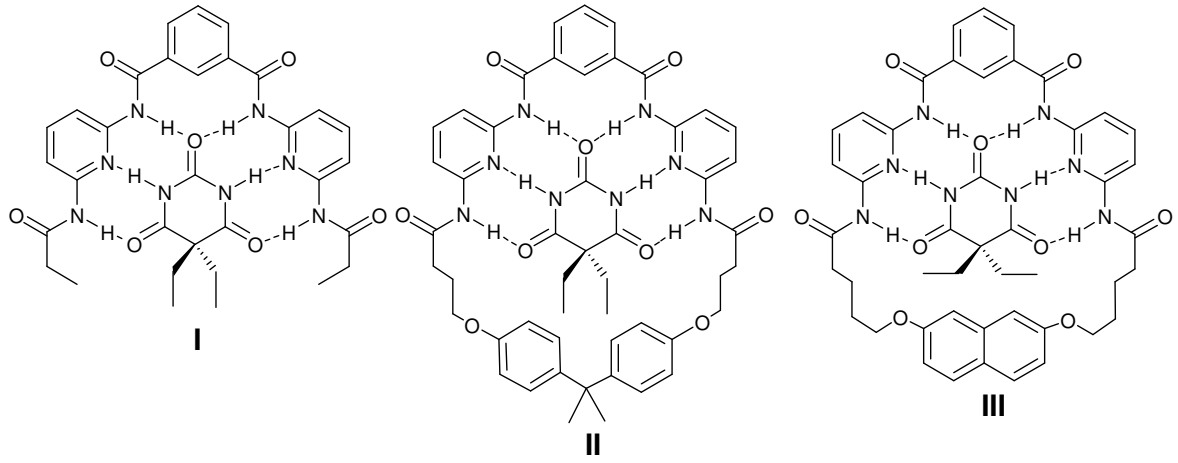

Figure 1.9. Hamilton's receptors complexes with barbital.[52]

Table 1.1. Binding constants of Hamilton's receptors with barbital at 25°C.[52]

log(K)	**(I)**	**(II)**	**(III)**
$CDCl_3$	4.3	6.1	
CH_2Cl_2		5.8	5.4

This soon became a classical example of H-bonded receptor to bind neutral molecules, as this binding motif was used in many other works. Hamilton's receptors and all receptors or

molecular devices derived from them can be described as consisting of two parts bond together:

- The upper part is a central "bridge" consisting of an aromatic centre, most frequently a benzene ring, substituted by two 2,6-diamidopyridine units. The two diamidopyridine units are there to form the 6 H-bonds with the barbiturate and the primary role of the aromatic centre is to be a spacer between those two units, so this part can be designed as the binding motif of the receptors, and is what defines them as Hamilton-like receptors. It has to be noted that the aromatic centre of this "bridge" can be different from the classical 1,3-substituted benzene of Hamilton's original receptor: it can bear some groups to improve its solubility, or to confer to it a specific functionality that would be switched on upon binding.
- Attached to the two terminal nitrogen atoms of this bridge, we can have either a closing loop, or pendant arms, possibly bearing other motifs. This lower part is typically what distinguishes two different receptors, modifies their binding affinity towards different barbiturates, the geometry and other properties of the complexes, and confer to these different receptors their functionalities for different applications.

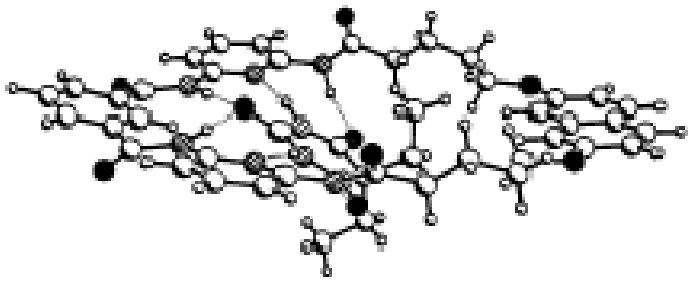

Figure 1.10. X-ray structure of the complex with barbital of one of Hamilton's receptors.[52b]

It has to be noted that each time crystal structures of the complexes formed with different versions of these receptors and barbiturates were obtained, the complexes were symmetrical when looked from above as illustrated in **Figure 1.10**, however the barbiturate was not exactly in the same medium plane than the two amidopyridine units but tilted with a

small angle, the oxygen of the central carbonyl of the barbiturate being in the medium plane and closer to the receptor, as shown in **Figure 1.10**. The value of this angle however was not the same with all receptors.

Although they were developed to bind specifically barbiturates, these receptors, because they possess two donor-acceptor-donor sites, can bind other substrates through H-bonds with some degree of complementarity. Of course cyanurates (derivatives of cyanuric acid, see **Figure 1.8**) have the same complementarity as barbital with these receptors and will be bonded as strongly, but other substrates with less complementarity will be bonded, such as ureas or carboxylic acids.

It has also to be noted that barbiturates are also involved in other types of complementary, H-bonded self-assembled superstructures, notably molecular films formed by self-assembly with triaminopyrimidine (as illustrated on **Scheme 1.1**)[6a] or melamine derivatives,[6c] which was the basis of many other works in supramolecular chemistry, in particular under the direction of J.-M. Lehn[2] and G. M. Whitesides.[60b,c]

1.1.4.4) Applications of Hamilton-like receptors

Many supramolecular systems have been derived from Hamilton's original barbiturate receptors. An overview of these systems involving *Hamilton-like receptors* can be made by reviewing the different characteristics and functions of these systems.

The first applications developed with these receptors were in catalysis.[61] Using his receptor for molecular recognition and stabilization of transition-state, Andrew Hamilton and his collaborators studied the catalysis of phosphoryl-transfer reactions.[61a] Following this idea of mimicking enzymatic mechanisms, reactions between derivatives of these receptors and barbiturates that were favored by the suitable prearrangement of the reagents upon binding were studied, in the case of thiolysis[61b,c] and decarboxylation of *N*-Carboxy-

imidazolidinone.[61d] More recently, the synthesis of catalysts containing the Hamilton binding motif was envisaged.[61e,f]

The next domain of application, also initiated by A. D. Hamilton and his collaborators, was to study the changes in fluorescence induced by binding. Energy transfer between receptors and barbiturates both tagged with different chromophores was studied,[62a] (see **Scheme 1.10**) and the first article describing fluorescent changes in these types of receptors not written by A. D. Hamilton was on the change upon complexation with different guests in the fluorescence spectrum of a receptor with two pyrenes attached on the lower part.[62b] It was later observed that Hamilton's receptors were slightly fluorescent on their own, and this was used to design a fluorescent probe where the receptor was incorporated in mixed self-assembled monolayers (SAMs) of alkanethiolates on gold.[62c] Other studies of binding luminescent ruthenium(II) tris(2,2'-bipyridine) tagged barbiturates have also been made and studied for electron transfer, such as the one given as an example in **Figure 1.8**.[62d,e]

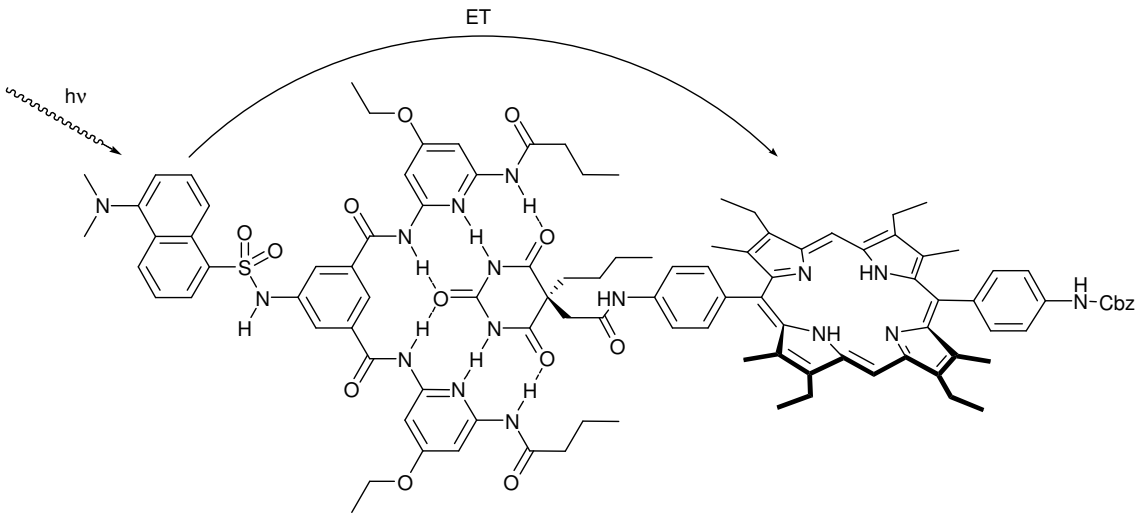

Scheme 1.12. Energy transfer through Hamilton's multichromophore complexes.[62a]

Photoinduced electron transfer (PET) inside a Hamilton-like complex has also been studied and used by different groups.[63] Barbiturates similar to the one in **Figure 1.8** were used for this application with receptors tagged with another metal complex on the central aromatic bridge.[63a] Complexes with similar barbiturates and receptors tagged also on the bridge by a

methyl viologen group were used more recently to study the PET process itself inside the complex.[63b] Ultra-fast PET was also performed by the Bassani group between receptors bearing oligo(thienylene vinylene) groups attached to the arms and fullerene-tagged barbiturates.[63c] Another example of PET with a different fullerene-tagged barbiturate involves a central perylene bisimide bearing two Hamilton receptors.[63d] The PET from a porphyrin-tagged receptor to a fullerene-tagged cyanurate has also been studied in a more recent article, showing that binding different metal ions in the porphyrin allowed to switch between energy and electron transfer.[63e]

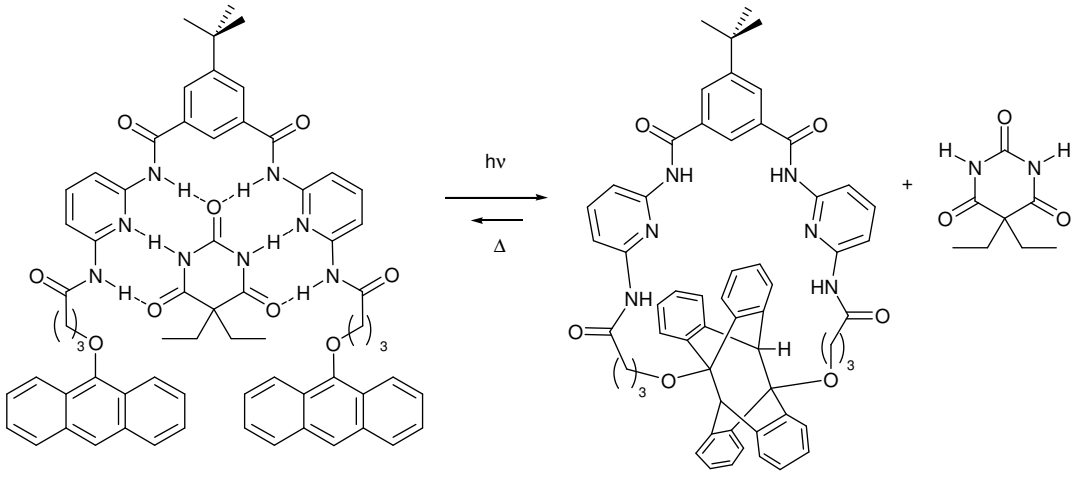

Scheme 1.13. Photoswitched binding of barbital by anthracene-tagged receptors.[51]

After fluorescence and PET, the next step was to use actual photochemical reactions inside complexes of this type. The first example[51] of such device has been mentioned above in the paragraph about anthracene photodimerisation. It was developed in a collaboration between the Tucker group and the team of D. Bassani in Bordeaux, and involves a series of Hamilton-like open receptors terminated by anthracene groups, that can be reversibly closed using anthracene photodimerisation,[46] leading to a change in the binding affinity with barbital (see **Scheme 1.13)**. Another photochromic device based on Hamilton-like receptors is the recent conception of an "ultimate lock-and-key system in which the key unlocks the lock",[64] that is a complex between a receptor where the closing part is a dithiane or trithane-based photolabile module which cleaves only in the presence of an external sensitizer, and a

barbiturate bearing this benzophenone sensitizer, so that upon irradiation of the complex the receptor closing part is cleaved.

Another promising work with these receptors in the context of photochemistry is the complexation of merocyanine dyes by merocyanine-tagged Hamilton-like receptors, leading to the orientation of merocyanines in a head to tail fashion, as wanted for applications in nonlinear optics.[65]

The idea of binding metallic cations in addition to the barbiturate with Hamilton-like systems is encountered in two different works.[66] The first of these two articles[66a] describes a Hamilton-like receptor with two triethyleneglycol substituted arms that can bind both sodium and barbiturates, and that gives a better binding constant both for sodium and barbiturate when the barbiturates also bears a third triethyleneglycol arm to bind Na^+ in a cryptate fashion. In a more recent article, [66b] the binding of zinc (II) ions by the two bipyridine ligands covalently bond to a Hamilton-like receptor changes the conformation of its cavity and stops it to bind barbital: in this context, the Zn^{2+} ions are described as negative allosteric co-factors, again by analogy with biochemical systems.

Also his contribution to the world of self-organised systems containing barbiturates and cyanurates was mainly based on the conception of molecular films,[6] J.-M. Lehn and his coworkers have also used the Hamilton motif. The first of his articles to use a Hamilton-like receptor (in a competition experiment) are about the dynamic formation and selection of a receptor for barbiturates by self-organisation,[67] in a dynamic covalent chemistry context. Also the receptor formed in this way does not fully belong to the family of Hamilton-like receptors, it also possesses two amidopyridine groups oriented towards the barbiturate and forming 4 complementary H-bonds. The next article[68] describes the conformational rearrangement of a receptor made by alternating 5 diamidopyridine motifs with 3 isophtalic bridges (which is basically the Hamilton motif repeated 3 times) in the presence of barbiturates and cyanurates.

The other contributions by this group all deal with supramolecular polymers[69] made by self-assembly of monomers bearing Hamilton-like receptors and/or cyanurate ends (see **Scheme 1.14**). The properties of these polymers were studied and it was observed that some of the particular mechanical properties of these polymers could be explained by the stacking of the H-bonded planes.

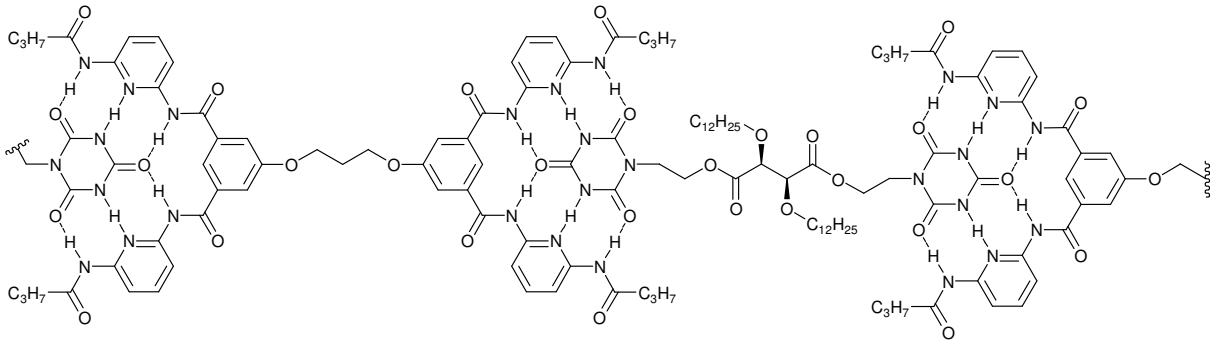

Scheme 1.14. Supramolecular polymers with cyanurates and H-bonded receptors.

This last phenomenon had already been used to make gelators[70] based on Hamilton's receptors substituted by cholesterol, whose gelation ability changed depending on the solvent and upon binding of barbital or other guests. In the same article, it was observed that Hamilton-like receptors have a tendency to self-associate by H-bonds, especially in aliphatic solvents, often leading to poor solubility. This problem was also encountered by another team working on dissolving Hamilton's receptors in PVC for building extraction devices for barbiturates.[71a] In another article, Hamilton's receptors were bound to polystyrene in order to selectively extract barbituric acid tagged compounds by chromatography.[71b]

Another contribution of the Tucker group to the world of Hamilton-like receptors was to design receptors where the bridging isophtalic acid was replaced by ferrocene-1,1' or ferrocene-1,3-dicarboxylic acid, in order to perform electrochemical sensing[72] (see **Scheme 1.15**). This structure was also encountered in another article[61e] that was already mentioned in the applications to catalysis.

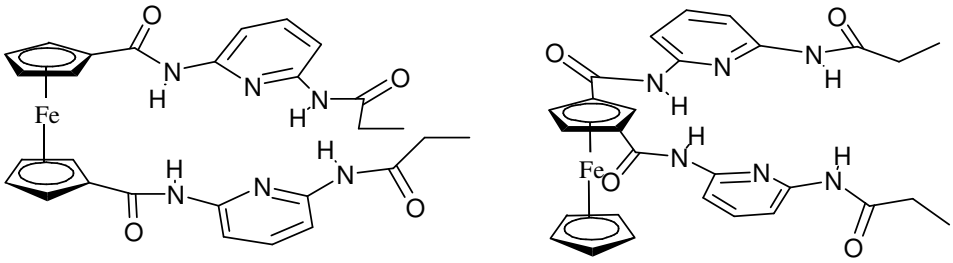

Scheme 1.15. Electrochemical sensors for barbiturates.

Chiral versions of the Hamilton's receptor have also been designed.[73] Receptors containing a *(R)*-BINOL or a modified deoxycholate moiety in the closing part of the receptor have been synthesised and used for making asymmetric 1,3-dipolar cycloadditions on achiral barbiturate-cinnamic acid conjugates,[73a] however the enantioselectivities of these reactions were quite low, and this was attributed to the fact that barbiturates are not bound in the same medium plane than the receptor, so the reacting part of the barbiturate can be far away from the chiral moiety of the receptor. Similar receptors also closed by a *(R)*-BINOL but too small to bind barbiturates were used for their versatile H-bonding affinities with many different substrates as chiral solvating agents (shift reagents) for chiral discrimination in ^{1}H NMR.[73b-e]

Hamilton's recognition motif has also been attached to polymers, in order to confer it binding properties with barbiturate-tagged products.[74] It was then applied to bind barbiturate-tagged nanoparticles to a surface.[74c,d] Another application in the domain of polymer science was the synthesis of polymers tagged with thymine- and cyanurate-, as well as diamino-pyridine (receptor for thymine) and Hamilton-like receptors (for cyanurates) groups, in order to investigate the concept of self-sorting in polymers.[74e]

Finally, the Hamilton motif has been used in the conception of dendrimers.[75] In the first of these articles,[75a] the Hamilton motif was attached to pre-synthesised amine-terminated dendrimers, leading to large dendrimers with 4 to 32 binding sites for barbiturates, then the fluorescence properties of these multivalent receptors and their complexes with different barbiturates were studied. The six other articles[75b-g] are all made by A. Hirsch's group, and all

concern supramolecular dendrimers obtained by binding cyanurates tagged with different functionalities to a core containing 3 to 6 times the Hamilton motif, as illustrated in **Scheme 1.16**.

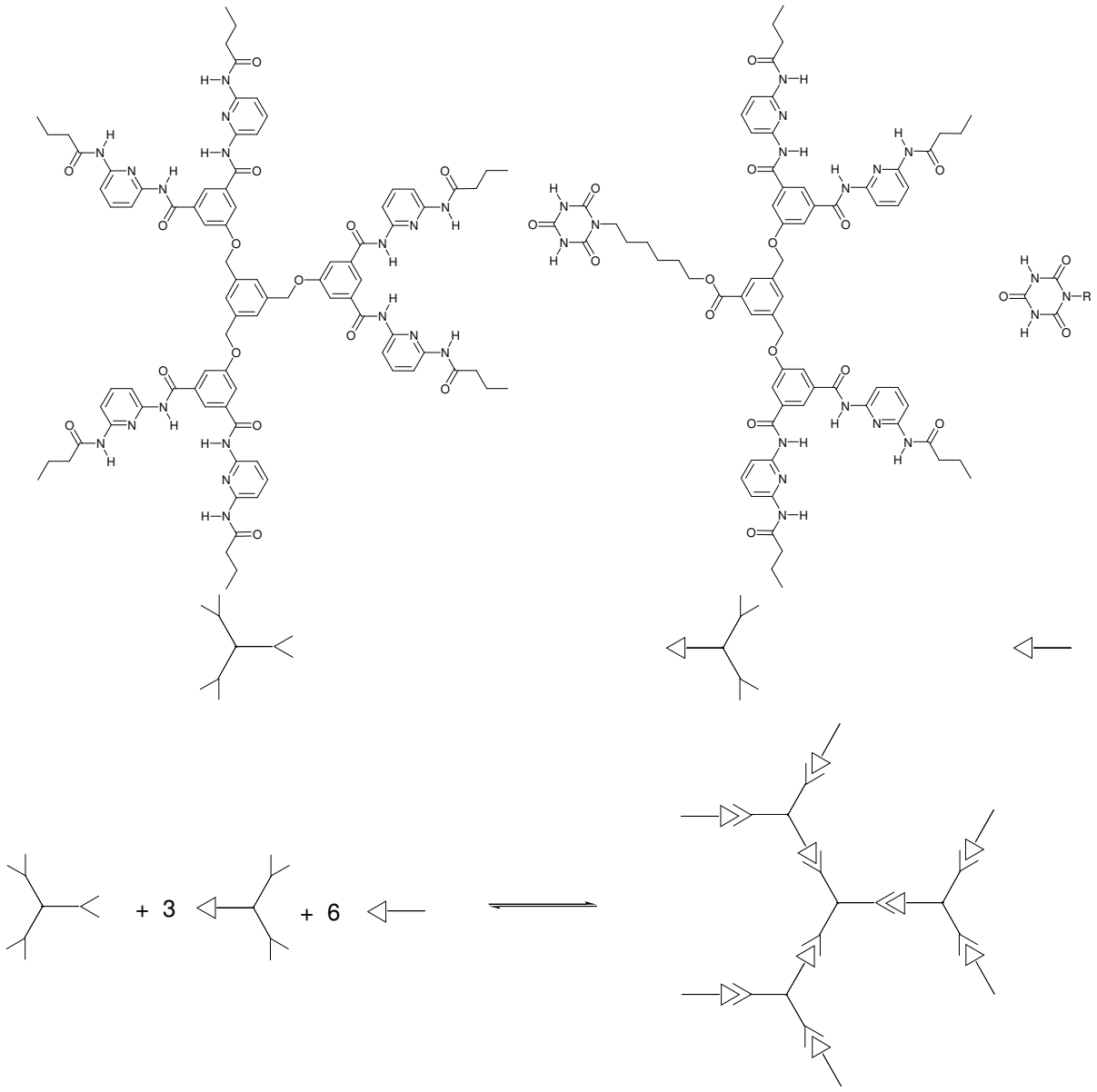

Scheme 1.16. Dendrimers based on Hamilton-like receptors.[75b]

1.2) Introduction to this project

1.2.1) Initial description and aims of the project

The project that this PhD thesis starts to explore derives from an observation of a property of Hamilton's receptors and devices derived from them. There are several examples of directed synthesis of interlocked structures such as catenanes and rotaxane synthesis where the necessary pre-formation was made using hydrogen bonds,[22f-h, 35, 76] but to the best of our knowledge the Hamilton motif, despite its privileged position in supramolecular chemistry as illustrated above, has never been used in generating such interlocked structures, also this idea has been evoked as an exercise in Eric Anslyn's textbook "*Modern Physical Organic Chemistry*".[77] By considering existing crystal structures as the one of **Figure 1.10**, it was thought that using a 5,5'-disubstituted barbituric acid with suitably long appendages, the 1:1 inclusion complexes formed with a macrocyclic Hamilton-like receptor would see the subtituents of the barbiturate protruding from front and back faces of the essentially planar receptor because of the geometry imposed by the unique sp^3-carbon atom on the otherwise planar barbiturate guest.

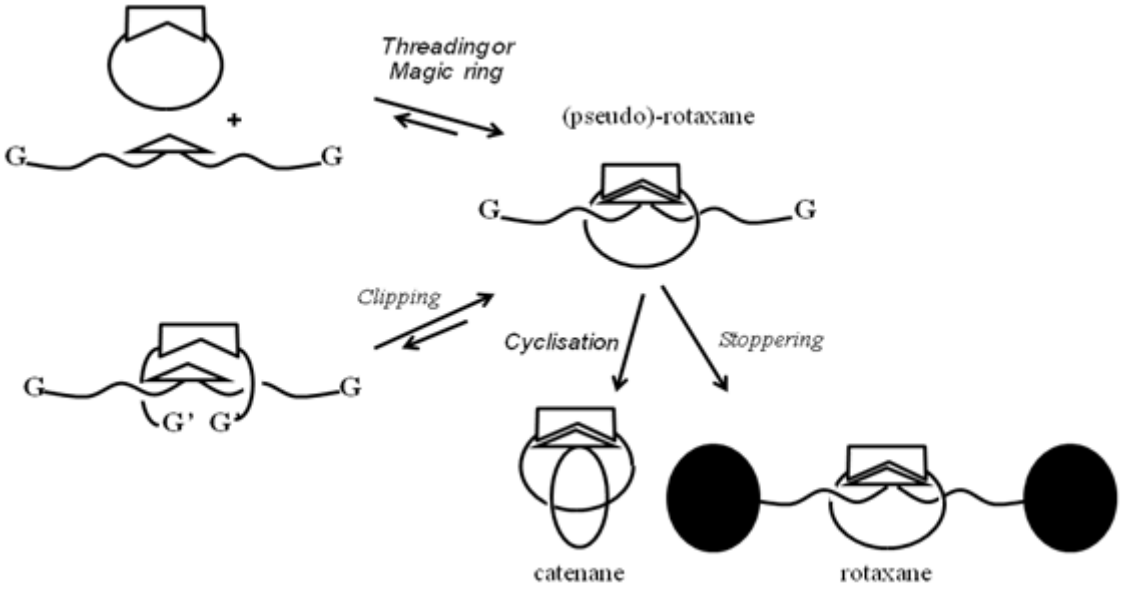

Scheme 1.17. Strategies for making interlocked structures.

This would be potentially conducive to the generation of mechanically-interlocked structures, such as catenanes via a ring-closing reaction between reacting groups at the extremities of the "arms" of the barbiturate, or rotaxanes by introducing stoppers instead. Or, if stoppers are already in place and prevent the formation of the rotaxane by *threading* through the Hamilton receptor, it was thought that another possibility was to use an open receptor and to use a ring closure reaction in order to form the rotaxane by *clipping*, or even to use the closed receptor in a *magic ring* approach. All these different strategies are illustrated in **Scheme 1.17**.

Another idea which was soon introduced in this work was to use anthracene photodimerisation as a ring closure reaction. It had already been used successfully in a previous work made by Y. Molard in J. H. R. Tucker's group that also involved Hamilton receptors, as already evoked (see **Scheme 1.13**).[51] A work that was based on introducing anthracene groups at the extremities of a Hamilton-like receptor for performing the photocyclomerisation of the receptor by anthracene dimerisation, combined with the considerations above on the interesting geometry of these complexes, naturally invited to do the opposite, that is to introduce anthracene groups at the extremities of a barbiturate and perform the photocyclomerisation of the barbiturate, which would lead to a catenane and thus, would be a *photocatenation*. Making *photocatenanes* using anthracene photodimerisation was also envisaged by Dr. N. McClenaghan and his Master student C. Lincheneau in Bordeaux,[78] so a collaboration with this group started on this project.

If the ring-closing reaction for the final formation of the catenane had to be anthracene dimerisation, then if another ring-closing reaction was to be used for the closure of the receptor it had to be of a different nature: the choice that was soon made was to use olefin metathesis, partly because it was already widely used in the synthesis of interlocked structures and as it is one of the simplest reaction that can be performed under thermodynamic control,

and partly because in a first time it was thought that the deformations and steric effects induced by the binding of a barbiturate in open Hamilton-like receptors terminated by a double bond would allow to control the reactivity and stereoselectivity of the ring-closing metathesis reaction. This was in fact a part of a larger project of attempting to obtain a form of supramolecular control of the reactivity and stereoselectivity in olefin metathesis. Also this will not be mentioned later in this thesis, some of the work that I have made during those four years and some of the work done by undergraduate students under my practical supervision in the laboratory was related to templated olefin metathesis.[79]

This research project was started with the intention of filling a gap in the literature, that is the formation of interlocked structures derived from Hamilton's receptors. These have been suggested previously[77] but in fact never synthesised. Providing a new way to obtain interlocked structures is always a significant development as there are still relatively few general templates to obtain these structures, which may have wide applications in different molecular machines in the near future with the development of nanotechnologies.[32a,b,c] Obtaining photocatenanes, that is catenanes resulting from a photochemical process, is another important new aim, and anthracene photodimerisation[46] is an interesting candidate reaction for fulfilling this objective.[78] Apart from interlocked structures, the Hamilton motif is presently widely used in many different applications.[61-72] More experimental data and a description of the different aspects of this complexation phenomenon, on both geometric and thermodynamic grounds, will allow a better understanding for all future applications of similar receptors.

1.2.2) Design of the molecules

In order to achieve the aim of obtaining interlocked structures by using the techniques described in the above paragraph, the receptors and barbiturates described in **Figure 1.11** were envisaged. In this figure, the barbiturates are represented in their two possible

photocyclised forms, and the receptors are represented in their forms closed by metathesis, and complexed with barbital.

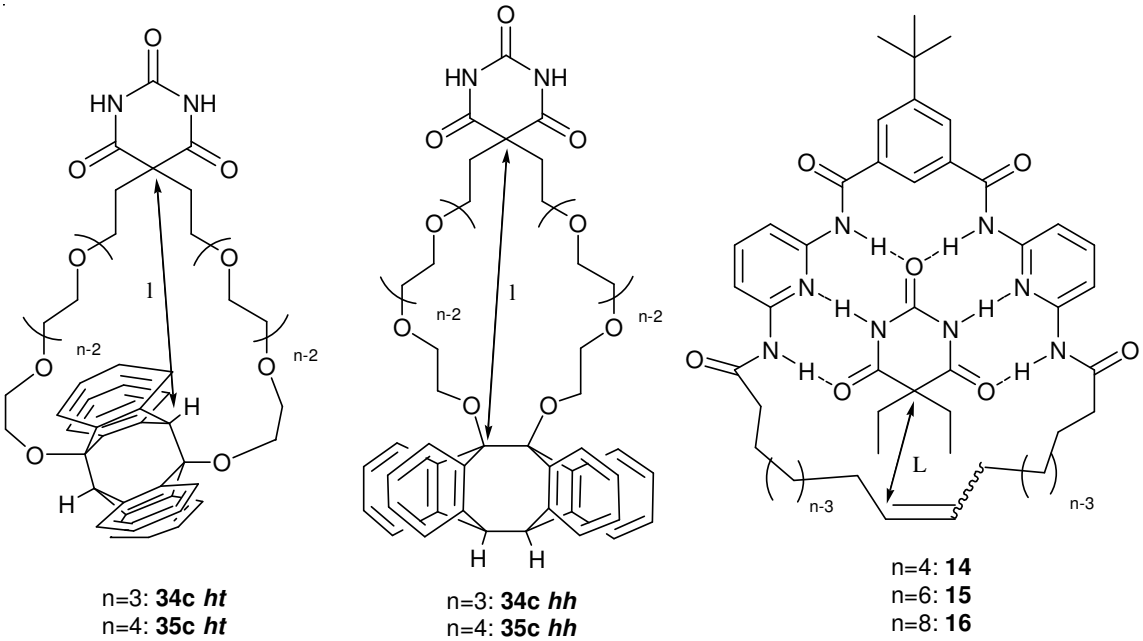

Figure 1.11. Structures envisaged for the barbiturates and receptors.

Having a double bond in the closing part of the receptor will allow opening and closing of the receptors by metathesis. The dimension of the ring in these receptors is directly related to the number of CH_2 units between the olefin and the C=O. The ring sizes of receptors **15** and **16** correspond approximately to the same ring size as A. D. Hamilton's original receptors in terms of atom number (II and III in **Figure 1.9**).[61] Receptor **14** would correspond to a smaller receptor. It was thought that it could be more rigid and may have a more clearly defined geometry which could yield more easily to interlocked structures.

The dimension of the anthracene-terminated barbiturates can be related to the number of ethylene glycol units in the chain between the barbiturate and the anthracene. Barbiturate **34** corresponds to a closed ring of 21 atoms, which is presently the smallest ring size for an interlocked structure obtained by threading, as discussed earlier.[26] Barbiturate **35** is significantly larger and as will be discussed below, seems more adapted to the synthesis of interlocked structures.

As described below, the feasibility of forming interlocked structures is discussed on the basis of the relative dimensions of the closed rings, represented by the distances *l* and *L*, defined as the distance between the central atom of the barbiturate and respectively the first atom of the anthracene unit or the first atom of the double bond (see **Figure 1.11**). This distance was measured on molecular models obtained using the MM2 force field in the software Chem3D Pro.[80] The results are presented in **Table 1.2**.

Table 1.2. Dimensions of the rings described in **Figure 1.1** according to Chem3D models.

Receptor	*L* (*trans*)	*L* (*cis*)
14 (*n* = 4)	5.3 Å	5.7 Å
15 (*n* = 6)	7.8 Å	7.9 Å
16 (*n* = 8)	9.9 Å	10.5 Å
Guest	*l* (*hh*)	*l* (*ht*)
34 (*n* = 3)	9.5 Å	7.8 Å
35 (*n* = 4)	13.5 Å	11.1 Å

If $l > L$, then cyclisation by dimerisation of the anthracene is more likely to occur beyond the receptor ring and the photocatenane will form more easily. According to these models, this will be the case for receptor **14** with both anthracene-terminated guests, for receptor **15** with both guests (but only if the *hh* dimer is formed with guest **34**), and for receptor **16** with guest **35** only. If $l \lesssim L$, then photocyclomerisation will be hampered by the presence of the alkyl chain between the anthracene units, leading to slower kinetics or smaller yields of catenanes. According to these models, this will be the case for receptor **15** with the *ht* dimer of guest **34**, and also probably with the *cis* form of receptor **16** with the *ht* dimer of **35**. If $l \ll L$, then the anthracene dimer will not form unless it can form inside the receptor

ring, essentially leading perched complexes. The models above predict this situation for receptor **16** and guest **34**. It has to be pointed out that even with $l < L$, catenanes can still be formed if cyclisation occurs on the side rather than at the opposite extremity of the receptor.

Other receptors and guests have been designed and synthesised in this thesis. The rationale for their design and more sophisticated *ab initio* DFT calculation performed for several of these systems will be described in the corresponding chapters.

1.2.3) Outline of the thesis

After this *Chapter 1*, the *introduction* to this thesis which reviewed the background of the domains touched by this thesis, *Chapter 2*, the first chapter of *results and discussion* of this thesis will be about the new Hamilton-like receptors designed for this project. In addition to their synthesis, this chapter will also study these receptors under different aspects: their ability to be opened or closed by olefin metathesis, and their binding properties with barbital which will be investigated by different methods, UV absorption, ITC and IR.

Chapter 3 will describe a first family of new barbiturates synthesised for this project, study their different properties, including fluorescence and photochemistry for the anthracene-tagged barbiturates.

Chapter 4 will study the binding of the barbiturates described in *chapter 3* to the receptors described in *chapter 2*, and will investigate the formation of catenanes or rotaxanes from these complexes, using olefin metathesis or anthracene photodimerisation.

The last chapter of results and discussion, *Chapter 5*, will introduce a second family of new barbiturates synthesised for this project, study their synthesis and the binding of one of them with the different receptors.

All the experimental results and procedures that are not directly needed for a comprehension and discussion of the results exposed in the other chapters but are necessary to

reproduce them experimentally are given in *Chapter 6*, *experimental part* of this thesis. Details of spectra and X-ray structures are given in *Appendix*.

In order to facilitate the reading, a chart of the most frequently mentioned molecules is folded at the last page of the thesis.

---

[1] *The Concise Oxford Dictionary*, edited by Judy Pearsall, Oxford University Press, 10th edition, **1999**.

[2] Lehn, J.-M. *Supramolecular Chemistry, Concepts and Perspectives*; V.C.H. ed., **1995**. Many of the definitions of the terms introduced in this introduction are taken from this book.

[3] Press realease of the Nobel Prize in Chemistry, 14 October 1987.

[4] Pauling, L. *Chemical And Engineering News* **1946**, *24*, 1375.

[5] Fischer, E. *Berichte der Deutschen Chemischen Gesellschaft* **1894**, *27*, 2985.

[6] (**a**) Lehn, J.-M.; Mascal, M.; DeCian, A.; Fischer, J. *Journal of the Chemical Society, Chemical Communications* **1990**, 479-481; (**b**) Lehn, J.-M.; Mascal, M.; DeCian, A.; Fischer, J. *Journal of the Chemical Society, Perkin Transactions 2* **1992**, 461-467; (**c**) Russell, K. C.; Lehn, J.-M.; Kyritsakas, N.; DeCian, A.; Fischer, J. *New Journal of Chemistry* **1998**, 123-128.

[7] Rowan, S. J.; Cantrill, S. J.; Cousins, G. R. L.; Sanders, J. K. M.; Stoddart, J. F. *Angewandte Chemie International Edition* **2002**, *41*, 898-952.

[8] Hunter, C. A. *Angewandte Chemie International Edition* **2004**, *43*, 5310-5324.

[9] (**a**) Dingley, A. J.; Grzesiek, S. *Journal of the American Chemical Society* **1998**, *120*, 8293-8297; (**b**) Cordier, F.; Rogowski, M.; Grzesiek, S.; Bax, A. *Journal of Magnetic Resonance* **1999**, *140*, 510-512; (**c**) Isaacs, E. D.; Shukla, A.; Platzman, P. M.; Hamann, D. R.; Barbiellini, B.; Tulk, C. A. *Physical Review Letters* **1999**, *82*, 600-603;

[10] Prins, L. J.; Reinhoudt, D. N.; Timmerman, P. *Angewandte Chemie International Edition* **2001**, *40*, 2382-2426.

[11] Gilson, M. K.; Given, J. A.; Bush, B. L.; McCammon, J. A. *Biophysical Journal* **1997**, *72*, 1047-1069.

[12] Cooper, A.; Johnson, C. M.; Lakey, J. H.; Nöllmann, M. *Biophysical Chemistry* **2001**, *93*, 215-230.

[13] Buurma, N. J.; Haq, I. *Methods* **2007**, *42*, 162–172.

[14] (**a**) Houk, K. N.; Leach, A. G.; Kim, S. P.; Zhang, X. *Angewandte Chemie International Edition* **2003**, *42*, 4872-4897; (**b**) Sharp, K. "Entropy–enthalpy compensation: Fact or artifact?" *Protein Science* **2001**, *10*, 661-667.

[15] (**a**) Westwell, M. S.; Searle, M. S.; Klein, J.; Williams, D. H. *Journal of Physical Chemistry* **1996**, *100*, 16000-16001; (**b**) Chang, C.-E.; Gilson, M. K. *Journal of the American Chemical Society* **2004**, *126*, 13156-13164.

[16] (**a**) Banks, R. L.; Bailey, G. C. *International Journal of Product Development*, **1964**, *3*, 170; (**b**) Eleuterio, H. S. *German Pat.* 1072811, **1960**; (**c**) Truett, W. L.; Johnson, D. R.; Robinson, I. M.; Montague, B. P. *Journal of the American Chemical Society.*, **1960**, *82*, 2337.

[17] (**a**) Chauvin Y. ; Hérisson, J.-L. *Die Makromolekular Chemie* **1971**, *141*, 161; (**b**) Chauvin, Y. *Angewandte Chemie International Edition*, 2006, **45**, 3740-3747 (Nobel lecture, see references within).

[18] Astruc, D. *New Journal of Chemistry*, 2005, **29**, 42-56.

[19] Schrock, R. R. *Angewandte Chemie International Edition*, 2006, **45**, 3748-3759 (Nobel lecture, see references within).

[20] Grubbs, R. H. *Angewandte Chemie International Edition*, 2006, **45**, 3760-3765 (Nobel lecture, see references within).

[21] (**a**) molecular knot: Dietrich-Buchecker, C.; Rapenne, G.; Sauvage, J.-P. *Chemical Communications* **1997**, 2053-2054; (**b**) handcuff-like catenane: Frey, J.; Kraus, T.; Heitz, V.; Sauvage, J.-P. *Chemical Communications* **2005**, *2005*, 5310-5312.

[22] Organometallic catenane obtained under thermodynamic control: (**a**) Gruter, G. J. M.; de Kanter, F. J. J.; Markies, P. R.; Nomoto, T.; Akkerman, O. S.; Bickelhaupt, F. *Journal of the American Chemical Society* **1993**, *115*, 12179-12180.; Fujita's "Magic ring catenanes": (**b**) Fujita, M.; Ibukuro, F.; Hagihara, H.; Ogura, K. *Nature* **1994**, *367*, 720-723; (**c**) Fujita, M.; Ibukuro, F.; Yamaguchi, K.; Ogura, K. *Journal of the American Chemical Society* **1995**, *117*, 4175-4176; (**d**) Fujita, M.; Ibukuro, F.; Seki, H.; Kamo, O.; Imanari, M.; Ogura, K. *Journal of the American Chemical Society* **1996**, *118*, 899-900; (**e**) Fujita, M.; Aoyagi, M.; Ibukuro, F.; Ogura, K.; Yamaguchi, K. *Journal of the American Chemical Society* **1998**, *120*, 611-612 ; "Magic ring catenanes" obtained by metathesis: (**f**) Kidd, T. J.; Leigh, D. A.; Wilson, A. J. *Journal of the American Chemical Society.* **1999**, *121*, 1599-1600; (**g**) "magic ring rotaxanes": Kilbinger, A. F. M.; Cantrill, S. J.; Waltman, A. W.; Day, M. W.; Grubbs, R. H. *Angewandte Chemie International Edition* **2003**, *42*, 3281-3285; (**h**) "magic rod rotaxanes": Hannam, J. S.; Kidd, T. J.; Leigh, D. A.; Wilson, A. J. *Org. Lett.* **2003**, *5*, 1907-1910.

[23] Schill, G. *Catenanes, Rotaxanes and Knots*; *Organic Chemistry, A Series of Monographs*, Vol. 22, Academic Press: New York, **1971**.

[24] Frisch, H. L.; Wasserman, E. *Journal of the American Chemical Society*, 1961, **83**, 3789-3795.

[25] Schill, G.; Beckmann, W.; Schweickert, N.; Fritz, H. *Chemische Berichte* **1986**, *119*, 2647-2655.

[26] (**a**) Zhuang, C.; Li, S.; Zhang, J.; Zhu, K.; Li, N.; Huang, F. *Organic Letters* **2007**, *9*, 5553-5556; (**b**) Hsu, C.-C.; Chen, N.-C.; Lai, C.-C.; Liu, S.-M.; Chiu, S.-H. *Angewandte Chemie International Edition* **2008**, *47*, 7475-7478.

[27] Gibson, H. W.; Nagvekar, D. S.; Yamaguchi, N.; Bhattacharjee, S.; Wang, H.; Vergne, M. J.; Hercules, D. M. *Macromolecules* **2004**, *37*, 7514-7529.

[28] (**a**) Wasserman, E.; Hill, M. *Journal of the American Chemical Society*, 1960, **82**, 4433-4434; (**b**) Wasserman, E. *Scientific American*, 1962, **207**, 94.

[29] Schill, G.; Lüttringhaus, A. *Angewandte Chemie International Edition* **1964**, *3*, 546-547.

[30] (**a**) Hudson, B.; Vinograd, J. *Nature* **1967**, *216*, 647-652; (**b**) Wang, J. C. *Annual Reviews of Biochemistry* **1996**, *65*, 635-692.

[31] Dietrich-Buchecker, C. O. Sauvage, J.-P. *Chemical Reviews* **1987**, *87*, 795-810 (review, see references within).

[32] (**a**) Amabilino, D. B.; Stoddart, J. F. *Chemical Reviews* **1995**, *95*, 2725-2828; (**b**) Cantrill, S. J.; Pease, A. R.; Stoddart, J. F. *Journal of the Chemical Society, Dalton Transactions* **2000**, 3715-3734; (**c**) Balzani, V.; Credi, A.; Raymo, F. M.; Stoddart, J. F. *Angewandte Chemie International Edition* **2000**, *39*, 3348-3391 (reviews, see references within); (**d**) Anelli, P. L.; Ashton, P. R.; Ballardini, R.; Balzani, V.; Delgado, M.; Gandolfi, M. T.; Goodnow, T. T.; Kaifer, A. E.; Philp, D.; Pietraszkiewicz, M.; Prodi, L.; Reddington, M. V.; Slawin, A. M. Z.; Spencer, N.; Stoddart, J. F.; Vicent, C.; Williams, D. J. *Journal of the American Chemical Society* **1992**, *114*, 193-218; (**e**) Cantrill, S. J.; Fulton, D. A.; Heiss, A. M.; Pease, A. R.; Stoddart, J. F.; White, A. J. P.; Williams, D. J. *Chemistry, a European Journal* **2000**, *6*, 2274-2287.

[33] Colquhoun, H. M.; Goudings, E. P.; Maud, J. M.; Stoddart, J. F.; Williams, D. J.; Wolstenholme, J. B. *Journal of the Chemical Society, Chemical Communications* **1983**, 1140 - 1142.

[34] Bissel, R. A.; Córdova, E.; Kaifer, A. E.; Stoddart, J. F. *Nature* **1994**, *329*, 133-137.

[35] (**a**) Johnston, A. G.; Leigh, D. A.; Pritchard, R. J.; Deegan, M. D. *Angewandte Chemie International Edition* **1995**, *34*, 1209-1212; (**b**) Johnston, A. G.; Leigh, D. A.; Nezhat, L.; Smart, J. P.; Deegan, M. D. *Angewandte Chemie International Edition* **1995**, *34*, 1212-1216;

(**c**) Leigh, D. A.; Murphy, A.; Smart, J. P.; Deleuze, M. S.; Zerbetto, F. *Journal of the American Chemical Society* **1998**, *120*, 6458-6467; (**d**) Deleuze, M. S.; Leigh, D. A.; Zerbetto, F. *Journal of the American Chemical Society* **1999**, *121*, 2364-2379; (**e**) Leigh, D. A.; Wong, J. K. Y.; Dehez, F.; Zerbetto, F. *Nature* **2003**, *424*, 174-179; (**f**) Gadret, G.; Zamboni, R.; Schouwink, P.; Mahrt, R. F.; Thies, J.; Loontjens, T.; Leigh, D. A. *Chemical Physics* **2001**, *269*, 381-388; (**g**) Altieri, A.; Bottari, G.; Dehez, F.; Leigh, D. A.; Wong, J. K. Y.; Zerbetto, F. *Angewandte Chemie International Edition* **2003**, *42*, 2296-2300.

36 (**a**) Chichak, K. S.; Cantrill, S. J.; Stoddart, J. F. *Chemical Communications* **2005**, 3391–3393; (**b**) Cantrill, S. J.; Chichak, K. S.; Peters, A. J.; Stoddart, J. F. *Accounts of Chemical Research* **2005**, *38*, 1-5.

37 Berná, J.; Leigh, D. A.; Lubomska, M.; Mendoza, S. M.; Pérez, E. M.; Rudolf, P.; Teobaldi, G.; Zerbetto, F. *Nature Materials* **2005**, *4*, 704-710.

38 (**a**) Nguyen, T. D.; Leung, K. C.-F.; Liong, M.; Pentecost, C. D.; Stoddart, J. F.; Zink, J. I. *Organic Letters* **2006**, *8*, 3363-3366; (**b**) Leung, K. C.-F.; Nguyen, T. D.; Stoddart, J. F.; Zink, J. I. *Chemistry of Materials* **2006**, *18*, 5919-5928.

39 (**a**) Green, J. E.; Choi, J. W.; Boukai, A.; Bunimovitch, Y.; Johnston-Halperin, E.; Delonno, E.; Luo, Y.; Sheriff, B. A.; Xu, K.; Shin, Y. S.; Tseng, H.-R.; Stoddart, J. F.; Heath, J. R. *Nature* **2007**, *445*, 414-417; (**b**) Lee, C.-F.; Leigh, D. A.; Pritchard, R. G.; Schultz, D.; Teat, S. J.; Timco, G. A.; Winpenny, R. E. P. *Nature* **2009**, *458*, 314-318.

40 Valeur, B. *Invitation à la fluorescence moléculaire*; 2004 ed.; De Boeck Université: Bruxelles, **2004**.

41 Rhys Williams, A. T.; Winfield, S. A.; Miller, J. N. *Analyst* **1983**, *108*, 1067-1071.

42 (**a**) de Silva, A. P.; de Silva, S. A. *Journal of the Chemical Society, Chemical Communications* **1986**, 1709-1710; (**b**) Bryan, A. J.; de Silva, A. P.; de Silva, S. A.; Rupasinghe, R. A. D. D.; Sandanayake, K. R. A. S. *Biosensors* **1989**, *4*; (**c**) Bissel, R. A.; Calle, E.; de Silva, A. P.; de Silva, S. A.; Gunaratne, H. Q. N.; Hawib-Jiwan, J.-L.; Peiris, S. L. A.; Rupasinghe, R. A. D. D.; Samarasinghe, T. K. S. D.; Sandanayake, K. R. A. S.; Soumillon, J.-P. *Journal of the Chemical Society, Perkin Transactions 2* **1992**, 1559-1564.

43 Sakamoto, H.; Takagaki, H.; Nakamura, M.; Kimura, K. *Analytical Chemistry* **2005**, *77*, 1999-2006.

44 (**a**) Melhuish, W. H. *Journal of Physical Chemistry* **1961**, *65*, 229-235; (**b**) Becker, H.-D. *Chemical Reviews* **1993**, *93*, 145-172; (**c**) Aubry, J.-M.; Peirlot, C.; Rigaudy, J.; Schmidt, R. *Accounts of Chemical Research* **2003**, *36*, 668-675.

[45] (**a**) Bouas-Laurent, H.; Castellan, A.; Desvergne, J.-P. *Pure and Applied Chemistry* **1980**, *52*, 2633-2648; (**b**) Bouas-Laurent, H.; Castellan, A.; Daney, M.; Desvergne, J.-P.; Guinand, G.; Marsau, P.; Riffaudt, M.-H. *Journal of the American Chemical Society* **1986**, *108*, 315-317.

[46] (**a**) structural aspects: Bouas-Laurent, H.; Castellan, A.; Desvergnes, J.-P.; Lapouyade, R. *Chemical Society Reviews* **2000**, *29*, 43-55; (**b**) mechanistic aspects: Bouas-Laurent, H.; Castellan, A.; Desvergnes, J.-P.; Lapouyade, R. *Chemical Society Reviews* **2001**, *30*, 248-263.

[47] (**a**) Chandross, E. A.; Ferguson, J. *Journal of Chemical Physics* **1966**, *45*, 3554-3564; (**b**) Ferguson, J.; Morita, M.; Puza, M. *Chemical Physics Letters* **1976**, *42*, 288-292; (**c**) Morita, M.; Kishi, T.; Tanaka, M.; Tanaka, J.; Ferguson, J.; Sakata, Y.; Misumi, S.; Hayashi, T.; Mataga, N. *Bulletin of the Chemical Society of Japan* **1978**, *51*, 3449-3457; (**d**) Ferguson, J.; Castellan, A.; Desvergne, J.-P.; Bouas-Laurent, H. *Chemical Physics Letters* **1981**, *78*, 446-450.

[48] (**a**) Moran, N. *"Novel Anthracene tagged DNA sensors"*; PhD Thesis, University of Exeter, **2006**; (**b**) Moran, N.; Bassani, D. M.; Desvergne, J.-P.; Keiper, S.; Lowden, P. A. S.; Tucker, J. H. R. *Chemical Communications* **2006**, 5003-5005; (**c**) Smith, E. E.; McClean, J. N.; Cooke, L. A.; Duprey, J.-L.; McCourt, M.; Fabani, M. M.; Tucker, J. H. R.; Vyle, J. S. *Tetrahedron Letters* **2007**, *48*, 6569-6572.

[49] (**a**) McSkimming, G.; Tucker, J. H. R.; Bouas-Laurent, H.; Desvergne, J.-P. *Angewandte Chemie International Edition* **2000**, *39*, 2167-2169 ; (**b**) McSkimming, G. *"Photo-active Anthracene Receptors for* s-*Block and* d-*Block Metals"*; PhD Thesis, University of Exeter, **2001**; (**c**) McSkimming, G.; Tucker, J. H. R.; Bouas-Laurent, H.; Desvergne, J.-P.; Coles, S. J.; Hursthouse, M. B.; Light, M. E. *Chemistry, a European Journal* **2002**, *8*, 3331-3342.

[50] Okada, M.; Harada, A. *Macromolecules* **2003**, *36*, 9701-9703.

[51] (**a**) Molard, Y.; Bassani, D. M.; Desvergne, J.-P.; Horton, P. N.; Hursthouse, M. B.; Tucker, J. H. R. *Angewandte Chemie International Edition* **2005**, *44*, 1072-1075; (**b**) Molard, Y.; Bassani, D. M.; Desvergne, J.-P.; Moran, N.; Tucker, J. H. R. *Journal of Organic Chemistry* **2006**, *71*, 8523-8531.

[52] (**a**) Chang, S.-K.; Hamilton, A. D. *Journal of the American Chemical Society.* **1988**, *110*, 1318-1319 ; (**b**) Chang, S.-K.; Van Engen, D. ; Fan, E.; Hamilton, A. D. *Journal of the American Chemical Society.* **1991**, *113*, 7640-7645.

[53] (**a**) von Baeyer, A. *Annalen der Chemie und Pharmacie* **1863**, *127*, 199-236; (**b**) von Baeyer, A. *Annalen der Chemie und Pharmacie* **1864**, *130*, 129-175.

[54] *Annales de Chimie et de Physique* **1818**, *8*, 201-206.

[55] Fischer, E.; von Mering, J. *Therapie der Gegenwart* **1903**, *44*, 97-101.

[56] (**a**) reaction with allyl bromide: U. S. pat., 1 042 265**, 1912**; (**b**) with benzyl chloride: Guyot, A.; Esteva, G. *Bulletin de la Société Chimique de France* **1908**, *(4) 3*, 803.

[57] (**a**) Michael, A. *Journal für Praktische Chemie* **1887**, *35*, 449-459; (**b**) Dox, A. W.; Yoder, L. *Journal of the American Chemical Society* **1922**, *44*, 1578-1581; (**c**) Dickey, J. B.; Gray, A. R. In *Organic Syntheses Coll. Vol. II* **1946**; p 60; (**d**) Cope, A. C.; McElvain, S. M. *Journal of the American Chemical Society* **1932**, *54*, 4319-4325; (**e**) Beres, J. A.; Pearson, D. E.; Bush, M. T. *Journal of Medicinal Chemistry* **1967**, *10*, 1078-1080; (**f**) Yoon, J. H.; Park, Y. J.; Lee, J. H.; Yoo, J.; Jun, C.-H. *Organic Letters* **2005**, *7*, 2889-2892.

[58] (**a**) Guyot, A.; Esteva, G. *Comptes rendus hebdomadaires de l'Académie des Sciences* **1909**, *148*, 564 ; (**b**) Dox, A. W.; Thomas, A. *Journal of the American Chemical Society* **1923**, *45*, 1811-1816; (**c**) McElvain, S. M. *Journal of the American Chemical Society* **1935**, *57*, 1303-1304; (**d**) Barnes, H. M.; McElvain, S. M. *Journal of the American Chemical Society* **1937**, *59*, 2348-2351; (**e**) Song, H. N.; Lee, H. J.; Kim, H. R.; Ryu, E. K.; Kim, J. N. *Synthetic Communications* **1999**, *29*, 3303-3311.

[59] (**a**) Kopinski, R. P.; Pinhey, J. T.; Rowe, B. A. *Australian Journal of Chemistry* **1984**, *37*, 1245-1254; (**b**) Jursic, B. S.; Neumann, D. M. *Tetrahedron Letters* **2001**, *42*, 4103-4107.

[60] (**a**) Seto, C. T.; Whitesides, G. M. *Journal of the American Chemical Society* **1990**, *112*, 6409-6411; (**b**) Zerkowski, J. A.; Seto, C. T.; Whitesides, G. M. *Journal of the American Chemical Society* **1992**, *114*, 5473-5475; (**c**) Zerkowski, J. A.; MacDonald, J. C.; Seto, C. T.; Wierda, D. A.; Whitesides, G. M. *Journal of the American Chemical Society* **1994**, *116*, 2382-2391.

[61] (**a**) Tecilla, P.; Chang, S.-K.; Hamilton, A. D. *Journal of the American Chemical Society* **1990**, *112*, 9586-9590; (**b**) Tecilla, P.; Hamilton, A. D. *Journal of the Chemical Society, Chemical Communications* **1990**, 1232-1234; (**c**) Tecilla, P.; Jubian, V.; Hamilton, A. D. *Tetrahedron* **1995**, *51*, 435-448; (**d**) Kluger, R.; Tsao, B. *Journal of the American Chemical Society* **1993**, *115*, 2089-2090; (**e**) Sørensen, H. S.; Larsen, J.; Rasmussen, B. S.; Laursen, B.; Hansen, S. G.; Skrydstrup, T.; Amatore, C.; Jutand, A. *Organomettalics* **2002**, *21*, 5243-5253; (**f**) Larsen, J.; Rasmussen, B. S.; Hazell, R. G.; Skrydstrup, T. *Chemical Communications* **2004**, 202-203.

[62] (**a**) Tecilla, P.; Dixon, R. P.; Slobodkin, G.; Alavi, D. S.; Waldeck, D. H.; Hamilton, A. D. *Journal of the American Chemical Society* **1990**, *112*, 9408-9410; (**b**) Aoki, I.; Harada, T.;

Sakaki, T.; Kawahara, Y.; Shinkai, S. *Journal of the Chemical Society, Chemical Communications* **1992**, 1341; (**c**) Motesharei, K.; Myles, D. C. *Journal of the American Chemical Society* **1994**, *116*, 7413-7414; (**d**) Chin, T.; Gao, Z.; Lelouche, I.; Shin, Y.-g.; Purandare, A.; Knapp, S.; Isied, S. S. *Journal of the American Chemical Society* **1997**, *119*, 12849-12858; (**e**) Salameh, A. S.; Ghaddar, T.; Isied, S. S. *Journal of Physical Organic Chemistry* **1999**, *12*, 257-254.

63 (**a**) Ghaddar, T. H.; Castner, E. W.; Isied, S. S. *Journal of the American Chemical Society* **2000**, *122*, 1233-1234; (**b**) Dirksen, A.; Kleverlaan, C. J.; Reek, J. N. H.; De Cola, L. *Journal of Physical Chemistry A* **2005**, *109*, 5248-5256; (**c**) McClenaghan, N. D.; Grote, Z.; Darriet, K.; Zimine, M.; Williams, R. M.; De Cola, L.; Bassani, D. M. *Organic Letters* **2005**, *7*, 807-810; (**d**) Zhuang, J.; Zhou, W.; Li, X.; Li, Y.; Wang, N.; He, X.; Liu, H.; Li, Y.; Jiang, L.; Huang, C.; Cui, S.; Wang, S.; Zhu, D. *Tetrahedron* **2005**, *61*, 8686-8693; (**e**) Wessendorf, F.; Gnichwitz, J.-F.; Sarova, G. H.; Hager, K.; Hartnagel, U.; Guldi, D. M.; Hirsch, A. *Journal of the American Chemical Society* **2007**, *129*, 16057-16071.

64 Lakkakula, S.; Mitkin, O. D.; Valiulin, R. A.; Kutateladze, A. G. *Organic Letters* **2007**, *9*, 1077-1079.

65 (**a**) Würthner, F.; Schmidt, J.; Stolte, M.; Wortmann, R. *Angewandte Chemie International Edition* **2006**, *45*, 3842-3846; (**b**) Schmidt, J.; Schmidt, R.; Würthner, F. *Journal of Organic Chemistry* **2008**, *73*, 6355-6362.

66 (**a**) Nabeshima, T.; Takahashi, T.; Hanami, T.; Kikuchi, A.; Kawaba, T.; Yano, Y. *Journal of Organic Chemistry* **1998**, *63*, 3802-3803; (**b**) Al-Sayah, M. H.; McDonald, R.; Branda, N. R. *European Journal of Organic Chemistry* **2004**, 173-182.

67 Berl, V.; Huc, I.; Lehn, J.-M.; DeCian, A.; Fischer, J. *European Journal of Organic Chemistry* **1999**, 3089-3094.

68 Berl, V.; Krische, M. J.; Huc, I.; Lehn, J.-M.; Schmutz, M. *Chemistry, a European Journal* **2000**, *6*, 1938-1946;

69 (**a**) Berl, V.; Schmutz, M.; Krische, M. J.; Khoury, R. G.; Lehn, J.-M. *Chemistry, a European Journal* **2002**, *8*, 1227-1244; (**b**) Kolomiets, E.; Lehn, J.-M. *Chemical Communications* **2005**, 1519-1521; (**c**) Kolomiets, E.; Buhler, E.; Candau, S. J.; Lehn, J.-M. *Macromolecules* **2006**, *39*, 1173-1181.

70 Inoue, K.; Ono, Y.; Kanekiyo, Y.; Ishi-i, T.; Yoshihara, K.; Shinkai, S. *Journal of Organic Chemistry* **1999**, *64*, 2933.

[71] (**a**) Li, S.; Sun, L.; Chung, Y.; Weber, S. G. *Analytical Chemistry* **1999**, *71*, 2146-2151; (**b**) Zhang, S.-Q.; Fukase, K.; Izumi, M.; Fukase, Y.; Kusumoto, S. *Synlett* **2001**, 590-596.

[72] (**a**) Westwood, J., *Metallocene Receptors for Neutral Molecules*, PhD Thesis, University of Exeter, Exeter, UK, **2001**; (**b**) Collinson, S. R.; Gelbrich, T.; Hursthouse, M. B.; Tucker, J. H. R. *Chemical Communications* **2001**, 555-556; (**c**) Tucker, J. H. R.; Collinson, S. R. *Chemical Society Reviews* **2002**, *31*, 147-156; (**d**) Westwood, J.; Coles, S. J.; Collinson, S. R.; Gasser, G.; Green, S. J.; Hursthouse, M. B.; Light, M. E.; Tucker, J. H. R. *Organomet.* **2004**, *23*, 946-951.

[73] (**a**) Rasmussen, B. S.; Unai, E.; Skrydstrup, T. *Journal of the Chemical Society, Perkin Transactions 1* **2002**, 1723-1733; (**b**) Ema, T.; Tanida, D.; Sakai, T. *Organic Letters* **2006**, *8*, 3773-3775; (**c**) Ema, T.; Tanida, D.; Sakai, T. *Journal of the American Chemical Society* **2007**, *129*, 10591-10596; (**d**) Ema, T.; Tanida, D.; Hamada, K.; Sakai, T. *Journal of Organic Chemistry* **2008**, *73*, 9129-9132; (**e**) Ema, T.; Tanida, D.; Sugita, K.; Sakai, T.; Miyazawa, K.-i.; Ohnishi, A. *Organic Letters* **2008**, *10*, 2365-2368.

[74] (**a**) Binder, W. H.; Kunz, M. J.; Kluger, C.; Hayn, G.; Saf, R. *Macromolecules* **2004**, *37*, 1749-1759; (**b**) Binder, W. H.; Kluger, C. *Macromolecules* **2004**, *37*, 9321-9330; (**c**) Binder, W. H.; Kluger, C.; Straif, C. J.; Friedbacher, G. *Macromolecules* **2005**, *38*, 9405-9410; (**d**) Binder, W. H.; Sachsenhofer, R.; Straif, C. J.; Zirbs, R. *Journal of Materials Chemistry* **2007**, *17*, 2125-2132; (**e**) Burd, C.; Weck, M. *Macromolecules* **2006**, *38*, 7225-7230.

[75] (**a**) Dirksen, A.; Hahn, U.; Schwanke, F.; Nieger, M.; Reek, J. N. H.; Vögtle, F.; De Cola, L. *Chemistry, a European Journal* **2004**, *10*, 2036-2047; (**b**) Franz, A.; Bauer, W.; Hirsch, A. *Angewandte Chemie International Edition* **2005**, *44*, 1564-1567; (**c**) Hager, K.; Franz, A.; Hirsch, A. *Chemistry, a European Journal* **2006**, *12*, 2663-2679; (**d**) Maurer, K.; Hager, K.; Hirsch, A. *European Journal of Organic Chemistry* **2006**, 3338-3347; (**e**) Hager, K.; Hartnagel, U.; Hirsch, A. *European Journal of Organic Chemistry* **2007**, 1942-1956; (**f**) Gnichwitz, J.-F.; Wielopolski, M.; Hartnagel, K.; Hartnagel, U.; Guldi, D. M.; Hirsch, A. *Journal of the American Chemical Society* **2008**, *130*, 8491-8501; (**g**) Grimm, F.; Hartnagel, K.; Wessendorf, F.; Hirsch, A. *Chemical Communications* **2009**, 1331-1333.

[76] (**a**) Carver, F. J.; Hunter, C. A.; Shannon, R. J. *Journal of the Chemical Society, Chemical Communications* **1994**, 1277-1280; (**b**) Vogtle, F.; Jager, R.; Hiindel, M.; Wens-Hildebrandt, S. *Pure and Applied Chemistry* **1996**, *68*, 225-232;

[77] Anslyn, E. V.; Dougherty, D. A. *Modern Physical Organic Chemistry*; University Science Books, **2006**. The idea of making a rotaxane based on Hamilton's complex is given in exercise 15 of chapter 4, p. 254.

[78] Lincheneau, C. *Photogénération de Molécules Entrelacées : Photocaténation*, Master report, Université Bordeaux 1, **2006**.

[79] (**a**) Rocher, M. *Using H-bonds to control the reactivity in olefin metathesis*, PhD 1st year report, University of Birmingham, **2006**; (**b**) Bhayat, K. *Olefin Metathesis: Controlling Selectivity by Use of Hydrogen Bonds*, Master Report, University of Birmingham, **2008**.

[80] Chem3D Pro is a part of the ChemOffice suite, © **2001** CambridgeSoft, 100 Cambridge Park Dr., Cambridge, MA 02140-2317 USA. For the MM2 force field, cf. Norman L. Allinger, *J. Am. Chem. Soc.* **1977**, *99*, *25*, 8127-8134.

2) NEW RECEPTORS

2.1) Synthesis

2.1.1) Design and strategy

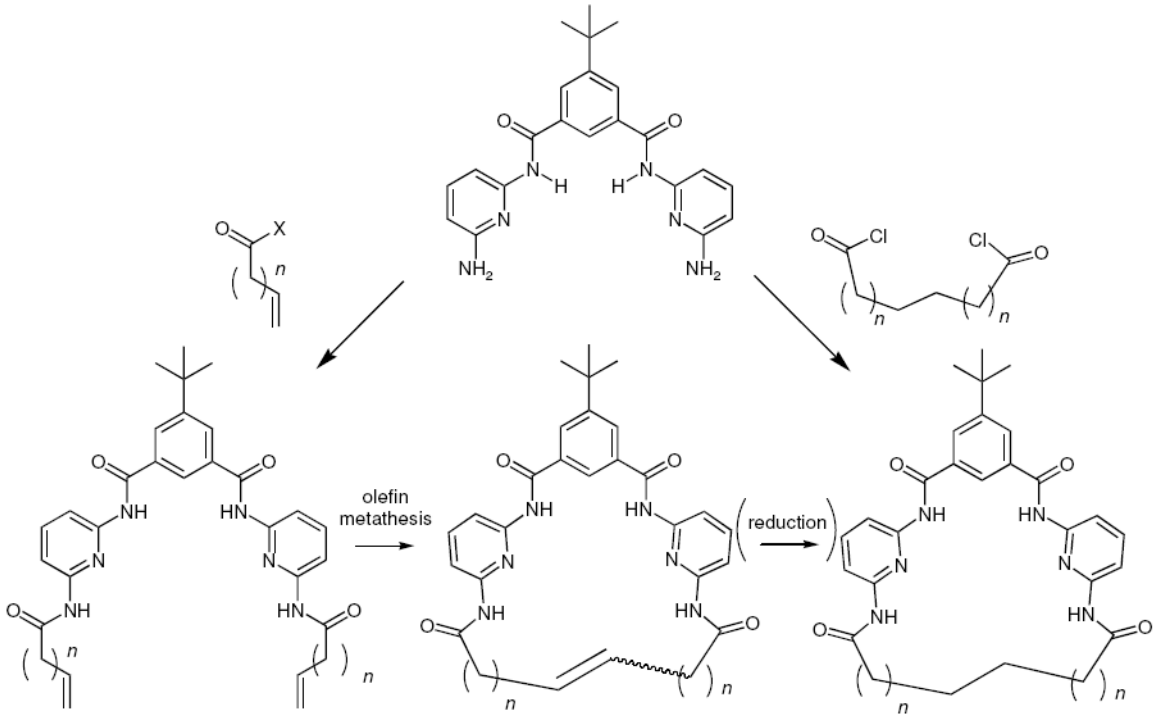

Figure 2.1. Design of the new receptors and strategy.

Three different kind of receptors for barbiturates containing the Hamilton[1] motif were synthesised:

- The first kind consists of open, uncyclised receptors substituted with alkyl chains terminated by free olefins. They can be obtained by substituting the central bridge with two equivalents of an acyl chloride bearing this olefin.
- The second kind consists of cyclised receptors obtained by ring-closing metathesis of the receptors of the first kind. They can exist in two forms, *cis* or *trans* which may be formed in different quantities depending on the conditions of the metathesis and may be difficult to separate.

- The last kind consists of cyclised receptors bearing no double bond. They are formally a reduced version of the receptors of the second kind, but can be easily obtained by macrocyclisation using the central bridge and a diacyl chloride with a long alkyl chain.

2.1.2) Precursors

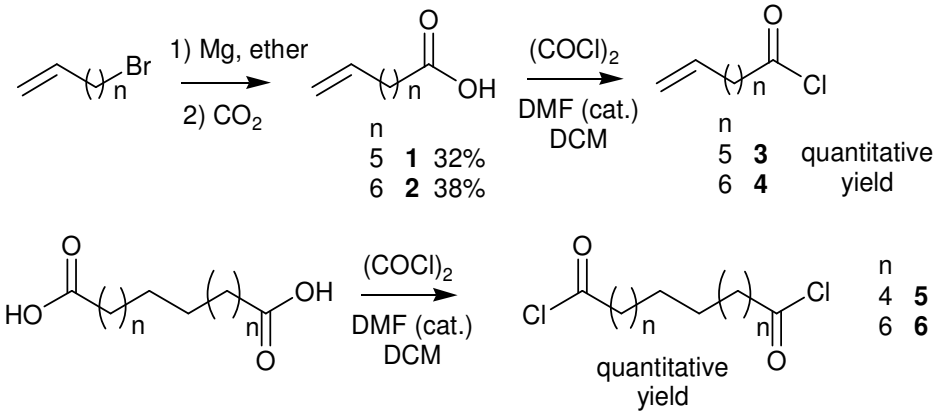

Scheme 2.1. Precursors of the "lower part" of the receptors.

For the synthesis of the "lower part" of the receptors (**Scheme 2.1**), the anhydride or the acyl chloride of the substituents were necessary. The pent-4-enoic anhydride ($n = 2$) and the 10-undecenoyl chloride ($n = 8$) are commercially available, but not the other acyl chlorides. Hept-6-enoic acid is commercially available, but not oct-7-enoic and non-8-enoic acids **1** and **2**, which had to be synthesised from the corresponding bromides by forming a Grignard reagent and reacting it with solid CO_2. They were obtained in moderate yields (32% and 38%). The acyl chlorides were obtained by adding an excess of oxalyl chloride and a few drops of DMF as a catalyst to a solution of the acid in DCM. The solvents and reagents in excess were then removed by evaporation to afford the products which were used without further purification for the next step. The diacyl chlorides used for the synthesis of the "reduced" receptors were obtained the same way.

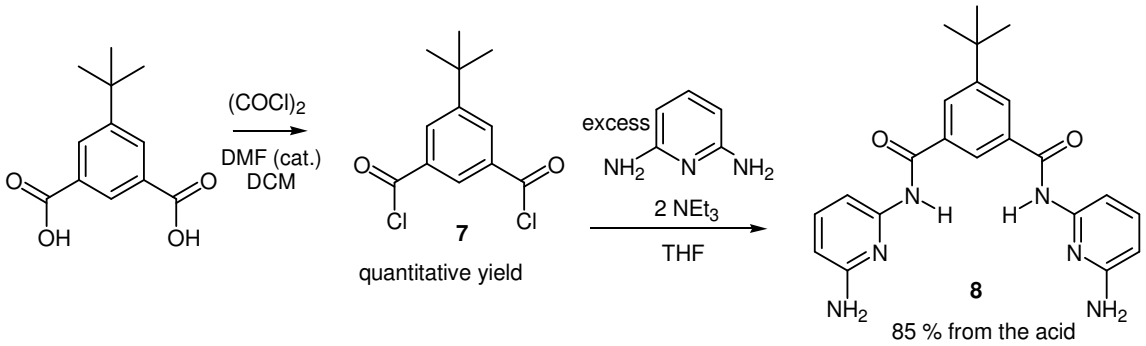

Scheme 2.2. Synthesis of the "bridge".

The "upper part" of the receptors was easily synthesised from the reaction of 2,6-diaminopyridine **7**, which in turn was made in quantitative yield from *tert*-butyl isophtalic acid. The "bridge" **8** was obtained in 85% yield after separation by flash chromatography on silica gel.

2.1.3) Uncyclised olefin terminated receptors

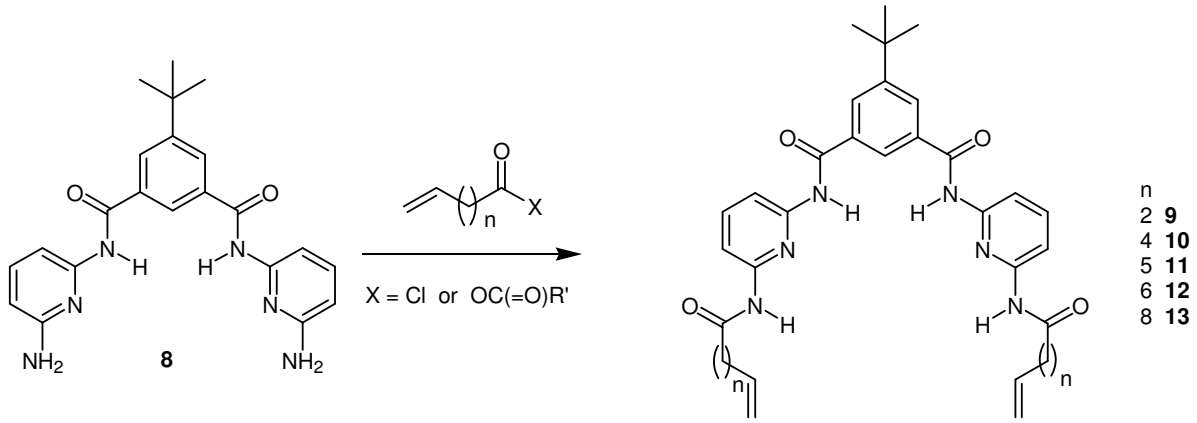

Scheme 2.3. Synthesis of uncyclised olefin terminated receptors.

The "bridge" **8** was reacted with the acyl chlorides described above, using triethylamine as a base. The yields of these reactions (see **Table 2.1** below) vary from low (7% for **11**) to high (93% for **12**). This variation is probably due to the varying purity of the acyl chloride used, as it is purified only by evaporation of the byproducts.

Table 2.1. Yields of uncyclised receptors.

Receptor	*n*	*Yield*	*Using…*
9	2	23%	4-pentenoic anhydride
10	4	56%	6-heptenoyl chloride (obtained from 6-heptenoic acid)
11	5	7%	7-octenoyl chloride (**3**) synthesised in 2 steps from 7-bromohept-1-ene
12	6	93%	8-nonenoyl chloride (**4**) synthesised in 2 steps from 8-bromooct-1-ene
13	8	66%	10-undecenoyl chloride

2.1.4) Ring-closing metathesis

The closing of these open receptors by metathesis had to be performed with a catalyst tolerant to the functional groups present in the receptors and barbiturates. The Grubbs' 1st generation catalyst has been proven to be tolerant to reactants containing amide subunits,[2] but the particular case of barbiturates (which are more acidic than other amides) was uncertain: in order to verify if Grubbs' 1st generation catalyst was active in the presence of a barbiturate, the ring-closure metathesis of diallyl-diethyl-malonate in the presence of 1 equivalent of barbital was attempted (see **Scheme 2.4**). The NMR of the crude at the end of the reaction revealed that the reaction was complete, confirming that Grubbs' 1st generation catalyst was tolerant to barbiturates.

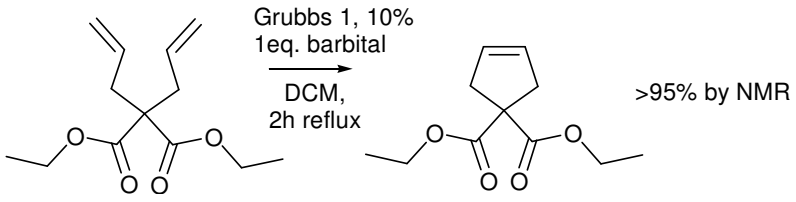

Scheme 2.4. Ring-closure metathesis of diallyl-diethyl-malonate in the presence of barbital.

There are also very few examples of the use of this catalyst with compounds containing a pyridine subunit where the lone pair on the nitrogen is free to compete with the phosphine ligands binding to the ruthenium centre of the catalyst. Some examples were found

where the lone pair of a pyridine nitrogen was involved in coordination to a copper[3] or platinum[4] cation, but only few references were found where olefin metathesis was used for ring-closure metathesis with non-complexed pyridine subunit.[5,3b] However in these two articles the nitrogen bearing a non-complexed lone pair could be considered as sterically protected. Consequently, it was uncertain whether cyclisation was possible with Grubbs' 1st generation catalyst in the absence of the barbiturate guest.

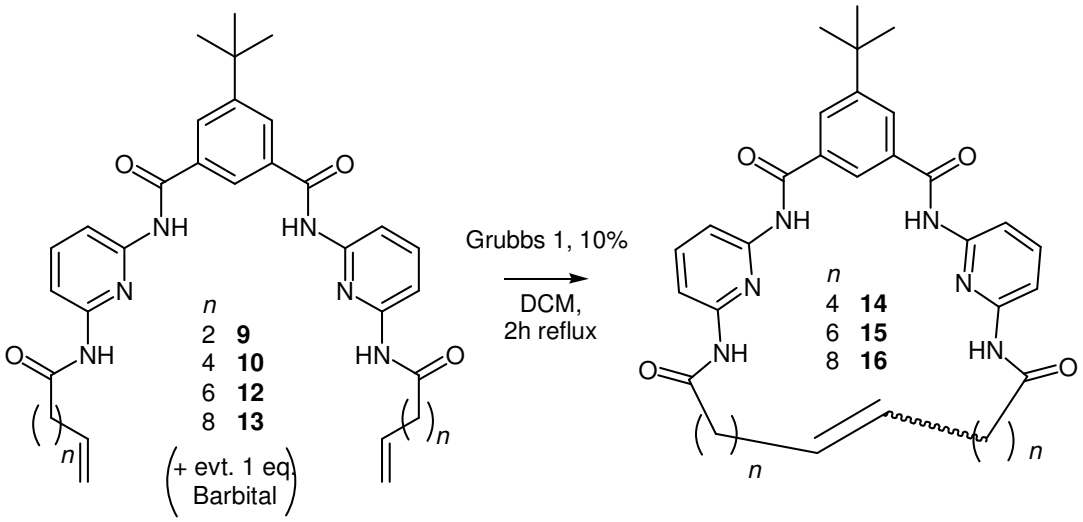

Scheme 2.5. Synthesis of the "closed" receptors by metathesis.

In order to verify whether the ring-closing metathesis reaction was going to work, a trial cyclisation was carried out, in the absence and in the presence of 1 equivalent of barbital. A small volume of solution of uncyclised receptors **9**, **10**, **12** or **13** or their 1:1 mixture with barbital, at a concentration of *3 mM*, with *10 mol%* of Grubbs' 1st generation catalyst, was heated to reflux during 2 hours, then the solvent was evaporated and the reacting mixtures were then directly analysed by NMR and mass spectrometry. **Figure 2.4** shows a region of the ^{1}H NMR spectrum for this experiment with **13** in the absence of barbital: the signals at *5.80* (**a**) and *4.96 ppm* (**b** & **c**) corresponding to the terminal olefin of the starting material have almost disappeared whereas a new ethylenic signal appears at *5.25 ppm*. These changes are consistent with the formation of cyclised product **16** as the main product. However, it is

possible that small amounts of solid that did not dissolve in $CDCl_3$ were polymeric or oligomeric material obtained by intermolecular metathesis.

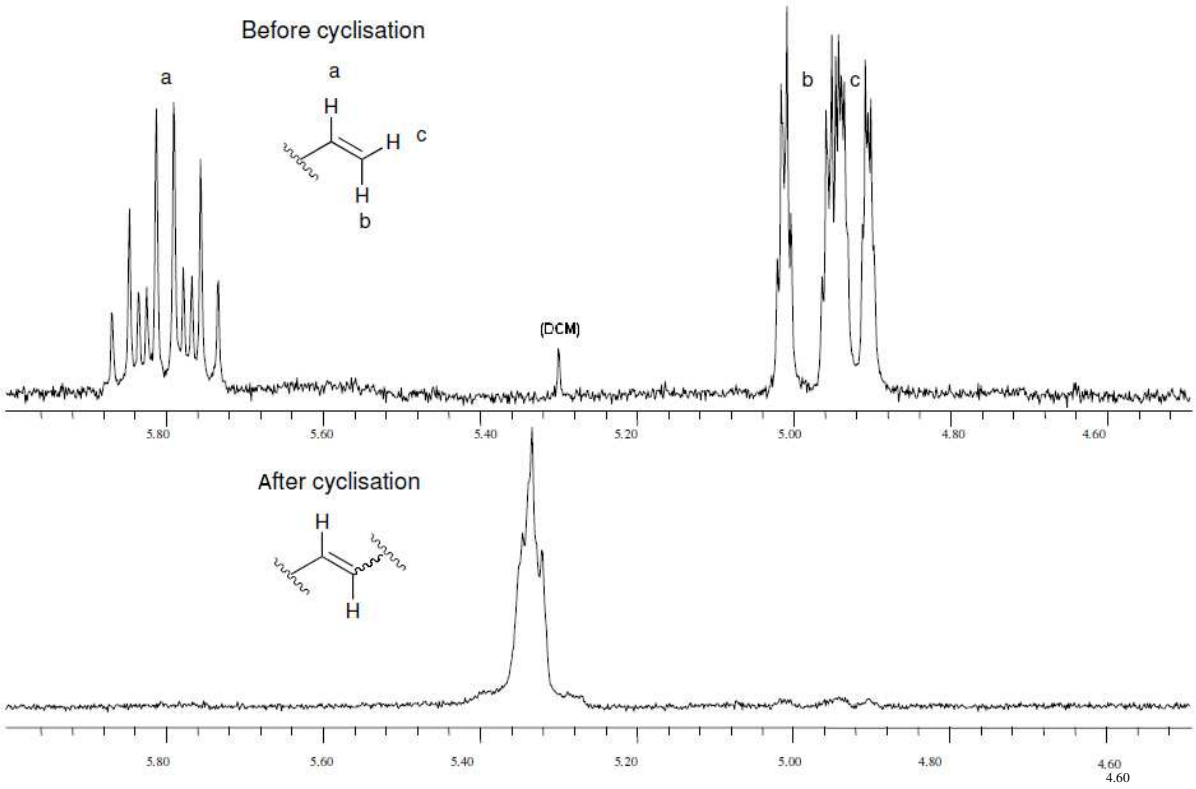

Figure 2.4. ^{1}H NMR of the receptor with n = 8 in $CDCl_3$ before and after metathesis, in the absence of barbital.

By comparing the integration of this new signal with remaining signals of the uncyclised receptor in each experiment, it was possible to measure how much cyclised product was obtained if we assume that no polymerisation or oligomerisation occurred. Finally, for the actual synthesis of **14**, **15** and **16** the cyclisation was made on a larger scale and the products were separated by flash chromatography and obtained as mixtures of *cis* and *trans* isomers (as shown by ^{13}C NMR, *vide infra*). The results of these experiments are given in **Table 2.2**.

Table 2.2. Yield and product distribution of the cyclised receptors obtained by metathesis.

n	*Starting uncyclised receptor*	*Product*	*Measured yield (NMR)*	*Isolated yield after chromatography*	cis / trans *in isolated product*
2	**9**	(no product)	≈0%	(not isolated)	(not applicable)
4	**10** **10 + barbital**	**14** **14 + barbital**	>95% 10%	44%	68 / 32
6	**12** **12 + barbital**	**15** **15 + barbital**	>85% >85%	39%	79 / 21
8	**13** **13 + barbital**	**16** **16 + barbital**	>95% >95%	73%	66 / 34

When starting from **9**, no cyclised product was obtained and only starting material was observed by ^{1}H NMR. As no insoluble solids were observed, this could be a good evidence that there are no effective competing intermolecular processes. The ring can probably not form with $n = 2$ because the distance between the two double bonds, imposed by the large aromatic groups, remains too large for cyclisation, although molecular models obtained using the MM2 force field in the software Chem3D Pro[6] suggest that the formation of this small ring is still possible. Another explanation for the difficulty of this reaction is that the short distance between the C=O and the double bond may result in deactivation of the intermediate formed through the formation of a Ru-O coordinative bond (see **Scheme 2.6**).

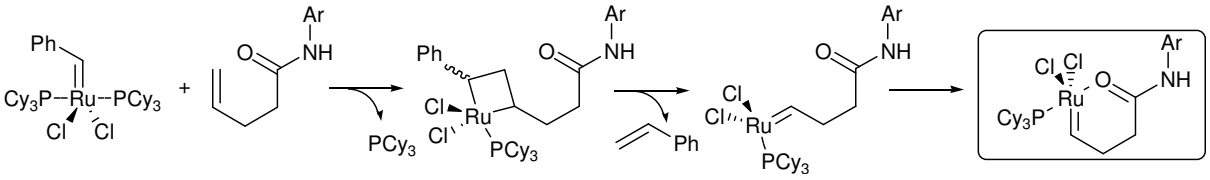

Scheme 2.6. Possible deactivation of the Grubbs catalyst when reacting with **9**.

As the cyclisation did not work with **9** alone, it was not tried in the presence of barbital. For the larger compounds **10**, **12** and **13**, the corresponding cyclised receptors were formed, in high yield according to the ^{1}H NMR spectra of the crude mixtures, but the isolated yields after chromatography were lower. It was interesting to note that when 1 equivalent of barbital was added to **10**, the cyclisation by metathesis was hampered; only 10% of cyclised product was observed by metathesis, the origin of which probably comes from the unbound receptor which

is in equilibrium with the complex in solution. This result can be explained by steric reasons; presumably the bound guest prevents the two terminal double bonds from coming into close proximity.

The determination of the *cis/trans* ratios (**Table 2.2**) was estimated by ^{13}C NMR since the ^{1}H NMR spectra of these receptors did not show any evidence for a mixture of two isomers, also this was not the case for the ^{1}H spectra of some of the complexes with barbiturates other than barbital where some evidence of this was observed (see *Chapters 4* and *5*). In constrast, the ^{13}C NMR spectra of these receptors clearly gave two distinct peaks of different intensity for many of the carbons. For each different carbon it was difficult to unambiguously determine which one belonged to the *cis* or the *trans* product, but the ratio between the smaller and the bigger peaks remained approximately constant for each carbon. However, according to a simulation using ChemNMR,[7] the CH_2 carbon closest to the double bond should appear at a different chemical shift depending on the configuration of the double bond: *27.3 ppm* if the double bond is *cis* and *33.3* if it is *trans*. Indeed this is what was observed by NMR (cf. *Chapter 6* for the detail of the spectra). Assuming that the ratio between the NMR signals of two carbons at the same position on each isomer of the molecule was proportional to the ratio of their concentrations, this average ratio was calculated as well as the standard deviation, which gave an uncertainty value close to 10%. We can conclude from this that the main product of these ring-closing metatheses is the *cis* isomer in each case. They were not separated and in the rest of this thesis they will be considered as one product, except when obviously an effect of the presence of two different isomers can be observed.

In order to assess the order of magnitude of the fluorescence of these receptors, the fluorescence quantum yield of receptor **16** was measured by comparing the integral over all wavelengths of its emission spectrum for an excitation wavelength of *324 nm* with the emission spectrum of an anthracene solution in the same conditions. The description of this

method is given in *Chapter 6*, as well as a figure showing the large difference between the low intensity of the emission of receptor **16** compared to anthracene. An experimental fluorescence quantum yield of $\Phi_F = 0.008$ was obtained. The study showed that these receptors are only very weakly fluorescent, as is the case with most pyridine-containing compounds in non protic solvents where the relaxation process that dominates by far is intersystem crossing.[8]

2.1.5) "Reduced" receptors

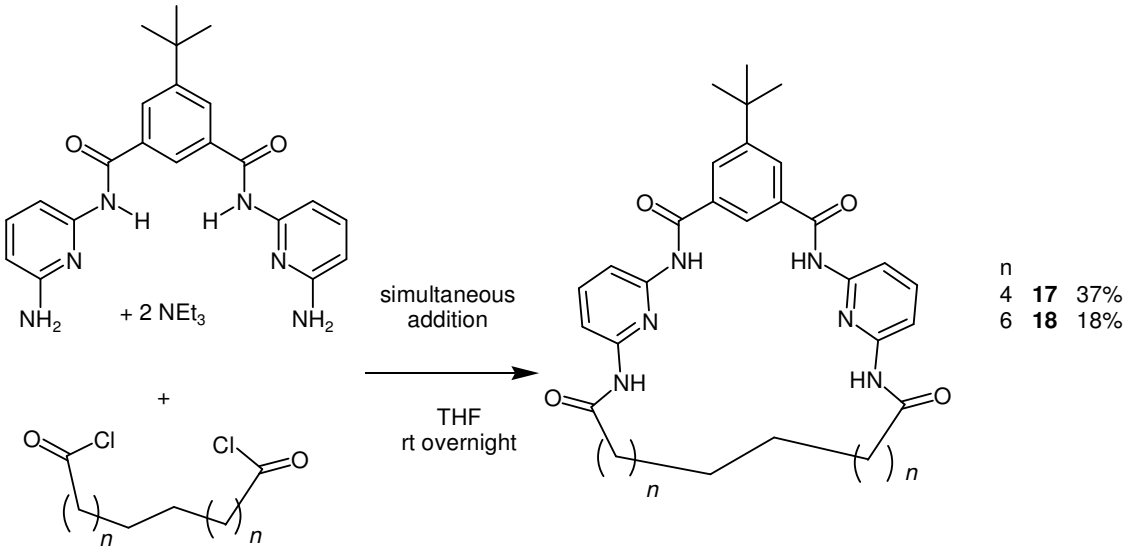

Scheme 2.7. Synthesis of "reduced" receptors.

Finally, the so-called "reduced" receptors were synthesised by macrocyclisation, through the simultaneous addition to the solvent of a solution of **8** containing two equivalents of triethylamine, and a solution of the diacyl chloride **5** or **6**. The yields were only moderate (37% and 18% respectively for **17** and **18**), as is often observed in macrocyclisation, where intermolecular reactions compete with the formation of the macrocycle.

In attempts to crystallise the complexes of these receptors with the barbiturate **39** (see *Chapter 5*), our colleagues N. McClenaghan, B. Kaufmann and J.-P. Desvergne from the University Bordeaux 1 (France) obtained good crystals of the receptors which allowed them

to determine the structures of these receptors in the solid state by X-ray diffraction. These structures are represented in **Figure 2.5**, and more details are given in *Appendix 1*.

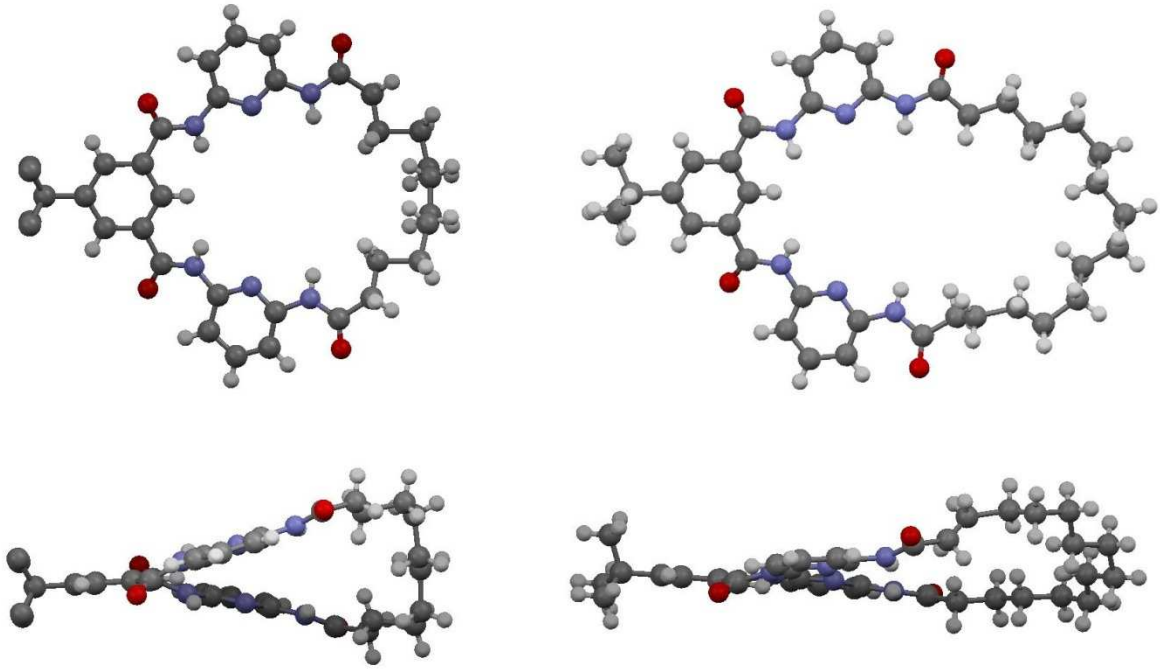

Figure 2.5. Structures of **17** (left) and **18** (right) in the solid state, as determined by XRD.

The structure of **18** is similar to Hamilton's receptors;[1] the "bridge" part is nearly planar with the two diamidopyridine subunits facing each each other, making the binding motif nearly planar. However, **17** is not as planar and the two diamidopyridine units are separated by an angle of *35*°, which makes it less complementary to the structure of barbituric acids.

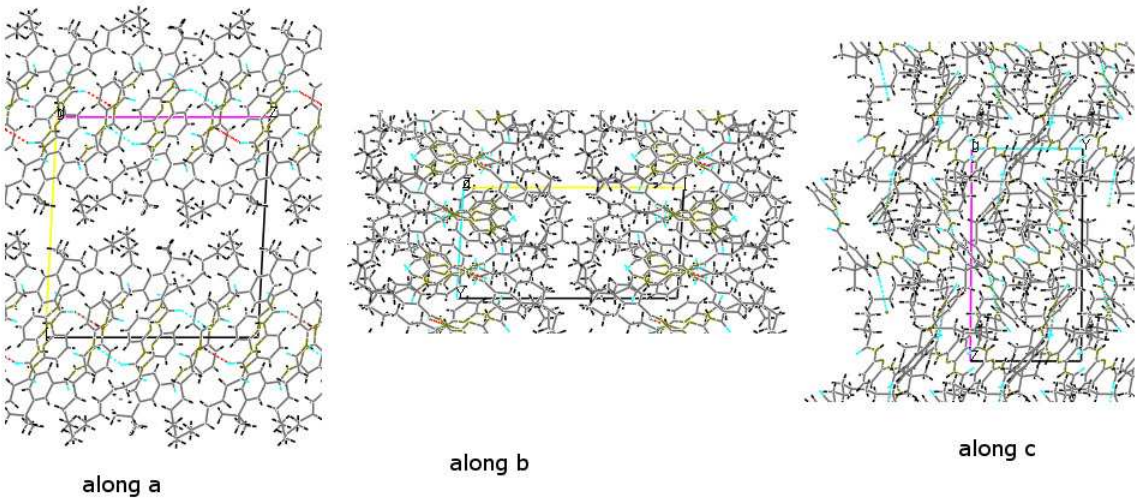

Figure 2.6. Crystal structure of **18** in the solid state along the 3 axes.

The crystal structure of **18** (**Figure 2.6**) also shows that in the solid state, the receptors are H-bonded to each other and form large sheets (perpendicular to the c axis of the cell) with the alkyl chains and *tert*-butyl groups on the outside. Along with other observations made by NMR (the NH signals in the ^{1}H NMR spectrum were found to change their chemical shift slightly depending on the concentration) and ITC (see below), this indicates that these receptors can probably aggregate to some extent in solution at high concentrations, a property that they share with other Hamilton-like receptors.[9]

2.2) Binding studies with barbital

2.2.1) Titrations followed by UV-vis spectrometry

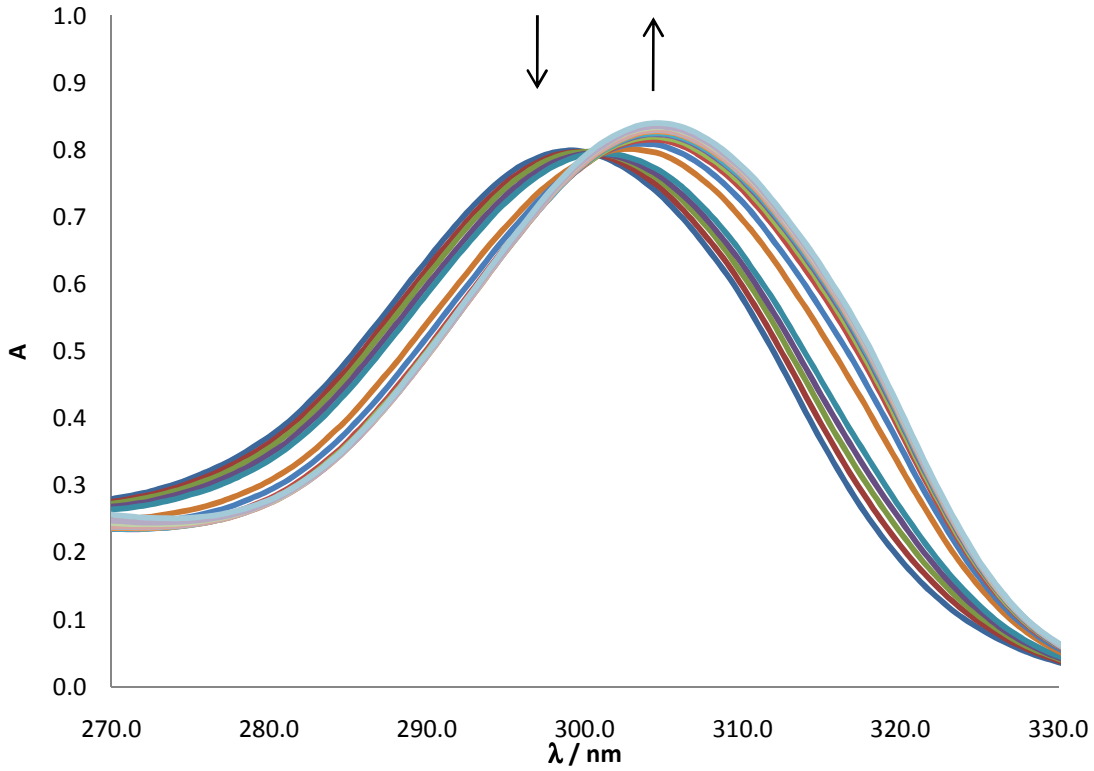

Figure 2.7. Variation of the corrected absorption spectra during the titration of **18** (*2.5.10^{-5} M* solution in DCM) with barbital (*0* to *3 equiv.*), at room temperature.

The binding constant of each receptor with barbital was measured by UV absorption, by monitoring the change in the pyridine band of each receptor (around *300 nm*) in the

presence of increasing amounts of barbital (see *Chapter 6* for further information). Whereas for all the receptors the maximum of absorption of the pyridine was close to $\lambda_{max} = 298\ nm$, for the complexes with barbital it was close to $\lambda_{max} = 303\ nm$ and ε_{max} was (depending on the receptor) either slightly bigger or smaller at this new maximum. Therefore the shape of the band changes as more complex is formed in solution (see **Figure 2.7**).

Table 2.3. *log(K)* for the formation of 1:1 complexes with barbital, obtained by UV titration in DCM at rt.

Receptor	*n*	*log(K)*	*Margin of error*
10	4	4.70	0.02
12	6	4.58	0.02
13	8	4.66	0.04
14	4	3.69	0.05
15	6	5.09	0.03
16	8	5.52	0.01
17	4	3.99	0.05
18	6	5.79	0.03

The data were treated with the software Letagrop[10] assuming that only 1:1 complexes could form, and the results are presented in **Table 2.3**. The errors are those given by the Letagrop software used to make the calculations from the UV data.

We can see that the binding constants are approximately the same for all the uncyclised receptors **10**, **12** and **13** ($log(K) \approx 4.65 \pm 0.09$). For the closed receptors however, the binding constants are very different: they are lower than in the open form for the two smaller receptors **14** and **17** (even if this last value is not certain, see below), and higher for the larger receptors **15**, **16** and **18**. Having a higher binding constant in the closed form was

also found with Hamilton's receptors[1] and can be understood in terms of the *macrocyclic effect*.[11a]

For the smaller receptors **14** and **17**, the X-ray structure of **17** suggests an explanation. The short alkyl linker forces the binding motif to adopt a conformation which is not favourable to the formation of 6 complementary hydrogen bonds with barbital, and possibly even prevents it from adopting a conformation similar to that of the open receptors. In the case of receptor **17**, it was difficult to obtain a good fit with this software for a 1:1 complex with the values of absorbance obtained. The result in **Table 2.3** was obtained after removing the last spectrum obtained with 115 equivalents of barbital which was clearly not passing through the isosbestic point (see *Chapter 6*). Considering the X-ray structure, it was considered that the two amidopyridine units which are not facing each other could be considered as two separate binding sites. In which case, barbital may bind through only three H-bonds, occupying only one binding site, and leaving the other to eventally bind another barbital molecule and form a complex with two barbital molecules. A better fit was obtained when assuming that both a 1:1 and a 2:1 complex could form, but the error in each result was larger. The obtained results were:

17 + **barbital** $\rightleftarrows$ **17•barbital** $\quad log(K_1) = 4.2 \pm 0.2$

17 + 2.**barbital** $\rightleftarrows$ **17•(barbital)**$_2$ $\quad log(K_2) = 7.2 \pm 0.3$

The binding constant for the binding of a second barbital to the first complex formed is:

17•barbital + **barbital** $\rightleftarrows$ **17•(barbital)**$_2$ $\quad log(K_2/K_1) = 3.0 \pm 0.5$

If the two binding sites were similar and independent, there would be a difference between K_1 and K_2/K_1 which would be explained only by statistical considerations. It can be easily demonstrated[12] that for a statistical effect $K_2/K_1 = K_1/4$. If we write *(F)* for concentration (in

mol.L^{-1}) of free sites and *(O)* the activity of occupied sites, and if we note the receptor **17** as R, barbital as B, and the 1:1 and 2:1 complexes as $R \bullet B$ and $R \bullet B_2$ respectively, we would have:

$$(F) = 2.(B) + (R \bullet B)$$

$$(O) = (R \bullet B) + 2.(R \bullet B_2)$$

If the barbital could bind on both binding sites in a similar way, then it could be possible to define a binding constant *K* for this binding site, and we would have at equilibrium:

$$K = \frac{(O)}{(R).(F)}$$

By replacing *(F)* and *(O)* by their expressions as a function of the concentration of actual species, and then replacing $(R \bullet B)$ and $(R \bullet B_2)$ by their expressions as a function of K_1, K_2, *(R)* and *(B)*, this expression is obtained:

$$K = \frac{K_1 + 2.K_2.(R)}{2 + K_1.(R)}$$

As according to our starting hypothesis *K* is a constant, it should not depend on *(R)* which can be replaced by *zero* or any value. This leads to the conclusion:

$$K_1 = 2.K$$

$$\frac{K_2}{K_1} = \frac{K}{2} = \frac{K_1}{4}$$

In our case, $log(K_1/4) = 3.6$ and $log(K_2/K_1) = 3.0$ so we observe that $K_2/K_1 < K_1/4$. Therefore, as could be reasonably expected for steric reasons, it is more difficult to bind the second molecule of barbital than the first.

2.2.2) Titrations followed by ITC

The binding of some of the receptors with barbital was also studied by ITC. The procedure followed is described in the experimental part (*Chapter 6*). The results of a first titration of receptor **18** with barbital using this method at *0.1 mM* are shown in **Figure 2.8**. The negative slope is unexpected in a simple binding curve. However if these initial data

points are removed and if the initial concentration is corrected in order to obtain a calculated value of $n = 1$ at the equivalence, it is possible to obtain a good fit with the data and to obtain a calculated value for the binding constant and associated thermodynamic parameters:

$log(K) = 5.46 \pm 0.03$, $\Delta H° = -14.59 \pm 0.13$ kcal.mol^{-1}, $\Delta S° = -24.0 \pm 0.5$ cal.mol^{-1}.K^{-1}.

A repetition of the experiment using the same concentrations gave very similar results (with the same negative slope at the beginning, and similar calculated concentration / binding constant / thermodynamic parameters within a 5% margin of error).

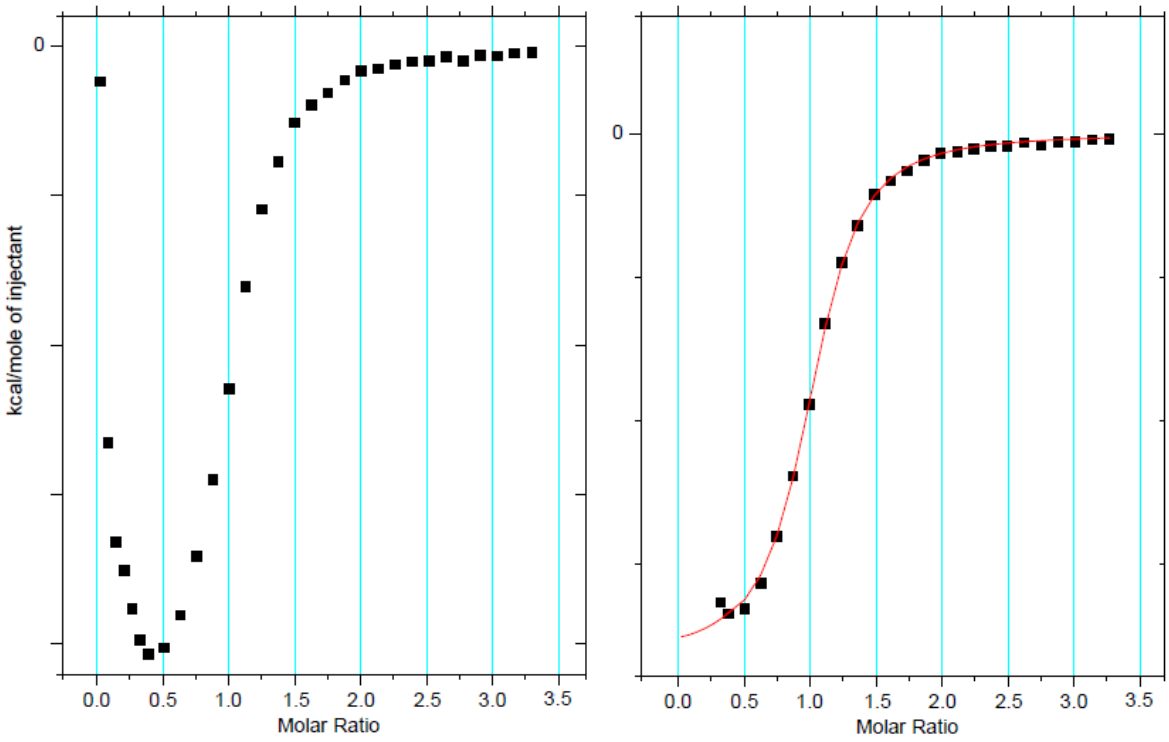

Figure 2.8. Titration of **18** by barbital at 0.1 mM: crude (left) and fitted after removing the first points (right).

By UV titration, the binding constant was evaluated as $log(K) = 5.79$. This is a different value but the order of magnitude remains the same. The negative slope observed at the beginning can be explained by an aggregation process.[9] If we consider that a dimer of the receptor is forming at high concentrations in DCM, then this negative slope would correspond to the displacement of the dissociation equilibrium in the direction of the monomer induced by the dilution and the binding of barbital to the monomer (see **Scheme 2.8**, note that the

structure of the dimer drawn here is purely hypothetical). The small heat release observed at the beginning increases to something more exothermic as more barbital is added, which is the effect of the addition of the positive ΔH of the dissociation, which is endothermic, and the negative ΔH of the complexation of barbital, which is exothermic. The fact that the initial concentration had to be corrected in order to obtain a value of $n = 1$ can also be related to this aggregation, as the aggregates of the receptors are probably poorly soluble.

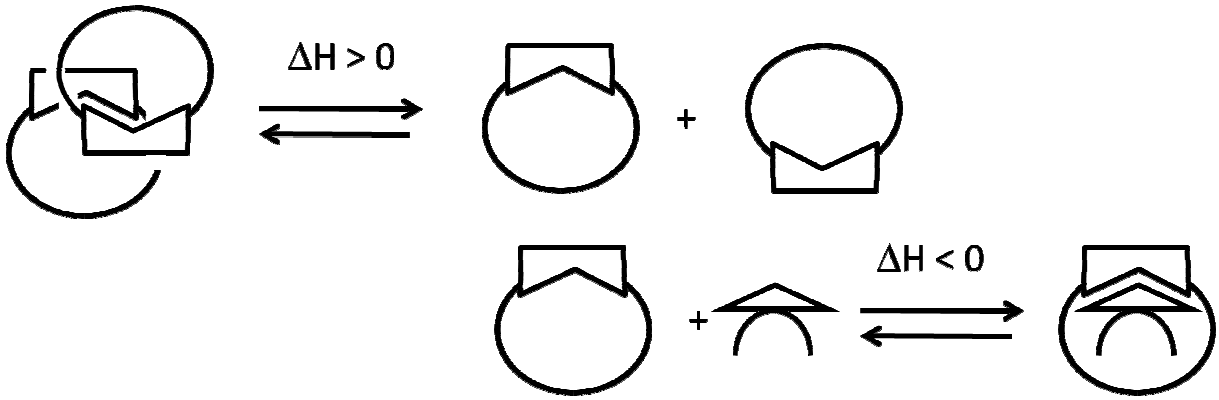

Scheme 2.8. Dissociation of the receptor aggregates (represented here as a dimer) can induce a thermal effect, as seen by ITC.

A dilution experiment with barbital was also made, by adding the same barbital solution to neat DCM. This is the usual technique in ITC titrations, where these values have to be subtracted from the heat changes values recorded in the titration between receptor and substrate. In this case, no heat of dilution could be registered, only apparently random noise (see *Appendix 3*), so the fit was done directly on the integrated titration data.

In order to verify that this negative slope was due to autoassociation of the receptor at high concentration, another titration was made with solutions that were five times more dilute (*0.02 mM*, see **Figure 2.9**). As the concentration was five times smaller, the heat changes recorded were also smaller, and the signal/noise ratio was less good which explains why the fit is not as good as previously observed. Nevertheless, it was observed that this time the general shape of the data remains close to what is expected for a binding interaction with

log(K) $\simeq$ *5.0*. The negative slope is no longer visible, as expected if this was really due to aggregation as explained above.

Finally the titrations were all made at an intermediate concentration (*0.05 mM*, see **Figure 2.9**) where the signal/noise ratio is reasonable and the negative slope in the first few data points is not seen. The results of these titrations are given in **Table 2.4**.

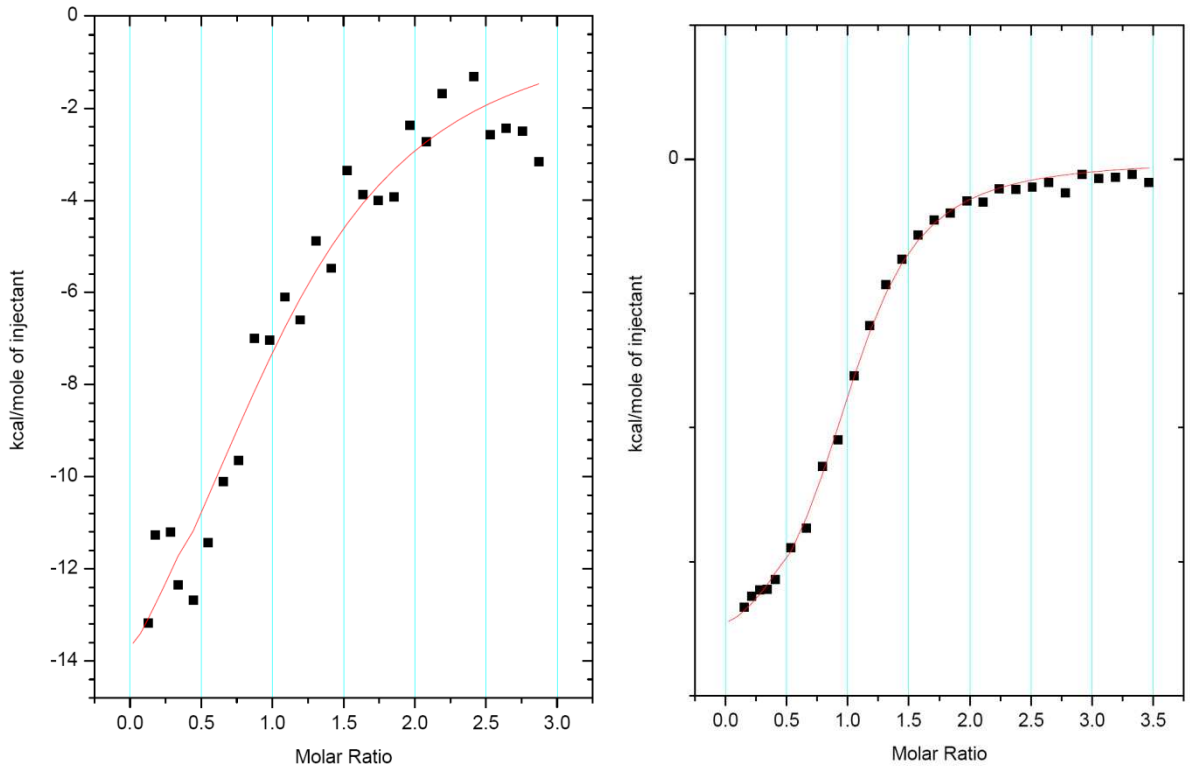

Figure 2.9. Titration of **18** with barbital at 0.02 and 0.05 mM.

Table 2.4. *log(K)*, *ΔH°* and *ΔS°* of 1:1 complexation with barbital measured by ITC in dichloromethane at *25 °C* (*298 K*).

receptor	*n*	*log(K)*	*ΔH° / kcal.mol^{-1}*	*ΔS° / cal.K^{-1}.mol^{-1}*
12	6	4.43 ± 0.02	-17.0 ± 0.8	-37 ± 3
16	8	4.85 ± 0.03	-15.5 ± 0.4	-30 ± 1
17	4	3.91 ± 0.03	-8.0 ± 0.3	-8.9 ± 0.8
18	6	5.33 ± 0.07	-15.0 ± 0.2	-25.8 ± 0.8

The errors given in **Table 2.4** are those given by the Origin software used to make the calculations from raw ITC data. The first observation that can be made is that the binding constants found with this method are of the same order of magnitude as those found by UV-Vis (**Table 2.3**), even if the values found by ITC are generally slightly smaller. This is likely to be an indirect consequence of the phenomenon of autoassociation of the receptors described above. For this reason, these values are probably less reliable than those found by UV-Vis titrations (**Table 2.3**), which were performed at a lower concentration where aggregation is less important. However, it can also be observed that when the *log(K)* of different complexes are compared to each other, similar trends are observed in the results obtained by ITC and UV-Vis titrations. Therefore, although there is a certain degree of uncertainty in these ITC results, it is still interesting to use the measured value of $\Delta H°$ and calculated $\Delta S°$ in order to explain these trends.

It can be seen that the values of $\Delta H°$ and $\Delta S°$ obtained by ITC for the binding of barbital to the two "closed" receptors **16** and **18** are very similar. The comparison between the enthalpic and entropic terms differences between the two complexes reveal that the augmentation of the binding constant with barbital from **16** to **18** is explained by the entropic term: From **16** to **18**, $\Delta(\Delta H°) = 0.5 \pm 0.6$ and $\Delta(-T.\Delta S°) = -1.3 \pm 0.5$ *kcal.mol*$^{-1}$, so it is the bigger entropic term that determines the negative sign of $\Delta(\Delta G°)$ and makes the barbital bind more strongly to **18** than to **16**. The same observation can be made between the open receptor **12** and its closed, reduced formed **18**: From **12** to **18**, $\Delta(\Delta H°) = 2.0 \pm 1.0$ and $\Delta(-T.\Delta S°) = -3.3 \pm 1.1$ *kcal.mol*$^{-1}$, so once again it is the entropic term that determines the negative sign of $\Delta(\Delta G°)$ and makes the barbital bind more strongly to **18** than to **12**.

It is important to note that the observation of higher binding constants for closed "Hamilton-like" receptors compared with their open forms (*i.e.* the *macrocyclic effect*[11a]) does not result in a ready explanation for the enthalpic or entropic nature of this effect. Studies on

the binding of metallic cations by crown ethers have shown that this effect is often related to favourable enthalpic changes but that there are also cases where it is the entropic term that explains it.[11b-c] An enthalpic contribution to the macrocyclic effect can be understood if a non-cyclic receptor has to adopt a conformation which is different from its own minimal energy conformation, a change that will add a positive term (unfavourable to binding) in the expression of $\Delta H°$, whereas in the cyclic receptor, this unfavourable contribution is already paid for as the receptor already has the desired conformation for binding. This may be the correct explanation for the macrocyclic effect observed with the original Hamilton receptors, which do not have any other substituents than diamidopyridine on the central bridging benzene ring.[1] Other work with "Hamilton-like" receptors have demonstrated that the preferred conformation of similar open receptors is not the one favourable to complexation.[13a-c] However in our receptors, there is a *tert*-butyl group, and other work[13c,d] suggests that having a bulky substituent in this position can restrict conformational freedom and contribute to the pre-organization of the uncyclised receptor for binding barbital.

On the other hand, an entropic contribution to the macrocyclic effect can be understood if the open receptor has to lose conformational freedom in order to bind the guest, whereas the cyclic one does not have to lose as much conformational freedom as it is already restricted. This is probably the dominant effect here. The opposite changes in $\Delta H°$ may be understood as a case of *entropy-enthalpy compensation*[14] (see *Chapter 1),* as a linear relationship of the kind $\Delta H° = \alpha + T_C.\Delta S°$ can be verified with $T_C = 182\ K$ and $\alpha = -10.2\ kcal.mol^{-1}$, but the margin of error on the data and the small number of values used for the regression will not allow a statistical verification of this model.

Finally, for the complex with **17**, it was difficult to obtain a good fit as reflected by the high margin of error in the results. This may be because the model used for fitting only considered the formation of the 1:1 complex and not the 2:1 complex. The difference with **18**

is explained mostly by enthalpic reasons, as $\Delta H°$ changes in the direction of a weaker binding ($\Delta(\Delta H°) = +\ 7.0\ kcal.mol^{-1}$) which makes the value of $\Delta H°$ nearly two times smaller than that for **16**. This is what would be expected if **17** binds barbital with only three hydrogen bonds instead of six. The absolute value of $\Delta S°$ has decreased by an even bigger factor, which makes that the term $-T.\Delta S°$ partly compensates the variation in $\Delta H°$ ($\Delta(-T.\Delta S°) = -\ 4.6\ kcal.mol^{-1}$). Again, if we consider that barbital is bound only on one side by three hydrogen bonds instead of six, then it has more freedom of motion in the complex, which will add a positive contribution to $\Delta S°$.

Another positive contribution equal to $R.ln(2) = 1.38\ cal.K^{-1}.mol^{-1}$ has to be added.[12] Its origin is statistical: as barbital can bind to the two binding sites, it is possible to consider the binding constant *Ks* and the thermodynamic parameters $\Delta X°_S$ for each binding site, and compare with the values K_C and $\Delta X°_C$ for the 1:1 complex. Then if we note *(S)* the concentration of free site, *(B)* the concentration of barbital, *(R)* the concentration of the receptor **17** and *(C)* the concentration of the complex, we have:

$$K_C = \frac{(C)}{(B).(R)}$$

$$(R) = 2.(S) \Longrightarrow K_S = \frac{(C)}{(B).(S)} = 2.K_C$$

$$\Delta G°_S = -R.T.ln(K_S) = -R.T.ln(K_C) - R.T.ln(2) = \Delta G°_C - R.T.ln(2)$$

As $\Delta H°_C$ represents the binding strength of barbital to the complex, it is equal to $\Delta H°_S$ for one of the two binding sites, however $\Delta S°_C$ and $\Delta S°_S$ will be different. The equation above will then be simplifed to $\Delta S°_C = \Delta S°_S + R.ln(2)$, which makes the term $R.ln(2)$ apparent. It can be concluded that these thermodynamic parameters are in good agreement with the formation of a 1:1 complex between **17** and barbital through three hydrogen bonds only, on one only of the two binding sites accessible to barbital.

2.2.3) Comparison of *ab initio* models, IR spectra and XRD structures

This work was done at the *Pôle Modélisation* of the *Institut des Sciences Moléculaires* (University Bordeaux I, France) by Dominique Cavagnat and Thierry Buffetau with the products synthesised in Birmingham, using a methodology developed by their group.[15] *Ab initio* models of **17**, **18**, barbital and their complexes were calculated (see **Figures 2.10** and **2.11** for the models of the complexes, and *Chapter 6* for experimental procedures).

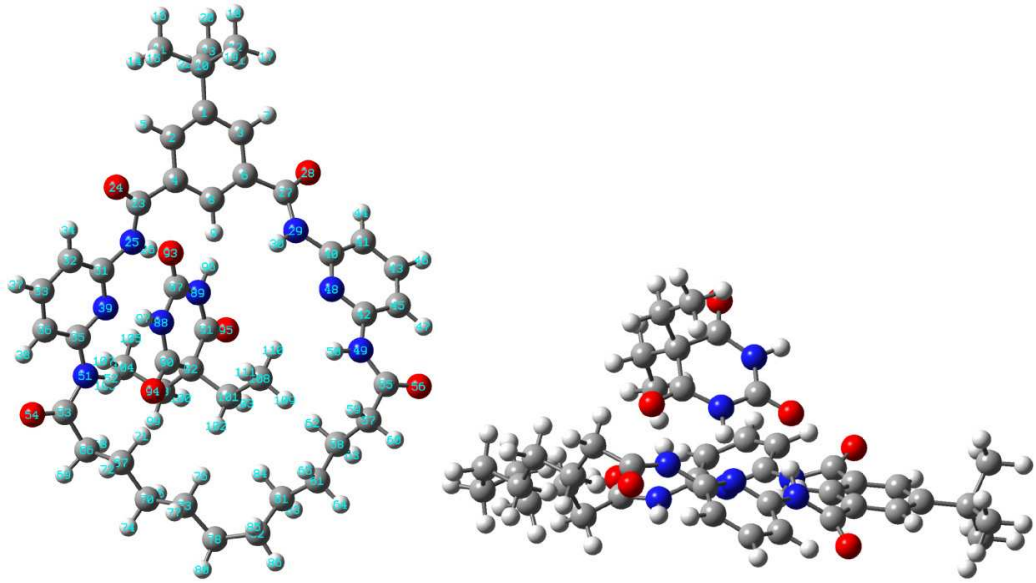

Figure 2.10. *Ab-initio* model of **17•barbital**.

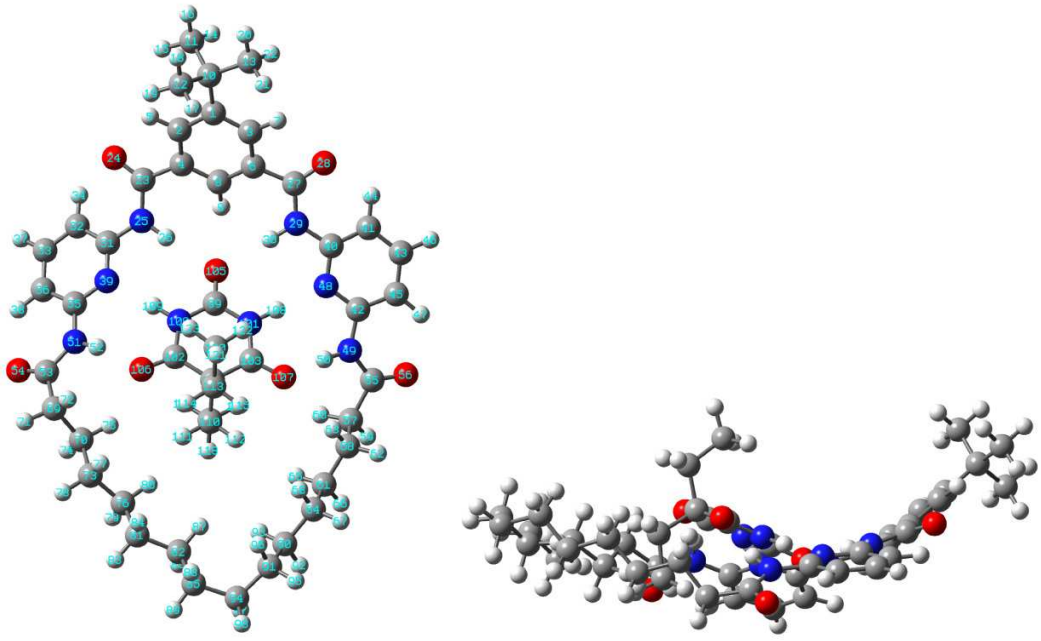

Figure 2.11. *Ab-initio* model of **18•barbital**.

The first observation on these models is that the general shape and conformation of both of **17** and **18** in the complexes are remarkably similar to what was seen on the X-ray structure of the receptors. However, the models of the receptors without barbital were different, especially the model of **18** where the same relatively large angle was observed between the planes of the two diamidopyridine moieties. According to the models of the complexes, **18** should bind barbital in a similar way to Hamilton's receptors by forming six complementary H-bonds, the barbital being in the middle of the cavity and the complex nearly symmetrical. It can also be observed that barbital is not entirely in the same medium plane as the two amidopyridine units: the oxygen atom of the central C=O is between the two amide that bind it, in the medium plane, but the rest of the molecule is tilted out of this plane with an angle of 35°. This means that one of the two ethyl groups of barbital is threading in the receptor while the other is entirely outside. However **17** should bind barbital through three H-bonds only, the barbital remaining outside of the cavity. Such a complex is obviously not a good basis for making interlocked structures. It is also clear that one of the diamidopyridine binding sites is still able to bind a second molecule of barbital. Calculations of *ab initio* models for this 2:1 complex are still ongoing.

Theoretical IR spectra of the single molecules and the complexes were then calculated from these models. A comparison between simulated and experimental IR spectra (see **Figure 2.12**) allow us to verify whether these models are in good agreement with experimental observations, with a few restrictions: the C-H vibrations may be different as Fermi resonances are not simulated with this model,[15a] and the intermolecular interactions (other than inside the complex) are not considered as the model is one of a molecule or complex "alone". This is what makes the experimental spectrum of barbital alone so different from its theoretical spectrum, as probably intermolecular hydrogen-bonds are forming at this concentration. The intensities of the C=O vibration bands are also difficult to predict because of the possible

hydrogen bonds to the solvent (chloroform). For the same reason, the experimental spectra of the 1:1 mixtures (at *5 mM*) contain a very weak band at *3422 cm^{-1}* that indicates the presence of a small amount of free receptor.

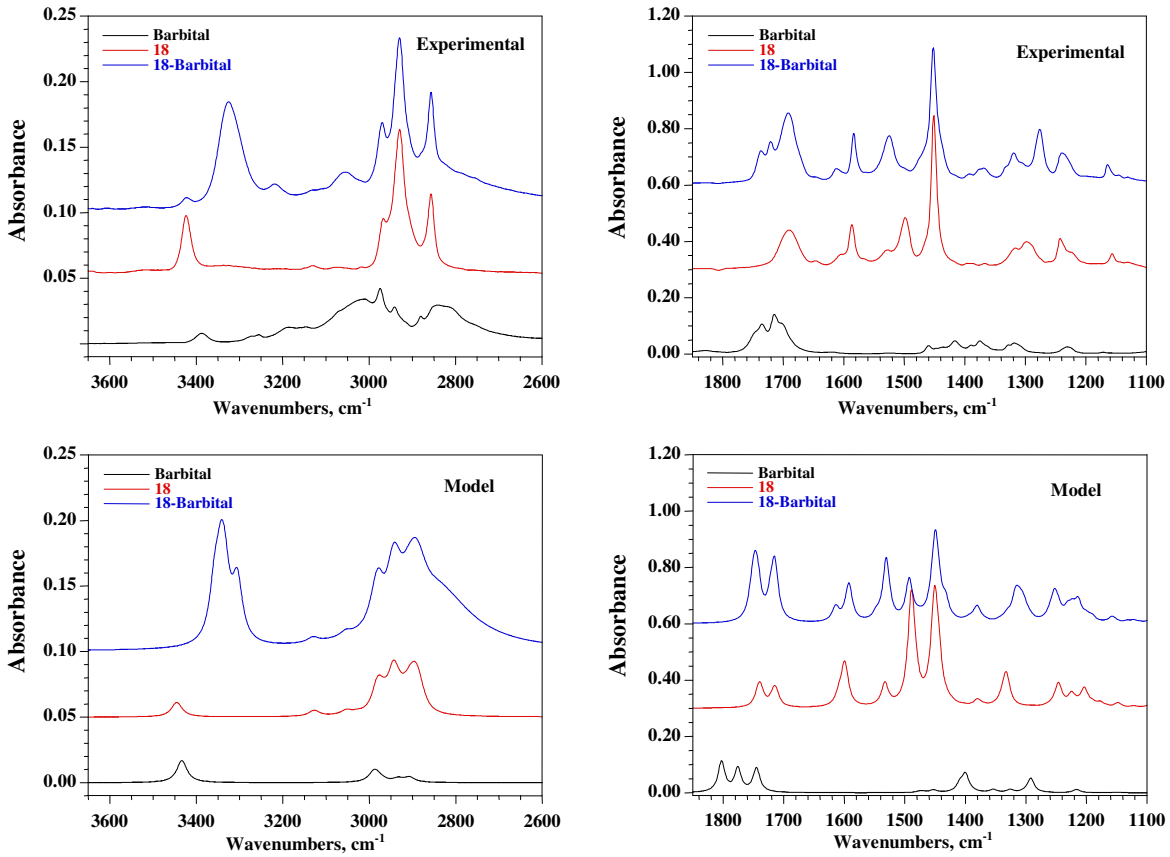

Figure 2.12a. Comparison of experimental and calculated IR spectra for **barbital**, "reduced" receptor **18** and their complex.

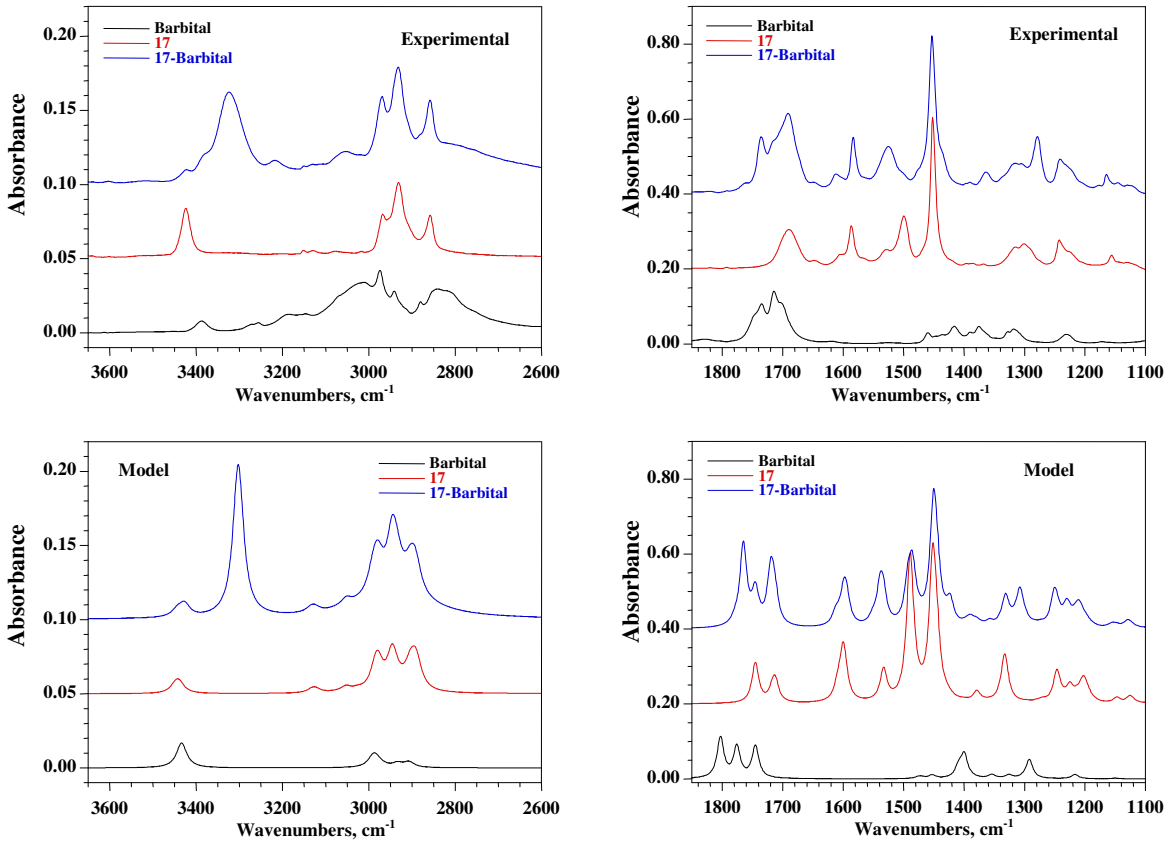

Figure 2.12b. Comparison of experimental and calculated IR spectra for **barbital**, "reduced" receptor **17** and their complex.

Knowing these restrictions, it can be observed that nevertheless for the complex of barbital with receptor **18**, there is a very good agreement between the calculated and experimental spectra, confirming that the 1:1 complex is probably formed. For the complex with **17**, the calculated and experimental spectra are also in relatively good agreement, however there are some features of the experimental spectrum that may indicate the presence of another complex. In particular, there is a shoulder at *3383 cm*$^{-1}$ in the spectrum of the complex with **17** which is absent from the theoretical and experimental spectra of **17** and therefore is not due to unbound receptor, but is also absent in the theoretical spectrum of the complex. This, combined with the lower intensity of the band at *3325 cm*$^{-1}$ compared to the complex with **18** probably indicate the presence of another 2:1 complex. The second barbital involved in the complex exhibits weaker hydrogen bonds with **17** since the new band appears at higher wavenumbers. This is consistent with the second binding constant from the UV data

being lower than expected from statistical considerations alone. This feature can also explain the lower intensity of the band observed at *1525 cm*$^{-1}$ (associated with the bending modes of the N-H groups hydrogen bonded with C=O of Barbital) for the complex with **17** (see the comparison of experimental spectra in **Figure 2.13**).

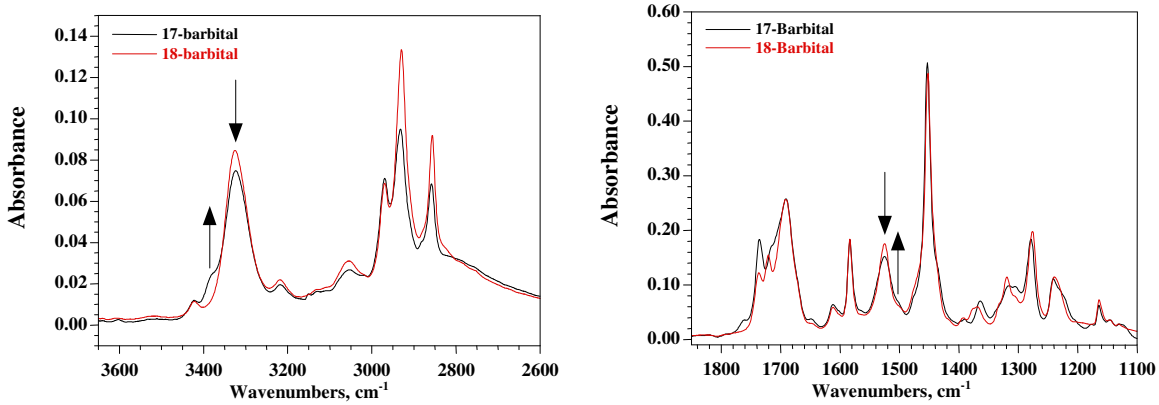

Figure 2.13. Comparison of experimental spectra of 1:1 mixtures of receptors **17** or **18** with barbital, and changes attributed to the 2:1 complex of **17** with barbital.

Finally, crystals of the complex of **18** with barbital were obtained by our colleagues from University Bordeaux 1, allowing them to determine the solid-state structure of theses complexes in the solid state by X-ray crystallography. The structure obtained is complex, with two slightly different complexes being present in the unit cell. One of these structures is presented in **Figure 2.14** and more details are given in *Appendix 1*. It is interesting to note that this structure is very close to the one predicted by *ab-initio* models, and strongly supports the feasibility of interlocked structures from similar complexes.

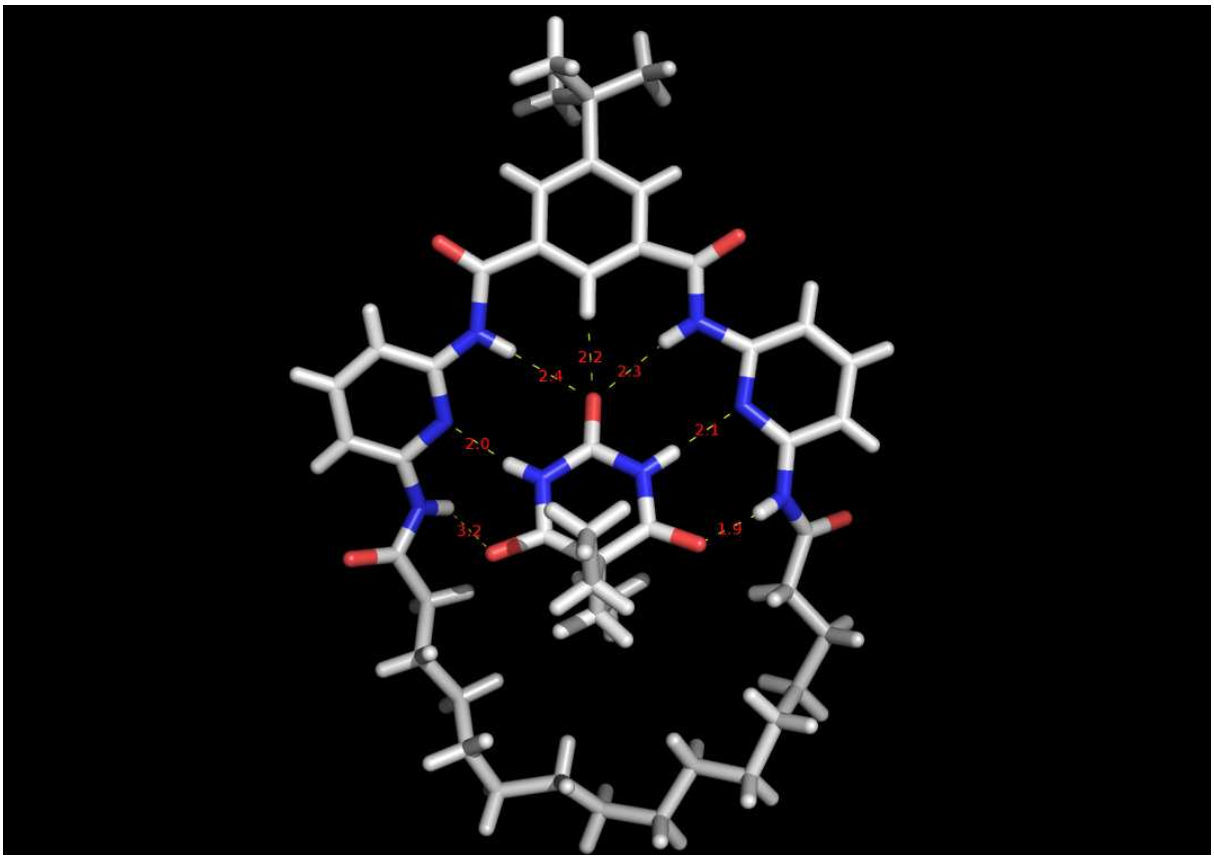

Figure 2.14. One of the two independent **18•barbital** complexes observed in the unit cell by X-ray diffraction. Disordered water has been omitted.

2.3) Conclusion and further work

A series of new receptors for barbiturates has been synthesised, and a study of their binding with barbital has allowed a better understanding of the differences in the binding abilities, not only *quantitatively* but also *qualitatively*. This has been made possible by the use of two techniques, ITC and comparison of experimental and simulated IR spectra. However all the different binding phenomena revealed by ITC and IR were not fully studied. In particular, a full study of the aggregation process observed with these receptors, including dilution experiments of the receptors, remains to be done. Once the thermodynamic parameters of this process are known, it would be possible to fit the ITC titration data with the software IC-ITC,[16b] which applies a more complete model of all the different possible events.[16a]

The different thermodynamic parameters obtained here may also lead to the conception of better receptors for barbiturates. It has been demonstrated that the size of the ring for obtaining a correct conformation for 1:1 complexes only and for obtaining an appropriate shape for interlocked structures is a crucial parameter. A poor binding and more difficult ring closing can also be related to the size of the ring. The importance of steric effects influencing preorganization through bulky substituents placed on the central benzene moiety opposite the binding site has also received a support from the interpretation of ITC results. Although the *cis* and *trans* isomers of the double-bonded closed receptors have not been separated, binding with barbital has not been shown to be noticeably different with these mixtures of isomers compared to single receptors.

---

[1] (**a**) Chang, S.-K.; Hamilton, A. D. *Journal of the American Chemical Society* **1988**, *110*, 1318-1319 ; (**b**) Chang, S.-K.; Van Engen, D. ; Fan, E.; Hamilton, A. D. *Journal of the American Chemical Society* **1991**, *113*, 7640-7645.

[2] Clark, T. D.; Ghadiri, M. R. *Journal of the American Chemical Society* **1995**, *117*, 12364-12365.

[3] (**a**) Dietrich-Buchecker, C.; Rapenne, G.; Sauvage, J.-P. *Chemical Communications* **1997**, *1997*, 2053-2054; (**b**) Frey, J.; Kraus, T.; Heitz, V.; Sauvage, J.-P. *Chemical Communications* **2005**, *2005*, 5310-5312.

[4] Chuchuryukin, A. V.; Dijkstra, H. P.; Suijkerbuijk, B. M. J. M.; Klein Gebbink, R. J. M.; van Klink, G. P. M.; Mills, A. M.; Spek, A. L.; van Koten, G. *Angewandte Chemie International Edition* **2003**, *115*, 238-240.

[5] Branowska, D.; Rykowski, A. *Tetrahedron* **2005**, *61*, 10713-10718.

[6] Chem3D Pro is a part of the ChemOffice suite, © **2001** CambridgeSoft, 100 Cambridge Park Dr., Cambridge, MA 02140-2317 USA. For the MM2 force field, cf. Norman L. Allinger, *J. Am. Chem. Soc.* **1977**, *99*, *25*, 8127-8134.

[7] Implemented in ChemDraw Ultra ®, © 1985-2001 CambridgeSoft Corporation. References given in ChemDraw: (**a**) Fürst, A.; Pretsch, E. *Analytica Chimica Acta* **1990**, *229*, 17; (**b**) Pretsch, E.; Fürst, A.; Badertscher M.; Bürgin, R.; Munk, M. E. *J. Chem. Inf. Comp. Sci.* **1992**, *32*, 291-295; (**c**) Bürgin Schaller, R.; Pretsch, E. *Analytica Chimica Acta* **1994**, *290*, 295; (**d**) Bürgin Schaller, R.; Arnold, C.; Pretsch, E. *Analytica Chimica Acta* **1995**, *312*, 95-105; (**e**)

Bürgin Schaller, R.; Munk, M. E.; Pretsch, E. *Journal of Chemical Information and Computer Sciences***1996**, *36*, 239-243.

[8] Valeur, B. *Invitation à la fluorescence moléculaire*; De Boeck Université, Bruxelles, **2004**.

[9] (**a**) Inoue, K.; Ono, Y.; Kanekiyo, Y.; Ishi-i, T.; Yoshihara, K.; Shinkai, S. *Journal of Organic Chemistry* **1999**, *64*, 2933; (**b**) Li, S.; Sun, L.; Chung, Y.; Weber, S. G. *Analytical Chemistry* **1999**, *71*, 2146-2151.

[10] Havel, J. *Haltafal-Spefo program*; Mazaryle University: Brno, Moravia, Czech Republic. References: (**a**) Sillen, L. G.; Warnqvist, B. *Arkiv för Kemi* **1968**, *31*, 315; (**b**) Sillen, L. G.; Warnqvist, B. *Arkiv för Kemi* **1968**, *31*, 377.

[11] (**a**) Cabbiness, D. K.; Margerum, D. W. *Journal of the American Chemical Society* **1969**, *91*, 6540-6541; (**b**) Haymore, B. L.; Lamb, J. D.; Izatt, R. M.; Christensen, J. J. *Inorganic Chemistry* **1982**, *21*, 1598-1602; (**c**) Izatt, R. M.; Bradshaw, J. S.; Nielsen, S. A.; Lamb, J. D.; Christensen, J. J.; Sen, D. *Chemical Reviews* **1985**, *85*, 271-339.

[12] Connors, K. A. *Binding Constants: The Measurement of Molecular Complex Stability*; Wiley, New-York, **1987**.

[13] (**a**) Chin, T.; Gao, Z.; Lelouche, I.; Shin, Y.-g.; Purandare, A.; Knapp, S.; Isied, S. S. *Journal of the American Chemical Society* **1997**, *119*, 12849-12858; (**b**) Berl, V.; Schmutz, M.; Krische, M. J.; Khoury, R. G.; Lehn, J.-M. *Chemistry, a European Journal* **2002**, *8*, 1227-1244; (**c**) Dirksen, A.; Hahn, U.; Schwanke, F.; Nieger, M.; Reek, J. N. H.; Vögtle, F.; De Cola, L. *Chemistry, a European Journal* **2004**, *10*, 2036-2047; (**d**) Schmidt, J.; Schmidt, R.; Würthner, F. *Journal of Organic Chemistry* **2008**, *73*, 6355-6362.

[14] (**a**) Houk, K. N.; Leach, A. G.; Kim, S. P.; Zhang, X. *Angewandte Chemie International Edition* **2003**, *42*, 4872-4897; (**b**) Sharp, K. *Protein Science* **2001**, *10*, 661-667.

[15] (**a**) Buffeteau, T.; Ducasse, L.; Brizard, A.; Huc, I.; Oda, R. *Journal of Physical Chemistry A* **2004**, *108*, 4080-4086; (**b**) Buffeteau, T.; Cavagnat, D.; Bouchet, A. ; Brotin, T. *Journal of Physical Chemistry A* **2007**, *111*, 1045-1051.

[16] (**a**) Buurma, N. J.; Haq, I. *Methods* **2007**, *42*, 162–172; (**b**) Buurma, N. J.; Haq, I. *Journal of Molecular Biology* **2008**, *381*, 607-621.

3) NEW FLEXIBLE BARBITURATES

3.1) Synthesis

3.1.1) Design and strategy

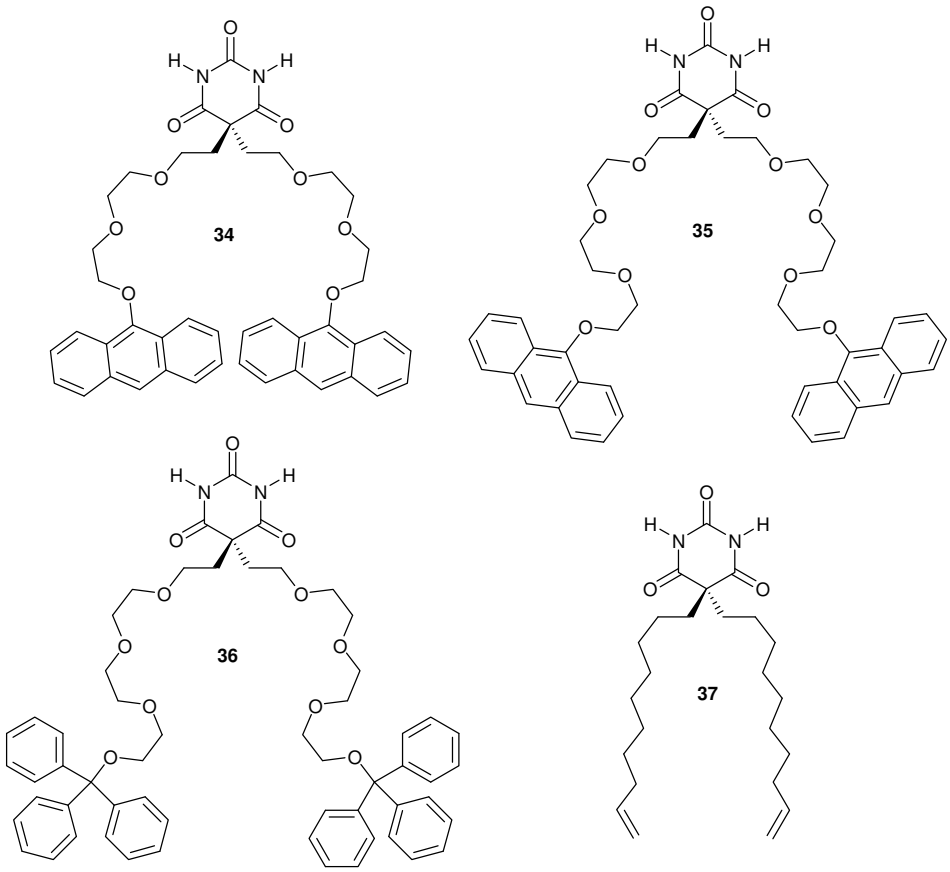

Scheme 3.1. Flexible barbiturates **34**, **35**, **36** and **37**.

In order to form interlocked structures with "Hamilton-like" receptors, our first approach, which will be referred to as the "flexible barbiturate approach", was to synthesise barbiturates substituted on the central carbon by two long, flexible chains terminated either by a stopper, or a reacting group. It was thought that if the terminal group was small enough to thread through a closed receptor, then a pseudo-rotaxane would be accessed, which would lead to a rotaxane by a stoppering reaction or a catenane by a ring-closing reaction. Alternatively, if its bulkiness would stop it threading through the cavity of a closed receptor,

then a rotaxane would be accessed either by binding it to an open receptor that could be closed by metathesis, or by using a "magic ring" approach.*

The strategy adopted to synthesise the stoppered guests was to synthesise the stoppered chain as a bromide or iodide first, and then to use it to make a disubstituted malonate that would be finally converted to a barbiturate using a procedure described in the literature.[1] The "flexible barbiturates" synthesised here are described in **Scheme 3.1**. In order to facilitate the reading of this chapter, their structures are also described on the chart folded at the last page of this thesis. The first barbiturates (**34** and **35**) were independently designed by C. Lincheneau and N. McClenaghan in Bordeaux,[2] before we merged our projects. They bore tri- or tetra-ethylene glycol arms terminated by anthracenes, in order to perform a ring closure using anthracene dimerisation.[3] The chain lengths were chosen on the basis of the models discussed in *Chapter 1* (pp. 45-48). Another barbiturate with a tetraethylene glycol arm terminated by a trityl group (**36**) was later synthesised because of the difficulties posed by anthracene (see below). Finally another barbiturate with an alkane chain terminated by a free olefin (**37**) was synthesised, in order to obtain a catenane by threading through one of the "reduced" receptors (**17** and **18**) and then performing a ring closing metathesis to form the catenane. Its chain length is slightly shorter than that of **34**, and will lead after ring-closing metathesis to a 19-membered ring, which is smaller than what has already been obtained for interlocked structures, but not theoretically impossible if the strategy adopted is clipping rather than threading (see discussion in *Chapter 1*, pp. 15-16).[4]

* This means an approach based on the equilibrium of open and closed forms of the receptors under the conditions of metathesis, cf. *Chapter 1* and references therein.

3.1.2) Malonate precursors

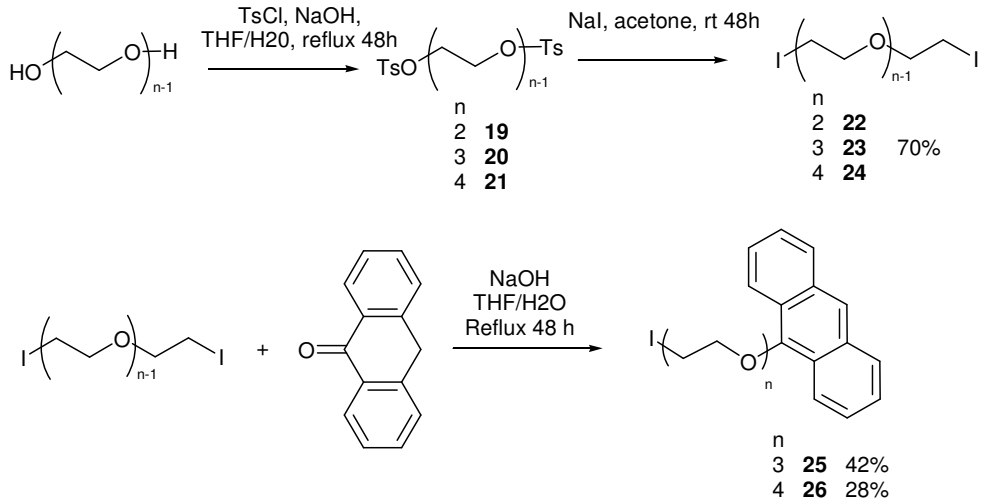

Scheme 3.2. Synthesis of the precursors **25** and **26** to the anthracene-substituted malonates **30** and **31**.

The synthesis of the iodo- pendant arms **25** and **26** of the anthracene-substituted barbiturates **34** and **35** was achieved by reacting a large excess of a diiodide, itself easily synthesised in two steps from tri- or tetra-ethylene glycol, with anthrone in a mixture of THF and water at reflux. This last reaction had to be performed in the dark (by covering the reacting flask with foil) in order to avoid anthracene photooxidation to anthraquinone, which would occur even in presence of trace amounts of oxygen. The anthracene-substituted arms were then isolated by column chromatography on silica gel. The yields after column chromatography were relatively poor and difficult to reproduce for two reasons:

- An excess of diiodide was used to avoid forming too much of the undesired di-anthracene substituted product, but this caused cracks in the silica and dispersion of the products on the column;
- As mentioned above, anthracene derivatives are easily oxidised in air in the presence of light and anthraquinone as well as hydroxy-iodo-arms were obtained as byproducts.

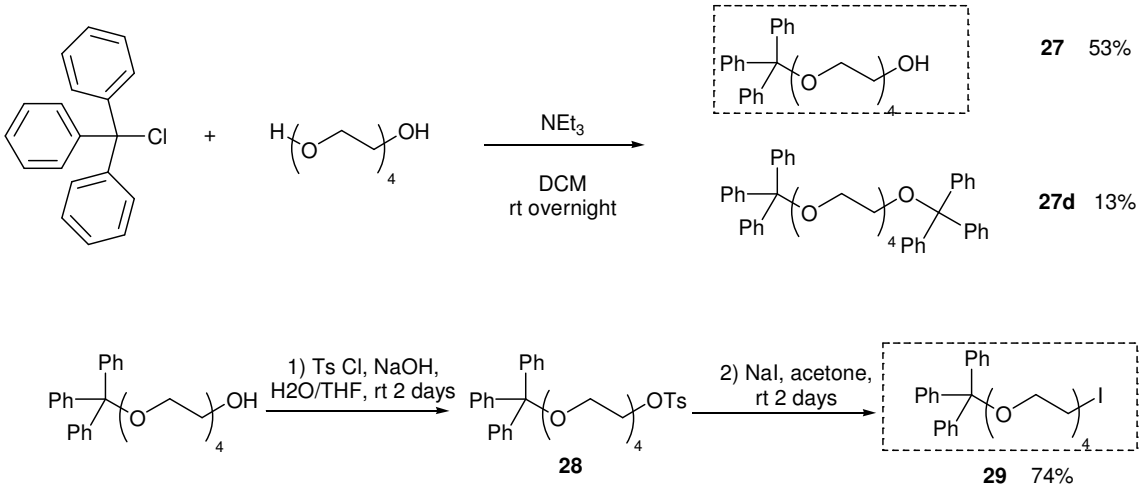

Scheme 3.3. Synthesis of the precursor to malonate **32**.

The iodo-pendant arm **29** of the trityl-substituted barbiturate **36** was synthesised in 53% yield by reacting one equivalent of trityl chloride with tetraethylene glycol and isolating the mono-trityl ether from the mixture by chromatography. It was then converted to the iodide in two steps in a very good yield of 74%, using similar conditions to those used for the synthesis of diodides **22**, **23** and **24**.

3.1.3) Malonates

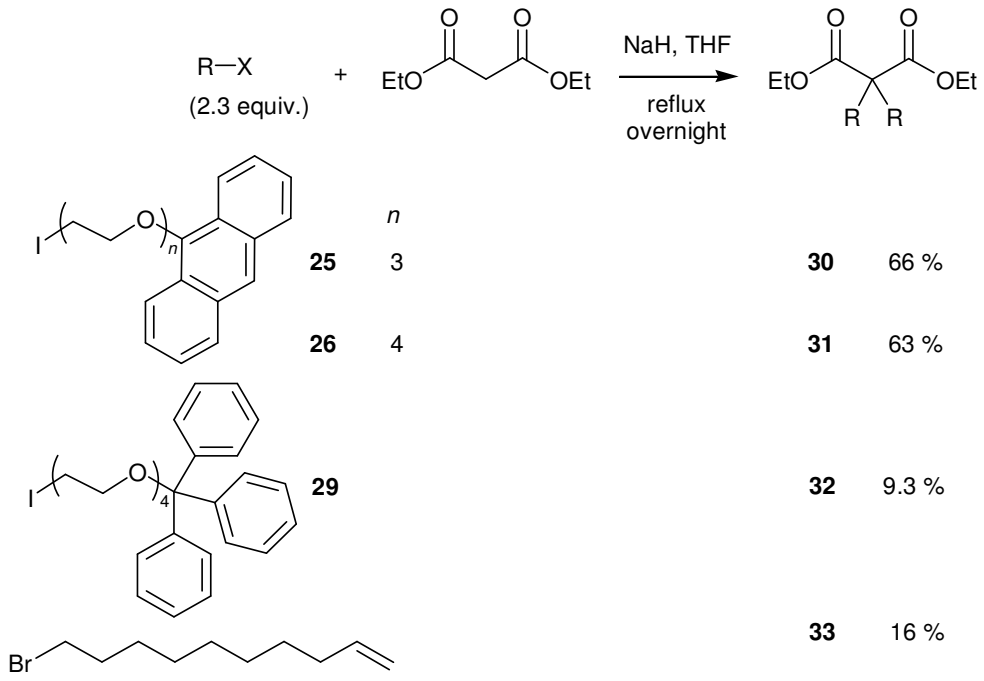

Scheme 3.4. Synthesis of the disubstituted malonates **30**, **31**, **32** and **33**.

The procedure followed was similar for all four malonates, diethylmalonate was deprotonated with 2 equivalents of sodium hydride in THF and reacted with 2 equivalents of the iodide or the bromide of the arm, then the product was separated from the crude by chromatography on silica gel. Reasonably good isolated yields (60% and 63%) of disubstituted malonates **30** and **31** were obtained when reacting with anthracene terminated iodides **25** and **26**. Some of the anthracene products were cleaved by oxidation to anthraquinone, which may suggest that the yield of the reaction was actually even higher. By comparison, the isolated yield of trityl terminated malonate **32** was very poor; the actual yield of the reaction may be however of the same order of magnitude, but as the trityl group is acid sensitive, it was probably partly hydrolysed by the silica when separating the product from the crude by chromatography. Finally for the olefin-terminated malonate **33**, the yield of isolated product was also lower than for **30** and **31**. This may be because commercial 1-bromodec-9-ene was used instead of the iodide, and as the reactivity of bromides is lower than that of iodides in nucleophilic substitutions, the reaction was probably not complete when stopped.

3.1.4) Conversion of malonates to barbiturates

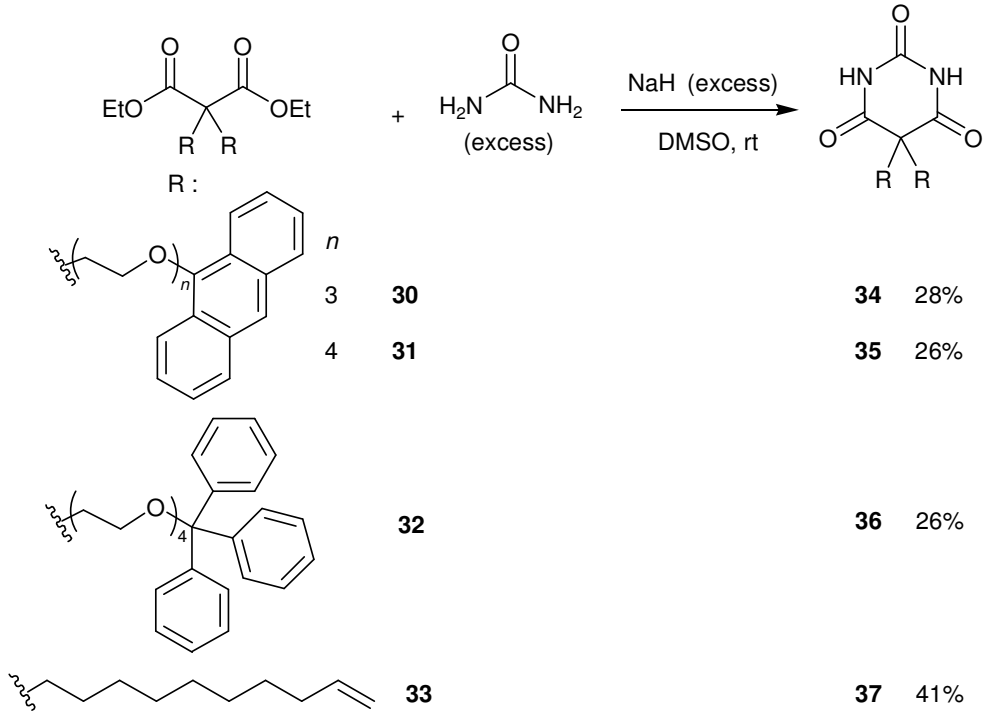

Scheme 3.5. Conversion of malonates to barbiturates.

The procedure followed was similar for all four barbiturates, they were reacted with an excess of sodium hydride and urea in DMSO, and then the product was separated from the crude by chromatography on silica gel. This time the best yield was obtained with the olefin terminated barbiturate **37**. The lower yield observed for the other barbiturates could be due to product decomposition, either by photooxidation of the anthracene-tagged barbiturates **34** and **35** or by hydrolysis of the trityl-tagged barbiturate **36**. Alternatively the actual yield of the reaction could be lower, which may be the case as the ethylene glycol arms chains are slightly more rigid than the alkyl chain of **37**, and this increased rigidity may increase the energy of the transition state in the reaction with urea through restriction of conformational freedom.

3.2) Photochemistry of the anthracene-tagged barbiturates

3.2.1) Fluorescence studies

3.2.1.1) Fluorescence spectra and quantum yields

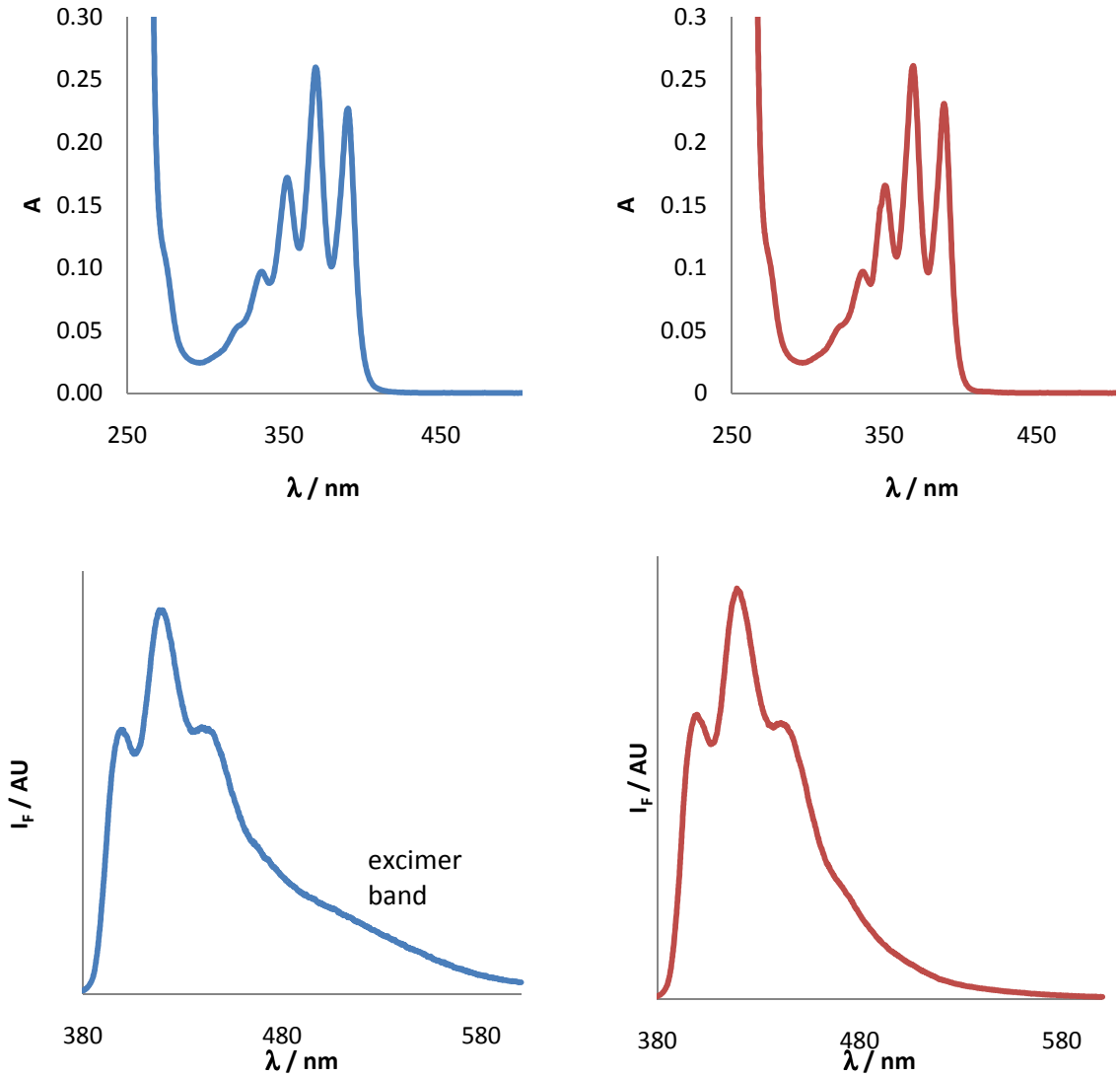

Figure 3.1. Absorption (top) and emission spectra (bottom) of degassed solutions of **34** (left) and **35** (right), 2×10^{-5} *M* in dichloromethane. Excitation wavelength: *365 nm*.

The emission spectra of solutions of **34** and **35** in degassed DCM were recorded with an excitation wavelength of *365 nm*, close to the maximum of absorption of the anthracene band (*369 nm*) (see **Figure 3.1**). For **34**, in addition to monomer emission, an *excimer band* at

around 530 nm was observed,* showing that the two anthracene units freely approach one another during the lifetime of the excited-state. This was not observed with **35** which had longer flexible arms.

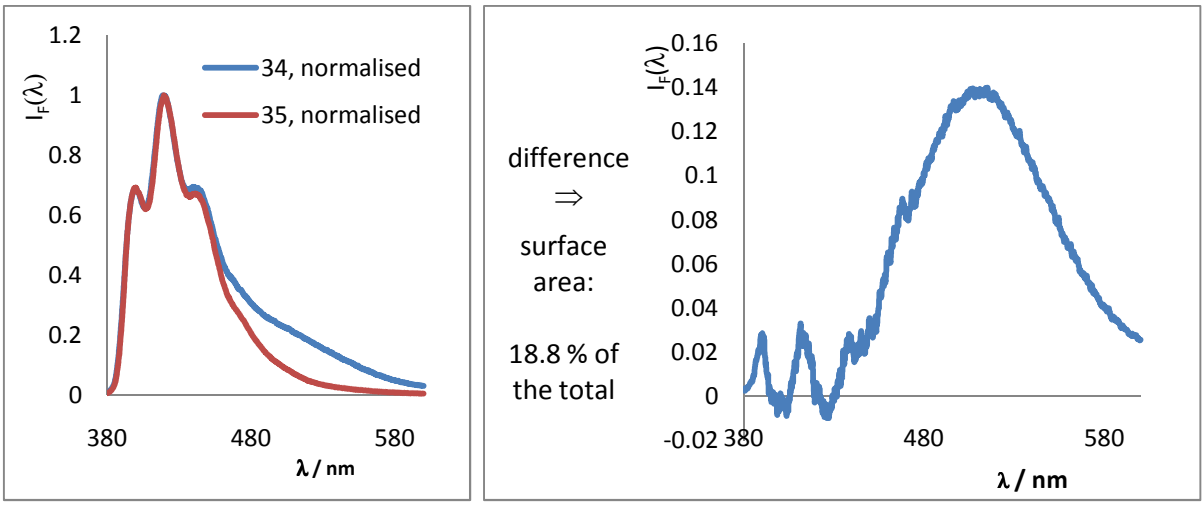

Figure 3.2. Excimer fluorescence band of **34** (right) obtained by difference of the normalised emission spectra of **34** and **35** (left), in dichloromethane, excitation wavelength *365 nm*.

By considering the whole spectrum, the fluorescence quantum yield of **34** was measured (cf. *Chapter 6* for a description of this method): a value $\Phi_{F,\,34\,total} = 0.184$ was obtained. The quantum yield of fluorescence of **35** was not measured. It is important to note that the quantum yield of fluorescence obtained for **34** is for the complete spectrum containing both the monomer and the excimer bands. In other words, the total number of molecules that fluoresce (in the monomer and the excimer form) is divided by the total number of molecules of **34** in solution that have been photoexcited. It is possible to evaluate the quantum yield of monomer emission alone by using a method already described in the literature:[5c] If it is assumed that in the case of **35** no excimer emission is present, then the spectrum of **35** should have the same shape as the emission spectrum of the monomer of **34**, in which case, by dividing those two spectra by their respective maxima and calculating the difference, a normalised spectrum of the excimer can be made (see **Figure 3.2**). The ratio

* An excimer is a complex formed between two identical molecules or molecular fragments, here two anthracene units, where one of the fragments is in an excited state (cf. *Chapter I*).

between the area of the surface covered by the excimer band to the surface area of the whole spectrum of **34** was then determined as *18.8%*, so the quantum yield of the monomer, which is related only to the fluorescence of the monomer, corresponds to the remaining *81.2%* of the total, that is $\Phi_{F,\ monomer} = 0.149$ and $\Phi_{F,\ excimer} = 0.035$.

Other information may be drawn from the spectrum of the excimer. Its maximum is for a wavelength of $\lambda_{max} \simeq 505\ nm$. It has been described in the literature[6] that the value of λ_{max} for the excimer was related to its geometry, with usually $\lambda_{max} \simeq 580\ nm$ for symmetrical excimers with completely overlapping orbitals, and lower wavelengths when the overlap was only partial, usually $\lambda_{max} \simeq 520\text{-}540\ nm$. The very low value obtained here suggests that the two anthracene units are not completely overlapping in this excimer.

3.2.1.2) Study of the fluorescence decay

The lifetimes of excited states were measured by time correlated single photon counting, an experimental method for observing the fluorescence decay.[7] The exact data found experimentally are reported in the experimental section (*Chapter 6*), but a simplified overview of these results is presented here. The solutions had to be thoroughly degassed in order to avoid photo-oxidation.

It was found that with **34**, the fluorescence intensity, expressed in arbitrary units, at the wavelength of the emission at *415 nm* (monomer band), was best fitted with a biexponential model:

$$I_{F\ 415\ nm}(t) = I_A . \mathrm{e}^{-\frac{t}{\tau_A}} + I_{B1} . \mathrm{e}^{-\frac{t}{\tau_B}}$$

with the following characteristic lifetime parameters: $\tau_A = 8.6\ ns$ and $\tau_B = 1.4\ ns$ and the pre-exponential factors $I_A = 0.1$ and $I_{B1} = 1.0$ (in arbitrary units).

At *510 nm*, in the excimer band, it was also a biexponential, with one of the lifetimes, $\tau_B = 1.4\ ns$, being the same as that at *415 nm*:

$$I_{F\,510\,nm}(t) = I_{B2}.\,e^{-\frac{t}{\tau_B}} + I_E.\,e^{-\frac{t}{\tau_E}}$$

with the following parameters: $I_{B2} = 0.06$, $I_E = 0.58$, and $\tau_E = 14.6$ *ns*.

These data can be interpreted using a simplified model that is similar to what has already been used on a related system in the literature:[5c] Two "monomeric" conformers of **34** exist in the excited state, which are noted *A* and *B* and each of them has a different lifetime (τ_A and τ_B), the second being shorter because it is leading to the excimer *E*, which lifetime has a lifetime of τ_E. These lifetimes can be related to the rate for different events, as shown in **Scheme 3.6**.

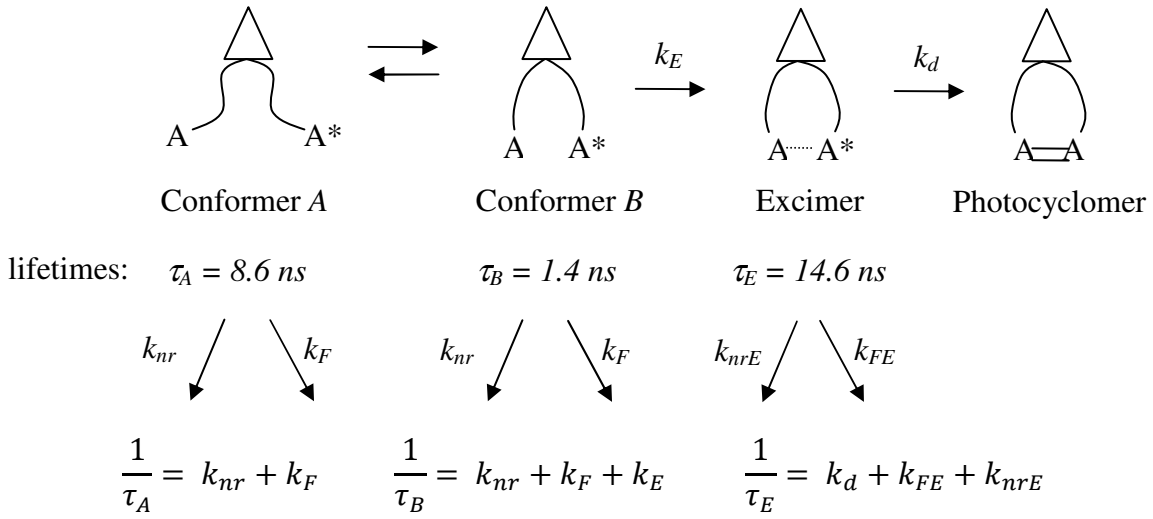

Scheme 3.6. Behaviour of the excited states of **34**.

In the equations in **Scheme 3.6**, k_{nr} is the rate constant for non-radiative relaxation of the monomeric excited state of **34** and k_F is the fluorescence rate constant of this monomer, these two rate constants being considered equal for conformers *A* and *B*. The rate constants for the conversion of *A* to *B* and *B* to *A* are ignored. The rate constant for the conversion of the monomer to the excimer is k_E. The rate constant for the reversion of the excimer to the monomer is considered small by comparison with other rate constants and is therefore ignored. k_{FE} and k_{nrE} are the rate constants for the fluorescence and non-radiative relaxation respectively of the excimer, and k_d is the rate constant for the reaction of anthracene

dimerisation reaction from the excimer. As no actual dimer of the starting molecule is formed but an intramolecular anthracene dimer, this reaction should be strictly termed *photocyclomerisation* and the photoproduct, *photocyclomer*.

This models leads directly to the rate constant for the formation of the excimer:

$$k_E = \frac{1}{\tau_B} - \frac{1}{\tau_A} = 6.0 \times 10^8\ s^{-1}.$$

As explained in *Chapter 1*, the quantum yield of fluorescence is given[8] by the following equation:

$$\Phi_F = \frac{1}{(M^*)_0} \int_0^\infty i_F(t).dt$$

In this equation, $(M^*)_0$ is the initial concentration of molecules in the excited state, and $i_F(t)$ is the *fluorescence intensity*, which has to be distinguished from the experimental $I_F(t)$ introduced above which was given in arbitrary units. In our case, the concentration of the monomer excited state $(M^*)_0$ decomposes in the sum of the concentrations of the two conformers *A* and *B*:

$$(M^*)_0 = (A^*)_0 + (B^*)_0$$

As the rate constant of fluorescence k_F is assumed to be the same for *A* and *B*, the expression of the intensity of fluorescence is:

$$i_F(t) = k_F.(A^*)_0.\mathrm{e}^{-\frac{t}{\tau_A}} + k_F.(B^*)_0.\mathrm{e}^{-\frac{t}{\tau_B}}$$

The experimental expression of the intensity of fluorescence given above was in arbitrary units, in other words there is a constant proportional factor *K* between these two expressions:

$$i_F(t) = k_F.(A^*)_0.\mathrm{e}^{-\frac{t}{\tau_A}} + k_F.(B^*)_0.\mathrm{e}^{-\frac{t}{\tau_B}} = K.I_A\mathrm{e}^{-\frac{t}{\tau_A}} + K.I_{B1}.\mathrm{e}^{-\frac{t}{\tau_B}}$$

This leads directly to $k_F.(A^*)_0 = K.I_A$ and $k_F.(B^*)_0 = K.I_{B1}$. This proportional factor *K* disappears by simplification when these expressions are reintroduced in the expression of $\Phi_{F,\,monomer}$:

$$\Phi_{F\ monomer} = \frac{k_F}{I_A + I_{B1}} \int_0^\infty \left(I_A \mathrm{e}^{-\frac{t}{\tau_A}} + I_{B1}.\mathrm{e}^{-\frac{t}{\tau_B}} \right).dt$$

Using the well known mathematical result of the integral of an exponential decay:

$$\int_0^\infty \mathrm{e}^{-\frac{t}{\tau}}.dt = \tau$$

The expression of $\Phi_{F,\ monomer}$ is equal to:

$$\Phi_{F\ monomer} = k_F.\frac{\tau_A.I_A + \tau_B.I_{B1}}{I_A + I_{B1}}$$

This last expression allows to evaluate the rate constant of fluorescence of the monomer k_F from the experimental values, as well as the rate constant of non-radiative relaxation k_{nr}:

$$k_F = \Phi_{F\ monomer}.\frac{I_A + I_{B1}}{\tau_A.I_A + \tau_B.I_{B1}} \quad \text{and} \quad k_{nr} = \frac{1}{\tau_A} - k_F$$

$$k_F = 7.3 \times 10^7\ s^{-1} \quad \text{and} \quad k_{nr} = 4.4 \times 10^7\ s^{-1}$$

According to the following equation,[8] the intensity of excimer emission (noted I_E) and monomer emission (noted I_M) can be related to their rate constants of fluorescence:

$$\frac{I_E}{I_M} = \frac{k_{FE}}{k_F}.\tau_E.k_E$$

Using the values measured or calculated before, this leads to the rate constant of fluorescence of the excimer:

$$k_{FE} = \frac{k_F.I_E}{\tau_E.k_E.I_M} = 1.9 \times 10^6\ s^{-1}$$

With **35**, the excimer emission was absent from the emission spectrum. However, as will be described later in this chapter, photodimerisation still occurred, which means that the two anthracene units can also freely approach one another. It is usually assumed that anthracene dimerisation occurs with the formation of an intermediate excimer,[3b] so in the case of **35**, an excimer probably forms but its fluorescence is not seen. This can be interpreted as

the rate constant of dimerisation from the excimer in this case being much larger than the rate constants of relaxation of the excimer, either through radiative (k_{FE}) or non radiative (k_{nrE}) processes. In other words an excimer species does not need to be introduced in the kinetic considerations for **35** as this species is only transient and nearly completely converts to the photocyclomer.

The fluorescence decay was also studied at *415 nm* and *510 nm*. As expected the same biexponential model was able to fit correctly the decay at both wavelength:

$$I_F(t) = I_A e^{-\frac{t}{\tau_A}} + I_B e^{-\frac{t}{\tau_B}}$$

with the following parameters: $I_A = 0.18$, $\tau_a = 7.0\ ns$; $I_B = 0.66$, $\tau_b = 3.4\ ns$. This indicates that once again two conformers of **35** are present and that each one leads to an excited state with a different lifetime, where the one with the shorter lifetime leads directly to the photocyclomer. In this case, the rate constant k_d for dimerisation of **35** can be calculated as done previously for the rate constant for excimer formation of **34**:

$$k_d = \frac{1}{\tau_B} - \frac{1}{\tau_A} = 1.5 \times 10^8\ s^{-1}$$

The rate constants of fluorescence and non-radiative decay of **35** can not be calculated as the fluorescence quantum yield of **35** was not measured, but their sum can be evaluated:

$$k_F + k_{nr} = \frac{1}{\tau_A} = 1.4 \times 10^8\ s^{-1}$$

It is interesting to note that for **34**, $k_F + k_{nr} = 1.2 \times 10^8\ s^{-1}$, which is a very similar value.

3.2.2) Photocyclomerisation and thermal return

When a degassed solution of **34** or **35** was irradiated at the wavelength of absorption of the anthracene groups (at *365 nm*), a photocyclomerisation reaction took place, as evidenced by NMR and UV-vis spectroscopy. In theory two different dimers can form, the *head to head dimer* (*hh*) or the *head to tail dimer* (*ht*) (see **Scheme 3.7**, and *Chapter 6* for the

experimental procedure). By UV, the anthracene band centred on *369 nm* disappeared (see **Figure 3.3**), and by ^{1}H NMR, the whole spectrum of each molecule was affected (see **Figure 3.4**).

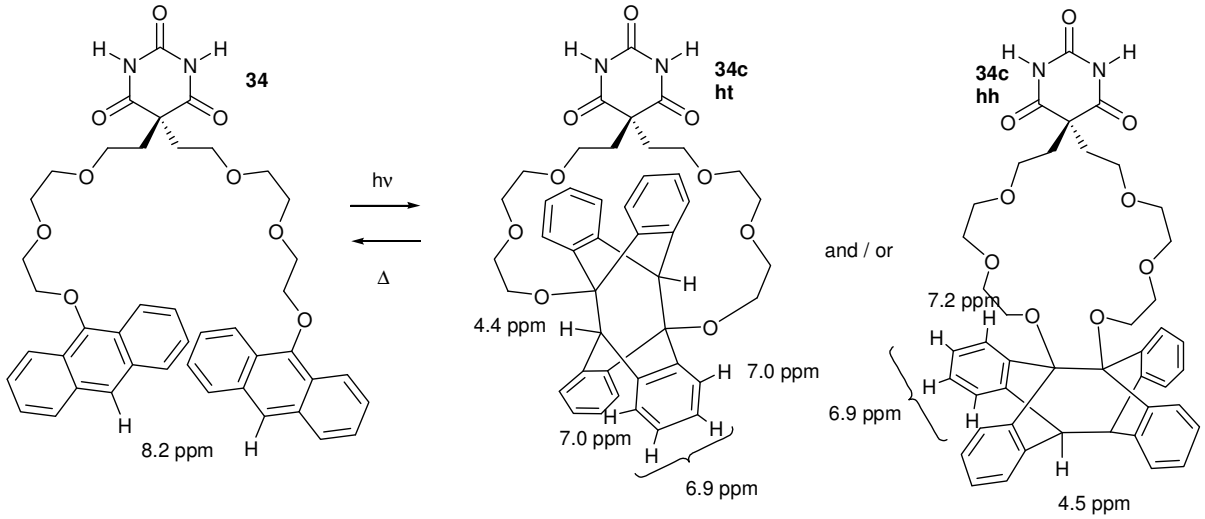

Scheme 3.7. Photocyclomerisation of **34**, with the structure of the two possible dimers, and some expected ^{1}H NMR shifts by comparison with 9-methoxyanthracene dimers.[9b]

Using these UV spectra, the quantum yields of dimerisation, Φ_d, of **34** and **35** were measured using Parker's actinometry method,[10] as described in *Chapter 6*. This involved fitting the experimental concentration values of remaining "monomeric" anthracene for different irradiation times using a model derived from the physico-chemical laws followed by the phenomenon (constant quantum yield, constant photonic flux, absorption described by Beer's law). The determination of the constant photonic flux was made using a known actinometer (potassium ferrioxalate) under the same irradiation conditions. The results are presented in **Table 3.1**.

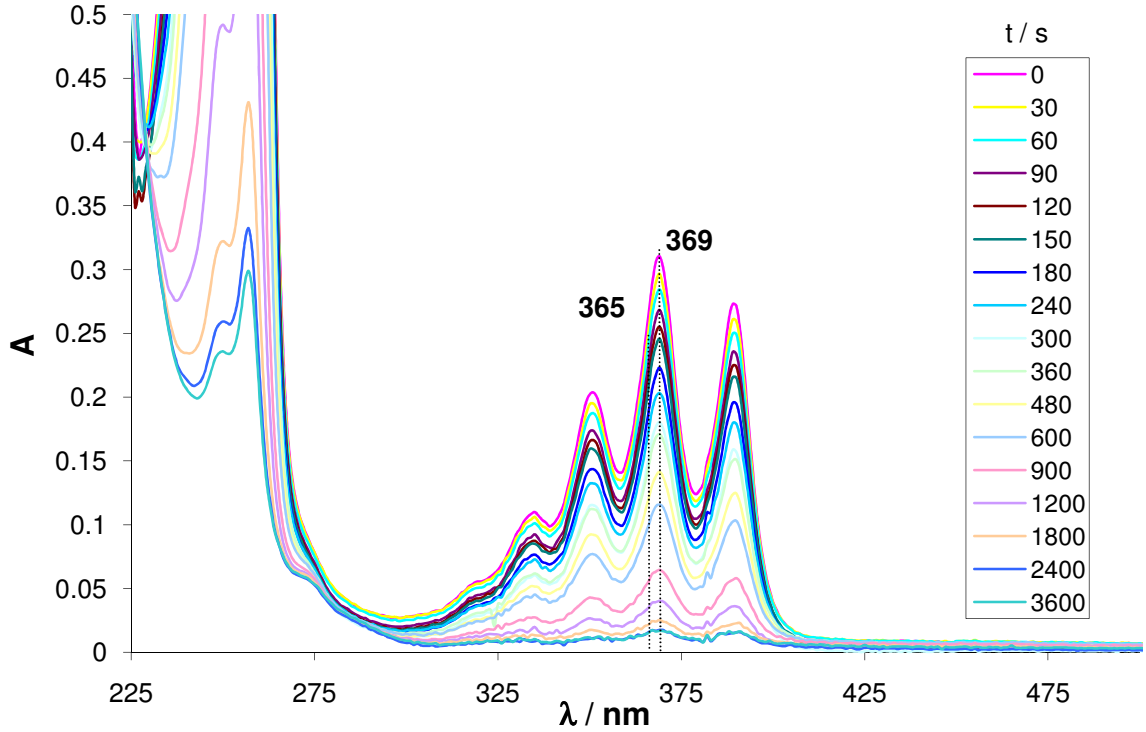

Figure 3.3. Changing electronic absorption spectra of a 2×10^{-5} *M* solution of **34** in degassed DCM upon irradiation at *365 nm*.

After complete conversion (*ie:* when the anthracene band had disappeared in the UV spectrum), the solutions were left in the dark at room temperature and the absorption at *369 nm* was measured at regular intervals in order to check the reappearance of monomeric anthracene by thermal return. The concentrations values were fitted with a monoexponential model, and the rate constants k_{ret} for thermal return at room temperature are also presented in **Table 3.1** (see *Chapter 6* for the procedure), as well as the half-life of the dimers, as given by the formula:

$$t_{1/2} = ln(2)/k_{ret}$$

Table 3.1. Quantum yields of photocyclomerisation and times of thermal return of **34** and **35**, measured by UV-vis. spectroscopy of solutions at 2×10^{-5} *M* in DCM, monochromatic irradiation at *365 nm*, Parker's actinometry; thermal return at room temperature.

Barbiturate	Φ_d	k_{ret} / s^{-1}	$t_{1/2}$
34	0.10	3.5×10^{-6}	2.3 days
35	0.28	7.6×10^{-4}	15 minutes

It can be observed that the quantum yield of photocyclomerisation for **35** is almost three times that of **34**, whereas the thermal return rate constant is more than 200 times greater. In other words, the dimer is easier to form and less kinetically stable in the case of **35**. The fact that the anthracene dimer forms fastest with **35** is consistent with the hypothesis expressed earlier that the dimerisation rate constant in the case of **35** is much larger than the fluorescence rate constant for the excimer, which explains why no excimer band was observed in the fluorescence spectrum of **35**. This could be due to geometric reasons, with different relative orientations of the anthracene units.

The quantum yields of dimerisation are of the same order of magnitude as those observed with similar systems.[3,5,11] The thermal return rate constants may reveal the geometry of the dimers; according to the literature,[3] the half-lives of *ht* dimers at room temperature are usually better expressed in years, whereas those of *hh* dimers are in hours. Here the time half-life of **35** is clearly very short even compared to the values expected for a *hh* dimer, and the half-life of **34** is close to the longer lifetimes observed for *hh* dimers[5c] but much too short for a *ht* dimers. For this reason, it is likely that the dimers formed are *head to head dimers*.

The NMR experiments (**Figure 3.4a** and **3.4b**) confirmed that the disappearance of the anthracene signals in the UV spectra were associated with the formation of anthracene dimers. In particular, a common feature characteristic of dimerisation appeared in the spectra of the solutions of **34c** and **35c**; the singlet at *8.2 ppm* corresponding to the proton opposite to the oxygen on the central anthracene aromatic ring (**e**) disappeared, and a new signal for the bridgehead proton (same proton, but in a new environment) appeared at *4.5 ppm* (**e'**). The fact that this is only one clear singlet indicates that only one type of dimer is formed in each case.

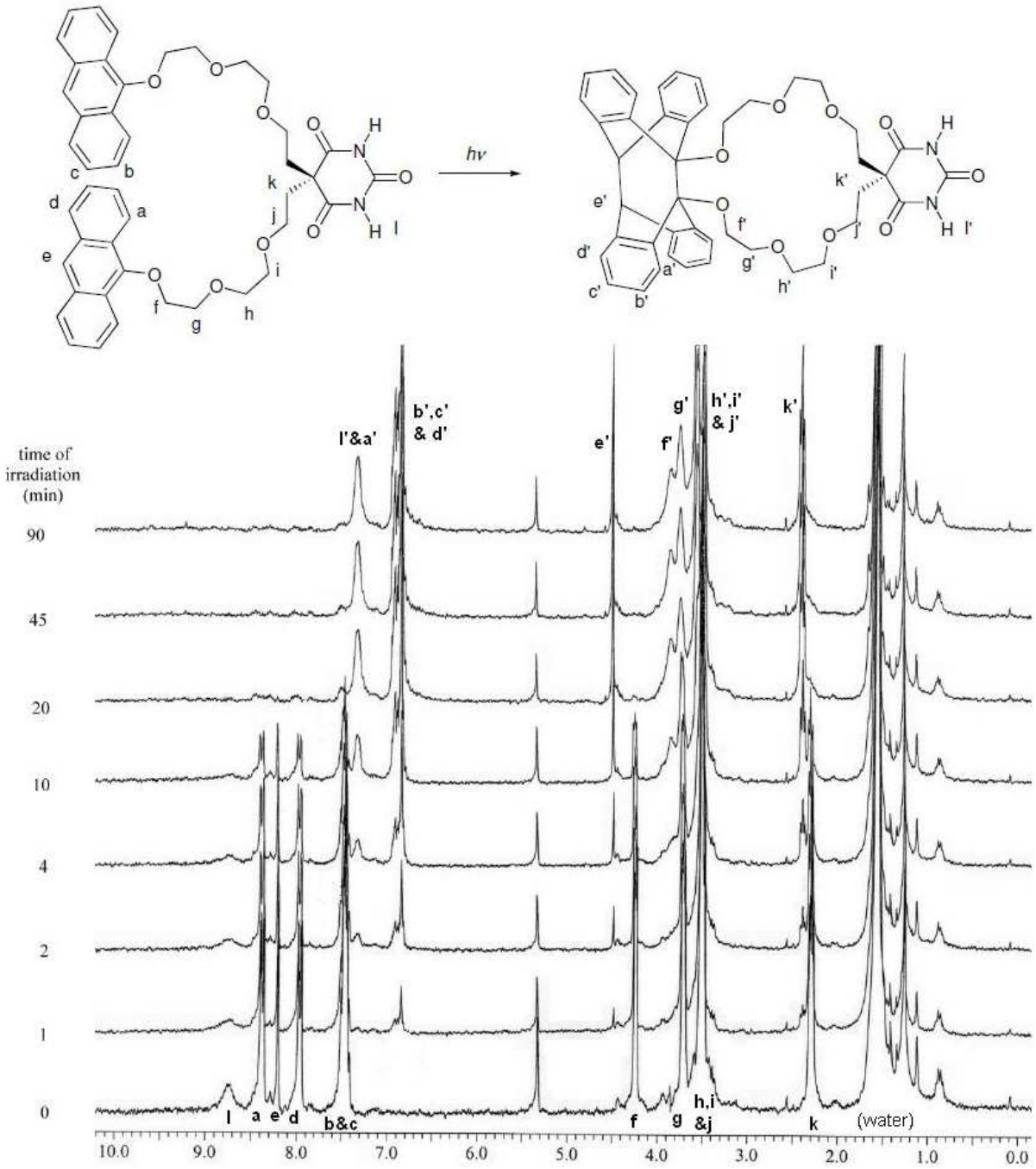

Figure 3.4a. Photocyclomerisation of **34** upon irradiation using a mercury lamp and a filter (saturated solution of lead acetate), followed by NMR in CD_2Cl_2, at a concentration of *2 mM*. Notice that the sample of **34** and/or the CD_2Cl_2 used was contaminated with water and other contaminants (unidentified peaks between *0* and *2 ppm*), which did not affect the changes observed upon irradiation.

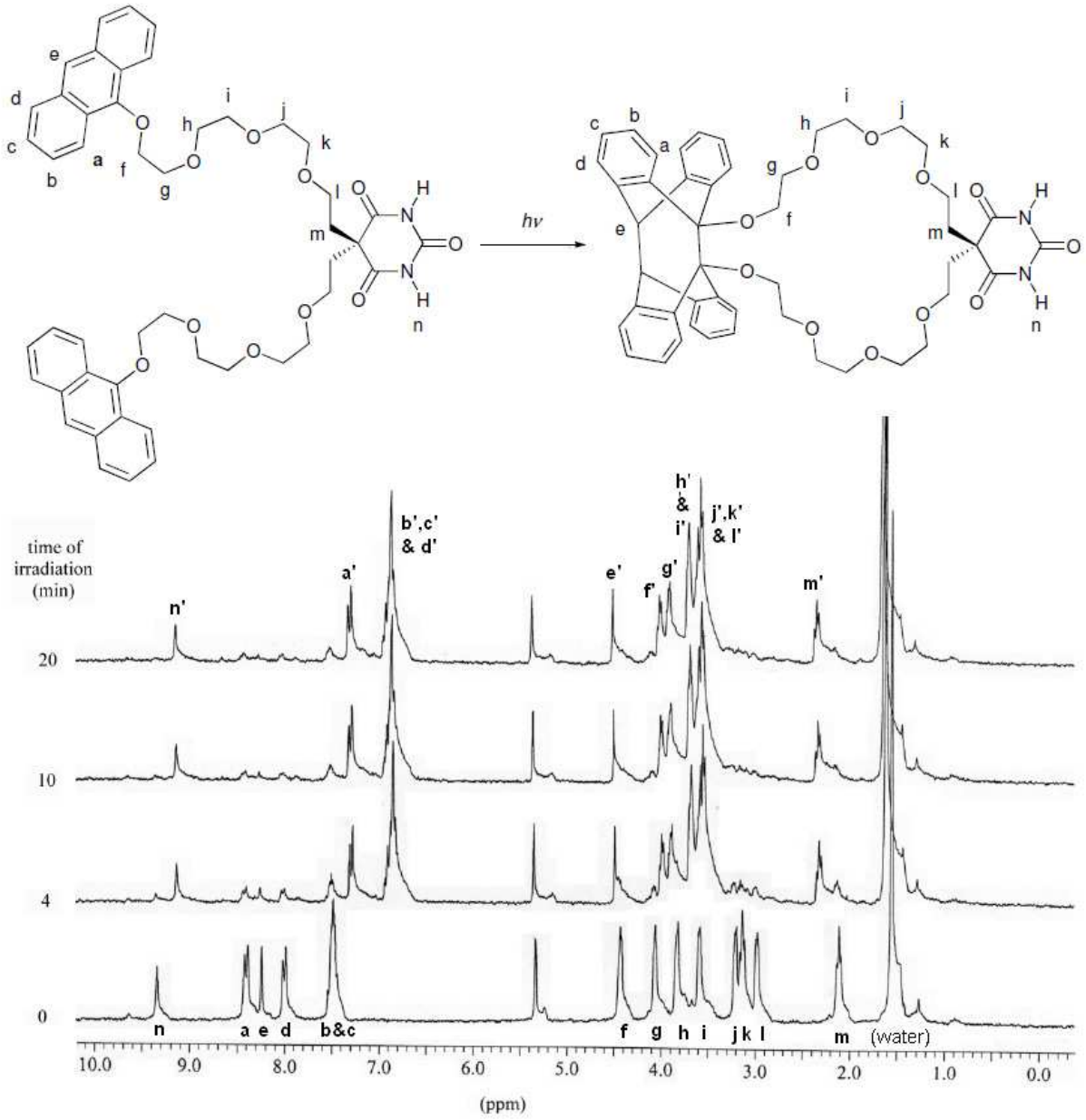

Figure 3.4b. Photocyclomerisation of **35** upon irradiation using a mercury lamp and a filter (saturated solution of lead acetate), followed by NMR in CD_2Cl_2, at a concentration of *2 mM*. Notice that the sample of **35** and/or the CD_2Cl_2 used was contaminated with water and other contaminants (unidentified peaks between *0* and *2 ppm*), which did not affect the changes observed upon irradiation.

The changes in the shifts of the aromatic protons are also characteristic of the formation of the anthracene dimer. It is however difficult to distinguish whether a *hh* or *ht* dimer has formed. A comparison of the two dimers of 9-(methoxy)anthracene in the literature[9] reveals that the signals for the aromatic protons closer to the substituent on the benzene ring (**a'**) should appear around *7.2 ppm* in the *hh* dimer, whereas in the *ht* dimer both

this proton and the proton *para* to it should form a multiplet at around *7.0 ppm* (see **Scheme 3.7**). In both cases, the integration patterns suggest a *hh* dimer, although in the case of **34c**, the spectrum is complicated by the presence of an NH signal (**l'**) at *7.2 ppm*.

It can also be observed that the signals for the CH_2 groups of the chain and the NH of the barbiturate shift upon photocyclomerisation. In particular, the NH signal (**l**) of **34** shifts from *8.7 ppm* in the non-cyclised form to *7.2 ppm* in the cyclised form (see **Figure 3.4**) and for **35** from *9.4 ppm* to *9.2 ppm*. This can be explained if in the non-cyclised form in solution, the NH partly binds to the polyethylene glycol chain through an intramolecular hydrogen bond, but not in the cyclised form. This explanation would also be consistent with the kinetic scheme used for explaining the results of fluorescence decay: the conformer *A* would be the conformer with the NH bond to the chain.

3.3) Conclusion and further work

The synthesis of these substituted barbiturates via the malonate has proved to be relatively easy. Different barbiturates can be designed in the same way, including different olefin-terminated barbiturates or trityl-phenol-stoppered barbiturates, where the stopper group would be less labile than the simple trityl stopper.[12]

Although the study of the fluorescence decay, quantum yields of fluorescence and photodimerisation have given much information on the photochemistry of **34** and **35**, more experiments are possible to get an even better understanding of their properties. The fluorescence quantum yield of **35** has not been measured, and variable temperature measurements might allow a better model to be established, in particular by measuring the rate of return from the excimer of **34** to the dissociated excited state.[11] Nevertheless, there were notable differences in photochemistry between **34** and **35**. In particular, it was observed that the internal anthracene dimer is formed more quickly with **35** than with **34**, making the lifetime of the excimer so short in the case of **35** that it can be ignored. The photocyclomer of

35 is also less thermally stable than that of **34**. Both of the barbiturates appear to form intramolecular *hh* dimers.

The binding of these barbiturates to "Hamilton-like" receptors, and attempts to obtain mechanically interlocked structures from these complexes, either by anthracene dimerisation or metathesis, will be studied in *Chapter 4*.

---

[1] (**a**) Procedure followed for the synthesis of disubstituted malonates: Hirose, T.; Hiratani, K.; Kasuga, K.; Saito, K.; Koike, T.; Kimura, E.; Nagawa, Y.; Nakanishi, H. *Journal of the Chemical Society, Dalton Transactions* **1992**, *1992*, 2679-2683; (**b**) conversion of malonate to barbiturate: Yoon, J. H.; Park, Y. J.; Lee, J. H.; Yoo, J.; Jun, C.-H. *Organic Letters* **2005**, *7*, 2889-2892.

[2] C. Lincheneau, *"Photogénération de Molécules Entrelacées : Photocaténation"*, Master report, Université Bordeaux 1, Bordeaux, **2006**.

[3] (**a**) structural aspects: Bouas-Laurent, H.; Castellan, A.; Desvergnes, J.-P.; Lapouyade, R. *Chemical Society Reviews* **2000**, *29*, 43-55; (**b**) mechanistic aspects: Bouas-Laurent, H.; Castellan, A.; Desvergnes, J.-P.; Lapouyade, R. *Chemical Society Reviews* **2001**, *30*, 248-263.

[4] Schill, G. *Catenanes, Rotaxanes and Knots*; *Organic Chemistry, A Series of Monographs*, Vol. 22, Academic Press: New York, **1971**.

[5] (**a**) McSkimming, G. *Photo-active Anthracene Receptors for* s-*Block and* d-*Block Metals*; PhD Thesis, University of Exeter, **2001**; (**b**) McSkimming, G.; Tucker, J. H. R.; Bouas-Laurent, H.; Desvergne, J.-P. *Angewandte Chemie International Edition* **2000**, *39*, 2167-2169; (**c**) McSkimming, G.; Tucker, J. H. R.; Bouas-Laurent, H.; Desvergne, J.-P.; Coles, S. J.; Hursthouse, M. B.; Light, M. E. *Chemistry, a European Journal* **2002**, *8*, 3331-3342.

[6] (**a**) Chandross, E. A.; Ferguson, J. *Journal of Chemical Physics* **1966**, *45*, 3554-3564; (**b**) Ferguson, J.; Morita, M.; Puza, M. *Chemical Physics Letters* **1976**, *42*, 288-292; (**c**) Morita, M.; Kishi, T.; Tanaka, M.; Tanaka, J.; Ferguson, J.; Sakata, Y.; Misumi, S.; Hayashi, T.; Mataga, N. *Bulletin of the Chemical Society of Japan* **1978**, *51*, 3449-3457; (**d**) Ferguson, J.; Castellan, A.; Desvergne, J.-P.; Bouas-Laurent, H. *Chemical Physics Letters* **1981**, *78*, 446-450.

[7] *Jobin Yvon Application Notes F-10 - Which Fluorescence Lifetime System is Best for You?*, URL: http://www.horiba.com/fileadmin/uploads/Scientific/Documents/Fluorescence/F-10.pdf.

[8] Valeur, B. *Invitation à la fluorescence moléculaire*; De Boeck Université: Bruxelles, **2004**.

[9] (**a**) Becker, H.-D. *Chemical Reviews* **1993**, *93*, 145-172; (**b**) Becker, H.-D.; Langer, V. *Journal of Organic Chemistry* **1993**, *58*, 4703-4708.

[10] (**a**) Parker, C. A. *Proceedings of the Royal Society A* **1953**, *220*, 104-116; (**b**) Hatchard, C. G.; Parker, C. A. *Proceedings of the Royal Society A* **1956**, *235*, 518-536.

[11] Marquis, D.; Desvergne, J.-P.; Bouas-Laurent, H. *Journal of Organic Chemistry* **1995**, *60*, 7984-7996.

[12] (**a**) Amabilino, D. B.; Ashton, P. R.; Boyd, S. E.; Gómez-López, M.; Hayes, W.; Stoddart, J. F. *Journal of Organic Chemistry* **1997**, *62*, 3062-3075; (**b**) Mahoney, J. M.; Shukla, R.; Marshall, R. A.; Beatty, A. M.; Zajicek, J.; Smith, B. D. *Journal of Organic Chemistry* **2002**, *67*, 1436-1440; (**c**) Chen, L.; Zhao, X.; Chen, Y.; Zhao, C.-X.; Jiang, X.-K.; Li, Z.-T. *Journal of Organic Chemistry* **2003**, *68*, 2704-2712.

4) APPROACH TO CATENANES WITH THE FLEXIBLE BARBITURATES

4.1) Binding studies

4.1.1) Titrations followed by UV-vis spectrometry

A first attempt at obtaining the binding constant between macrocycle **16** and guests **34** and **35** in a similar way to what was done with barbital was unsuccessful, as the software Letagrop could not accurately fit the data. It appeared that this was due to absorption by the anthracene unit of the guests, which was leading to high absorption values when more than 3 equivalents of barbiturate were added, and masking the slight changes in the pyridine band that related to complexation. Assuming that the absorption of the anthracene containing guest would not change upon complexation of the barbiturate moiety to the receptor, it was thought that its absorption could be subtracted from the spectrum, which would allow the data to fit with Letagrop (see **Figure 4.1**).

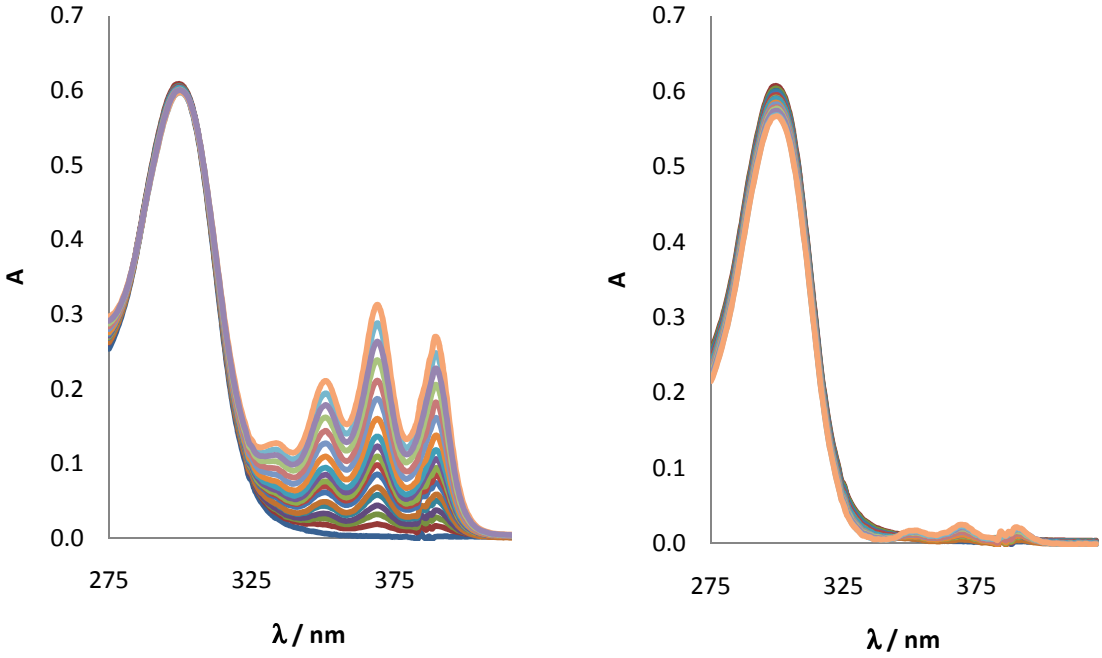

Figure 4.1. Absorption of the solution during the titration of a solution of **35** (2×10^{-5} M) by **12** (uncyclised receptor, *n* = *6*), from *0* to *1.2 equiv.* in DCM at room temperature, before (left) and after (right) correction of the correction due to the anthracene moiety of **35**.

However, as only low excesses of barbiturates were used and as the process of correcting the absorption due to the anthracene was also increasing the experimental error with the "corrected" absorption values, a relatively high margin of error in the binding constant resulted and sometimes a fit was difficult to obtain. The values for these binding constants are given in **Table 4.1**, along with the margin of errors given by Letagrop.[1]

Table 4.1. Binding constants for guests **34**, **35** and **36** obtained by titrations in DCM at room temperature, followed by UV, calculated with Letagrop.

complex	*n*	*log(K)*	*margin of error*
16•34	8	4.61 (barbital: 5.52)	0.04
12•35	6	3.73 (barbital: 4.58)	0.03
15•35	6	4.06 (barbital: 5.09)	0.07
16•35	8	3.65 (barbital: 5.52)	0.01
18•36	6	4.357 (barbital: 5.79)	0.001

What can be observed first is that, notwithstanding the uncertainty over the real margins of error, all the binding constants seem to be lower for each receptor than those with barbital, which can be explained on steric grounds. In order to enable a comparison of the finer differences between the binding constants with different guest compounds, **36**, which has trityl groups instead of anthracene groups, was also tested. As **36** does not absorb in the anthracene region, an excellent fit and margin of error was obtained for a binding constant of *log(K) = 4.36*, which is similar to the value of *log(K) = 4.06* found for the titration of **15** with **35**. As **18** is the reduced form of **15** and **36** is similar to **35** where the anthracene groups have been replaced by trityl groups, this result is not unexpected and indicates at least that the order of magnitude of the binding constants found with the anthracene-tagged barbiturates is correct.

The binding constant for the "open" receptor **12** with **35** has an intermediate value between the binding constants for the "closed" receptors **16** and **15** with **35.** This is different

to what was observed with barbital, where the binding constant was smaller with the open receptors than with the closed receptors, as expected because of the macrocyclic effect. It can be interpreted by the role of steric effects: in the complexes with the closed receptors, the favourable macrocyclic effect is outweighed by larger unfavourable steric effects with the closed receptors than with the open receptors.

Steric effects can again be involved to explain the differences in binding strength between the different complexes. A comparison between **16•35** and **15•35** reveals a higher binding constant for the smaller receptor **15**, and a comparison between **16•35** and **16•34** reveals a higher binding constant for the smaller barbiturate **34**. These results appear to be influenced by the size of the ring of the receptor relative to the length of the anthracene-terminated arms of the barbiturate. If the arms of the barbiturate are approximately as long as the dimension of the ring (as in **16•35**), then the binding constant is smaller because of the steric clash between the anthracene ends of the barbiturate and the alkyl group of the receptor. If they are longer (as in **15•35**) or shorter (as in **16•34**), then this steric interaction is less likely to take place.

4.1.2) Titrations followed by fluorescence

Titrations of the anthracene-tagged barbituric acids **34** and **35** with different receptors were also undertaken by monitoring the emission or excitation spectra of a solution of the barbiturate at a concentration of $2 \times 10^{-5}\ M$ at room temperature in the presence of increasing amounts of the receptor. With **34**, three titrations were made using the receptors **14**, **16** and **18**, and another titration was made between **35** and **15**.

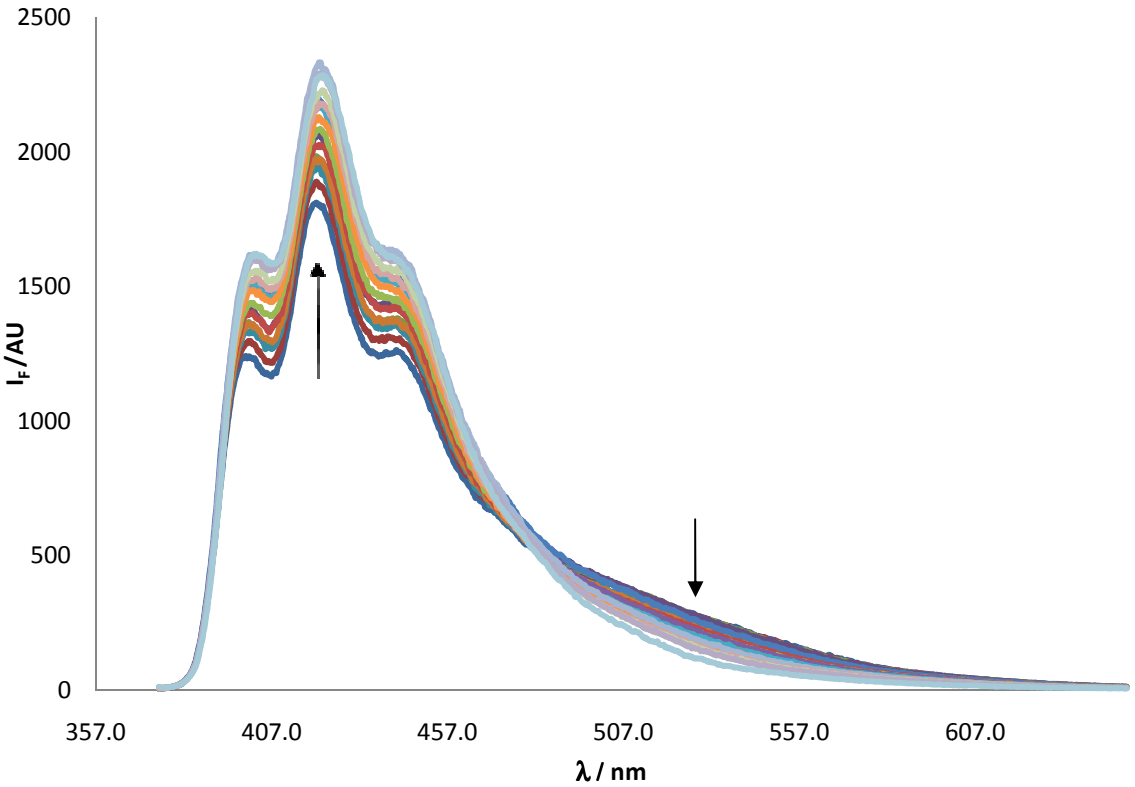

Figure 4.2. Changes in the emission spectrum of a solution of **34** in DCM (initial concentration 2×10^{-5} *M*) upon addition of **18** (from *0* to *2.0 equiv.*), $\lambda_{exc.} = 369$ *nm*.

Emission spectra were recorded with an excitation wavelength of $\lambda_{exc.} = 369$ *nm* for emission wavelengths ranging from *375* to *650 nm*. In the titrations with receptors **18** or **16** added to **34** and with **15** added to **35**, an increase in the anthracene monomer emission was observed upon addition of the receptor, which was interpreted as a sign of formation of the complex.[2] However in the case of **34** (whose fluorescence spectrum, contrary to **35**, presents an excimer band, cf. *Chapter 3*), the increase in monomer emission was accompanied by a decrease in the excimer emission (see **Figure 4.2**), which indicates that the rate constant for the formation of the excimer from the anthracene singlet excited state is probably lower in the complexes **16•34** and **18•34** than it is in free **34**. The increase in emission of the monomer is then interpreted as an effect of the disappearance of the excimer with **34**, and possibly due to the disappearance of a non-emissive excimer in the case of **35**.[2]

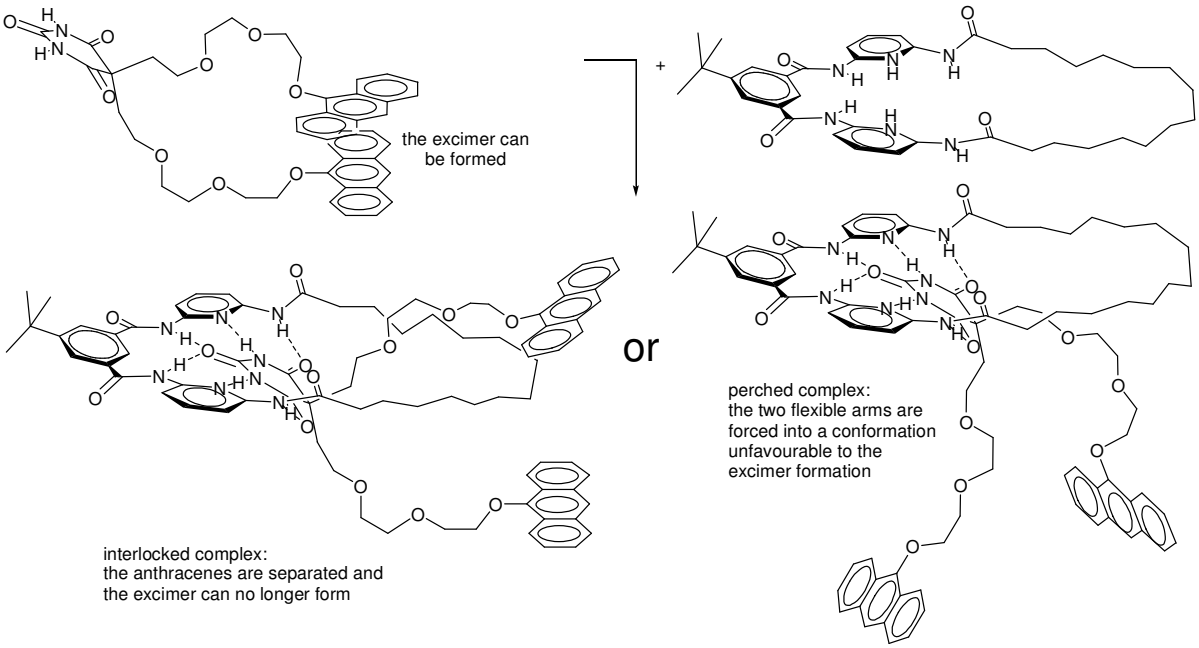

Scheme 4.1. Possible geometric origin of the disappearance of the excimer in the complex of **34** with the closed receptor **18**.

The disappearance of the excimer can be attributed to a blocking of the approach of the two terminal anthracene groups. As shown in **Scheme 4.1**, if the barbiturate is actually threading through the receptor to form an interlocked complex, the intervening macrocyclic ring of receptors **18** and **16** can repel the two anthracene-terminated arms and make their mutual approach more difficult. But if the barbiturate is actually not threading through the receptor and forms a "perched complex", it is also possible that this occurs because of an unfavourable conformation for excimer formation as the guest is complexed.

In the titrations of **34** with **18** and **16**, excitation spectra were also recorded upon addition of the receptor, by recording the emission of the anthracene ($\lambda_{em.} = 420\ nm$) for excitation wavelengths ranging from *220* to *400 nm* (see **Figure 4.3**). As observed with the emission spectra, the emission obtained when irradiating in the anthracene absorption band (between *330* and *390 nm*) increased with the amount of receptor. But the emission was also seen to increase for excitation at the wavelength of the pyridine band of the receptor (around *300 nm*). This can be understood as the result of an electronic energy transfer from the excited pyridine to the lower lying anthracene excited state, which results in subsequent anthracene

fluorescence. As explained in *Chapter 1*, energy transfer from "Hamilton-like" receptors to fluorescent-tagged barbiturates has been observed previously.[3] Due to the short excited-state lifetimes (a few *ns*) and the short range of energy transfer processes (a few *nm*), as well as the dilute nature of the solutions (a few μM), the quenching of the excited pyridine confirms complex formation. Thus static quenching is predominant, rather than diffusion limited, more commonly observed for long-lived excited states.[4] When more than one equivalent of receptor was added, this pyridine band started to diminish (the light blue curve in **Figure 4.3** that crosses the other curves is for *2 equiv.* of receptor). This clearly indicates that the energy transfer occurs between the components of one complex and not from the free receptor in solution.

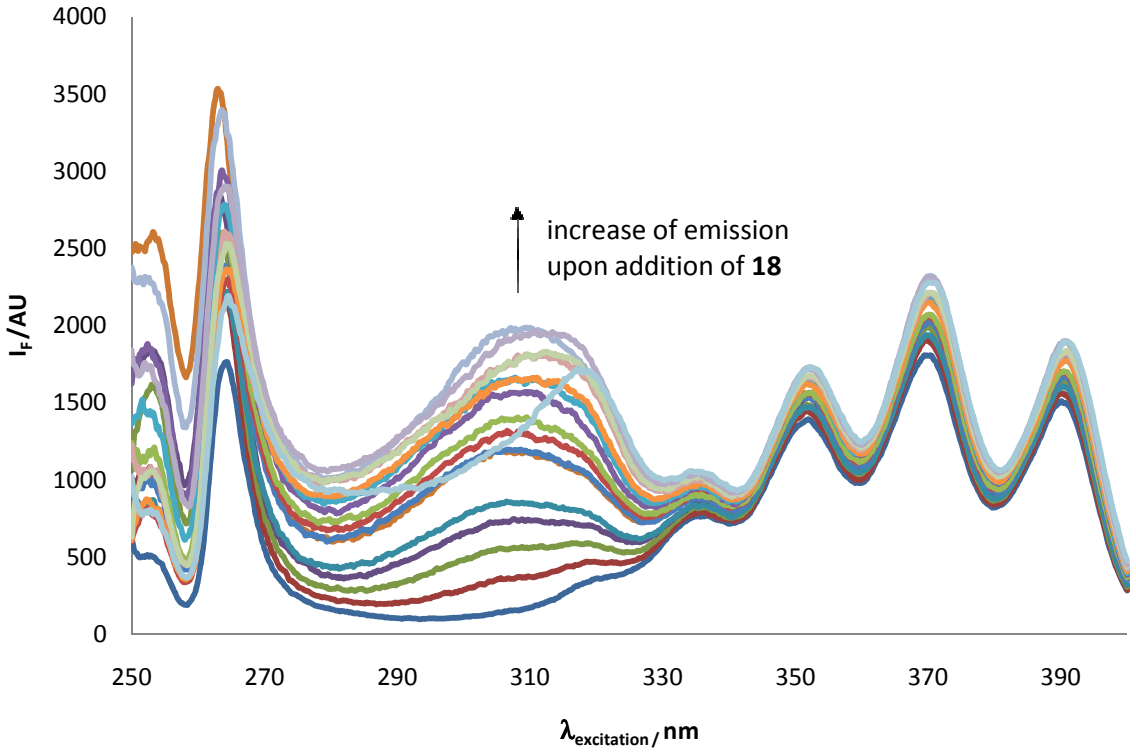

Figure 4.3. Changes in the excitation spectrum of a solution of **34** in DCM (initial concentration 2×10^{-5} *M*) upon addition of **18** (from *0* to *2.0 equiv.*), $\lambda_{em.} = 420$ *nm*.

In the titration between **34** and receptor **14**, only small variations in the intensity of the emission spectra were observed, with the general shape of the emission spectrum unaltered and the excimer band remaining. In the emission spectrum of a solution of **34** containing an

excess of the receptor **17**, which is the "reduced" version of **14** and has the same size, it was seen that diminution of the excimer emission still occurred but the change was less than that observed with the larger receptor **18** under the same conditions (see **Figure 4.4**). An excitation spectrum of this solution also showed that some energy transfer existed between the pyridine of the receptor and the anthracene of the guest, which indicates close approach and confirms that a complex is actually forming. This energy transfer, however, is also lower than that with **18**, as indicated by the comparison of the excitation spectra (**Figure 4.4**). This can be related to a lower binding affinity of **34** to **17** than to **18**, which would mean that less complex is formed and thus energy transfer is less efficient.

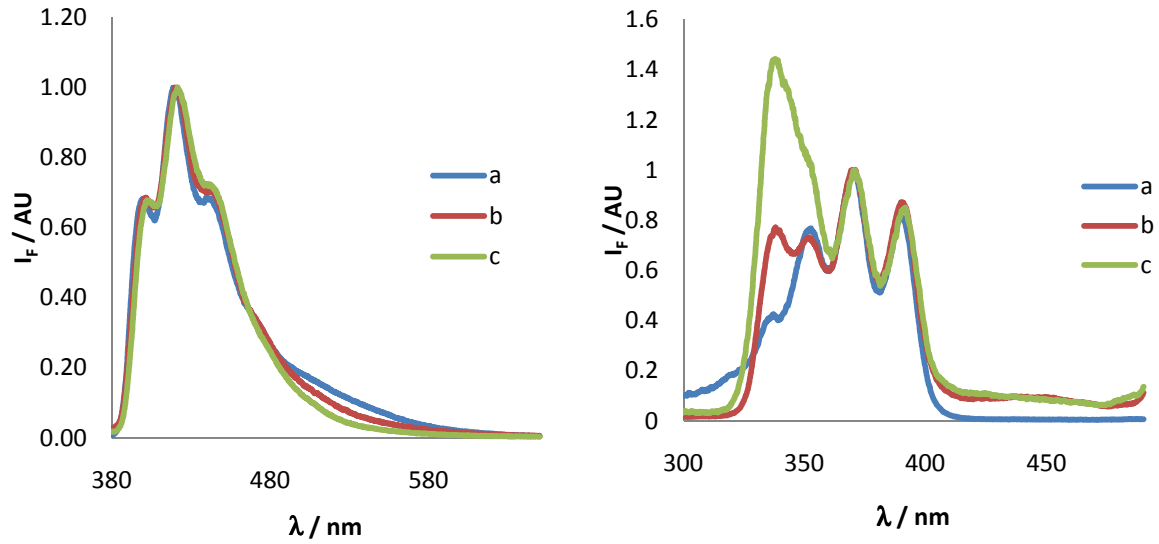

Figure 4.4. Comparison of the emission spectra ($\lambda_{exc.}$ = *420 nm*, left) and excitation spectra ($\lambda_{em.}$ = *500 nm*, right) of (a) **34**, (b) mixture of **34** (*1.8 mM*) and **17** (*20 mM*), and (c) mixture of **34** and **18**, same concentrations. All spectra are normalised to show the same intensity for the maximum of anthracene emission / resp. absorption.

Finally, the fluorescence data obtained in the experiments described above (both emission and excitation spectra) were used for calculating the binding constants using the software Letagrop.[1] The results are given in **Table 4.2**, where the margin of error are given by Letagrop. For **14•34**, the data could not be fitted by Letagrop because of the small changes that were observed. The values of *log(K)* found by this method are larger than those found by UV. This can be due to experimental error, because the values of fluorescence emission are

strictly proportional to concentration only for very low concentrations,[4] but it can also be due to a genuine difference as it has already been described in the literature[2,5] that binding constants of molecules to anthracene-tagged receptors can be higher when one of the anthracenes is in an excited state.

Table 4.2. Binding constants calculated from the titrations by fluorescence in DCM at room temperature.

complex	*n*	*log(K)*	*margin of error*
16•34 By emission	8	5.1 (absorption: 4.61)	0.2
16•34 By excitation	8	5.2	0.2
18•34 By emission	6	5.1	0.2
18•34 By excitation	6	5.1	0.3
15•35 By emission	6	4.9 (absorption: 4.06)	0.1

4.1.3) Titration followed by ITC

The binding constant for the olefin-terminated barbiturate **37** and **18** was measured by ITC in DCM at *25°C* (*298 K*). The results found were as follows:

$$log(K) = 4.62 \pm 0.04 \text{ (vs. } 5.33 \pm 0.07 \text{ for barbital)}$$

$$\Delta H° = -9.6 \pm 0.9 \text{ kcal.mol}^{-1} \text{ (vs. } -15.0 \pm 0.2 \text{ for barbital),}$$

$$\Delta S° = -11.0 \pm 3.0 \text{ cal.K}^{-1}\text{.mol}^{-1} \text{ (vs. } -25.8 \pm 0.8 \text{ for barbital).}$$

In comparison to barbital, it can be seen that the value is lower, and of the same order of magnitude as the binding constants found for **34**, **35** and **36** by UV. It can be observed that it is the enthalpic term $\Delta H°$ that explains the difference with barbital, with $\Delta H°$ more endothermic ($\Delta(\Delta H°) = +5.4$ kcal.mol^{-1}), whereas the term $-T.\Delta S°$ partly compensates this variation ($\Delta(-T\Delta S°) = -4.4$ kcal.mol^{-1}). This is somewhat similar, although the differences are less important, to what was observed with the complex between **17** and barbital, where

these observations were related to the barbital binding by only 3 hydrogen bonds to the receptor (see *Chapter 2*). In this case, it may indicate again that the complex formed in this case is somehow structurally different from the complexes with barbital. For example, the two lateral chains may force the barbiturate to sit in a position which is not ideal for strong H-bond interactions. This enthalpic contribution to a lower binding constant is partly compensated by a favourable entropic contribution, which can be interpreted as the result of increased freedom of motion, which could be a result of different types of complex being present in solution (*e. g.* perched and threaded) in equilibrium.

4.2) Closing of the receptors by olefin metathesis

As was done with barbital (cf. *Chapter 2*), the effect of metathesis on the complexes of the trityl-stoppered barbiturate **36** with the different receptors was studied by doing the following experiments: 1:1 mixtures of **36** with different receptors in solution in $CDCl_3$ were prepared, at a concentration of *6 mM*. When the receptor contained a double bond or a terminal olefin, a metathesis reaction was performed (addition of 10 mol% of Grubbs 1st generation catalyst, then reflux 30 minutes). The solutions were analysed by ^{1}H NMR and mass spectrometry (ES^+ and MALDI) both before and after metathesis, in order to verify that metathesis occurred, to check any differences in the structure of the products, and to test if rotaxanes could be detected.

The NMR of the 1:1 mixture with the non-cyclic receptor **12** is presented in **Figure 4.5**. Only the downfield part of the NMR spectrum is shown, which depicts the aromatic signals of the receptor (but not those of the trityl-barbiturate that start just on the right of this region) and the NH signals. It can be seen that these NH signals are significantly shifted upon complexation with **36** due to the expected H-bonding interactions The NH of the receptor closest to the benzene bridge (**c**)^{2b} shifts from *7.7* to *9.6 ppm*, the other NH of the receptor (**g**) shifts from *8.7* to *10.1 ppm*, and the barbiturate NH (**h**) shifts from *9.3* to *12.3 ppm*.

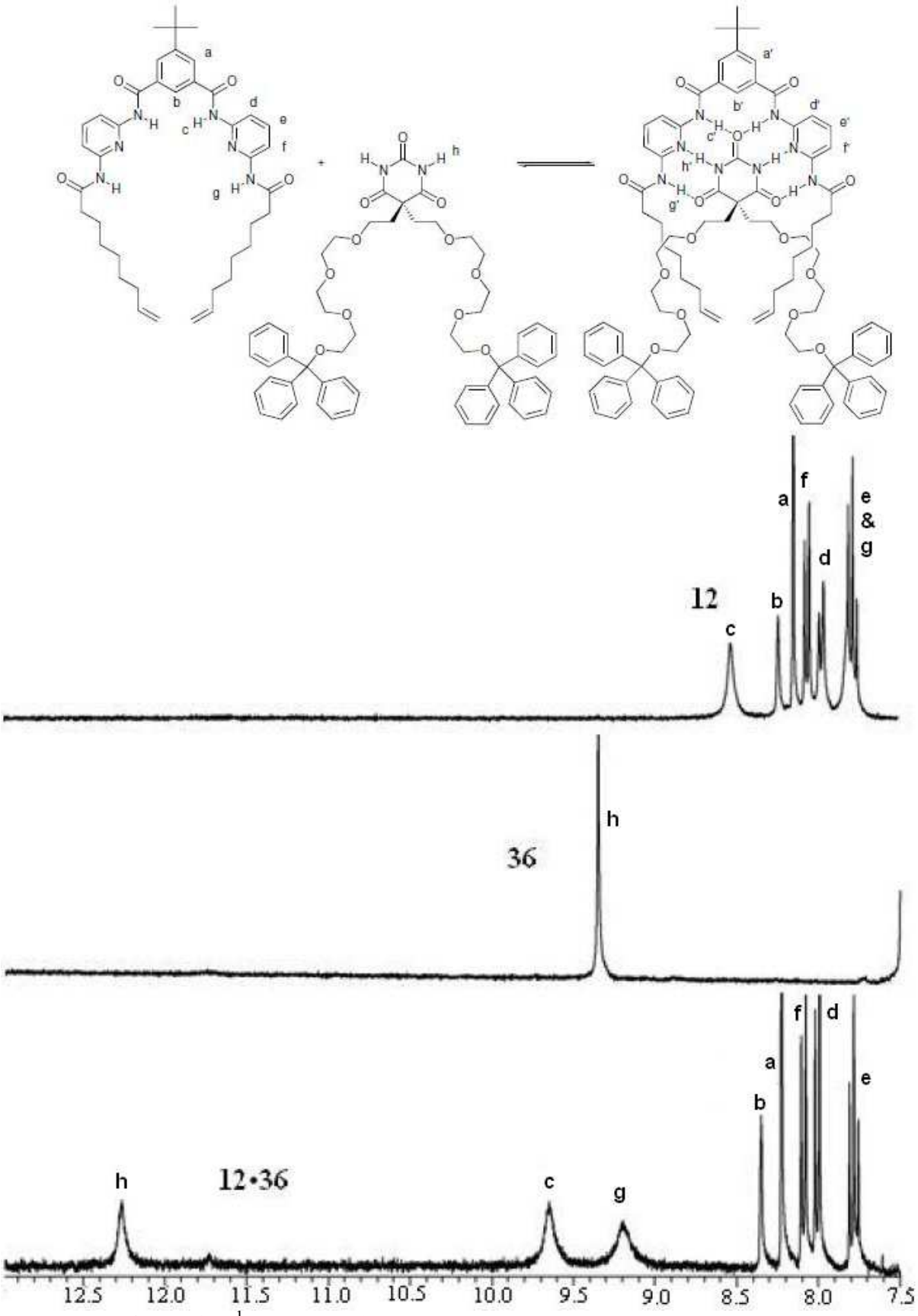

Figure 4.5. ^{1}H NMR of **12**, **36** and their 1:1 mixture in $CDCl_3$, *6 mM*.

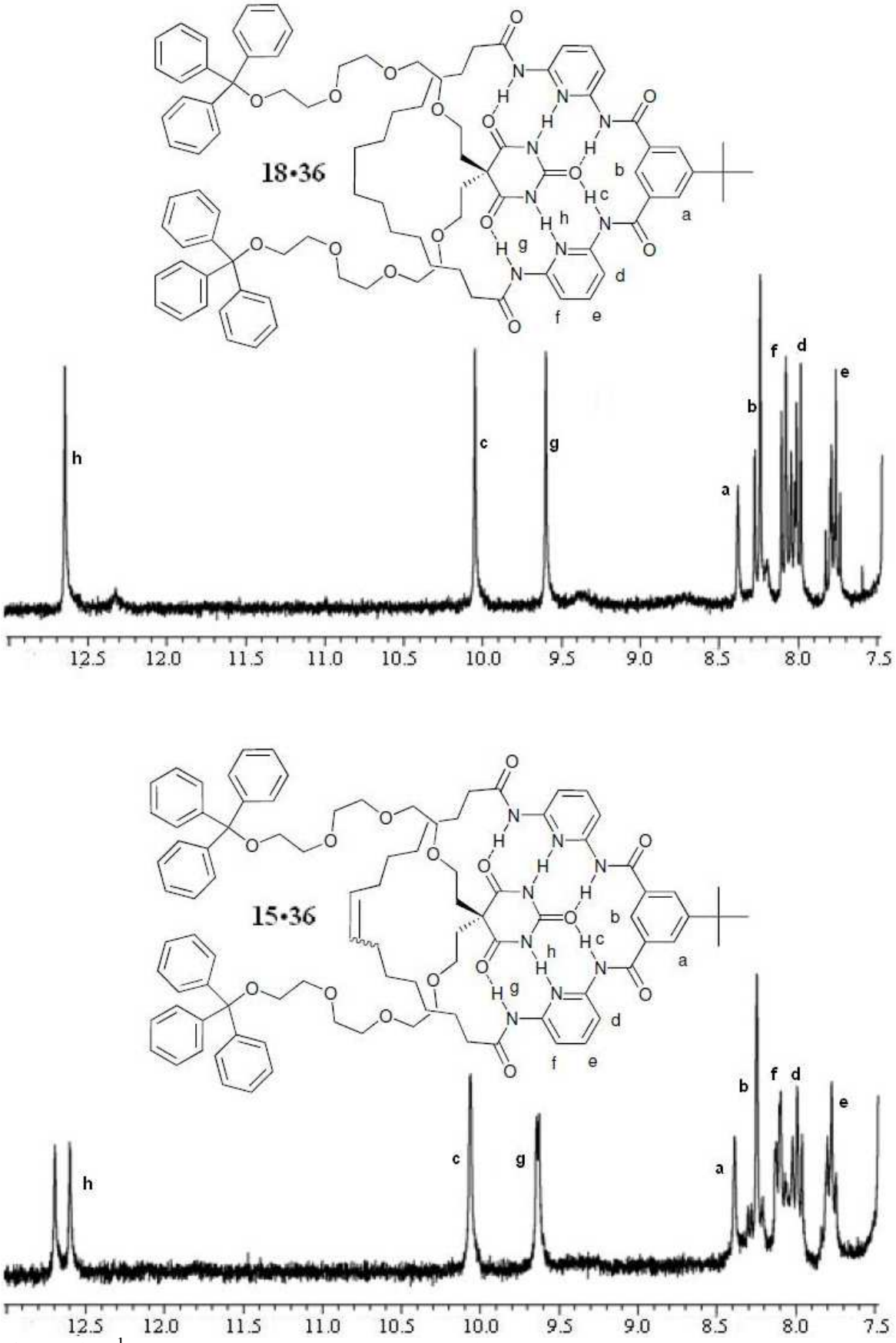

Figure 4.6. ^{1}H NMR spectra of 1:1 mixtures of **18** and **36** (top) and **15** and **36** (bottom) , in $CDCl_3$, *6 mM*.

With receptor **18**, which does not possess an olefinic double bond, the top spectrum in **Figure 4.6** was obtained. A comparison with the spectrum of **12•36** (**Figure 4.5**) shows two differences: the downfield shift of the NH peaks (**c**, **h** & **g**) is greater, which is consistent with a stronger binding interaction, and the shape of these peaks is thinner, which may indicate that the relative freedom of motion of the two components is less, at least on the NMR timescale. With receptor **15**, which only differs from **18** by the presence of an olefinic double bond, the bottom spectrum in **Figure 4.6** was obtained. While the two spectra reveal that the shifts of the NH protons are similar and the peaks are approximately as sharp in both, the main difference is that with **15** the barbiturate NH peak and the peak for the NH protons of the receptor closest to the central benzene bridge are split into two peaks of approximately similar height. The chemical shifts observed with **15•36** are as follows: *9.62 & 9.64 ppm* for the split NH signal (**g**), *10.06 ppm* for the other NH of the receptor (**c**), *10.60 & 12.69 ppm* for the barbiturate NH (**h**).

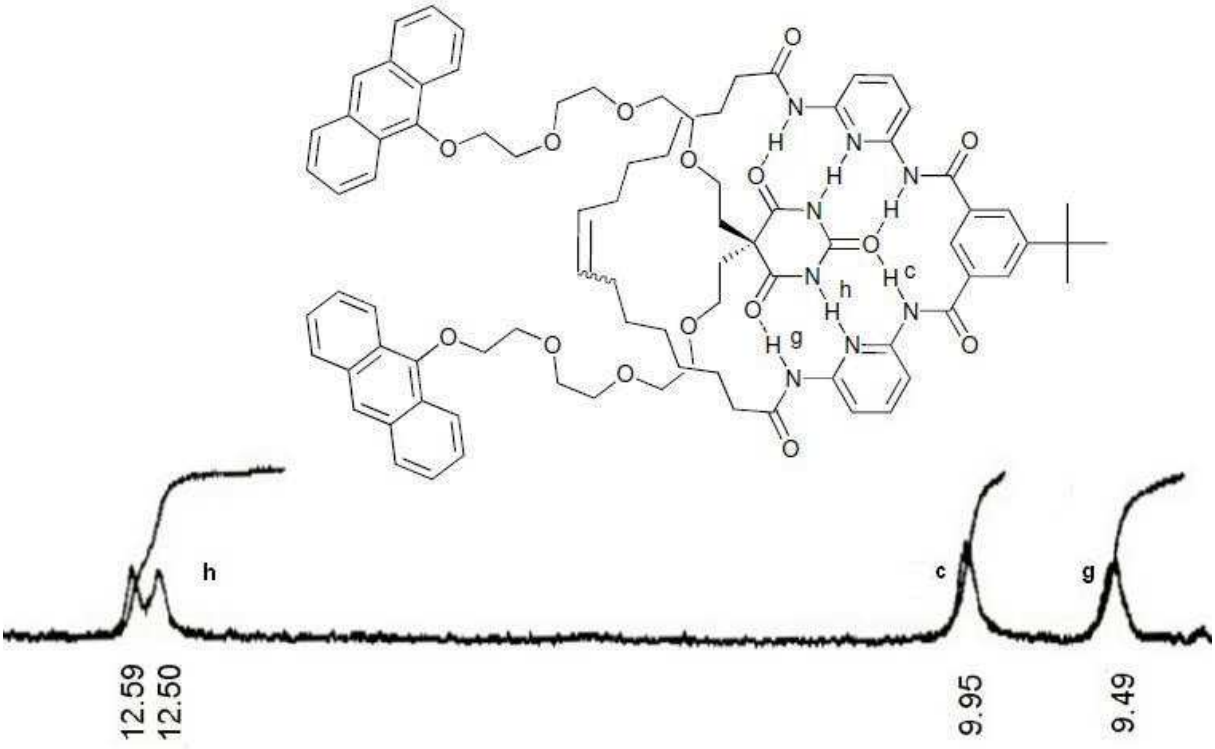

Figure 4.7. ^{1}H NMR spectrum of **15•35** in CD_2Cl_2, *2 mM*.

It was also noted that a similar splitting of the NH signals was observed in the complexes of receptors **14**, **15** and **16** with anthracene tagged barbiturates **34** and **35** (cf. **Figure 4.7** and also **Figures 4.9** to **4.14**) but not with the "reduced" receptors **17** and **18**. This splitting of the NH signals (**c**, **h** & **g**) upon complexation is therefore seen with all the flexible barbiturates terminated by bulky groups (but not with barbital nor with **37**) and only with the double-bonded cyclic receptors (*i. e.* not with the "reduced" receptors).

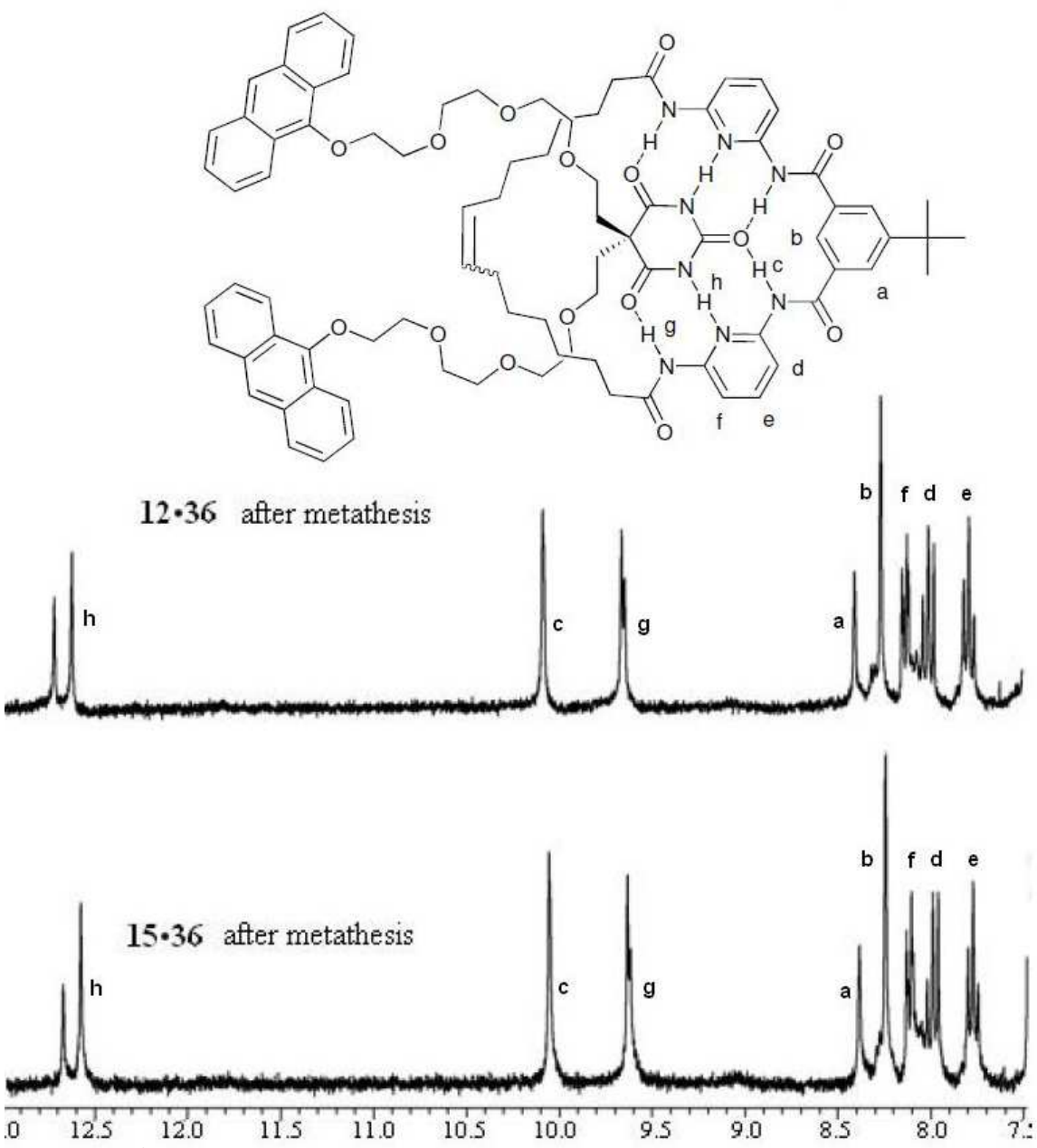

Figure 4.8. ^{1}H NMR spectra of 1:1 mixtures **12** and **36** (top) and **15** and **36** (bottom) after metathesis, in $CDCl_3$, *6 mM*.

When a metathesis reaction was performed on the solution of a solution of a 1:1 mixture of acyclic **12** and **36**, the result was as shown in **Figure 4.8**: the peaks were the same as in the spectrum of **15•36** (**Figure 4.6** bottom) but the relative heights of the different peaks were different. The same thing was observed when performing metathesis on the complex **15•36**: after metathesis, the height of the peaks changed to become nearly identical to what was obtained having done the metathesis on **12•36**.

How can this be explained? Clearly, two different complexes are formed between **36** and **15**. It is possible to imagine two different geometries for the complex, one interlocked or *threaded*, and one non-interlocked or *perched*. But if this was the explanation, it would also be observed with **18**, where the only difference is the absence of a double bond. Furthermore, the fact that both complexes are present in the 1:1 mixture of **15** and **36** even before metathesis would indicate that the perched and interlocked structures would be in thermodynamic equilibrium, which implies that it should not be affected by a metathesis experiment, where clearly it is. In other words, the fact that the ratio between the complexes is affected by metathesis implies that the two complexes are *not* in thermodynamic equilibrium with one another, except under the conditions of metathesis. This leads to another explanation, which is that the two *cis* and *trans* isomers of **15** actually bind **36** slightly differently, leading to different signals in the ^{1}H NMR spectrum. It is interesting to notice that if this is the correct explanation, the binding of the guest can actually modify the *cis-trans* ratio after metathesis. But if this is the correct explanation, then the *cis-trans* ratio would be approximately 50/50 in the mixture used as the two signals corresponding to the two complexes with **15** have approximately the same integration, which contradicts the value of 79/21 determined by ^{13}C NMR (cf. *Chapter 2*). This difference could be due to the fact that integral heights in ^{13}C spectra are not accurate but it is more likely to do with the fact that **15**

was re-synthesised for this experiment: the proportion of *cis* and *trans* isomers may have been different in the two samples.

The interpretation of the mass spectrometry results (see *Appendix 2*) is difficult as the two techniques used (ES^+ and MALDI) can show associated adducts that in fact are not (or very weakly) associated under other experimental conditions.[6] The results were studied in the positive ion mode and it is clear that some of these species are only weakly ionising to form cations in these conditions. In one of the experiments (**14•36** - after metathesis), a dimer of the receptor was observed: this was related to its aggregation (cf. *Chapter 2*). The mass of the complex was also seen in two cases (**18•36**, and **14•36** - after metathesis) but this cannot be considered as evidence for the formation of a rotaxane since it could simply be a perched complex.

4.3) Attempts to obtain catenanes by anthracene photodimerisation

4.3.1) Changes in photochemistry upon complexation

The quantum yields of dimerisation and rate constants of thermal returns of the complexes of the anthracene-tagged barbiturates with the receptor **16** were measured using the same method as for the barbiturates (see *Chapter 6* for the experimental procedure) by monitoring the disappearance of the anthracene absorption band in the UV-Vis. spectrum of solutions of mixtures of the complexes. The results are presented in **Table 4.3**.

Table 4.3. Quantum yields of photocyclomerisation and times of thermal return of 1:1 mixtures of barbiturates **34** and **35** with **16**, measured by UV-vis. spectroscopy, in DCM at room temperature

Complex	Φ_d	k_{ret} / s^{-1}	$t_{1/2}$
16•34	0.0014 (**34** alone: 0.10)	$2.3.10^{-4}$ (**34** alone: $3.5.10^{-6}$)	50 minutes (**34** alone: 2.3 days)
16•35	0.026 (**35** alone: 0.28)	$2.7.10^{-4}$ (**35** alone: $7.6.10^{-4}$)	43 minutes (**35** alone: 15 minutes)

The ease of formation and the stability of the intramolecular anthracene dimers are clearly affected by complexation. It can be observed that the quantum yields are smaller upon complexation, more than 10 times for **35** and more than 70 times for **34**. The rate constant for thermal return is 65 times faster upon complexation for **34**, but 3 times slower for **35**. The dramatic changes observed with **34** can be interpreted in the same way as the disappearance of the excimer: the two anthracene groups, for geometric reasons, cannot easily approach one another in this complex; however it is not impossible to form an anthracene dimer, but it is also less stable than the dimer formed in the free form, as indicated by the higher rate constant for the thermal return. This is probably for steric reasons as more strain would make ring opening easier. With **35**, the dimer is also more difficult to form in the complex than in the free form, but the drop in the quantum yield is less pronounced. However surprisingly the dimer formed is in this case slightly more stable than the one formed in the free form.

4.3.2) Photocyclomerisation followed by NMR and mass spectrometry

In order to follow anthracene dimerisation in the H-bonded complexes in more detail, solutions of 1:1 mixtures of **34** or **35** with receptors **14**, **15** and **16** at a concentration of *2 mM* in CD_2Cl_2 were prepared, and a series of ^1H NMR spectra were made as a function of irradiation time (see *Chapter 6* for the experimental conditions). The results of these experiments are given in **Figures 4.9** to **4.14**,* and have to be compared with the spectra of the irradiation of the barbiturates **34** and **35** alone (**Figure 3.4** in *Chapter 3*). The aim of these experiments was to check the feasibility of the photocyclomerisation in the complexes, which is a necessary preliminary to obtain catenanes by this method, and to check for any differences in the structures of the complexes and kinetics of the photochemical reactions.

* NB: In **Figures 4.9** to **4.19**, a schematic representation of the molecules is given in order to attribute the signals. Although interlocked structures are represented, no assumption is made on whether it is interlocked or perched.

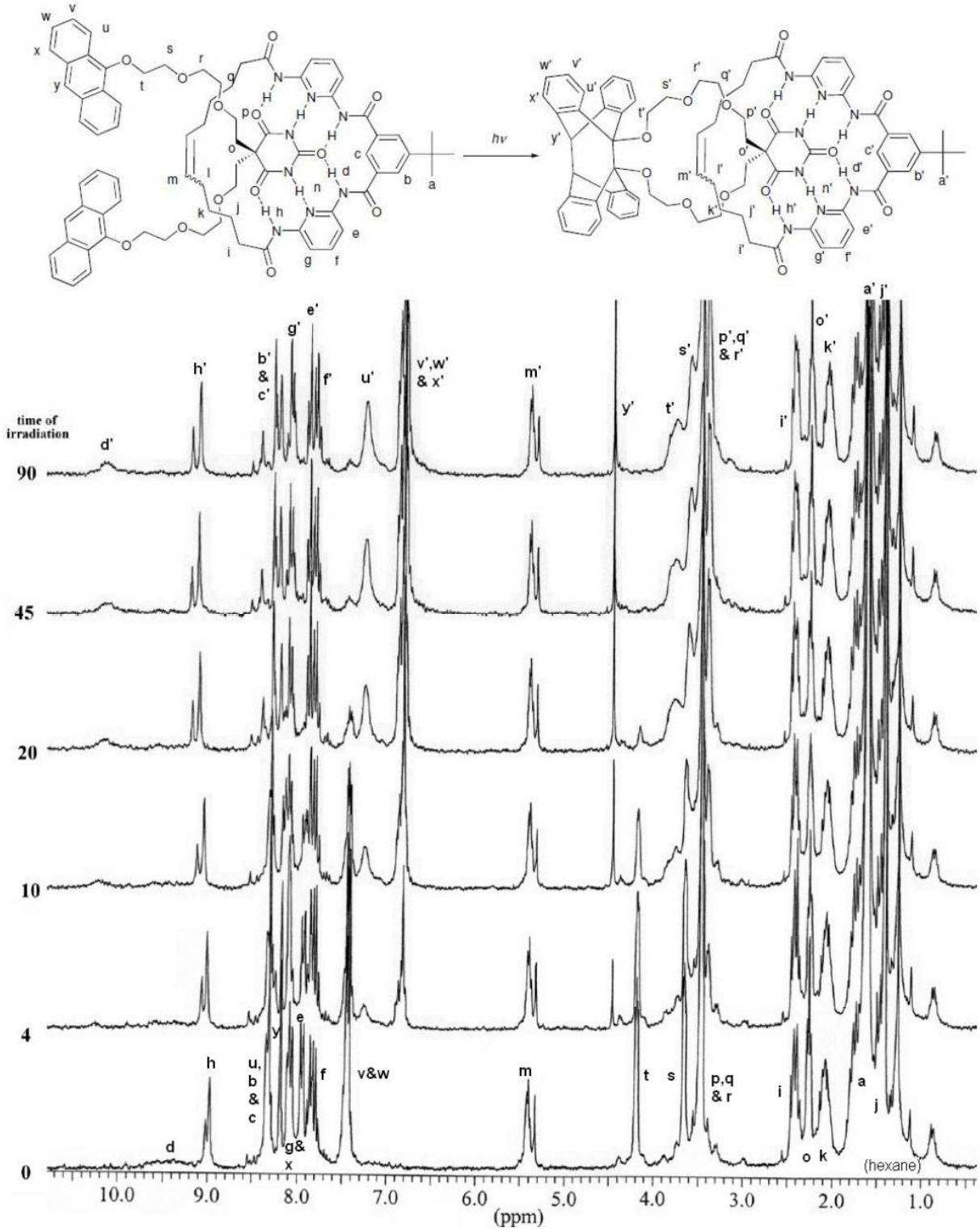

Figure 4.9. ^{1}H NMR of the complex **14•34** in CD_2Cl_2 upon irradiation over 90 minutes.

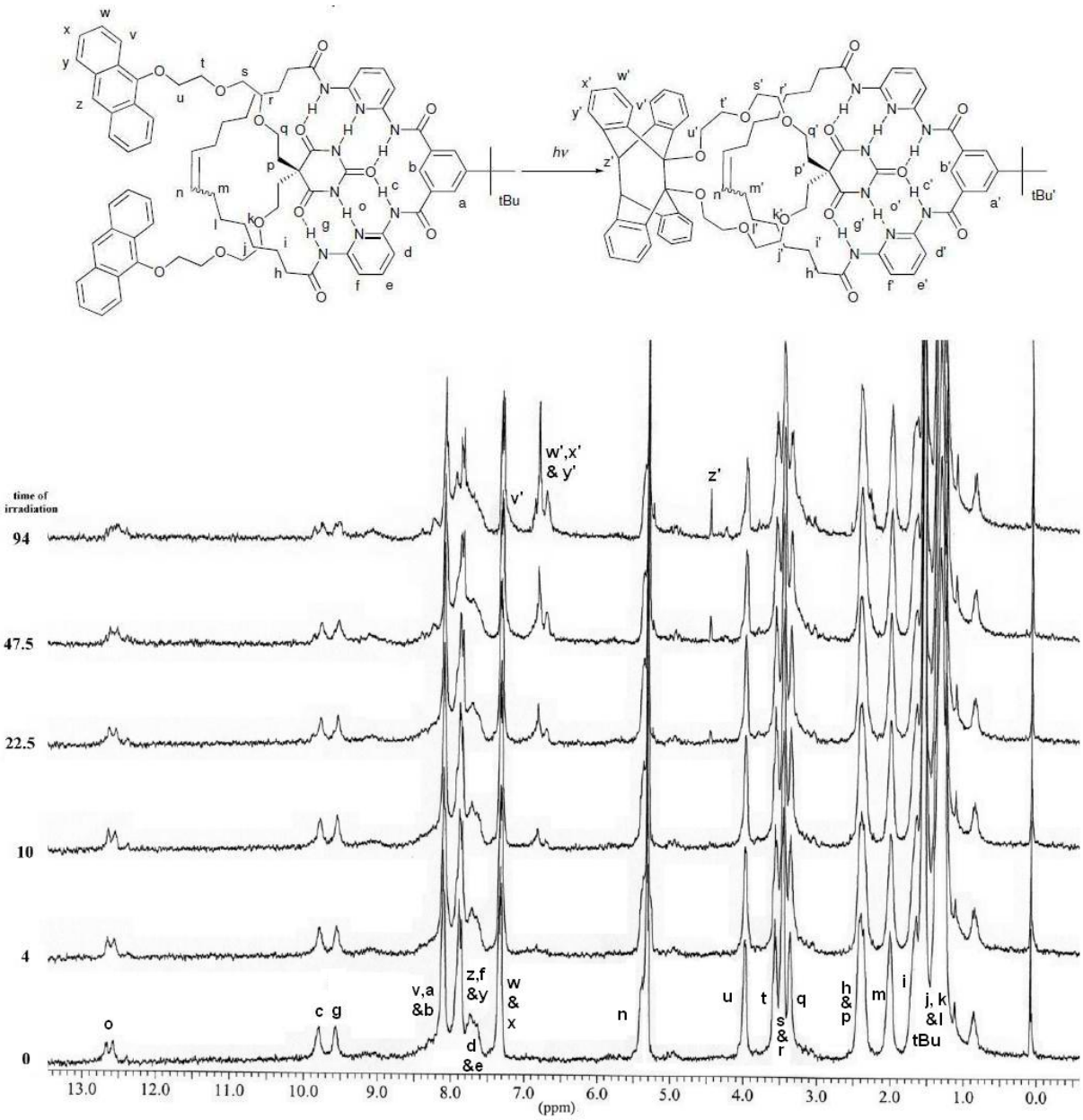

Figure 4.10. ^{1}H NMR of the complex **15•34** in CD_2Cl_2 upon irradiation over 94 minutes.

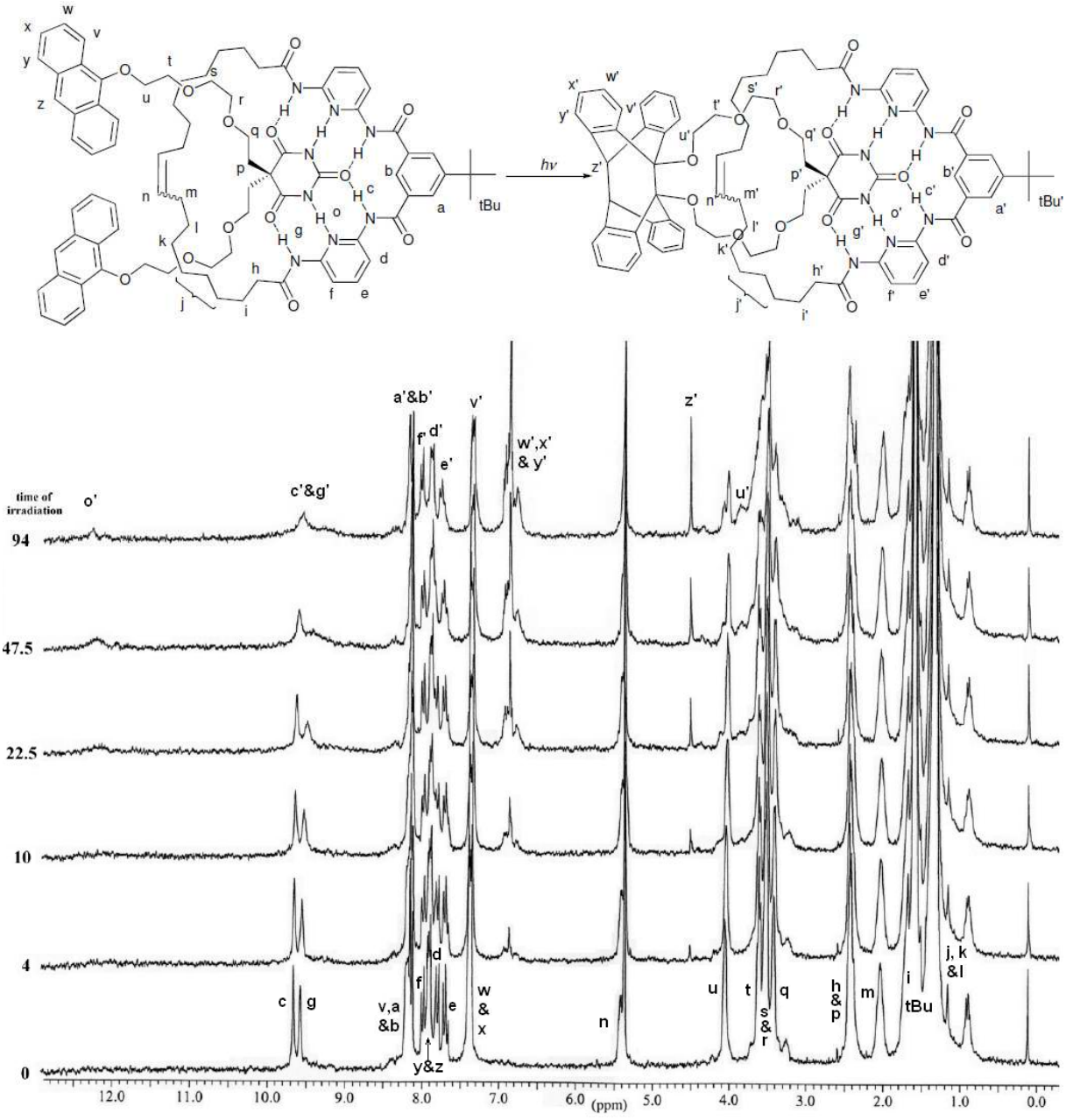

Figure 4.11. ^{1}H NMR of the complex **16•34** in CD_2Cl_2 upon irradiation over 94 minutes.

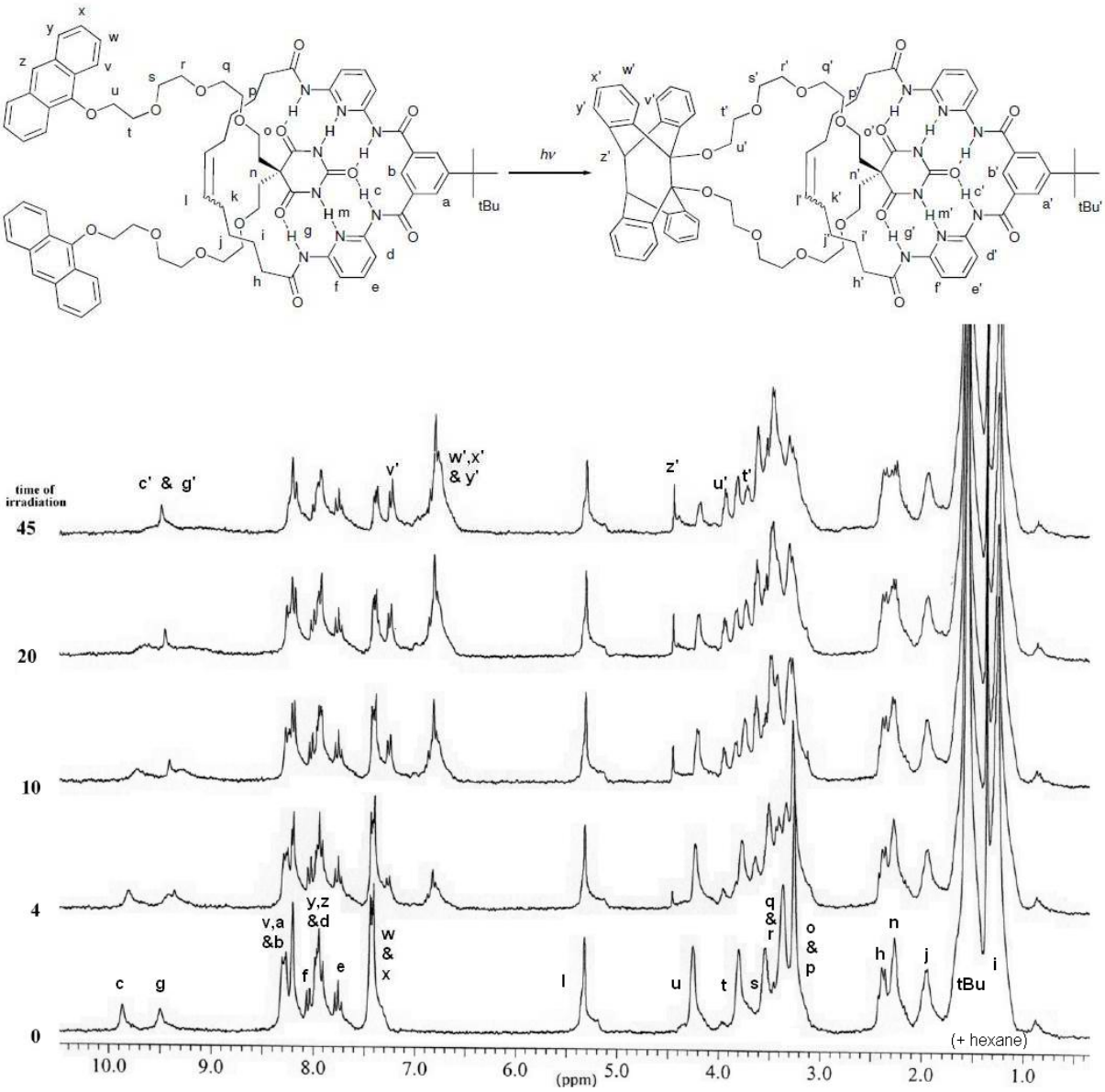

Figure 4.12. ^{1}H NMR of the complex **14•35** in CD_2Cl_2 upon irradiation over 45 minutes.

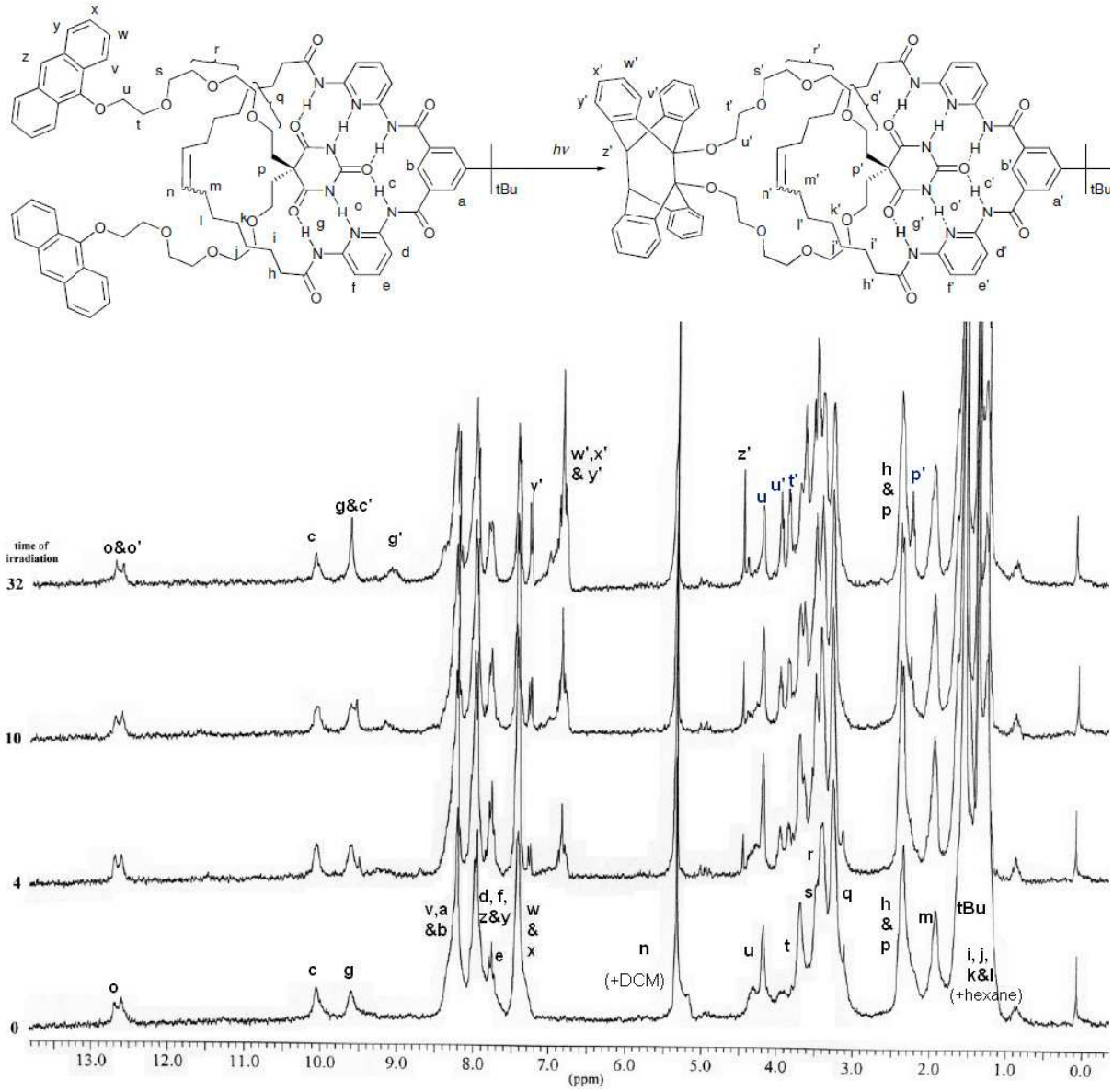

Figure 4.13. ^{1}H NMR of the complex **15•35** in CD_2Cl_2 upon irradiation over 32 minutes.

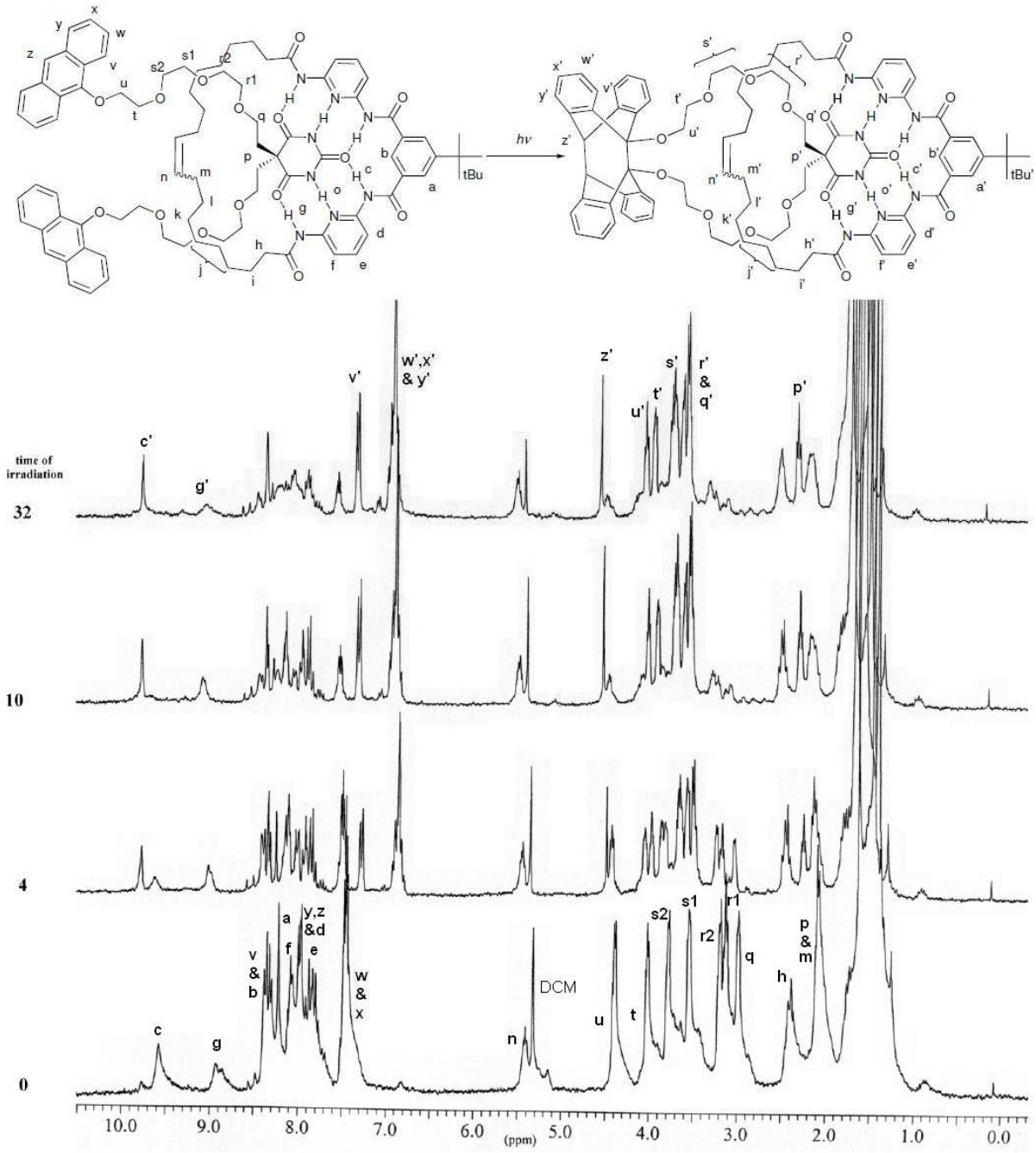

Figure 4.14. ^{1}H NMR of the complex **16•35** in CD_2Cl_2 upon irradiation over 32 minutes.

The appearance of an anthracene dimer is demonstrated in each case by the appearance of the singlet of the bridgehead proton, which appears at *ca. 4.5 ppm*. Quantum yields of dimerisation were not evaluated with precision here but as the conditions of irradiation were similar for every NMR tube, it can be assumed that the main differences observed in the irradiation time required for complete conversion to the dimer are related to differences in the quantum yields. With **34**, the photocyclomerisation was approximately as fast in the free

barbiturate as it was in the complex with **14**, slower with **16** and even slower with **15**. This is consistent with what was observed with the disappearance of the excimer, showing a more difficult approach of the anthracenes in the complexes with **15** and **16**. With **35** however, photocyclomerisation was faster in the complex with **16**, and slower with the two other receptors. It is as if the approach of the two anthracenes is not hampered at all in the complex with **16** whereas it is in the other complexes. A tentative explanation is that these observations are consistent with the formation of mostly interlocked complexes in the case of **34**, where the difficulty to form the dimer seems to be related to the distance between the macrocyclic ring of the receptor and the anthracenes (in between the anthracenes in the case of **16** and **15** and closer to the barbiturate centre in the case of **14**) whereas with **35**, perched complexes are indicated, as the difficulty to form the dimer seems to be related to the deformation imposed to the chains (greater with smaller receptors than with larger). It can also be observed that the signals corresponding to the CH_2 groups of the chain of the barbiturate are more numerous in the complexes of **35** with **14** and **15**, indicating that these two chains may not be in similar environments. This is consistent with the explanation above.

Similar experiments were also undertaken with **34** and the "reduced" receptors **17** and **18**. NMR spectra of 1:1 mixtures of the receptors with **34c** (photocyclised **34**) were also recorded. Then at the end of all these experiments, an excess of barbital was added to the tube and a final NMR was recorded. The solutions obtained were also analysed by MALDI mass spectrometry, in order to verify that catenanes were obtained. The ^{1}H NMR spectra of these experiments are given in **Figures 4.15** to **4.18**, and the MALDI spectra are presented in *Appendix 2*.

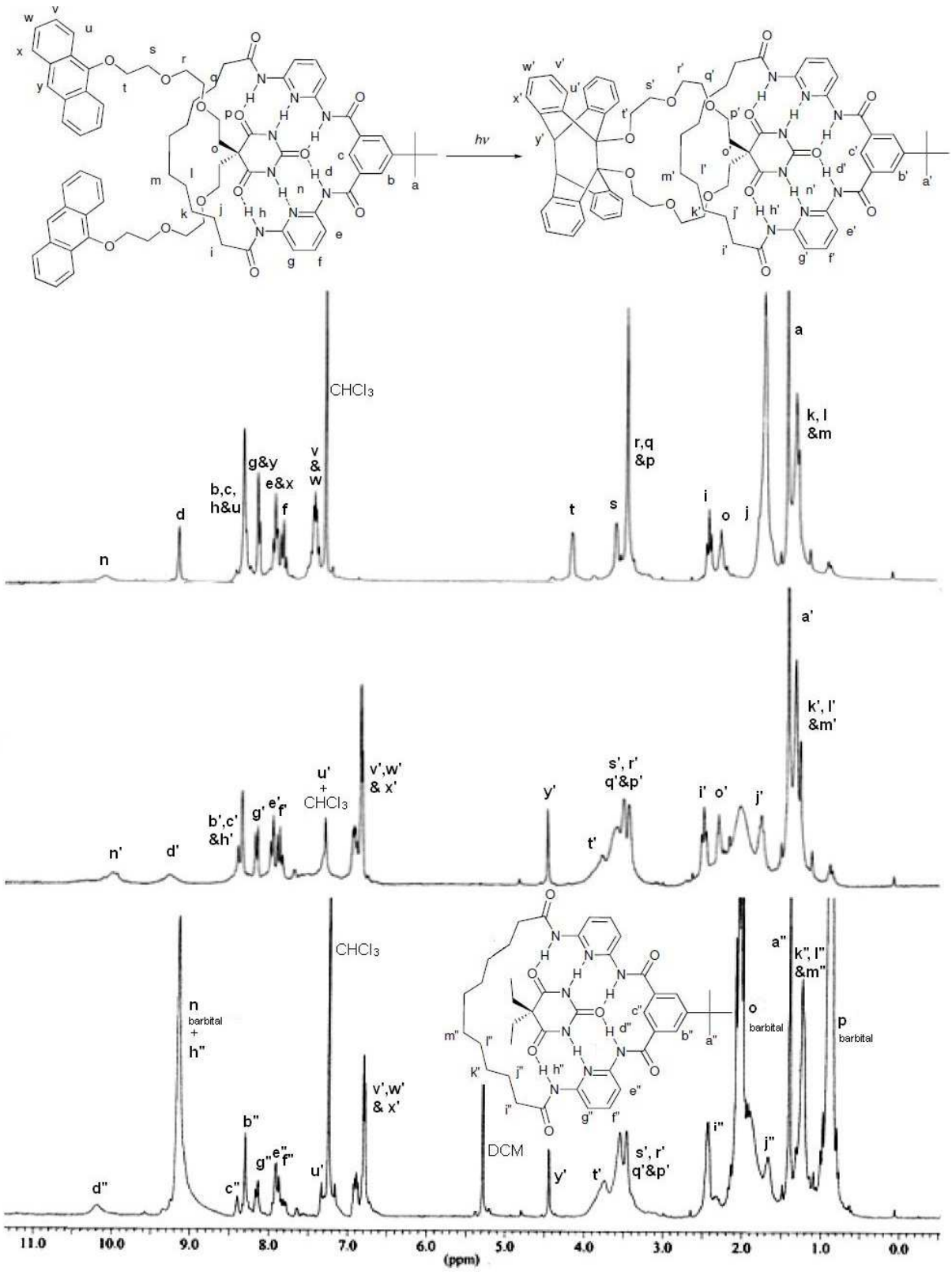

Figure 4.15. ^{1}H NMR ($CDCl_3$) of the 1:1 mixture of **17** and **34** before irradiation, after *90 min* of irradiation and after addition of an excess of barbital (contains DCM).

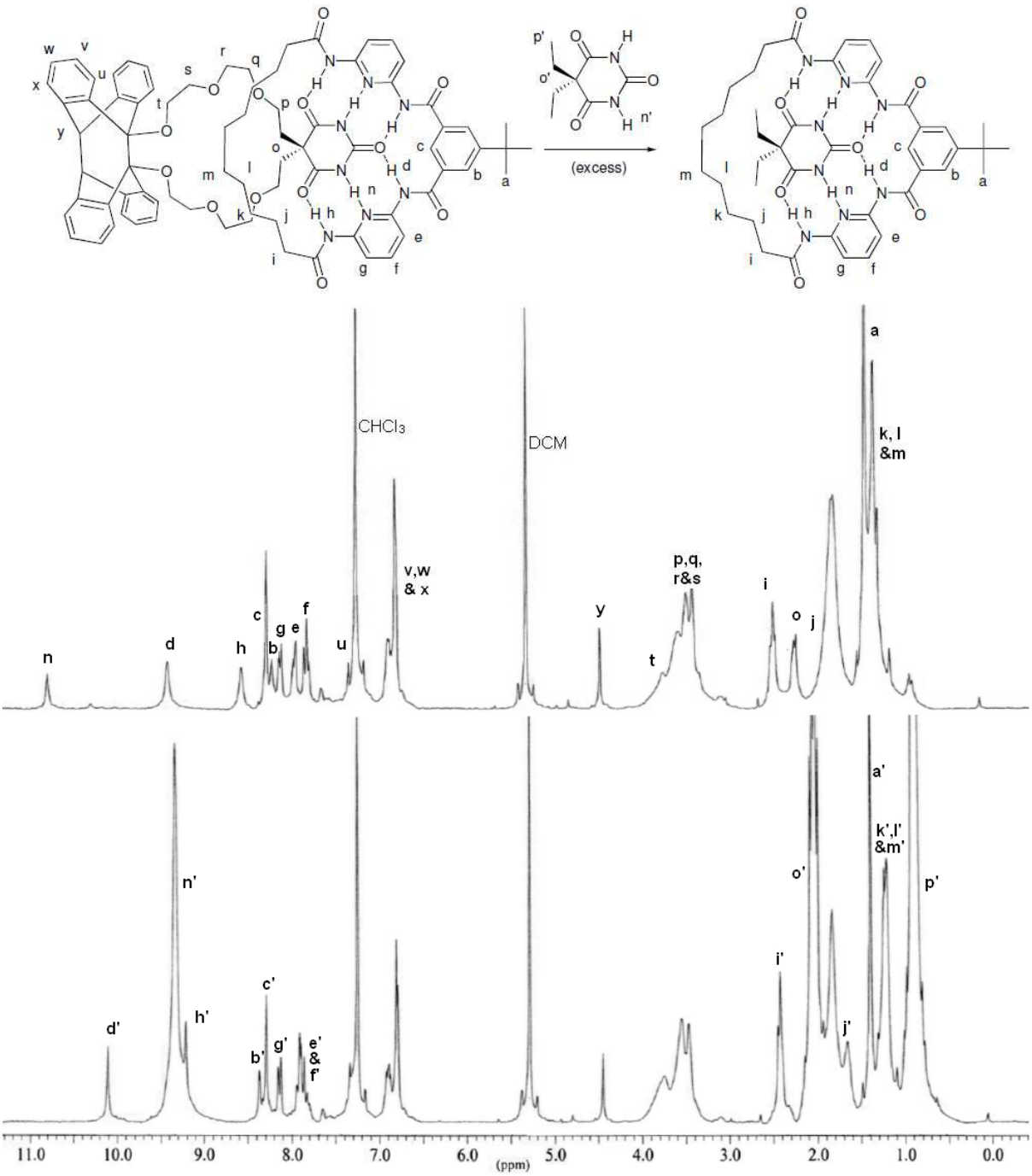

Figure 4.16. ^{1}H NMR ($CDCl_3$) of the 1:1 mixture of **17** and **34c** photocyclised separately and after addition of an excess of barbital.

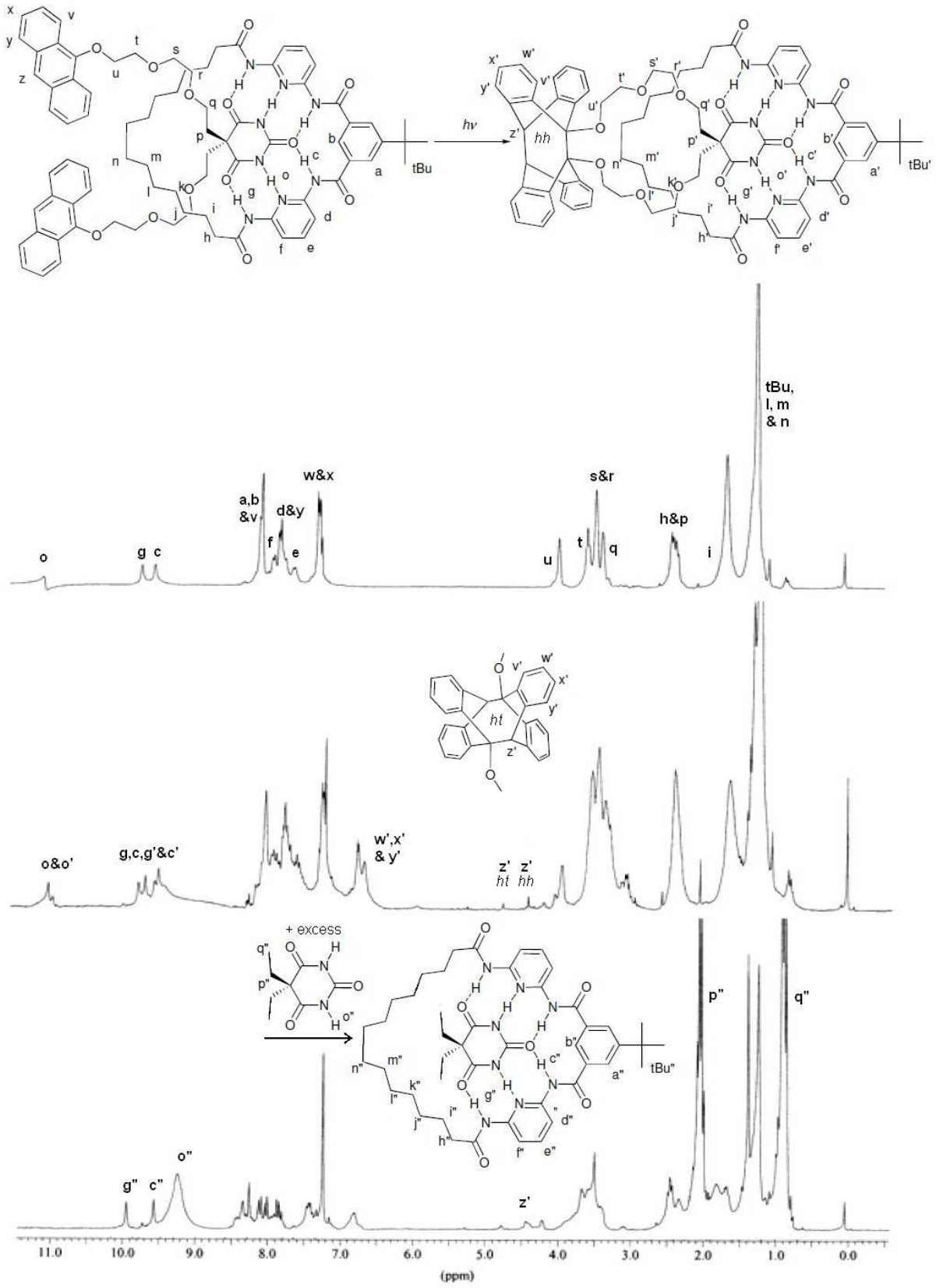

Figure 4.17. ^{1}H NMR ($CDCl_3$) of the complex **18•34** before irradiation, after *90 min* of irradiation and after addition of an excess of barbital.

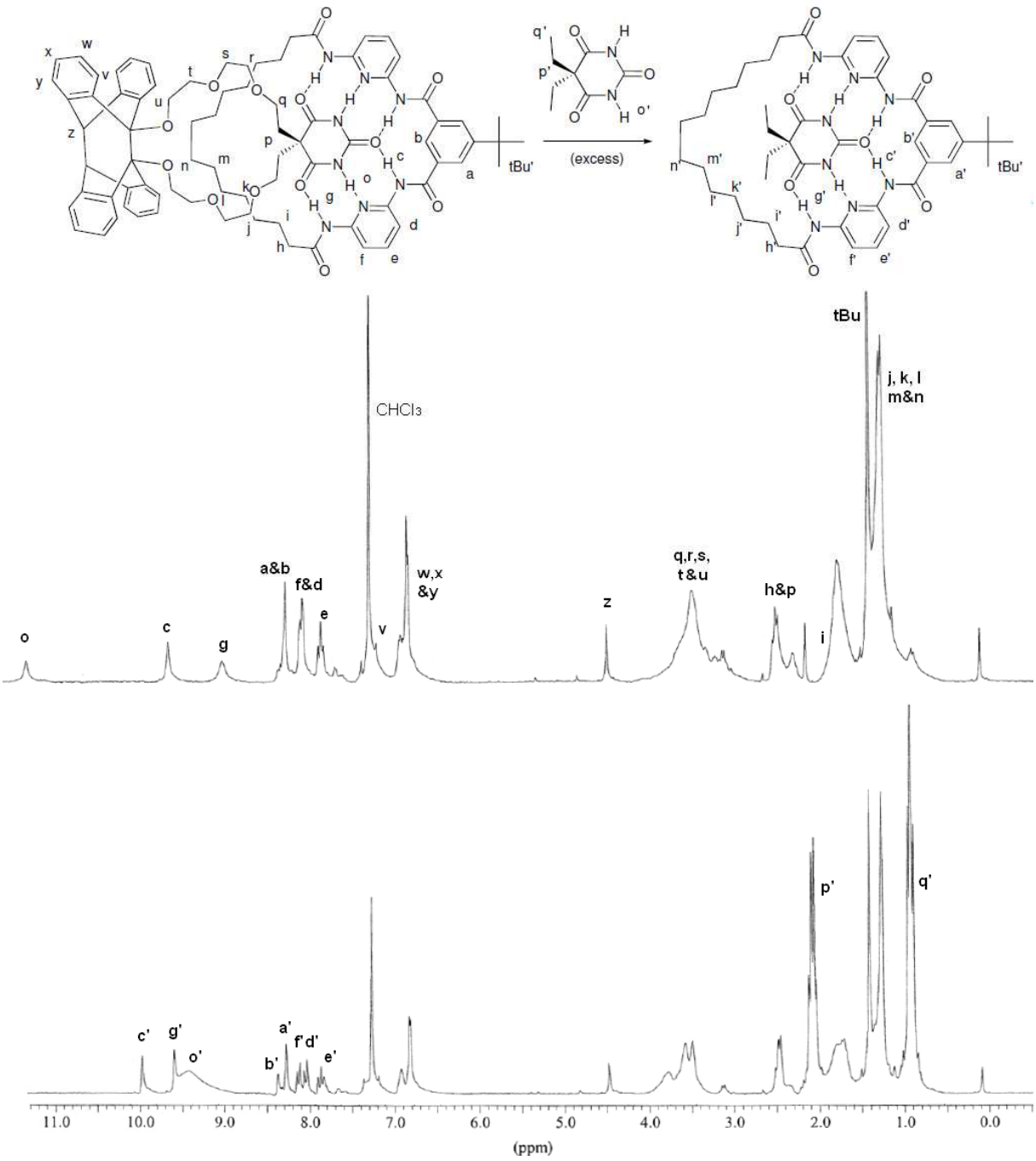

Figure 4.18. ^{1}H NMR ($CDCl_3$) of the complex **18•34c** formed separately and after addition of an excess of barbital.

In the case of **18**, it was seen that two different singlet signals corresponding to the bridgehead proton appeared in ^{1}H NMR, one at the same position (*4.5 ppm*) observed in all the other cases, and another at *4.8 ppm*. It was thought that this could be due to a faster photodimerisation of **34** outside the complex than bound to the receptor. In order to prove that, a 5:1 mixture of receptor **18** and barbiturate **34** was made and irradiated in the same

conditions: this time only the singlet at *4.8 ppm* appeared, showing that it was actually the position of the bridgehead proton of the cyclised complex (see **Figure 4.19**)

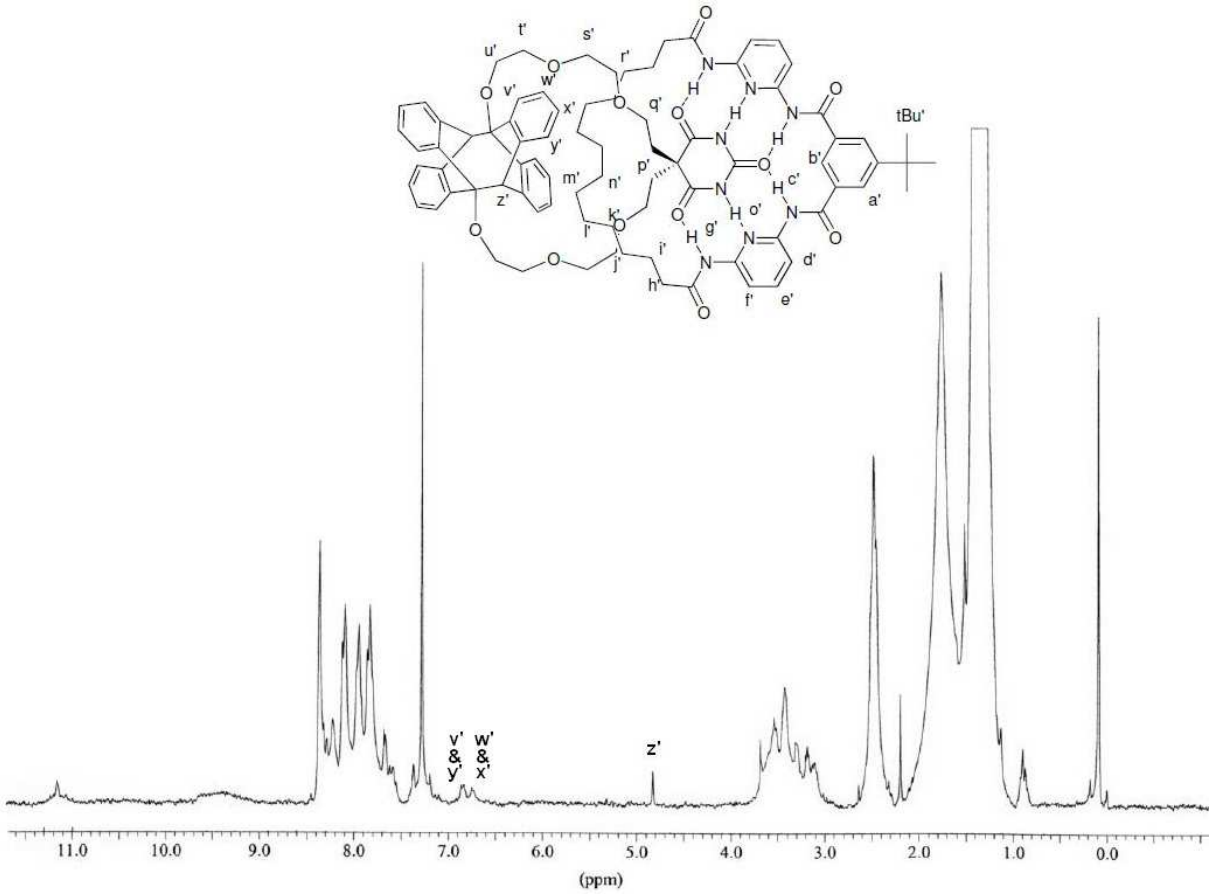

Figure 4.19. ^{1}H NMR of a 5:1 mixture of **18** and **34** after *90 min* of irradiation

For the case of the 1:1 mixture of **34c** and **18**, only the bridgehead proton at *4.5 ppm* was seen, which clearly indicates that this bridgehead proton is in different environments when the photocyclomerisation is undertaken in the presence or absence of receptor **18**, and that the *4.5 ppm* value is not affected by the complexation. Therefore, probably a different photocyclomer, with a different structure, is forming in the complex which cannot be an unsymmetrical anthracene dimer as the bridgehead proton is still present in the ^{1}H NMR spectrum as a singlet. Thus the *4.8 ppm* signal could either indicate a *head to head dimer* in a different environment, for example an interlocked structure, or a *head to tail dimer*, which seems more likely as the shape and chemical shifts of the aromatic protons in the dimer (two

multiplets corresponding to **v'** & **y'** and **w'** & **x'** in **Figure 4.19**) are consistent with this structure.[7]

As explained for the experiments with **36** discussed earlier in this chapter, MALDI was probably not the ideal technique for following these experiments. In addition to the low cation formation of the barbiturates and complexes and the presence of many peaks of associated species, the laser used in the desorption process may heat the sample and open up the anthracene dimer. As in the experiments with **36**, dimers of receptor were sometimes observed and related to aggregation. If the peaks corresponding to the complexes that were observed after the photocyclomerisation was performed on the complexes, were still present after addition of barbital, but no longer after addition of barbital to the solutions of the complexes of the receptors with barbiturates photocyclomerised separately, this would be considered as an evidence for catenane formation. This is what was observed, but these experiments, all the peaks corresponding to the barbiturates or the complexes were weak and at the limit of the background noise, which makes this evidence dubious.

4.4) Using olefin terminated barbiturate

Given that anthracene photodimerisation to form photocatenanes was proven problematic, a series of experiments were carried out to determine whether the olefin metathesis performed on the complex **17•37** could generate any catenane: a *1 mM* solution of a 1:1 mixture of **17** and **37** in $CDCl_3$ was prepared, which was then heated to reflux in the presence of *10 mol%* of Grubbs' 1st generation catalyst. Finally an excess of barbital was added. After each of these steps, it was analysed by ^{1}H NMR and mass spectrometry. For comparison, a mixture of **17** and **37c** (cyclised **37**), which can contain only perched complex, was also made and analysed before and after addition of barbital. The different products that can be detected are illustrated in **Scheme 4.2**.

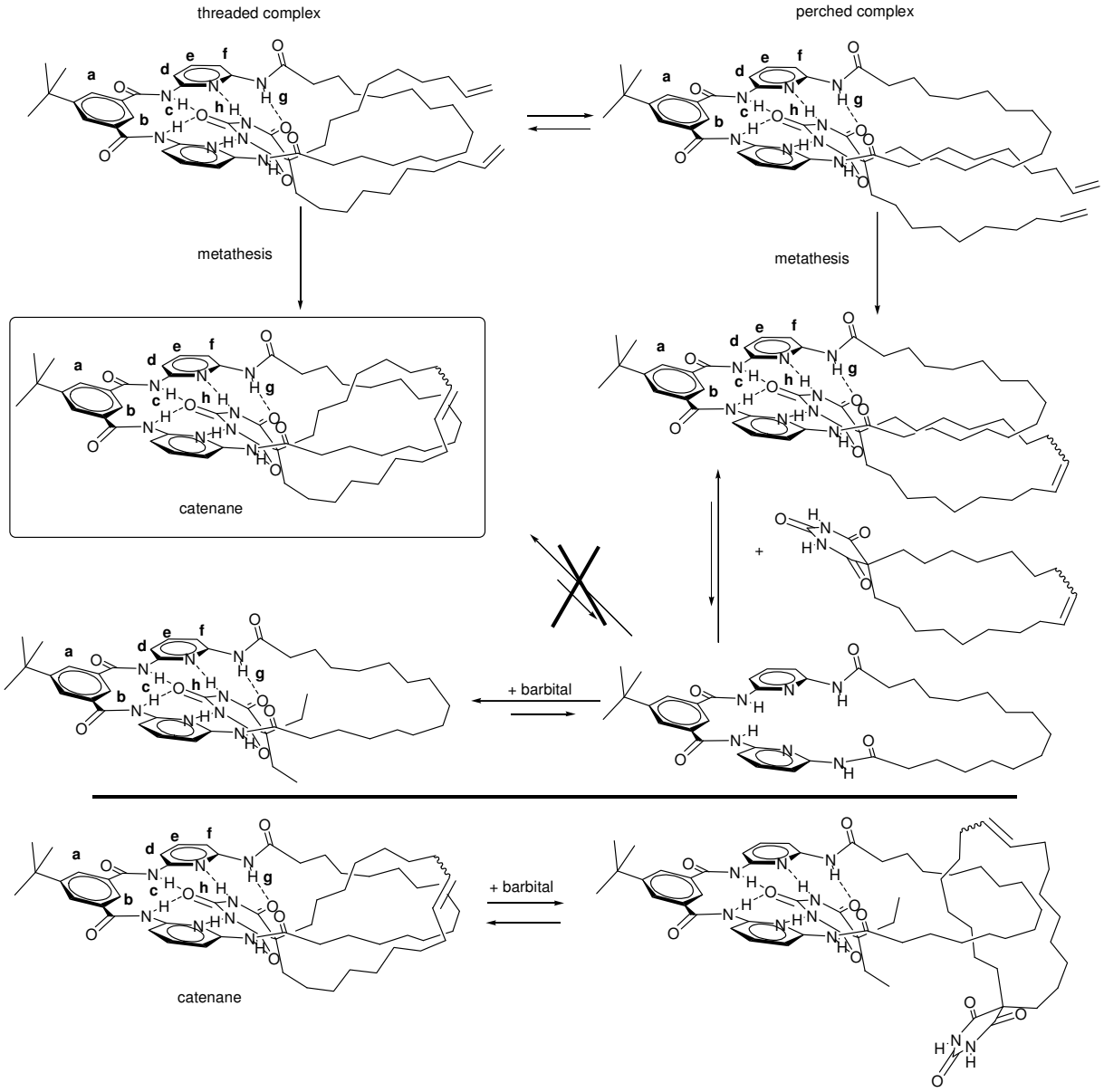

Scheme 4.2. Different possible products obtained by either performing a metathesis on a 1:1 mixture of **18** and **37**, or by making a 1:1 mixture of **18** and **37c** (cyclised **37**), and what can be obtained after adding an excess of barbital to these different products.

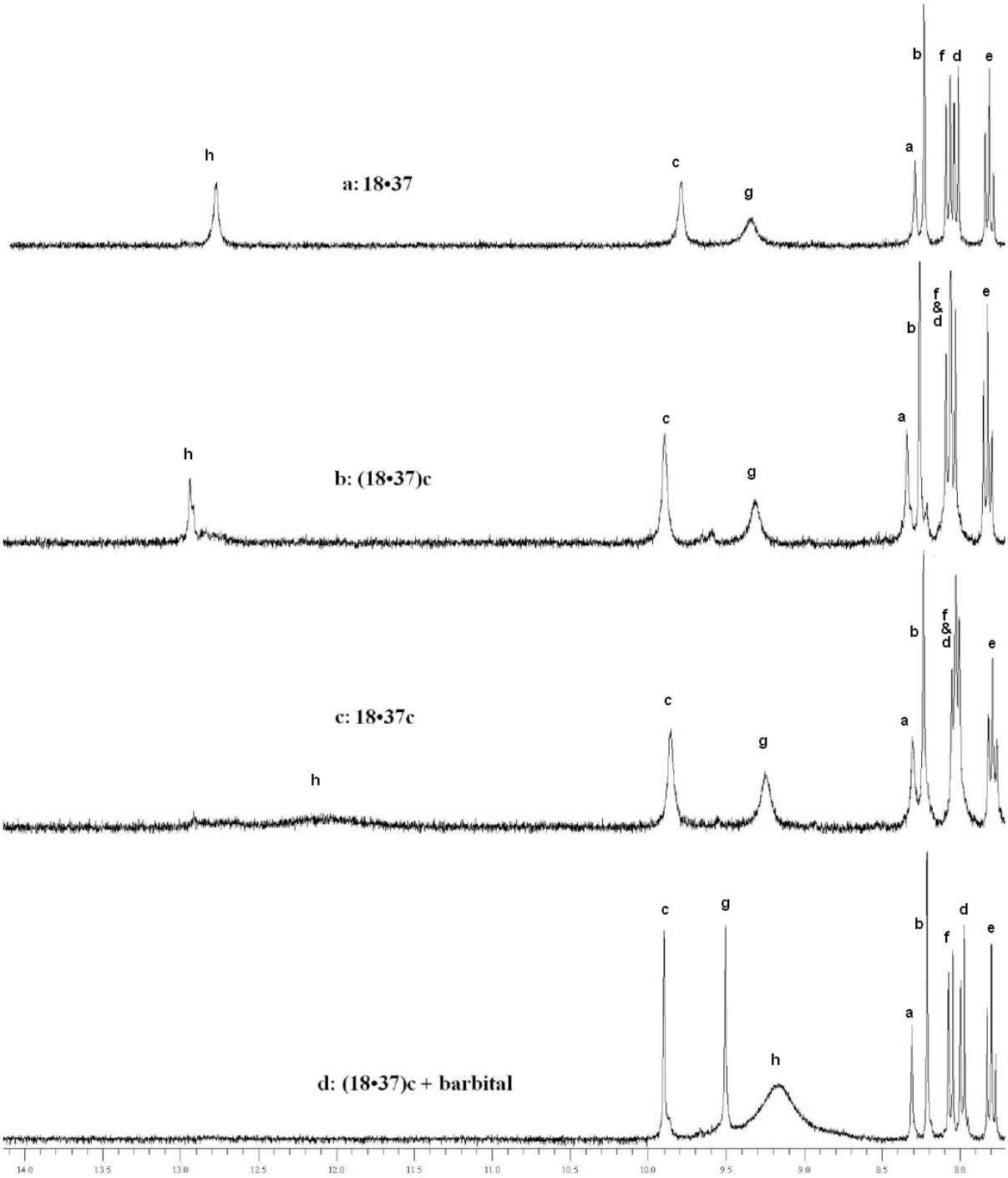

Figure 4.20. ^{1}H NMR spectra of a 1:1 mixture of **18** and **37**, *1 mM* in $CDCl_3$, (a) before and (b) after metathesis with *10 mol%* of Grubbs' first generation catalyst. For comparison, (c) mixture of **18** and **37c** (pre-metathesised **37**, slight excess). (d): Same mixture as (b) after addition of an excess of barbital.

The NMR spectra (**Figure 4.20**) reveal that the metathesis was complete after 2 hours at reflux, but that the spectrum of the metathesised mixture could not be distinguished by NMR from the mixture of the receptor with the pre-metathesised barbiturate, even after addition of an excess of barbital. This indicates that if some catenane has formed, then either it has done

so in small amounts, or it can bind barbital as suggested in the last equilibrium drawn in **Scheme 4.2**.

The mass spectra were made first of all by MALDI by looking at the positive ions, but unfortunately the barbiturates and the complexes were not seen. Therefore, new spectra were made by electrospray in the negative ions (ES^-), which allowed both the receptor and the barbiturate masses to be shown very clearly, as well as the complexes. The peaks for the complexes were relatively small but clearly distinct from the background noise. These mass spectra are presented in *Appendix 2*.

These mass spectra can be analysed as follows: in the 1:1 mixture of the barbiturate **37** with the receptor **18**, all the peaks for the starting materials and the 1:1 complex **37•18** can be clearly seen. After metathesis, we can see the peaks of the non-cyclised barbiturate **37** and its cyclised version **37c**, the receptor **18** and the two 1:1 complexes **37•18** and **37c•18**. There is also another unexplained peak which is probably an impurity in one of the starting materials as it was also seen in the spectrum before metathesis (though much smaller).

After adding an excess of barbital, the 1:1 complex with the uncyclised barbiturate **37•18** is no longer seen as would be expected if it has been displaced by barbital. However, the peak for the 1:1 complex with the cyclised barbiturate **37c•18** is still present, as would be expected if some of it was not displaced by barbital because of the mechanical bond. Therefore these results are at least consistent with the formation of a catenane. No peak corresponding to the mass of this complex plus barbital was seen, which indicates that the complex (**37c•18**)**•barbital**, described at the end of **Scheme 4.2**, was probably not formed.

The mass spectrum of the mixture of **18** with **37c** looked quite similar to the spectrum of the metathesised mixture, but surprisingly an additional peak was seen for a mass corresponding to two times **37c** plus one times **18**. As no peak corresponding to two times the mass of **37c** was seen in the ES^- spectrum of **37c** (NB: it was seen in MALDI but this can be a

weakly bound dimer),[6] it is unlikely that an actual "covalent dimer" of **37** was formed by metathesis. It is more likely that this peak corresponds to a 2:1 complex between **37** and **18**. After addition of an excess of barbital, the peak of the complexes **18•37c** and **18•(37c)**$_2$ both disappeared. This confirms that the **18•37c** peak remaining in the spectrum of the metathesised mixture after addition of barbital is likely to correspond to the catenane.

As was already mentioned in *Chapter III* (p. 86), the ring of **37c** is a 19 membered ring, whereas the smallest rings already known in isolated interlocked structures are 21-membered rings.[8] However, all these small-ring rotaxanes have been obtained by threading of the chain in the ring, whereas in our case the ring has been clipped around the chain by olefin metathesis. It was already pointed out in one of the seminal works of G. Schill on the limit of ring size in interlocked structures[9] that "*catenanes of small ring sizes will most likely be obtained by ring-contraction reactions*". However, the generally accepted theoretical limit in ring size predicted by molecular models with cycloalkane rings is of 20 atoms.[10]

In order to explain how a catenane of this type could have been formed, models of the two possible *cis* and *trans* isomers of the catenane formed by **18** and **37c** were calculated at the *Pôle Modélisation* of the *Institut des Sciences Moléculaires* (University Bordeaux I, France) by Dominique Cavagnat and Thierry Buffetau, using a methodology developed by their group.[11] They were optimised starting from the crystallographic stucture of the complex of **18** and barbital (cf. *Chapter II*, pp. 81-82) and adding the closing ring. These structures are presented in **Figure 4.21**.

It can be seen from these models that the closing double bond is positioned so that the hydrogen atoms bound to the sp^2 carbons are not pointing in the direction of the chain around which the ring has been clipped. It can be argued that for this reason, there is more space for the interlocked alkyl chain than there would be if the ring consisted of only methylene groups.

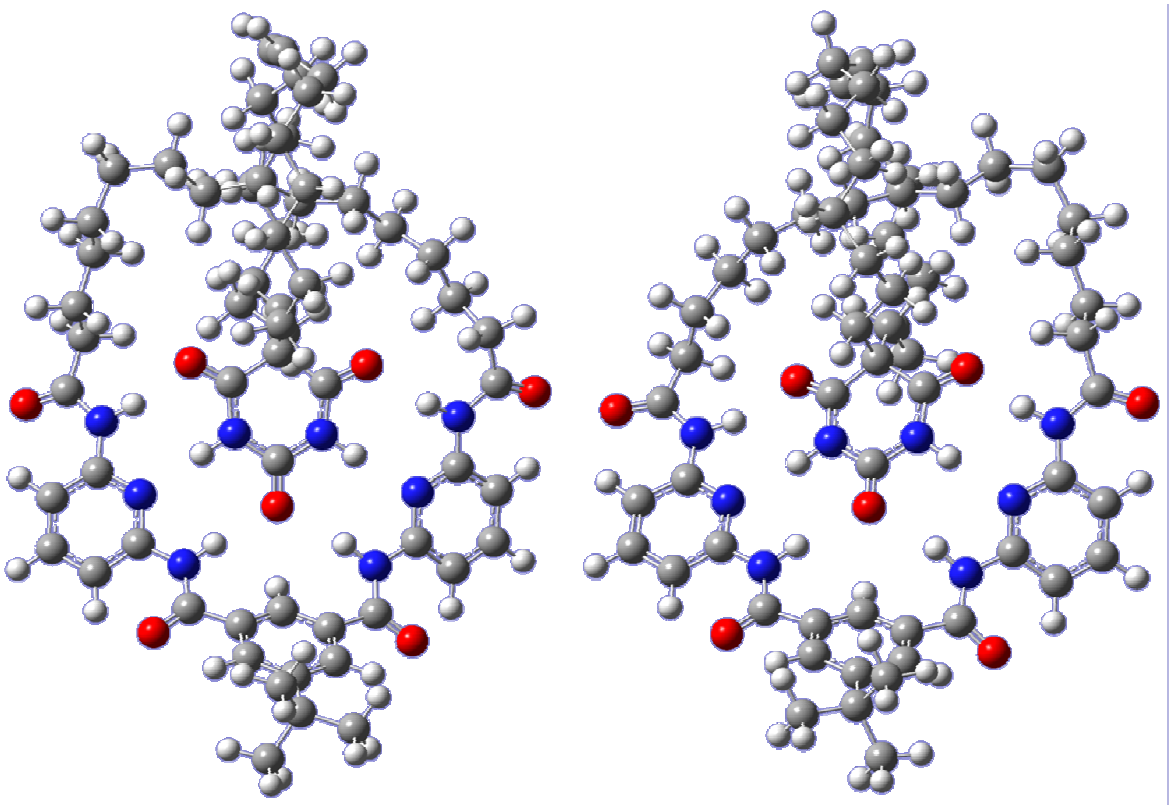

Figure 4.21. Calculated ab-initio structures of the isomers *cis* (left) and *trans* (right) of the catenane formed by **18** and **37c**.

4.5) Conclusion and further work

It has been demonstrated that long-chained barbiturates have lower binding affinity towards "Hamilton-like" receptors than barbital. This lower affinity is probably due to steric effects and to the fact that both threaded and perched complexes can form. Further ITC titrations between the different barbiturates and these receptors could give more insight into the reasons behind these difference in binding constants. It would also be, in the case of the anthracene-tagged barbiturates, a nice alternative to UV where anthracene absorption makes the results uncertain.

These barbiturates also seem to be more sensitive than barbital to subtle structural variations in the different receptors, as shown by the shifts in the NH ^{1}H NMR signals that differs for *cis* and *trans* receptors. However this was not observed with **37** where the extremities of the barbiturate's side chains are not bulky. Another effect of the interaction

between the extremities of the barbiturate's side chains with the macrocyclic ring of the receptor is the control of the excimer band formation as well as the modification of the quantum yield of photocyclomerisation. Even without formation of interlocked structures, it seems that binding to these types of receptor may be a way to control the diastereoselectivity and kinetics of ring-closing reactions, either on the barbiturate or the receptor.

Energy transfer from the receptor to the guest in the complexes with anthracene-tagged barbiturates was observed and some evidence was given that it was likely to be related to the strength of the complexation.

Evidence for an interlocked structure formed from a Hamilton-like receptor and a substituted barbiturate (**18** and **37** respectively) is provided by the observation of a peak in the mass spectrum corresponding to the expected mass of the catenane which is still present after adding an excess of barbital. These experimental results are very encouraging, but definitive proof for the formation of a new interlocked structure would normally come with X-ray crystallography. If this result has been interpreted correctly, it also demonstrates the feasibility of accessing interlocked structures with a 19 membered ring by a clipping approach. In this case, the catenane observed here is the smallest in terms of ring size, and its structure is supported by molecular models.

On the other hand, the formation of the photocatenanes is much less certain, as the method followed (detection by MALDI) was not sufficient in the time available. Re-iteration of these experiments, but followed by electrospray in the negative ion mode and with a systematic competition experiment with barbital, could eventually give better information on whether photocatenanes can be obtained by this method or not.

At this stage, it is too early to state that Hamilton-like complexes are a good basis to make interlocked structures, because the yield of any catenane produced was poor. This may be because "perched" complexes are easily formed instead of threaded complexes, but any

evidence for this topography is indirect. In order to prove this, X-Ray diffraction of the products would be necessary, but for the moment, different attempts to obtain crystals of the complexes with long-chain appended barbiturates have been unsuccessful. As was done in *Chapter 2*, *ab-initio* models a comparison of calculated and experimental IR spectra could also be informative regarding the geometry of the complexes. However the size and great flexibility of these molecules would make such models difficult to perform for the complexes before ring closure.

In order to avoid the formation of such perched complexes, we envisaged to synthesise new barbiturates with more rigid arms, which will be the subject of the next chapter.

---

[1] Havel, J. *Haltafal-Spefo program*; Mazaryle University: Brno, Moravia, Czech Republic. References: (**a**) Sillen, L. G.; Warnqvist, B. *Arkiv för Kemi* **1968**, *31*, 315; (**b**) Sillen, L. G.; Warnqvist, B. *Arkiv för Kemi* **1968**, *31*, 377.

[2] (**a**) Molard, Y.; Bassani, D. M.; Desvergne, J.-P.; Horton, P. N.; Hursthouse, M. B.; Tucker, J. H. R. *Angewandte Chemie International Edition* **2005**, *44*, 1072-1075; (**b**) Molard, Y.; Bassani, D. M.; Desvergne, J.-P.; Moran, N.; Tucker, J. H. R. *Journal of Organic Chemistry* **2006**, *71*, 8523-8531.

[3] (**a**) Tecilla, P.; Dixon, R. P.; Slobodkin, G.; Alavi, D. S.; Waldeck, D. H.; Hamilton, A. D. *Journal of the American Chemical Society* **1990**, *112*, 9408-9410; (**b**) Aoki, I.; Harada, T.; Sakaki, T.; Kawahara, Y.; Shinkai, S. *Journal of the Chemical Society, Chemical Communications* **1992**, 1341; (**c**) Motesharei, K.; Myles, D. C. *Journal of the American Chemical Society* **1994**, *116*, 7413-7414; (**d**) Chin, T.; Gao, Z.; Lelouche, I.; Shin, Y.-g.; Purandare, A.; Knapp, S.; Isied, S. S. *Journal of the American Chemical Society* **1997**, *119*, 12849-12858; (**e**) Salameh, A. S.; Ghaddar, T.; Isied, S. S. *Journal of Physical Organic Chemistry* **1999**, *12*, 257-254.

[4] Valeur, B. *Invitation à la fluorescence moléculaire*; 2004 ed.; De Boeck Université: Bruxelles, **2004**.

[5] Marquis, D.; Desvergne, J.-P. *Chemical Physics Letters* **1994**, *230*, 131-136.

[6] Gross, J. H. *Mass spectrometry - a textbook*; Springer-Verlag: Berlin Heidelberg, **2004**, p. 433.

[7] (**a**) Becker, H.-D. *Chemical Reviews* **1993**, *93*, 145-172; (**b**) Becker, H.-D.; Langer, V. *Journal of Organic Chemistry* **1993**, *58*, 4703-4708.

[8] (**a**) Schill, G.; Beckmann, W.; Schweickert, N.; Fritz, H. *Chemische Berichte* **1986**, *119*, 2647-2655; (**b**) Zhuang, C.; Li, S.; Zhang, J.; Zhu, K.; Li, N.; Huang, F. *Organic Letters* **2007**, *9*, 5553-5556; (**c**) Hsu, C.-C.; Chen, N.-C.; Lai, C.-C.; Liu, S.-M.; Chiu, S.-H. *Angewandte Chemie International Edition* **2008**, *47*, 7475-7478. Indirect evidence of threading of an alkyl chain in a 20 membered ring have also been obtained: (**e**) Gibson, H. W.; Nagvekar, D. S.; Yamaguchi, N.; Bhattacharjee, S.; Wang, H.; Vergne, M. J.; Hercules, D. M. *Macromolecules* **2004**, *37*, 7514-7529.

[9] Schill, G. *Catenanes, Rotaxanes and Knots*; *Organic Chemistry, A Series of Monographs*, Vol. 22, Academic Press: New York, **1971**.

[10] Frisch, H. L.; Wasserman, E. *Journal of the American Chemical Society* **1961**, *83*, 3789-3795.

[11] (**a**) Buffeteau, T.; Ducasse, L.; Brizard, A.; Huc, I.; Oda, R. *Journal of Physical Chemistry A* **2004**, *108*, 4080-4086; (**b**) Buffeteau, T.; Cavagnat, D.; Bouchet, A. ; Brotin, T. *Journal of Physical Chemistry A* **2007**, *111*, 1045-1051.

5) NEW RIGID BARBITURATES

5.1) Synthesis

5.1.1) Starting point and design

As concluded in *Chapter 4*, the attempts to use flexible barbiturates as components of interlocked structures were less than satisfactory, since the desired products were only ever obtained in trace amounts at best. In order to avoid the formation of "perched" complexes, the synthesis of new barbiturates with less flexible arms was envisaged. The synthesis of 5,5'-bis(*para*-hydroxyphenyl)-barbituric acid (**38**) from alloxan monohydrate and phenol had previously been described in the literature using a classical Friedel-Crafts reaction[1] (see **Scheme 5.1**). This compound has two phenyl groups directly substituted on the central ring, and was seen as a good starting point to synthesise barbiturate derivatives that would be more rigid than those containing directly appended ethylene-glycol or alkyl chains.

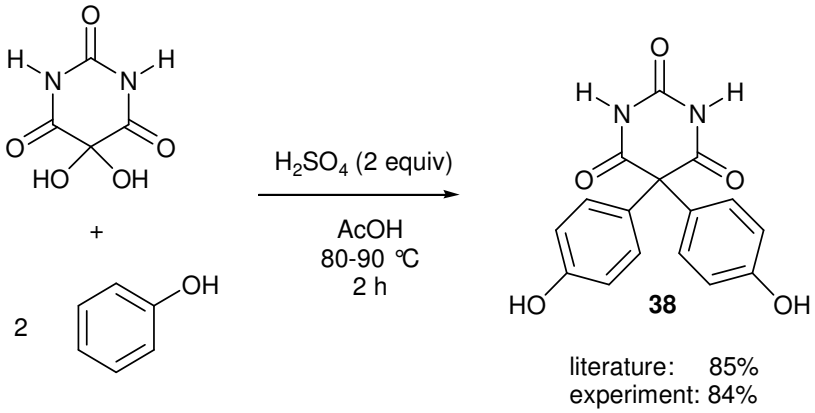

Scheme 5.1. Synthesis of **38** by Friedel-Crafts reaction.[1]

By linking arms terminated by either stoppers or reacting groups on the oxygen sites of this barbiturate, it was thought that a threaded complex could then be formed fairly readily, which would then lead to an interlocked structure. For example, terminal olefin groups would be small enough to easily thread into a macrocyclic receptor like **17** or **18**, and ring closing

olefin metathesis on the complex would then give a catenane. This chapter focuses on attempts to obtain these new olefin-terminated barbiturates, and on binding studies with a simpler barbiturate that has a similar structure.

The reaction described in **Scheme 5.1** was repeated successfully in a yield of *84%*, which was almost as good as the one of *85%* quoted in the literature.[1] X-ray diffraction on the crystalline product also allowed its solid state structure to be determined (**Figures 5.1**, **5.2** and *Appendix 1*).

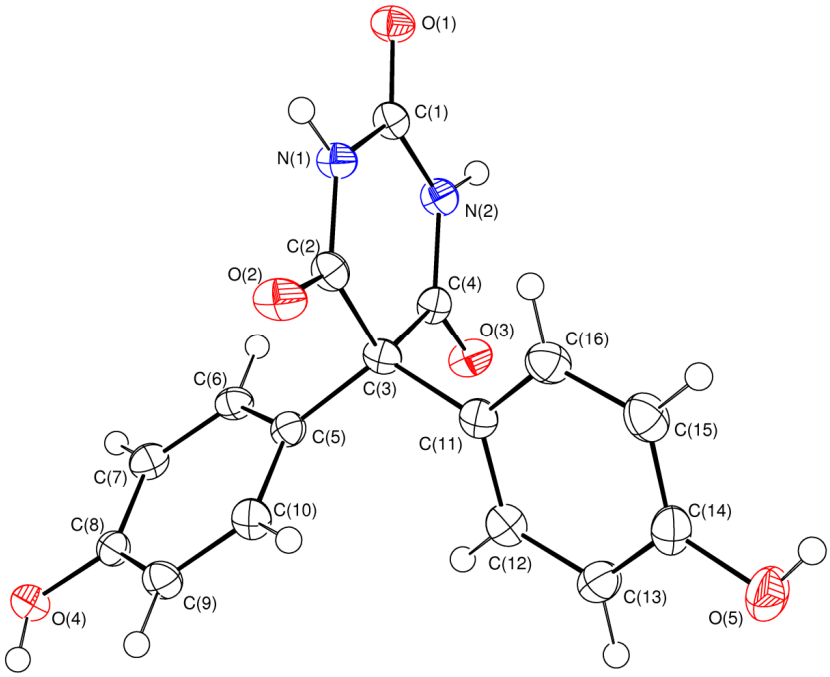

Figure 5.1. X-Ray crystal structure of **38**.

It can be observed that the barbituric acid moiety is nearly planar. The two phenyl groups are not in the same plane perpendicular to the plane of the barbiturate, but are twisted with respect to one another. The angles that they make with the medium plane of the barbiturates are practically equal for the two phenyl rings (*77°* for the plane of the ring C(5)-C(10), and *80°* for the plane of the ring C(11)-C(16)). This makes the axis defined by C(1), O(1) and C(3) as nearly an element of symmetry of the molecule by rotation through *180°*. The angle between the two phenyl planes is *59°*. This twisting is due to the possible

steric interactions between the hydrogen atoms born by C(10) and C(12). The angle C(5)-C(3)-C(11), which governs the axes from which arms attached to the oxygen atoms would start, is *115°* in this structure.

As shown in **Figure 5.2**, there are intermolecular hydrogen bonds formed in the solid state between the OH, CO and NH groups.

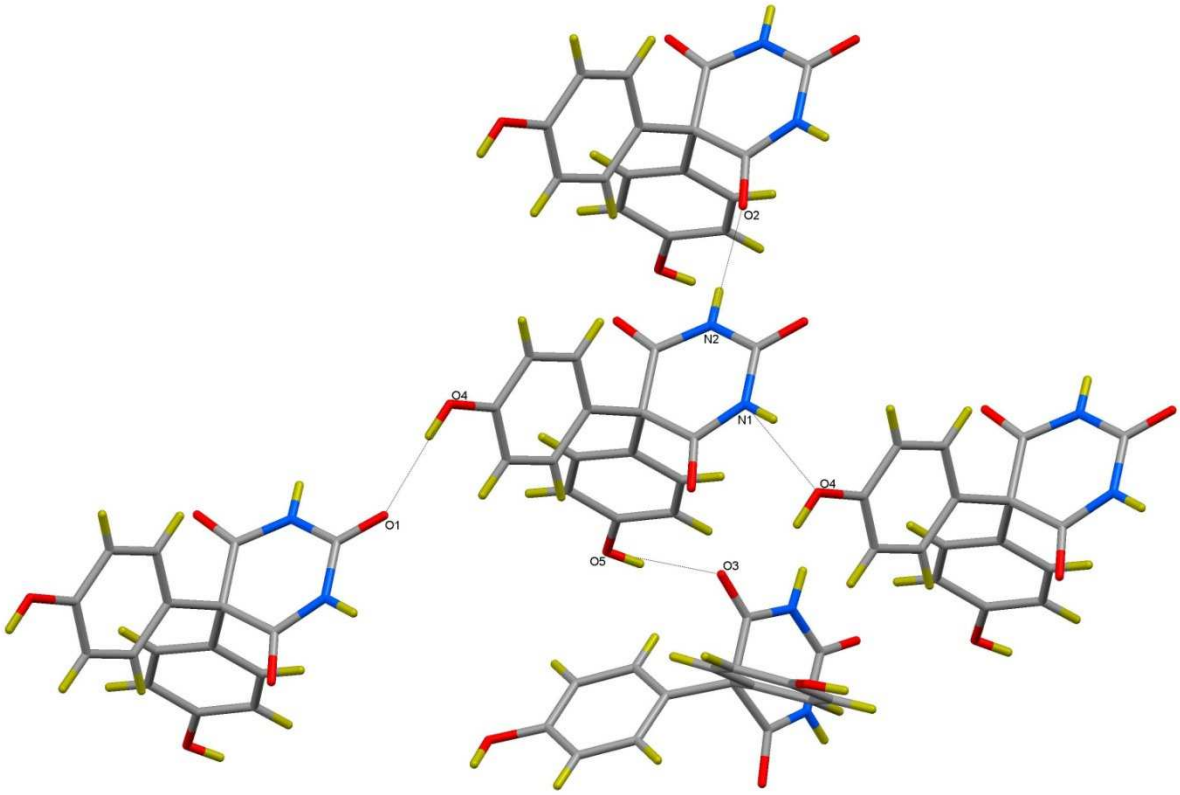

Figure 5.2. H-bonds between molecules of **38** in the solid state as determined by XRD.

5.1.2) Direct substitution[2a]

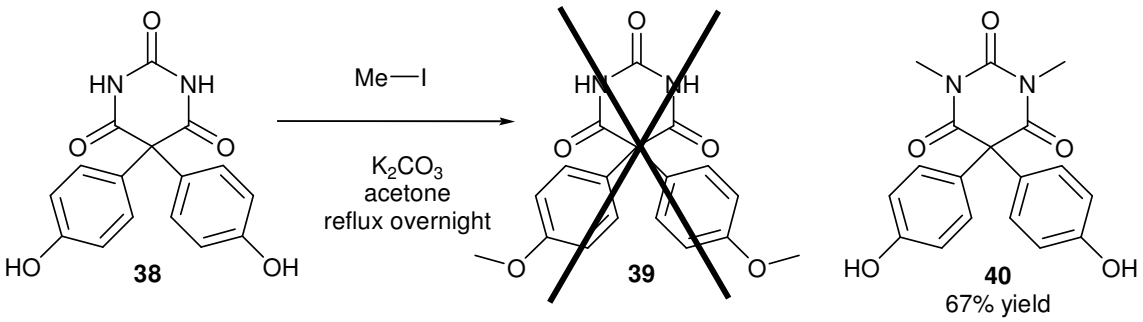

Scheme 5.2. Direct substitution with methyl iodide.

First of all, direct nucleophilic substitution of **38** was attempted in order to obtain O-substituted products. Initially various alkyl iodides were attempted under different conditions, but reactivity was poor.[2a] However a reaction with methyl iodide proceeded readily and a disubstituted product was obtained. However, its IR spectrum (see **Figure 5.3**) revealed that it was not the desired product **39** as substitution had in fact occurred on the N site, leading to **40** (see **Scheme 5.2**). When the reaction was repeated using DBU (1,8-Diazabicyclo[5.4.0]undec-7-ene, an hindered base) instead of potassium carbonate, the same product was obtained.[2a]

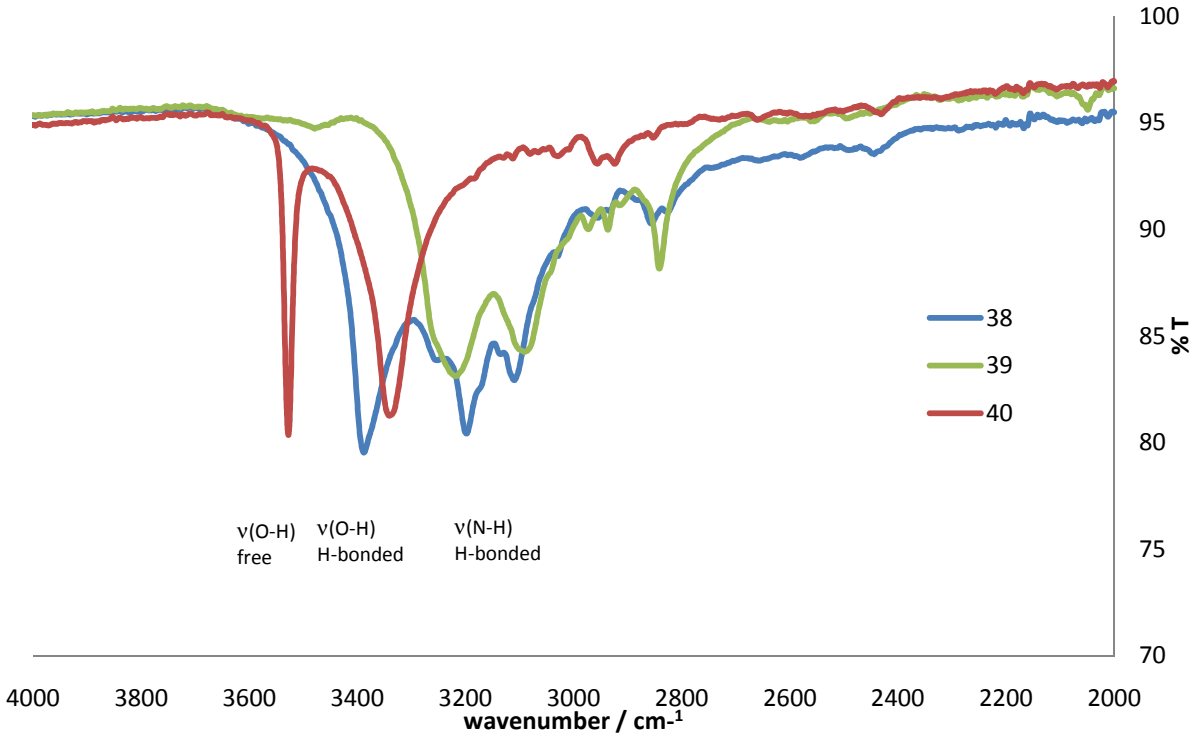

Figure 5.3. IR spectra of **38**, **39** and **40**.

In order to confirm that the product obtained by this reaction was indeed **40**, **39** was synthesised from alloxan monohydrate and anisole using a similar procedure[1] as that for **38**, leading to **39** in *25%* yield. A comparison of the IR spectra (see **Figure 5.3**) of **39** and **40** confirms this difference, as the ν(O-H) stretching band at *3341 cm*$^{-1}$ in the spectrum of **40** is not seen in the spectrum of **39**, whereas the ν(N-H) stretching band at *3217 cm*$^{-1}$ in the

spectrum of **39** is not seen in the spectrum of **40**. The spectrum of **38**, by contrast, contains these two bands. This difference is also visible by ^{1}H NMR; the chemical shifts for the OH protons in **39** and for the NH protons in **40** vary in different spectra with concentration and therefore cannot be used easily to confirm the structure. However the signal for the N-Me group in **40** arises at *3.27 ppm* and that for the O-Me group in **39** arises at *3.79 ppm*.

It was thought that the reason for the substitution at the NH position instead of the OH position was because of the higher acidity of the NH group. Comparing the *pKa* of similar compounds described in the literature, the *pKa* of the NH[3] should be close to *7.3* whereas the *pKa* of the OH[3b, 4] should be close to *9.4*. However it is likely that both sites can be deprotonated in the conditions of this reaction, or that it is the intermediate formed after a first step of nucleophilic substitution that is deprotonated. In this case it is the reactivity of both sites in the nucleophilic substitution that has to be compared. According to the theory of hard and soft acids and bases (HSAB),[5] the deprotonated nitrogen site is a softer base than the deprotonated phenol site, both because the electronegativity of the nitrogen is lower than the electronegativity of the oxygen and because the charge of the anion will be delocalised on the carbonyl. For this reason, according to the HSAB principle that *hard acids prefer to bond to hard bases and soft acids to soft bases*, the alkyl halide, which can be considered as a soft electrophile, is more likely to bond to the nitrogen site.

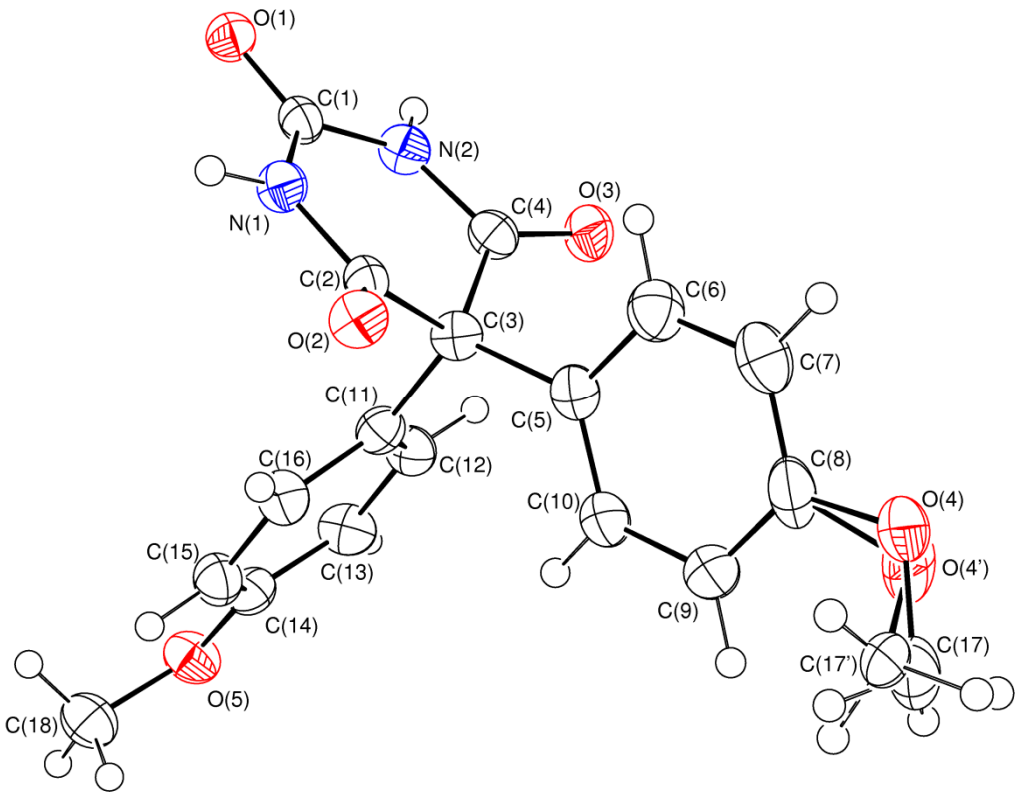

Figure 5.4: XRD of **39**.

An X-ray structure of **39** was also obtained (see **Figure 5.4**), showing at the molecular scale and in the solid state a structure which is quite different from that of **38**. In this structure, the position of one of the OMe groups, corresponding to O(4) and C(17), was found to be disordered over two positions with an occupancy ratio of *72:28*. As in **38**, the phenyl groups are not in the same plane and the main reason for this is certainly again the steric interaction between the hydrogen atoms born by C(10) and C(12). But this time the barbiturate ring is not entirely planar. If we call "plane of the barbiturate" the medium plane formed by C(4)-N(2)-C(1)-N(1)-C(2) and O(1), which atoms are all very close to planarity, the carbon C(3) is slightly out of this plane, at a distance of *0.42 Å*, and this plane makes an angle of *30°* with the plane defined by the atoms C(2)-C(3)-C(4). O(2) and O(3) are also slightly out of the plane of the barbiturate but on the other side: the medium plane of C(2)-O(2) and C(4)-O(3) forms an angle of *29°* with the plane of the barbiturate, and the two oxygen atoms are at an average distance of *0.31 Å* of this plane. This position of C(3) out of the medium plane allows

both phenyl rings to have particularly distinct orientations. One of them (C(5)-C(10)) makes an angle of *89°* with the plane of the barbiturate, whereas the other (C(11)-C(16)) makes an angle of *86°* with the other phenyl group, and of *90°* with the plane of the barbiturate. In other words the medium planes of the three rings are nearly all perpendicular to each other. The two phenyl rings are also distinct in the sense that the medium plane of C(5)-C(10) is nearly a plane of symmetry of the molecule. This means that C(6) and C(7) on one side and C(10) and C(9) on the other side of this ring are in different environments, whereas the ring C(11)-C(16) is divided in two by this plane of symmetry, which means that C(12) and C(13) on one side and C(16) and C(15) on the other side of this ring have nearly symmetrical environments.

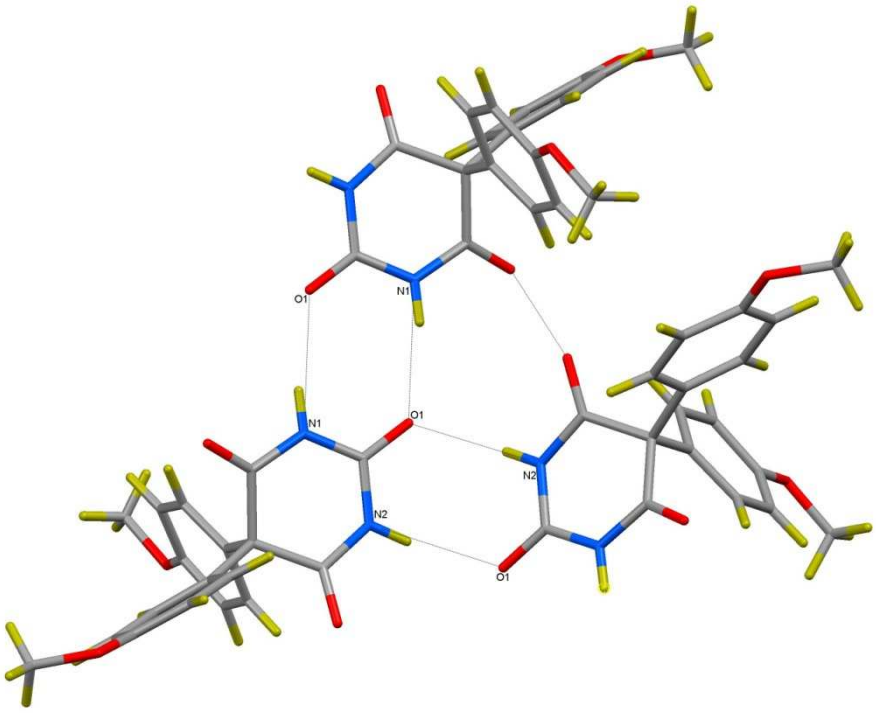

Figure 5.5. H-bonds between molecules of **39** in the solid state as determined by XRD.

Figure 5.5 shows only the minor OMe position, but the way that hydrogen bonds are formed between molecules in the solid state are similar. It can be observed that contrary to what was observed with **38**, the hydrogen bonds form only between the terminal CO and the NH of the barbituric acid moieties whereas the oxygens of the OMe groups and the other CO of the barbiturate are not involved.

5.1.3) Malonate strategy

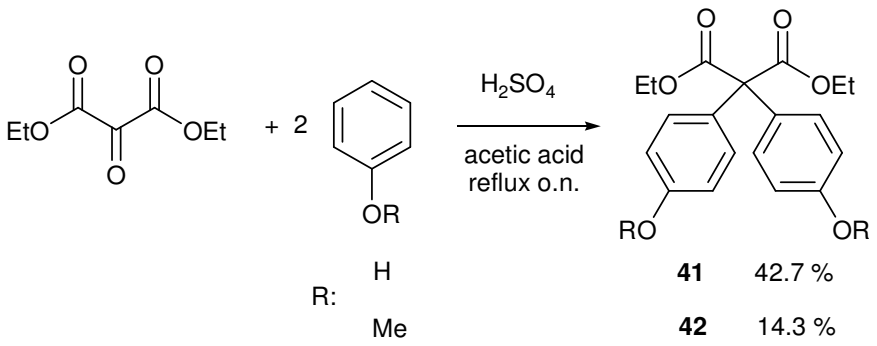

Scheme 5.3. New rigid malonates obtained by Friedel-Crafts reaction.

As the direct substitution of **38** was difficult, a strategy similar to the one described in *Chapter 3* was then adopted. Diethyl bis-(*para*-hydroxyphenyl) malonate (**41**) was obtained from diethyl ketomalonate and phenol by a Friedel-Crafts reaction in similar conditions to those used for **38**, in *43%* yield. The methyl-substituted barbiturate **42** was also obtained by the same method, using anisole instead of phenol, in *14%* yield (see **Scheme 5.3**). The bis-substitution of this malonate on the oxygen site by different alkyl iodide and bromides was then realised, as illustrated in **Scheme 5.4**:

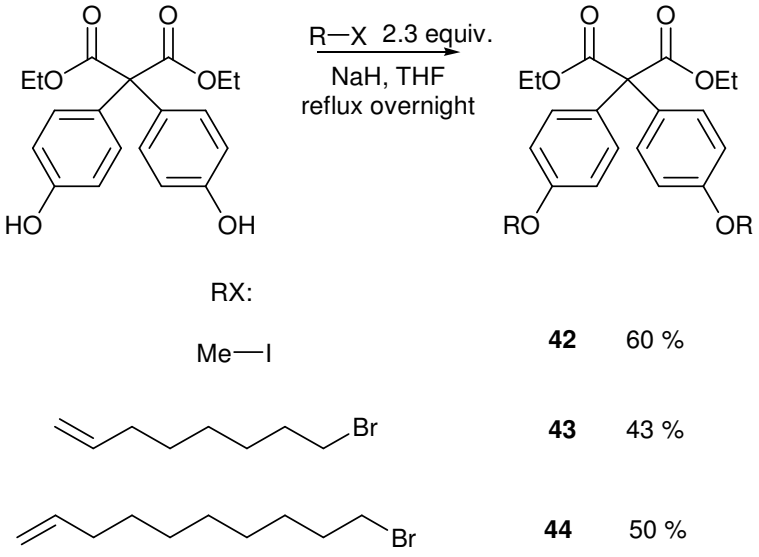

Scheme 5.4. Substitution on the O site of **41**.

The yields of these reactions were moderate but slightly better with methyl iodide, which is probably due to iodide being a better leaving group than bromide. In each case the mono-substituted products were also isolated by chromatography at the end of the reaction.

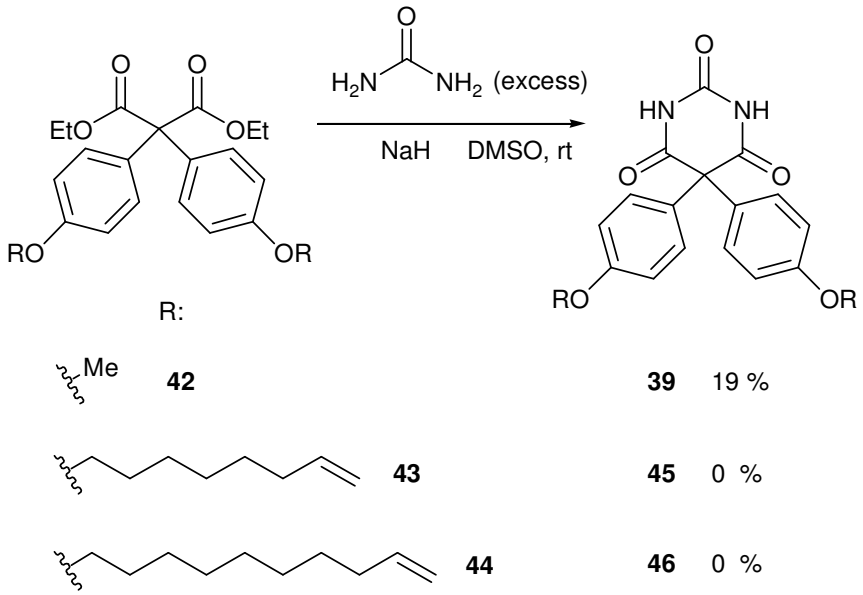

Scheme 5.5. Conversion of rigid malonates to rigid barbiturates.

The conversion of these malonates to the barbiturates was then studied, at first using the same conditions described in *Chapter 3* (using sodium hydride in dimethylsulfoxide), as described in **Scheme 5.5**. Unfortunately, except for the conversion of **42** which gave **39** in *19%* yield, none of the target barbiturates were identified at the end of these reactions. This may be due to the difficult reproducibility of the reactions in DMSO. This solvent is hygroscopic and traces of decarboxylated hydrolysed starting material were observed by mass spectrometry. More interestingly, products of oxidation of these byproducts were also observed (see **Scheme 5.6**). The only oxidant in the reaction mixture is DMSO, so it is likely that this side reaction has a similar mechanism to Swern oxidation[6] where DMSO is the actual oxidant.

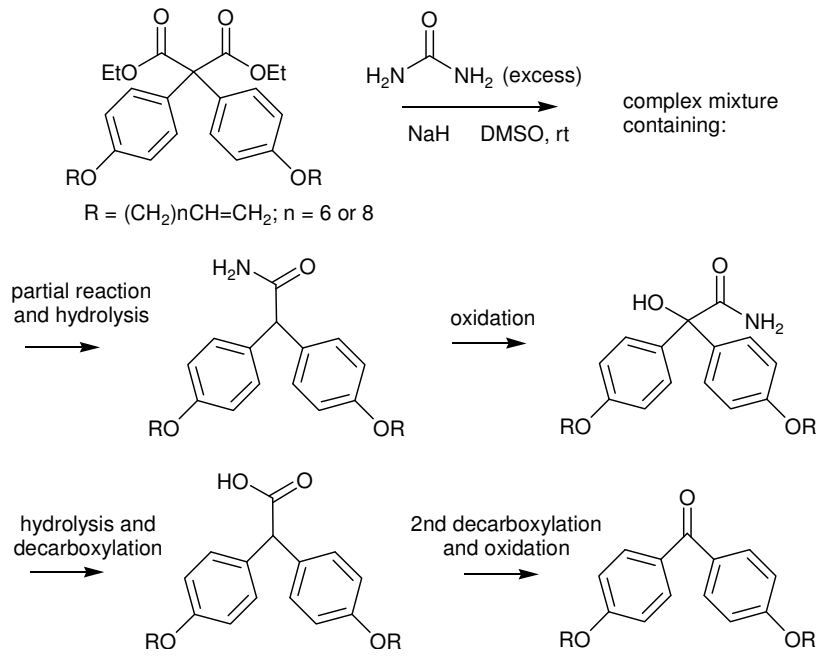

Scheme 5.6. Products of side reactions observed in mass spectrometry in attempts to convert **43** and **44** to **45** and **46**.

Different conditions were then tried for the conversions of **43** to **45**. The reaction was repeated using sodium hydride in DMF and sodium ethoxide in ethanol. In each case, the yields were always zero, and while no traces of oxidation were observed, the products of hydrolysis and partial reaction were still present.

5.1.4) Friedel-Crafts reactions

As **39** was obtained by a Friedel-Crafts reaction, it was thought that this could be a way of directly obtaining substituted barbiturates starting from alloxan monohydrate. However, considering the harsh conditions of this reaction (in boiling acetic acid with two equivalents of H_2SO_4), functional groups appropriate for interlocked structure formation would be affected by these conditions. For example, aromatic stoppers would undergo competitive Friedel-Crafts reactions, and olefins would also take part in other side reactions including isomerisation and hydrolysis. This corresponds to what was observed (**Scheme 5.7**); the olefin-terminated phenol ether **47** was obtained in an excellent yield from phenol and 10-bromodec-1-ene, but the Friedel-Crafts reaction with alloxan monohydrate under the same

conditions as used for **38** gave in the end a crude reaction mixture where, according to the NMR, the terminal olefin group had disappeared.

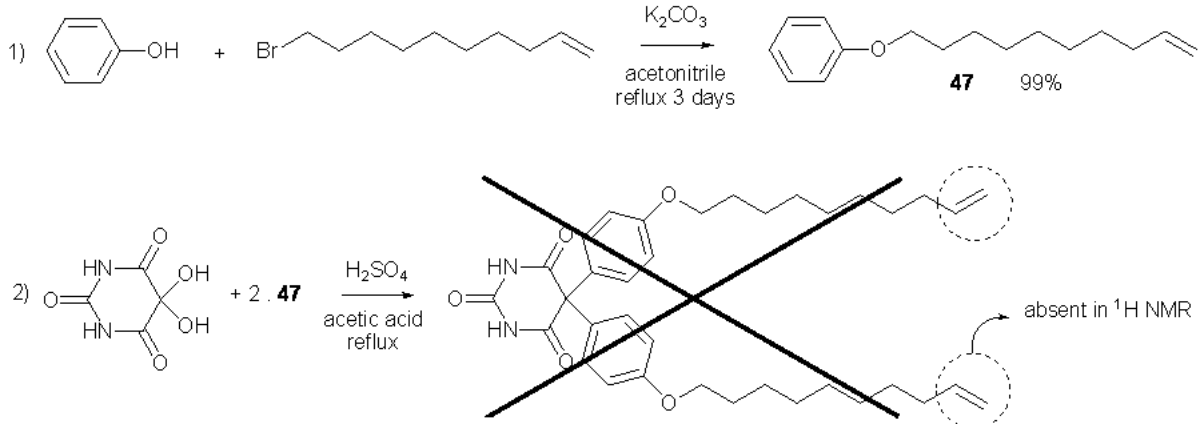

Scheme 5.7. Attempt to obtain **46** by direct Friedel-Crafts.

It is interesting to compare the different Friedel-Crafts reactions described in this chapter. The yields of these reactions are given in **Table 5.1**.

Table 5.1. Yields of Friedel-Crafts reactions.

Starting ketone	Starting aromatic	Product	Yield
Alloxan monohydrate	Phenol	**38**	84%
Alloxan monohydrate	Anisole	**39**	25%
Diethyl ketomalonate	Phenol	**41**	43%
Diethyl ketomalonate	Anisole	**42**	14%
Alloxan monohydrate	**47**	**46**	0%

It can be observed that the maximum yield is obtained when starting from alloxan monohydrate and phenol as the starting materials. The yield is more than three times lower when using anisole instead of phenol, which is consistent with the general observation that phenol ethers are less reactive in Friedel-Crafts reactions than phenols.[7] The yield is also approximately two times lower when using diethyl ketomalonate instead of alloxan monohydrate; this can be because some trans-esterification between the malonate and acetic acid is taking place, giving ethyl acetate and hydrolysed malonate.

5.1.5) Protection

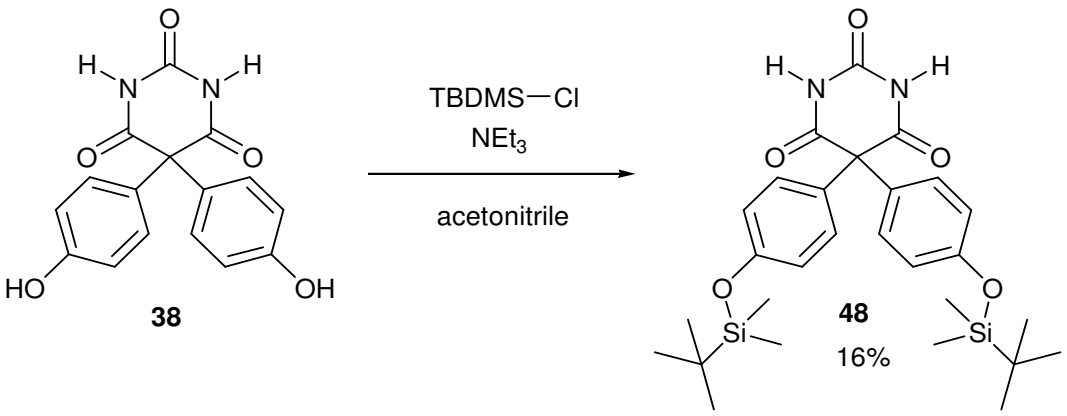

Scheme 5.8. Protection of the O-sites of **38** to give protected barbiturate **48**.

Contrary to what was observed with carbon electrophiles used in other substitutions, a substitution of **38** with *tert*-butyldimethylsilyl chloride gave a disubstituted product in *16%* yield (**Scheme 5.8**) which was substituted on the O site, as can be seen by its IR spectrum which contains a ν(O-H) band and no ν(N-H) band (**Figure 5.5**). This seems to be governed by the principle of HSAB,[5] the N site being softer than the O site and its relative softness being increased by charge delocalisation.

It was thought that if **48** was deprotected in situ in the presence of an excess of a suitable electrophile, then the substitution could occur on the O position as this would be the first anion formed, but an attempt to obtain **46** by this strategy led to the N-substituted product **49** in *69%* yield (see **Scheme 5.9**). The fact that the substituents of **49** are situated on the N sites is again demonstrated by the disappearance of the ν(O-H) band and the reappearance of the ν(N-H) band in its IR spectrum (see **Figure 5.6**). This is more evidence that the regioselectivity of these substitution reactions is governed by HSAB,[5] but it also demonstrates that there is no need for another base other than *tert*-butylamonium fluoride to perform this reaction from a TBDMS protected product.

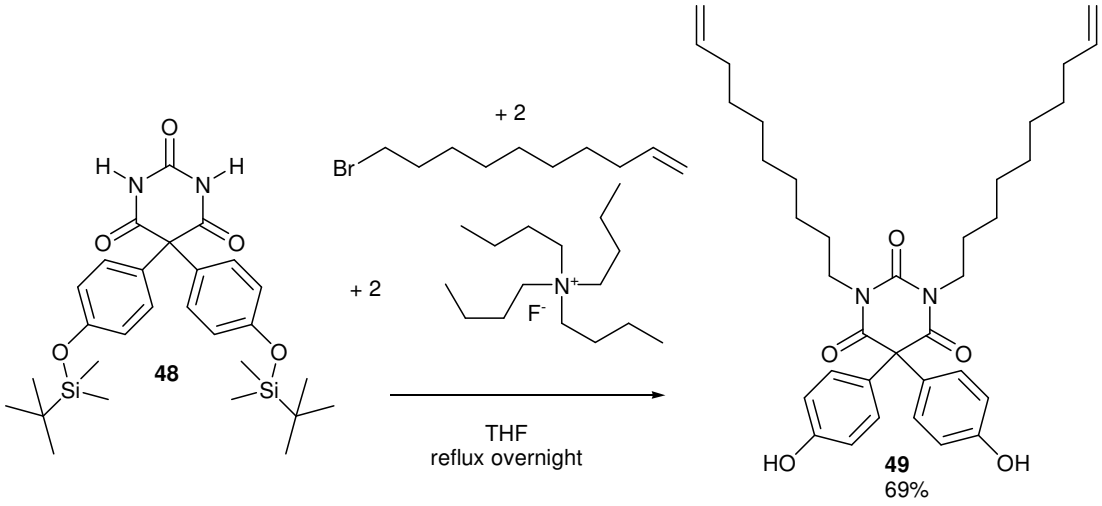

Scheme 5.9. One pot deprotection of **48** and substitution on the N site to give **49**.

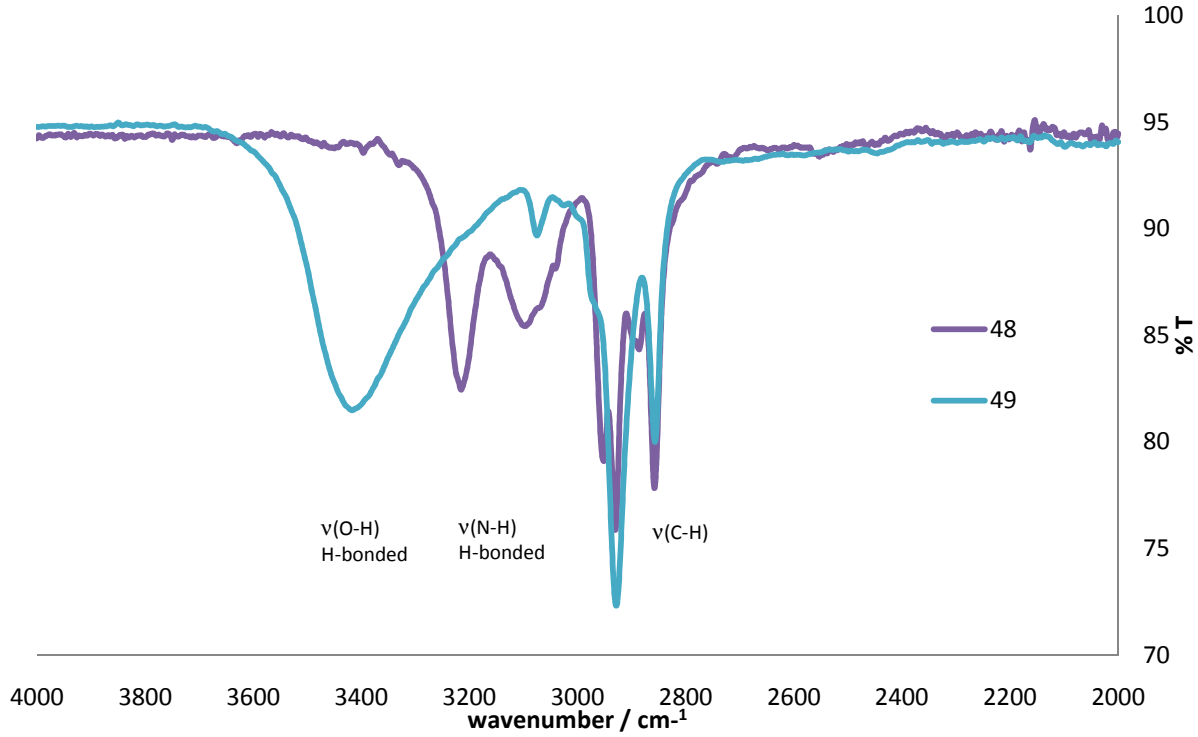

Figure 5.6. IR spectra of **48** and **49**.

5.2) Binding studies

5.2.1) ^{1}H NMR of a complex

As far as we are aware, barbiturate derivatives with two bulky aromatic groups directly substituted on the central carbon such as **39** have not previously been used as guest

molecules for "Hamilton-like" hosts. It was therefore important to establish that the extra steric bulk did not adversely affect their binding properties.

A ^{1}H NMR spectrum of a 1:1 mixture of **39** with **15** was made (*5 mM* in $CDCl_3$). It was compared with spectra if **15** alone and 1:1 mixture of **15** with barbital (**Figure 5.7**). As with barbital and other barbiturates, the NH both of the receptor and the barbiturate shifted downfield, which indicated that a complex is forming. It was also interesting to notice that the signal of the olefinic proton of **15** was split in two signals of different integrations upon binding. This was interpreted as further evidence that two different isomers of **15**, *cis* and *trans*, were present, as discussed in previous chapters.

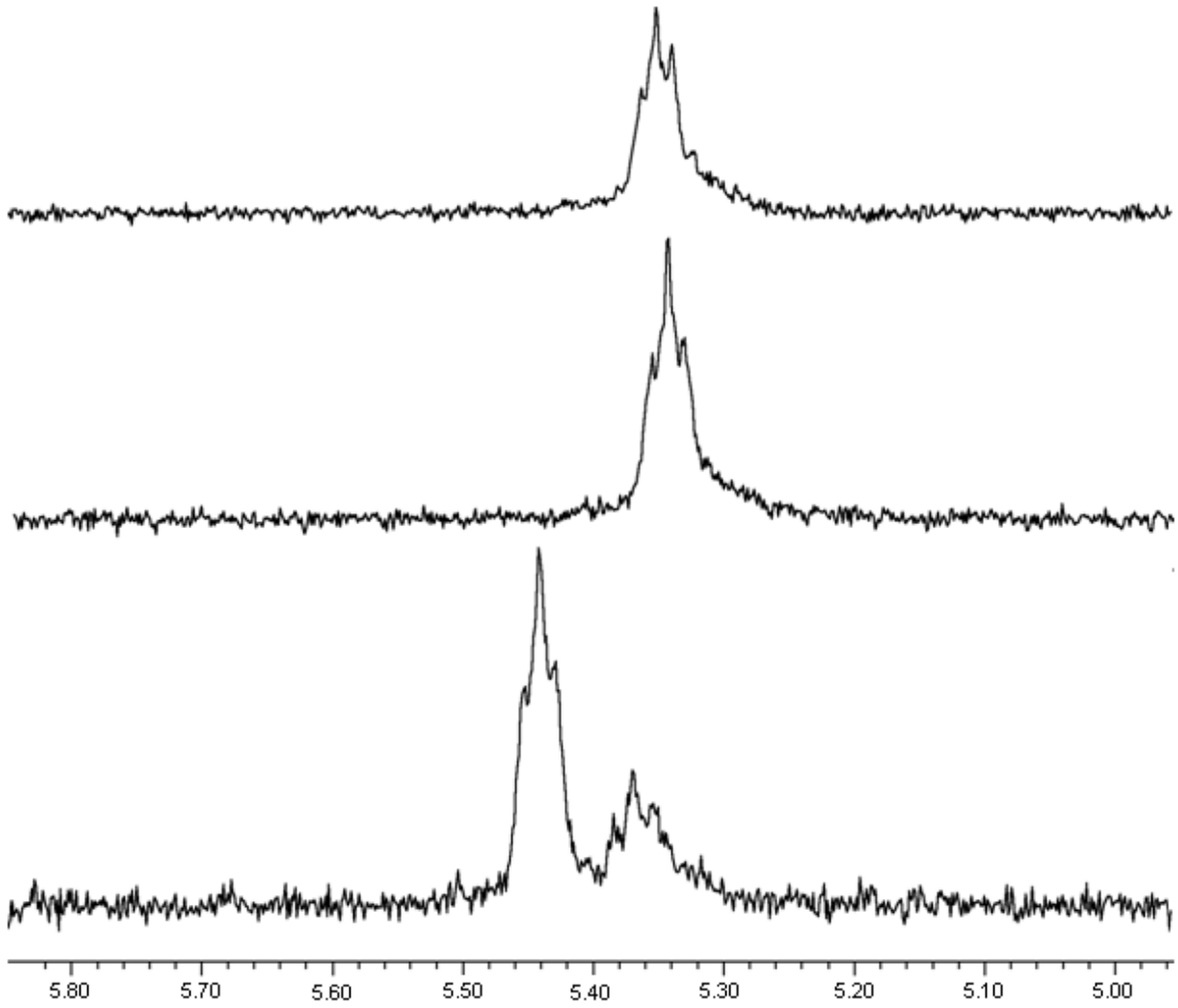

Figure 5.7. Detail of the ^{1}H NMR spectra of **15**, 1:1 mixture of **15** and barbital, and 1:1 mixture of **15** with **39**, all in $CDCl_3$ at a concentration of *5 mM*.

5.2.2) Titrations followed by UV-vis spectroscopy

In a similar way to what was done with anthracene-substituted flexible barbiturates (see *Chapter 4*) the absorption due to the phenoxy groups of **39** had to be corrected, leading to an increase in the margin of error and difficulty in fitting the data. The binding constants found by this method for 1:1 complexes are given in **Table 5.2**, where the error is given by Letagrop. As for the anthracene-substituted barbiturates, the actual error on the result may be higher.

Table 5.2. Binding constants between **39** and **17** and **18** at room temperature, in dichloromethane, determined by UV-vis titration

receptor	*n*	*log(K)*	*Error*
17	4	4.18 (with barbital: 4.2)	0.03
18	6	4.98 (with barbital: 5.79)	0.06

The first observation that can be made is that barbiturate **39** actually binds to cyclic receptors **17** and **18** with similar affinities to barbital. In fact, if the binding constant with **18** is lower than it is with barbital, as expected because of the steric interactions, the binding constant with **17** is surprisingly very similar to the binding constant for **17** and barbital. Furthermore, contrary to what was observed with barbital, no better fit was obtained when assuming that a 2:1 complex could also form with **17**. It is reasonable to think that this second complex could not form because of the potential steric interactions of the phenyl groups.

5.2.3) Titrations followed by ITC

The phenomenon of a negative slope at the beginning of the data that had been observed in titrations with barbital (cf. *Chapter 2*) was also observed here. Therefore titrations were made at a concentration of $0.05\ mol.L^{-1}$ in order both to minimize this problem and obtain a satisfactory signal/noise ratio. Contrary to what was observed with barbital, a small

heat of dilution of **39** was recorded, which had to be removed from the values of heat changes obtained during the titrations before the fit. The results of the titrations are given in **Table 5.3**.

Table 5.3. *log(K)*, $\Delta H°$ and $\Delta S°$ of 1:1 complexation of open and closed receptors with **39** measured by ITC in dichloromethane at room temperature, and comparison with binding constants of other barbiturates.

receptor	*n*	*log(K)*	$\Delta H°$ / *kcal.mol*$^{-1}$	$\Delta S°$ / *cal.K*$^{-1}$*.mol*$^{-1}$
12	6	4.35 ± 0.02 (barbital: 4.43 ± 0.02)	-21 ± 1 (barbital: -17.0 ± 0.8)	-51 ± 3 (barbital: -37 ± 3)
18	6	4.82 ± 0.03 (barbital: 5.33 ± 0.07, **37**: 4.62 ± 0.04)	-15.3 ± 0.5 (barbital: -15.0 ± 0.2, **37**: -9.6 ± 0.9)	-29 ± 2 (barbital: -25.8 ± 0.8, **37**: -11 ± 3)

The binding of **39** to "open" receptor **12** gives rise to surprisingly big variations of $\Delta H°$ and $\Delta S°$ compared to the binding of barbital. However the large unfavourable $\Delta S°$ is nearly completely compensated by a large favourable value of $\Delta H°$, leading only to a small diminution of the binding constant. The large variation of $\Delta S°$ can be attributed to an important loss of freedom of motion, which may be associated with C-H / π binding interaction that may force the pendant chain of the receptor to remain close to the barbiturate. This additional binding would also explain the larger value of $\Delta H°$.

The binding of **39** to **18** gives a $\Delta H°$ value close to the one found for the binding of barbital to **18** (within the margin of error), but a slightly less favourable $\Delta S°$. The small difference in $\Delta H°$ indicates that either the hydrogen bonds formed are as strong as those with barbital, which means that **39** adopts a similar geometrical position as barbital in the complex (which is counter-intuitive because of the possible steric effects), or that some additional weak binding interactions compensate any loss in hydrogen bonds. Once again the small change in $\Delta S°$ can be explained by a larger loss of freedom of motion that results from the complexation of **39** compared with barbital. Another informative comparison can be made between data for the binding to **18** of **39** and **37**, which are respectively "rigid" and "flexible" barbiturates. The lower entropic cost for the binding of the flexible barbiturate **37** may

indicate that this time the barbiturate **39** can adopt fewer geometrical positions than **37**, which would be an advantage for the formation of interlocked structures if it means that it is only or mostly the threaded complex that is formed, and not the perched complex.

5.2.4) Comparison of ab initio models, IR spectra and XRD structures

As was explained in *Chapter 2*, this work was done in Bordeaux by D. Cavagnat and T. Buffetau using a methodology developed by their group.[8] Models of the complexes were established (see **Figure 5.8**) in order to calculate their theoretical IR spectra which were compared with their experimental spectra in solution (see **Figure 5.9**).

The model of the complex of **18** and **39** is quite similar to the model of the complex of **18** and barbital. The barbiturate is bound by six complementary hydrogen bonds and is completely threaded. The model of the complex of **17** and **39** also bears similarities to the complex of **17** with barbital, as the barbiturate is bound only on one side by three hydrogen bonds as was observed in the model **17•barbital**. However, this time one of the two rigid phenoxy substituents is forced to be threaded in the macrocycle, and protrudes in front of the other amidopyridine unit, blocking the arrival of another barbiturate. This gives an explanation for why no 2:1 complex could be observed in UV-vis. measurements. This phenoxy group may also be involved in favourable C-H / π interactions between the aromatic ring and the hydrogens bound to the aliphatic closing chain.

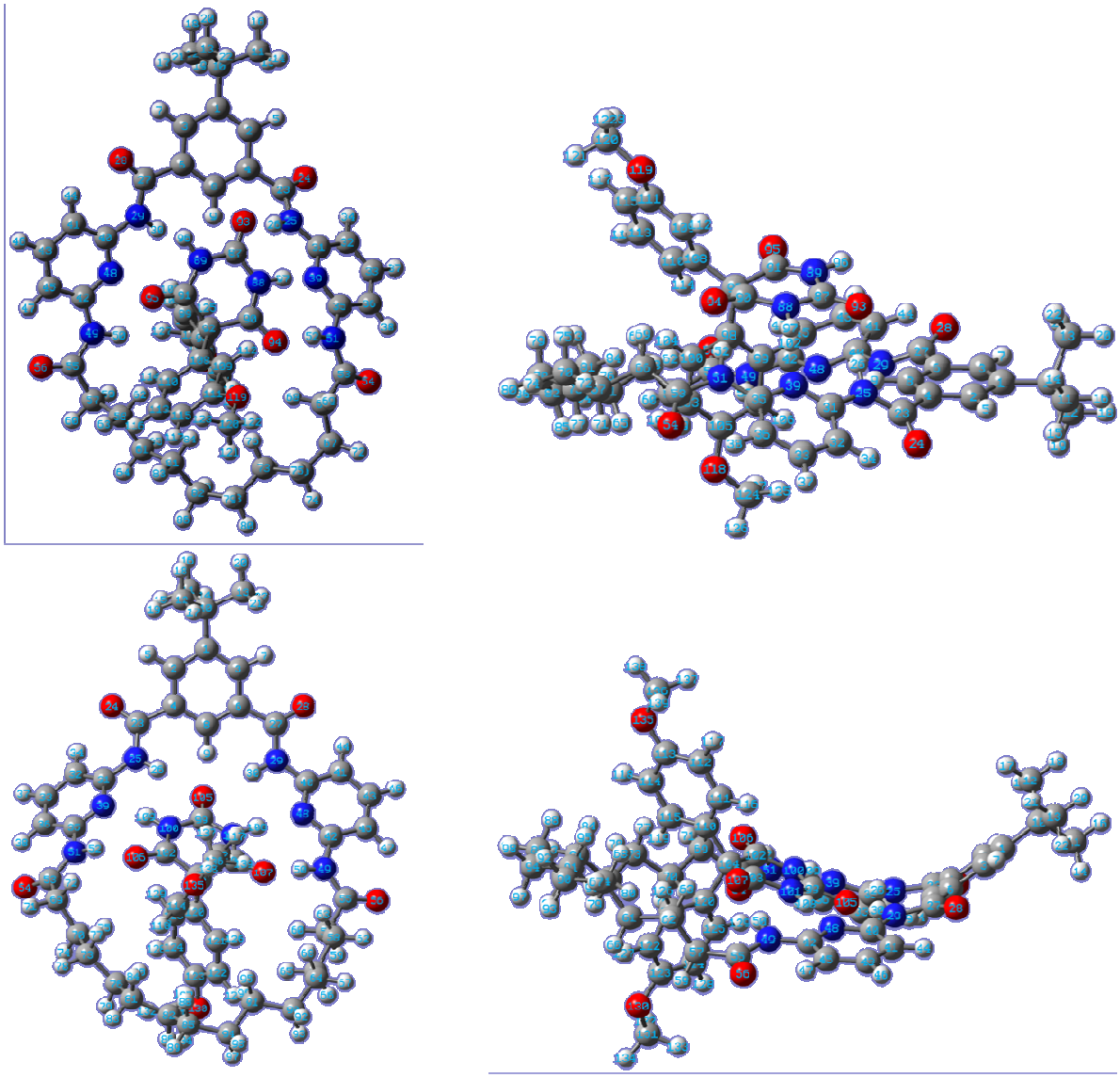

Figure 5.8. Models of **17•39** (above) and **18•39** (below).

With **18**, as was seen with barbital, the calculated and experimental IR spectra were very similar, which is in good agreement with what was observed by ITC. With **17**, the calculated and experimental spectra are also in good agreement. This time, contrary to what was observed with barbital, the IR spectrum affords no evidence for a 2:1 complex, therefore the model can be considered as a realistic representation of what happens in solution.

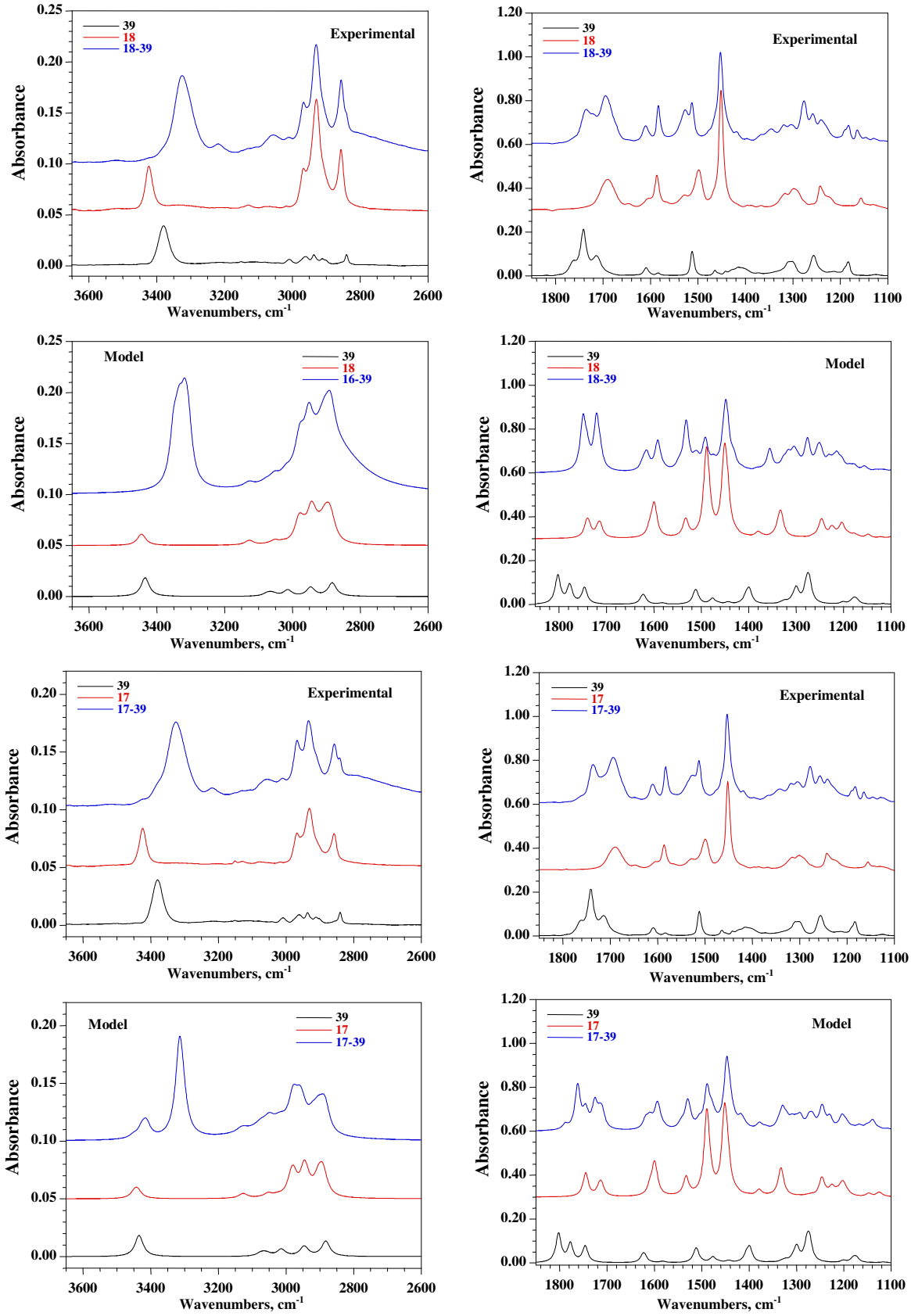

Figure 5.9. Comparison of experimental and calculated IR spectra for **39**, "reduced" receptors **17** (above) and **18** (below) and their complexes.

Finally, crystals of the complex between **18** and **39** were obtained by our colleagues from University Bordeaux 1, allowing them to determine the solid-state structure of these complexes in the solid state by X-ray crystallography. The structure obtained is presented in **Figure 5.10** and more details are given in *Appendix 1*.

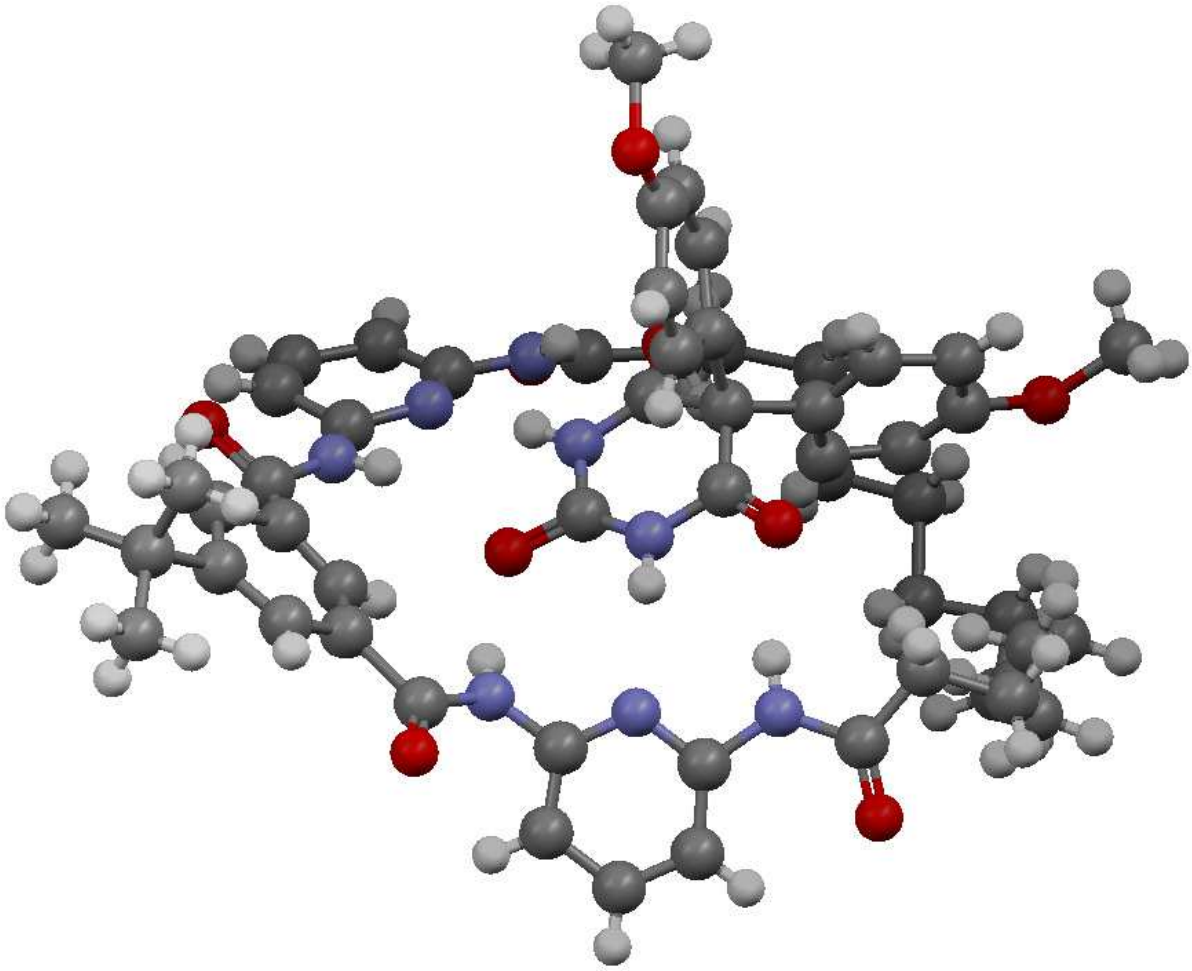

Figure 5.10. Structure of the **18•39** complex determined by X-ray diffraction.

It is interesting to note that contrary to what was observed with barbital, this structure is very different to the one predicted by *ab-initio* models. In the solid state, the complex formed is clearly perched and not threaded. However, it can be argued that the gas-phase model probably gives a better description of what happens in solution (as it is backed by consistent IR-spectra). In the solid state, interactions between different complexes play a more important role, in particular intermolecular H-bonds, which are present in this structure.

5.3) Conclusion and further work

Binding studies with **39** indicate that barbiturates directly substituted with two bulky groups such as aromatic rings bind efficiently to Hamilton-like sites, even with receptors that are too small to form six complementary hydrogen bonds with barbital. The *ab-initio* models are generally in good agreement with the experimental IR spectra, ITC and UV titrations, but not with the structure obtained by XRD for the complex with **18**. Except for this last result which can be interpreted as a phenomenon occurring only in the solid state, these studies tend to confirm the intuition that led to their synthesis, that these rigid guests have a structure that is more appropriate to the formation of interlocked structures than "flexible" barbiturates such as barbital. For this reason, rigid barbiturates with bulky groups and long appendages are promising candidates for obtaining interlocked structures.

Friedel-Crafts reactions are reliable for obtaining the basic structure of two *para*-phenoxy groups linked to the sp^3 carbon of the barbiturate ring. However this only applies to simple and robust starting materials that do not contain other reactive groups such as aromatic stoppers or terminal olefins. The starting barbiturate or malonate can be made, but then other strategies have to be used in order to introduce the desired functions on the barbiturate.

The conversion of malonates to barbiturates when the substituents of the malonate are bulky has also proved to be very difficult, which is probably because of steric reasons. There is good experimental evidence that the regioselectivity of nucleophilic substitutions on **38** is governed by HSAB,[5] which results in a reaction on the N position rather than the O when using a carbon electrophile.

The right strategy (**Scheme 5.10**) will then probably be to protect the O sites of **38** with TBDMS, then the N sites with Boc, then to deprotect the O with tBAF and substitute the desired pendant arm on the O, then finally to deprotect the N. There is at least one example of

a similar strategy in the literature,[9] but it is not on a barbiturate, which suggests that the last step (deprotection of the N-Boc) may be difficult and require acid conditions, but nevertheless less harsh than those used in the Friedel-Crafts reactions described above.

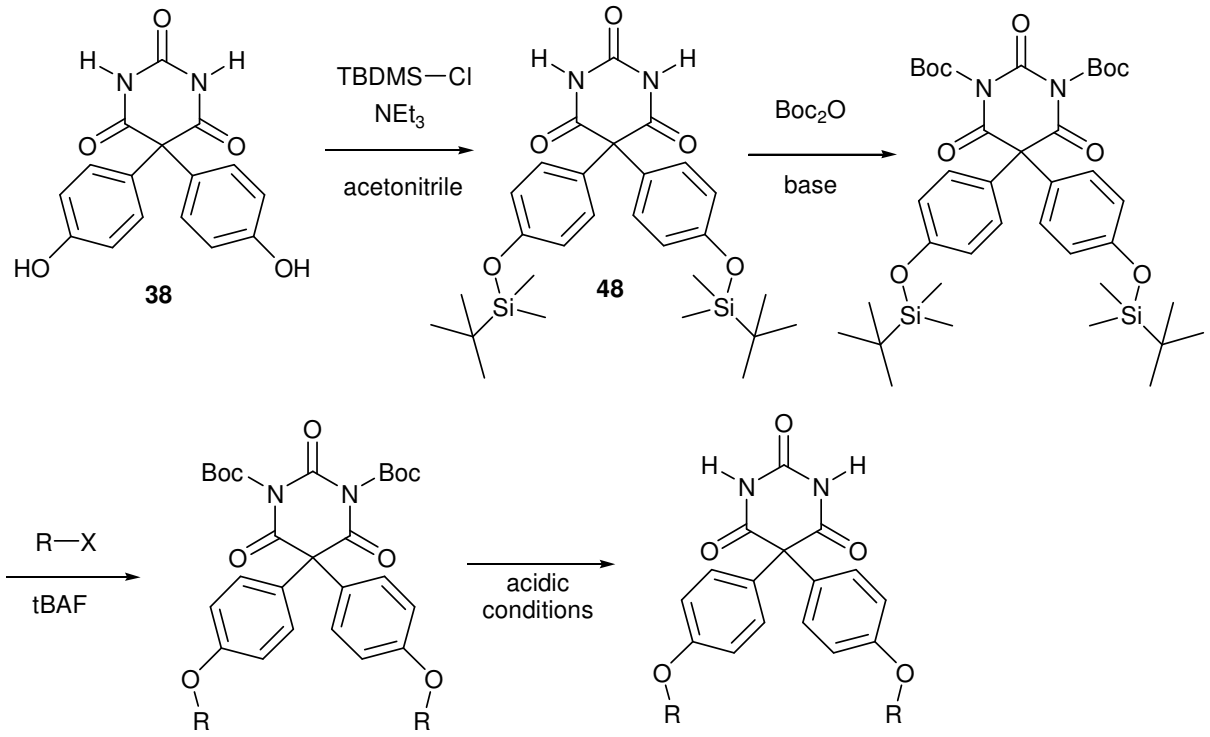

Scheme 5.10. Protection / deprotection strategy for accessing new rigid barbiturates.

---

[1] H. N. Song, H. J. Lee, H. R. Kim, E. K. Ryu and J. N. Kim, *Synthetic Communications*, 1999, **29**, 3303-3311.

[2] (**a**) Manchester, J. *Synthesis of interlocked structures using Barbiturate templates and Anthracene dimerisation*, MSci project report, University of Birmingham - School of Chemistry, **2008**; (**b**) Saraswat, A. *Synthesis of Catenanes Using Hamilton-like Hosts and Barbiturate Guests*, MSci project report, University of Birmingham - School of Chemistry, **2009**.

[3] (**a**) Wood, J. K. *Journal of the Chemical Society* **1906**, *89*, 1831-1839; (**b**) Butler, T. C. *Journal of Pharmacology and Experimental Therapeutics* **1956**, *116*, 326-336.

[4] Clara, M.; Strenn, B.; Saracevic, E.; Reuzinger, N. *Chemosphere* **2004**, *56*, 843-851.

[5] March, J.; Smith, M. B. "*Lewis Acid and Bases: Hard and Soft Acids and Bases*", in "*Chapter 8 - Acid and Bases"* of *March's Advanced Organic Chemistry - Reactions, Mechanisms and Structure*; 5 ed.; Wiley, Ed.; Wiley: New-York, **2001**, pp. 338-342 for an

overview of the HSAB theory, and pp. 438-445 for an application to nucleophilic substitutions.

6 March, J.; Smith, M. B. "*Oxidation or Dehydrogenation of Alcohols to Aldehydes and Ketones*", in "*Chapter 19 - Oxidations and Reductions"* of *March's Advanced Organic Chemistry - Reactions, Mechanisms and Structure*; 5 ed.; Wiley, Ed.; Wiley: New-York, **2001**, pp. 1514-1517.

7 March, J.; Smith, M. B. "*Friedel-Crafts Alkylation*", in "*Chapter 11 - Aromatic Electrophilic Substitution"* of *March's Advanced Organic Chemistry - Reactions, Mechanisms and Structure*; 5 ed.; Wiley, Ed.; Wiley: New-York, **2001**, p 707-711.

8 (**a**) Buffeteau, T.; Ducasse, L.; Brizard, A.; Huc, I.; Oda, R. *Journal of Physical Chemistry A*, **2004**, *108*, 4080-4086; (**b**) Buffeteau, T.; Cavagnat, D.; Bouchet, A. ; Brotin, T. *Journal of Physical Chemistry A*, **2007**, *111*, 1045-1051.

9 Peyrottes, S.; Coussot, G.; Lefebvre, I.; Imbach, J.-L.; Gosselin, G.; Aubertin, A.-M.; Prigaud, C. *Journal of Medicinal Chemistry* **2003**, *46*, 782-793.

6) EXPERIMENTAL

6.1) Syntheses

6.1.1) General considerations

All starting materials were purchased from Aldrich or Lancaster. The solvents were ordered from Sigma. The solvents used for reactions were dried by classical methods: distillation from calcium hydride for DCM (dichloromethane), hexane and acetonitrile, distillation from sodium wires and benzophenone for THF (tetrahydrofuran) and diethyl ether. Toluene, acetone and ethyl acetate were not dried. All reactions were carried out under N_2. When the product of the reaction contained the anthracene substructure, the reaction vessels were covered with foil to prevent any effect of light. Unless otherwise stated, the column chromatographies were made with silica gel (Merck, 230-400 mesh).

The NMR spectra were recorded on Bruker AC300 or AV300 spectrometers (300 MHz). The mass spectra were recorded on VG Zabspec mass spectrometer.

6.1.2) Experimental procedures and analysis of the products

1 (7-octenoic acid)[1]

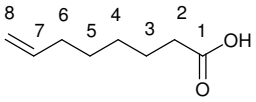

0.5 mL of a solution of 7-bromohept-1-ene (0.40 mL, 2.62 mmol) in diethyl ether (11 mL) was added to a suspension of magnesium powder (77.4 mg, 3.18 mmol) in diethyl ether (3 mL). The mixture was heated to reflux. When the solution became turbid, the heating was stopped and the rest of the solution was added drop wise, so that the reflux was maintained. It was left stirring without heating during 1h, refluxed 15 min and finally cooled to 0°C. The solution was then removed with a syringe and added to a mixture of powdered dry ice (CO_2, 5 g, 114 mmol) and diethyl ether (2 mL). After 30 min of stirring, water and ammonium chloride were added. This solution was filtered

and extracted with 20 mL of ether. The aqueous phase was acidified with concentrated HCl until it became turbid, then it was re-extracted with diethyl ether. This second organic phase was dried over $MgSO_4$, filtered and evaporated, giving 131.5 mg of **1** as an orange liquid (0.925 mmol, 35%). ^{1}H NMR ($CDCl_3$, 300 MHz): δ = 10.06 (br. s, 1 H, OH), 5.79 (ddt, J_t = 6.7, J_{d1} = 10.3 and J_{d2} = 17.1 Hz, 1 H, 7), 4.97 (m, 2 H, 8), 2.35 (t, J = 7.5 Hz, 2 H, 2), 2.05 (q, J = 7.0 Hz, 2 H, 6), 1.64 (quint, J = 7.3 Hz, 2 H, 3), 1.38 (m, 4 H, 4 & 5). The analysis is in agreement with the literature data.[1]

2 (8-nonenoic acid)[2]

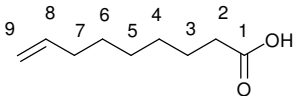

A solution of 8-bromooct-1-ene (4.9 g, 25.6 mmol) in diethyl ether (50 mL) was added drop wise to a suspension of magnesium powder (670 mg, 27.6 mmol) in diethyl ether (75 mL) at reflux. After 1h30 min of reflux, it was cooled to 0°C and powdered dry ice (CO_2, 30 g, 682 mmol) was added. After breaking the solids by vigorous stirring, a solution of sodium hydroxide (1.7 g) in water (100 mL) was added. The mixture was filtered and the organic phase was extracted with 20 mL of diethyl ether. The aqueous phase was acidified with concentrated HCl until pH < 2, then it was re-extracted with 2 × 30 mL of diethyl ether. This second organic phase was dried with $MgSO_4$, filtered and evaporated, giving 2.18 g of **2** as an colorless liquid (14.0 mmol, 54.5% yield). ^{1}H NMR ($CDCl_3$, 300 MHz): δ = 10.85 (br. s, 1 H, OH), 5.79 (ddt, J_t = 6.7, J_{d1} = 10 and J_{d2} = 17 Hz, 1 H, 8), 4.96 (m, 2 H, 9), 2.34 (t, J = 7.5 Hz, 2 H, 2), 2.05 (q, J = 6.7 Hz, 2 H, 7), 1.69 (quint, J = 7.4 Hz, 2 H, 3), 1.34 (m, 6 H, 4, 5 & 6). Mass spectrum (EI^+): m/z = 156 {$M^{\bullet+}$}, 138 (loss of water), 114 (Mc Lafferty). The analysis is in agreement with the literature data.[2]

6-heptenoyl chloride (n = 4)

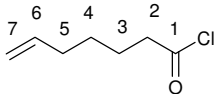

Oxalyl chloride (10 mL, 115 mmol) was added drop wise to a solution of 6-heptenoic acid (3.35 g, 26.3 mmol) and DMF (0.1 mL) in DCM

(100 mL) at 0°C. The solution was left stirring overnight at room temperature, and the solvent was evaporated under reduced pressure. 3.42 g of orange oil and black solid were obtained. It was proved by NMR that the oil was the pure desired product whereas the solid contained impurities. The oil was used for the next step without further purification. ^{1}H NMR ($CDCl_3$, 300 MHz): δ = 5.77 (ddt, J_t = 6.9, J_{d1} = 11.1 and J_{d2} = 16.2 Hz, 1 H, 6), 5.00 (m, 2 H, 7), 2.90 (t, J = 7.16 Hz, 2 H, 2), 2.08 (q, J = 7.11 Hz, 2 H, 5), 1.72 (quint, J = 7.4 Hz, 2 H, 3), 1.45 (quint, J = 7.5 Hz, 2 H, 4).

3 (7-octenoyl chloride)

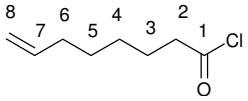

Oxalyl chloride (3 mL, 34.4 mmol) was added drop wise at 0°C to a solution of **1** (131 mg, 0.92 mmol) and DMF (0.1 mL) in DCM (10 mL). After 20h of stirring at room temperature, the solvents and excess oxalyl chloride were evaporated to afford 150 mg of solid which was used for the next step without further purification. ($CDCl_3$, 300 MHz): δ = 5.75 (m, 1 H, 7), 4.99 (m, 2 H, 8), 2.88 (t, J = 7.3 Hz, 2 H, 2), 2.05 (q, J = 6.5 Hz, 2 H, 6), 1.71 (quint, J = 7.3 Hz, 2 H, 3), 1.38 (m, 4 H, 4 & 5), + oxalic acid (11.4 ppm) and DMF (2 s near 3.0 ppm).

4 (8-nonenoyl chloride)

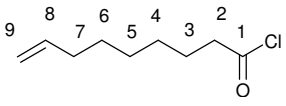

Oxalyl chloride (1.2 mL, 13.7 mmol) was added drop wise at 0°C to a solution of **2** (470 mg, 3.0 mmol) and DMF (20 µL) in DCM (20 mL). After 20h of stirring at room temperature, the solvents and excess oxalyl chloride were evaporated to afford 530 mg of solid which was used for the next step without further purification. ^{1}H NMR ($CDCl_3$, 300 MHz): δ = 5.79 (ddt, J_t = 6.7, J_{d1} = 10 and J_{d2} = 17 Hz, 1 H, 8), 4.98 (m, 2 H, 9), 2.88 (t, J = 7.3 Hz, 2 H, 2), 2.04 (q, J = 6.9 Hz, 2 H, 7), 1.71 (quint, J = 7.2 Hz, 2 H, 3), 1.36 (m, 6 H, 4, 5 & 6), + oxalic acid (11.0 ppm) and DMF (8.21, 3.09 and 2.96 ppm).

5 (dodecanedioyl chloride)

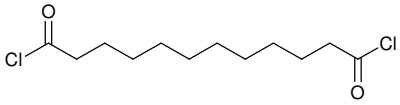

Dodecanedioic acid (229 mg, 1.0 mmol) was dissolved in a mixture of DCM (100 mL) and THF (20 mL). One drop of DMF was added. To this stirred suspension, oxalyl chloride (660 µL, 7.8 mmol) was added at 0°C. The mixture was left stirring at room temperature overnight, then the volatiles were evaporated, giving 364 mg of **5** as an oily solid which was used for the next step without further purification.

6 (hexadecanedioyl chloride)

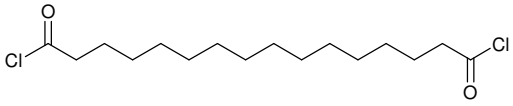

Oxalyl chloride (660 µL, 4.73 mmol) was added at 0°C to a solution of hexadecanedioic acid (286 mg, 1 mmol) and DMF (one drop) in THF (100 mL). The mixture was left stirring at room temperature overnight, then the volatiles were evaporated, giving **6** as a crude (green liquid and black solid) which was used for the next step without further purification.

7 (5-*tert*-Butyl isophthaloyl dichloride)[3]

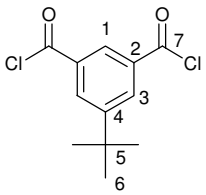

Oxalyl chloride (17 g, 0.134 mol) was added to a solution of 5-*tert*-butyl isophthaloic acid (5 g, 22.5 mmol) in DCM (60 mL). One drop of DMF (approx. 0.05 mL) was added: a gas release was observed. The solution was left stirring 20h at room temperature. Then the solvent was evaporated, affording 7.0 g of a yellow solution which crystallised partly in a yellow oily solid and partly in a white crystalline solid. By analysis, the white solid is pure **7** and the yellow solid is the same with traces of DMF and water (quantitative yield). ^{1}H NMR ($CDCl_3$, 300 MHz): δ = 8.67 (t, J = 1.7 Hz, 2 H, 3), 8.40 (d, J = 1.6 Hz, 1 H, 1), 1.40 (s, 9 H, 6). IR (ν, cm^{-1}): 3100 (m, $C_{sp}{}^2$-H), 2967 (m, $C_{sp}{}^3$-H), 1758 (s, conjugated carbonyl chloride C=O), 1588 (w, conjugated

aromatic C=C), 1474 & 1437 (w, aromatic C=C), 1368 (w, C_{sp}^3-H), 1214 & 1149 (w, C_{sp}^3-H), 992 (w, C_{sp}^3-H), 687 (s, C-Cl). The analysis is in agreement with the literature data.[3]

8 (*N*,*N'*-Bis-(6-aminopyridin-2-yl)-5-*tert*-butyl isophthalamide)

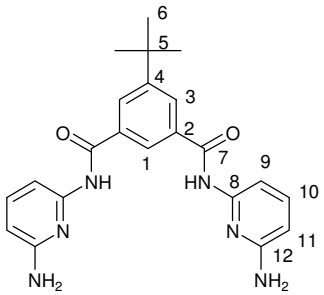

A solution of **7** (1.05 g, 4.05 mmol) in THF (50 mL) was added dropwise at room temperature to a solution of 2,6-diaminopyridine (4.13 g, 37.8 mmol) and triethylamine (1.18 mL, 8.5 mmol) in THF (100 mL). The mixture was left stirring 20h at room temperature, then the solvent was evaporated and 150 mL of water were added to the crude. After 10 min of stirring, the mixture was filtered and the 1.4 g of grey wet solid that were obtained were separated by flash chromatography (eluent: DCM/THF 3:1) to give 1.39 g of desired product as a beige solid (3.43 mmol, 85% yield). mp 142°C. ^{1}H NMR ($CDCl_3$, 300 MHz): δ = 9.31 (br. s, 2 H, NH), 8.27 (t, J = 1.6 Hz, 1 H, 1), 8.12 (d, J = 1.5 Hz, 2 H, 3), 7.63 (d, J = 7.3 Hz, 2 H, 9), 7.43 (t, J = 8.1, 2 H, 10), 6.24 (d, J = 7.8 Hz, 2 H, 11), 4.47 (br. s, 4 H, NH2), 1.32 (s, 9 H, 6). ^{13}C NMR (DMSO-d_6, 300 MHz): δ = 165.07 (7), 158.52 (8), 151.31 (4), 150.35 (12), 138.91 (10), 134.07 (2), 127.93 (3), 124.20 (1), 104.00 (9), 101.79 (11), 30.87 (6), 30.35 (5). Mass spectrum (ES^+, exact mass): m/z = 427.1851 {M + Na^+}, calculated: 427.1858. Elemental analysis: found: H, 6.16; C, 65.48; N, 18.35; calculated with 0.5 equiv. THF: H, 6.53; C, 65.47; N, 18.57.

9 (5-*tert*-Butyl-*N*,*N'*-bis-(6-pent-4-enoylamino-pyridin-2-yl)-isophthalamide)

A solution of pent-4-enoic anhydride (109 µL, 0.596 mmol) in THF (25 mL) was added slowly to a solution of **8** (100 mg, 0.247 mmol) and triethylamine (88 µL, 0.631 mmol) in THF (40 mL). The mixture was heated and left stirring at reflux overnight. Then the solvent was evaporated and the crude was re- $NaHCO_3$, dried over $MgSO_4$, filtered and evaporated.

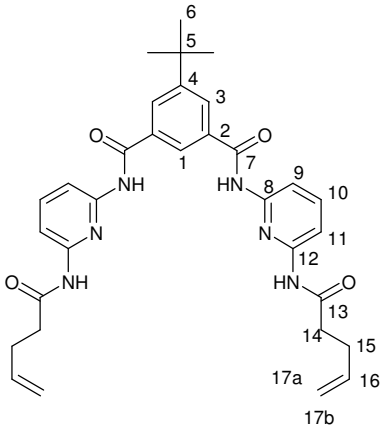

The yellow solid obtained washed with hexane, to give 77.6 mg of **9** as a white solid (0.136 mmol, 23% yield).dissolved in dichloromethane, washed with aqueous 5% ^{1}H NMR ($CDCl_3$, 300 MHz): δ = 9.10 (br. s, 2 H, NH between 7 and 8), 8.36 (br. s, 2 H, 3), 8.28 (br. s, 1 H, 1), 8.17 (br. s, 2 H, NH between 12 and 13), 8.02 (d, J = 7.0 Hz, 2 H, 11), 7.90 (d, J = 6.3 Hz, 2 H, 9), 7.73 (t, J = 8.1 Hz, 2 H, 10), 5.84 (m, 2 H, 16),5.08 (br. d, J = 17.4 Hz, 2 H, 17a), 5.01 (br. d, J = 11.5 Hz, 2 H, 17b), 2.54 (m, 8 H, 14 & 15), 1.38 (s, 9 H, 6).Mass spectrum (ES$^+$): *m/z* = 607 {M + K$^+$}, 591 {M + Na$^+$}, 569 {M + H$^+$}. Elemental analysis: found: H, 6.73; C, 68.82; N, 13.03; calculated with 0.5 equiv. hexane: H, 7.08; C, 68.72; N, 13.74.

10 (5-*tert*-Butyl-*N*,*N*′-bis-(6-hept-6-enoylamino-pyridin-2-yl)-isophthalamide)

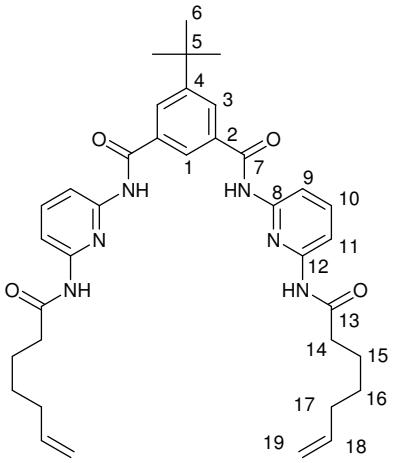

A solution of **6-heptenoyl chloride** (788 mg, 5.37 mmol) in THF (40 mL) was added slowly to a solution of **8** (891 mg, 2.20 mmol) and triethylamine (0.85 mL, 6.1 mmol) in THF (120 mL). The mixture was left stirring at room temperature overnight, then the solvent was evaporated and the crude was re-disolved in dichloromethane, washed with 4 × 50 mL of aqueous $NaHCO_3$ (5%) + NaCl solution, dried over $MgSO_4$, filtered and evaporated. The solid obtained was washed with 2 × 150 mL hexane, to give 764 mg of **10** as a yellowish solid (55.5%). mp 182°C. ^{1}H NMR ($CDCl_3$, 300 MHz): δ = 8.48 (br. s, 2 H, NH between 7 and 8), 8.23 (m, 1 H, 1), 8.14 (d, J = 1.5 Hz, 2 H, 3), 8.05 (d, J = 8.1 Hz, 2 H, 11), 7.97 (d, J = 8.0 Hz, 2 H, 9), 7.77 (t and s, J_t = 8.0 Hz, 4 H, 10 & NH between 12 and 13), 5.80 (ddt, J_t = 6.7, J_{d1} = 10.2 and J_{d2} = 17.0 Hz, 2 H, 18), 5.00 (m, 4 H, 19), 2.41 (t, J = 7.5 Hz, 4 H, 14), 2.10 (q, J = 7.1 Hz, 4 H, 17), 1.76 (quint., J = 7.7 Hz, 4 H, 15), 1.49 (quint., J = 7.6 Hz,

4 H, 16), 1.40 (s, 9 H, 6). ^{13}C NMR ($CDCl_3$, 300 MHz): δ 171.84 (13), 165.24 (7), 153.29 (8), 149.79 (12), 149.49 (4), 140.87 (10), 138.19 (18), 134.37 (2), 128.47 (3), 122.60 (1), 114.82 (19), 110.04 (9), 109.76 (11), 37.42 (14), 35.17 (5), 33.36 (17), 31.06 (6), 28.34 (16), 24.71 (15). Mass spectrum (ES+, exact mass): m/z = 647.3337 $\{M + Na^+\}$, calculated : 647.3322. Elemental analysis: found: C, 67.77; H, 7.31; N, 13.65; calculated with 0.66 equiv. of water: C, 67.90; H, 7.18; N, 13.20.

11 (5-*tert*-Butyl-*N*,*N*′-bis-(6-oct-7-enoylamino-pyridin-2-yl)-isophthalamide)

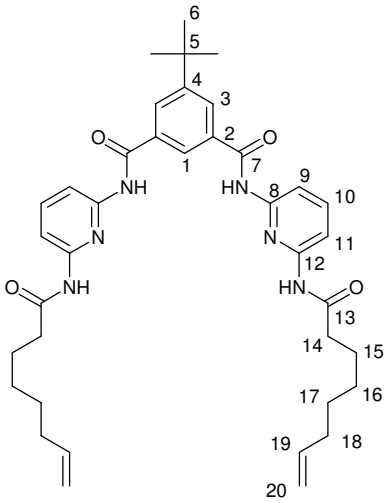

A solution of **3** as obtained at the last step (containing DMF and oxalic acid) (150 mg) in THF (20 mL) and DCM (20 mL) was added slowly to a solution of **8** (155 mg, 0.383 mmol) and triethylamine (1.2 mL, 8.61 mmol) in THF (60 mL). The mixture was left stirring at room temperature overnight, then the solvent was evaporated and the crude was re-dissolved in DCM (15 mL), washed with aqueous 5% $NaHCO_3$, dried over $MgSO_4$, filtered and evaporated, to give 207.3 mg of red viscous oil. It was separated by flash chromatography (silica gel, eluent DCM / ethyl acetate 30 / 70) to give 17.1 mg of **11** as a yellow solid (6.8% yield). ^{1}H NMR ($CDCl_3$, 300 MHz): δ = 8.33 (s, 2 H, NH between 7 and 8), 8.18 (m, 5 H, 1, 3 & 11), 8.10 (m, 4 H, 9 & NH between 12 and 13), 7.72 (t, J = 7.9 Hz, 2 H, 10), 5.78 (m, 2 H, 19), 4.95 (m, 4 H, 20), 2.40 (t, J = 7.53 Hz, 4 H, 14), 2.03 (m, 4 H, 18), 1.72 (m, 4 H, 15), 1.63 (m, 17 H, 6, 16 & 17) + traces of monosubstituted product (6.3 ppm, d, J = 7.9 Hz, free NH_2).

12 (5-*tert*-Butyl-*N*,*N*′-bis-(6-non-8-enoylamino-pyridin-2-yl)-isophthalamide)

A solution of **4** (530 mg, 3.0 mmol) in THF (100 mL) was added slowly to a solution of **8** (500 mg, 1.24 mmol) and triethylamine (0.5 mL, 3.6 mmol) in THF (150 mL). The mixture

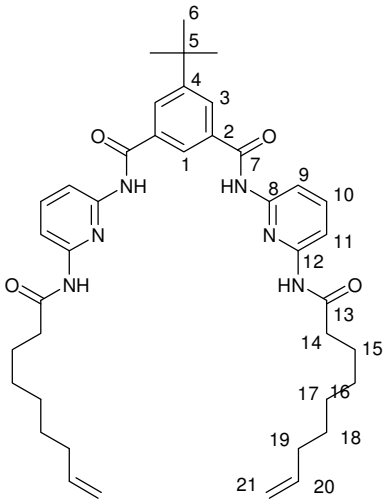

was left stirring at room temperature overnight, then the solvent was evaporated and the crude was re-dissolved in DCM (200 mL), washed with an aqueous solution of $NaHCO_3$ (5%) and NaCl (5%), dried with $MgSO_4$, filtered and evaporated. The yellow solid obtained was re-dissolved in 10 mL of DCM and methanol, and 250 mL of hexane were added, causing the precipitation of a solid which was filtered, re-dissolved in DCM and methanol and evaporated, to afford 787 mg of **12** as a white solid (93% yield). mp 175°C. ^{1}H NMR ($CDCl_3$, 300 MHz): δ = 8.67 (m, 2 H, NH between 7 and 8), 8.18 (m, 3 H, 1 and 3), 7.99 (m,4 H, 11 & 9), 7.73 (m, 4 H, 10 & NH between 12 and 13), 5.78 (m, 2 H, 20), 4.94 (m, 4 H, 21), 2.38 (m, 4 H, 14), 2.01 (m, 4 H, 19), 1.70 (m, 4 H, 15), 1.63 (m, 21 H, 6, 16, 17 & 18). ^{13}C NMR ($CDCl_3$, 300 MHz): δ = 171.76 (13), 164.91 (7), 153.41 (8), 149.73 (12), 149.32 (4), 140.95 (10), 138.87 (20), 134.49 (5), 128.31 (3), 122.60 (6), 114.34 (21), 110.07 (9), 109.68 (11), 37.70 (14), 35.21 (2), 33.64 (19), 31.12 (1), 29.01 (18), 28.77 (17), 28.65 (16), 25.25 (17). Mass spectrum (ES+, exact mass): *m/z* = 703.3953 $\{M + Na^+\}$, calculated : 703.3948. Elemental analysis: found: C, 70.28; H, 7.78; N, 12.28; calculated: C, 70.56; H, 7.70; N, 12.34.

13 (5-*tert*-Butyl-*N*,*N*′-bis-(6-undec-10-enoylamino-pyridin-2-yl)-isophthalamide)

A solution of 10-undecenoyl chloride (0.26 mL, 0.25 g, 1.2 mmol) in THF (15 mL) was added to a solution of **8** (202 mg, 0.50 mmol) and triethylamine (0.17 mL, 1.2 mmol) in THF (85 mL) at 0°C. The mixture was left stirring overnight at room temperature, then the solvent was evaporated and the crude was re-dissolved in dichloromethane, washed with 4 × 25 mL of aqueous 5% $NaHCO_3$, dried with $MgSO_4$, filtered and evaporated. The yellow solid obtained was washed with 2 × 50 mL of hexane, to give 243 mg of **13** as a yellow solid

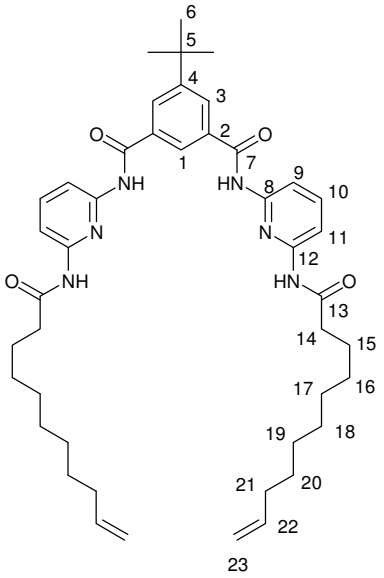

(66% yield). mp 130°C. ^{1}H NMR ($CDCl_3$, 300 MHz): δ = 8.38 (s, 2 H, NH between 7 and 8), 8.21 (s, 1 H, 1), 8.13 (s, 2 H, 3), 8.06 (d, J = 8.1 Hz, 2 H, 11), 7.98 (d, J = 8.0 Hz, 2 H, 9), 7.78 (t, J = 8.0 Hz, 2 H, 10), 7.67 (s, 2 H, NH between 12 and 13), 5.80 (ddt, J_t = 6.8, J_{d1} = 10.2, J_{d2} = 16.9 Hz, 2 H, 22), 4.96 (m, 4 H, 23), 2.40 (t, J = 7.4 Hz, 4 H, 14), 2.03 (q, J = 7.0 Hz, 4 H, 21), 1.74 (quint., J = 7.2 Hz, 4 H, 15), 1.42 (s, 9 H, 6), 1.32 (m, 20 H, 16, 17, 18, 19, 20). ^{13}C NMR ($CDCl_3$, 300 MHz): δ = 171.76 (13), 164.94 (7), 153.39 (8), 149.73 (12), 149.37 (4), 140.99 (10), 139.09 (22), 134.49 (2), 128.33 (3), 122.65 (1), 114.16 (23),110.04 (9), 109.70 (11), 37.76 (14), 35.22 (5), 33.73 (21), 31.14 (6), 29.28 (18 or 19), 29.26 (19 or 18), 29.17 (20), 29.03 (17), 28.85 (16), 25.30 (15). Mass spectrum (ES^+, exact mass): m/z = 759.4586 {M + Na^+}, calculated: 759.4574. Elemental analysis: found: C, 70.48; H, 8.30; N, 10.99; calculated with 0.5 equiv. ethyl acetate: C, 70.74; H, 8.26; N, 10.76.

Ring closure metathesis experiment on 9

A solution of Grubbs' 1st generation catalyst (bis(tricyclohexylphosphine)benzylidene ruthenium(IV) dichloride) (6 mg) in DCM (2 mL) was added drop wise to a solution of **9** (40 mg) in DCM (8 mL) under reflux. The mixture was left stirring at reflux overnight. Then the solvent was evaporated to give 48.9 mg of green solid which was analysed by mass spectrometry, ^{1}H and ^{31}P NMR: it is a mixture of starting material, Grubbs' catalyst and products of decomposition of the catalyst.

14 (ring closure metathesis experiment on **10**)

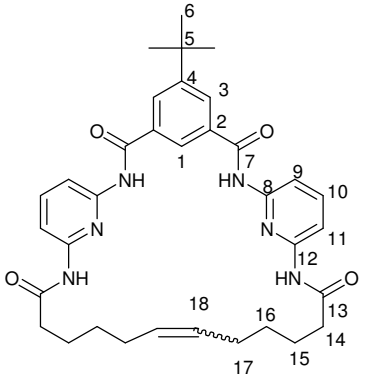

A solution of Grubbs' 1st generation catalyst (66.6 mg, 80.9 µmol) in DCM (50 mL) was added drop wise to a solution of **10** (500 mg, 801 µmol) in DCM (10 mL) at reflux. The mixture was heated to reflux and left stirring for 5 hours, then the solvent was evaporated to give 62.1 mg of green solid which was washed with hexane to give a yellow oil. Flash chromatography on silica (eluent: DCM / ethyl acetate with increasing ratio of ethyl acetate) finally gave 209.2 mg of **14** (351 µmol, 44% yield) as a brown solid**,** mixture of *cis* and *trans* isomers (approx. 68% *cis* ± 6% according to ^{13}C NMR). mp 298°C. ^{1}H NMR ($CDCl_3$, 300 MHz): δ = 8.38 (m, 5 H, 1, 3 & NH between 7 and 8), 8.13 (d, J = 8.3, 2 H, 9), 7.97 (d, J = 8.1, 2 H, 11), 7.82 (t, J = 8.3 Hz, 2 H, 10), 7.69 (br. s., 2 H, NH between 12 and 13), 5.40 (m, 2 H, 18), 2.43 (m, 4 H, 14), 2.08 (m, 4 H; 17), 1.79 (m, 4 H, 15), 1.50 (m, 4 H, 16), 1.42 (s, 9 H, 6). ^{13}C NMR ($CDCl_3$, 300 MHz): δ = 172.50 (13), 165.15 (7 *trans*), 164.88 (7 *cis*), 153.60 (8 *cis*), 153.53 (8 *trans*), 149.99 (6 *cis*), 149.96 (6 *trans*), 149.92 (4 *cis*), 149.86 (4 *trans*), 140.81 (10 *cis*), 140.69 (10 *trans*), 133.68 (2 *trans*), 133.49 (2 *cis*), 129.63 (18 *cis*), 129.80 (3), 130.04 (18 *trans*), 120.86 (1), 109.59 (9), 109.45 (11 *trans*), 109.35 (11 *cis*), 37.45 (14 *trans*), 37.19 (14 *cis*), 35.16 (5), 31.59 (17 *trans*), 31.00 (6 *cis*), 30.98 (6 *trans*), 28.75 (16 *cis*), 28.30 (16 *trans*), 26.37 (17 *cis*), 24.84 (15 *cis*), 24.38 (15 trans). Mass spectrum (ES^+, exact mass): m/z = 619.3009{M + Na^+}, calculated: 619.3006. Elemental analysis: found: C, 65.37; H, 6.79; N, 13.02; calculated with 0.4 equiv. dichloromethane: C, 65.51; H, 6.52; N, 13.33.

15 (ring closure metathesis experiment on **12**)

A solution of Grubbs' 1st generation catalyst (48.5 mg, 59.0 µmol) in DCM (40 mL) was added drop wise to a solution of **12** (404 mg, 593 µmol) in DCM (150 mL) at reflux. The

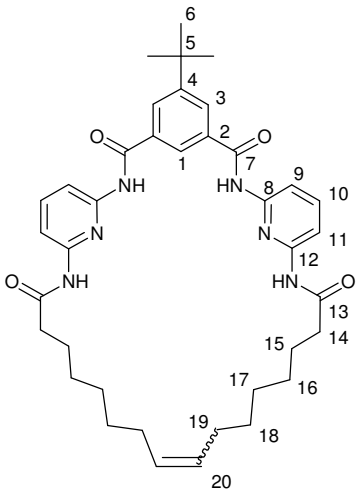

mixture was heated to reflux and left stirring during 4 hours, then the solvent was evaporated to give a green solid which was separated by flash chromatography on silica (eluent: DCM / ethyl acetate with increasing ratio of ethyl acetate), to give finally 151.2 mg of **15** (231.6 µmol, 39% yield) as a mixture of *cis* and *trans* isomers (approx. 79% *cis* ± 5% according to ^{13}C NMR). mp > 300°C. ^{1}H NMR ($CDCl_3$, 300 MHz): δ = 8.32 (m, 3 H, 1 & 3), 8.11 (m, 2 H, 9), 8.00 (d, *J* = 8.6, 2 H, 11), 7.81 (m, 4 H, 10 & NH between 7 and 8), 7.62 (m, 2 H, NH between 12 and 13), 5.35 (m, 2 H, 20), 2.39 (m, 4 H, 14), 1.98 (m, 4 H, 19), 1.75 (m, 4 H, 15), 1.41 (s, 9 H, 6), 1.36 (m, 12 H, 16, 17 & 18). ^{13}C NMR ($CDCl_3$ + 5% MeOH, 300 MHz): δ = 172.30 (13), 165.41 (7), 153.62 (8), 149.86 (12), 149.84 (4), 140.84 (10 *cis*), 140.73 (10 *trans*), 134.04 (2), 130.29 (20 *trans*), 129.89 (3 *cis*), 129.80 (20 *cis*), 129.76 (3 *trans*), 120.46 (1), 109.70 (9), 109.62 (11 *trans*), 109.59 (11 *cis*), 39.80 (5 *cis*), 37.79 (14 *trans*), 37.60 (5 *trans*), 35.15 (14 *cis*), 31.91 (19 *trans*), 30.98 (6), 29.11 (18 *cis*), 28.76 (18 *trans*), 28.68 (17 *cis*), 28.38 (19 *cis*), 27.93 (17 *trans*), 26.65 (16), 25.42 (15 *trans*), 25.21 (15 *cis*). Mass spectrum (ES^+, exact mass): *m/z* = 675.3651{M + Na^+}, calculated: 675.3635. Elemental analysis: found: C, 70.02; H, 7.79; N, 11.88; calculated with 0.25 equiv. hexane and 0.25 equiv. ethyl acetate: C, 69.85; H, 7.74; N, 12.07.

16 (ring closure metathesis experiment on **13**)

A solution of Grubbs' 1st generation catalyst (14 mg, 17.0 µmol) in DCM (5 mL) was added drop wise to a solution of **13** (99 mg, 134 µmol) in DCM (20 mL). The mixture was heated to reflux and left stirring during 2 hours, then the solvent was evaporated to give 93 mg of green solid. A flash chromatography (eluent: pentane / ethyl acetate with increasing ratio of ethyl acetate), finally gave 70 mg of isolated **16** as a mixture of *cis* and *trans* isomers (approx.

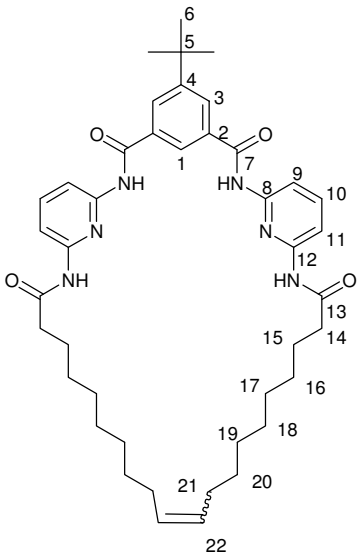

66% *cis* ± 6% according to ^{13}C NMR) (98.7 mmol, 73.5% yield). mp > 300°C ^{1}H NMR ($CDCl_3$, 300 MHz): δ = 8.54 (s, 2 H, NH between 7 and 8), 8.28 and 8.25 (m, 3 H, 1 & 3), 8.05 (br. s, 2 H, NH between 12 and 13), 7.98 (m, 2 H, 9), 7.78 (m, 4 H, 10 & 11), 5.33 (t, J = 3.7 Hz, 2 H, 22), 2.38 (t, J = 7.3 Hz, 4 H, 14), 1.98 (m, 4 H, 21), 1.73 (quint., J = 7.2 Hz, 4 H, 15), 1.38 (s, 9 H, 6), 1.28 (m, 20 H, 16, 17, 18, 19 & 20). ^{13}C NMR ($CDCl_3$, 300 MHz): δ = 171.97 (13), 165.29 (7), 153.91 (8), 149.79 (12), 149.63 (4), 140.96 (10 *trans*), 140.87 (10 *cis*), 134.20 (2 *trans*), 134.03 (2 *cis*), 130.47 (22 *trans*), 129.95 (22 *cis*), 129.74 (3 *trans*), 128.67 (3 *cis*), 114.20 (1), 110.31 (9 *cis*), 110.09 (9 *trans*), 109.83 (11), 37.80 (14), 35.24 (5), 32.14 (21 *trans*), 31.03 (6), 29.45 (18 *cis*), 29.28 (19 *cis*), 29.15 (18 *trans*), 29.11 (19 *trans*), 29.06 (17 & 20), 28.81 (16 *cis*) 28.27 (16 *trans*), 26.90 (21 *cis*), 25.50 (15 *trans*), 25.34 (15 *cis*). Mass spectrum (ES^+, exact mass): *m/z* = 731.4289 {M + Na^+}, calculated: 731.4261. Elemental analysis: found: C, 71.10; H, 7.93; N, 11.68; calculated: C, 71.16; H, 7.96; N, 11.85.

17

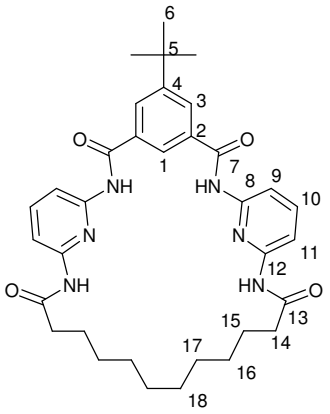

A solution of **dodecanedioyl chloride** (1 mmol, 364 mg as obtained) in a mixture of THF (90 mL) and DCM (15 mL), and a solution of **8** (400 mg, 0.989 mmol) and triethylamine (660 µL, 4.73 mmol) in a mixture of THF (90 mL) and DCM (10 mL), were added simultaneously to THF (40 mL) over one hour. The mixture was left stirring overnight at room temperature. Then the solvents and volatiles were evaporated. The crude obtained was re-dissolved in DCM (100 mL), washed with 1 M NaOH solution (50 mL), then with 5% $NaHCO_3$ solution (3 × 50 mL), dried with $MgSO_4$, filtered and evaporated. The

mixture obtained was separated by flash chromatography (eluent: DCM / ethyl acetate with increasing ratio of ethyl acetate), giving **17** as a beige solid (217 mg,36.6% yield). mp > 300°C. ^{1}H NMR ($CDCl_3$, 300 MHz): δ = 8.36 (d, J = 1.8 Hz, 2 H, 3), 8.34 (s, 2 H, NH between 7 and 8), 8.14 (d, J = 8.1 Hz, 2 H, 9), 8.00 (d, J = 8.2 Hz, 2 H, 11), 7.83 (br. s, 1 H, 1), 7.82 (tr, J = 8.0 Hz, 2 H, 10), 7.67 (s, 1 H, NH between 12 and 13), 2.42 (t, J = 7.5 Hz, 4 H, 14), 1.78 (quint, J = 7.1 Hz, 4 H, 15), 1.42 (s, 9 H, 6), 1.32 (m, 12 H, 16, 17 & 18). ^{13}C NMR ($CDCl_3$, 300 MHz): δ = 171.80 (13), 164.62 (7), 154.07 (8), 149.71 (12), 149.64 (4), 141.14 (10), 133.87 (2), 130.20 (3), 119.76 (1), 109.85 (9), 109.59 (11), 37.63 (14), 35.29 (5), 31.07 (6), 28.39 (18), 28.27 (17), 28.03 (16), 25.08 (15). Mass spectrum (ES^+): m/z = 621.3172 $\{M + H^+\}$, calculated : 621.3165. Elemental analysis: found: C, 64.84; H, 7.22; N, 13.04; calculated with 2 equiv. water: C, 64.33; H, 7.30; N, 13.24. Crystals of the product have been obtained in DCM and in acetone. The resulting crystal structures, as determined by X-ray diffraction, contain respectively one molecule of DCM and one of acetone. They are presented in *Appendix 1*.

18

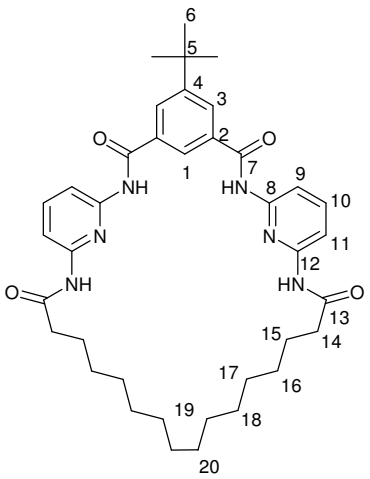

A solution of **hexadecanedioyl chloride** (1 mmol, as obtained) in THF (100 mL), and a solution of **8** (400 mg, 0.989 mmol) and triethylamine (660 µL, 4.73 mmol) in THF (100 mL), were added simultaneously to THF (50 mL) over 1 hour. The mixture was left stirringovernight at room temperature, then the solvents and volatiles were evaporated. The crude obtained was re--dissolved in DCM (250 mL) and 1% NaOH solution (50 mL) was added. The solid that precipitated was filtered, and the organic phase was separated, washed with 5% $NaHCO_3$ solution (3 × 50 mL), dried with $MgSO_4$, filtered and evaporated. The mixture obtained was separated by flash chromatography (eluent: DCM/ethyl

acetate with increasing ratio of ethyl acetate), giving **18** as a white solid (119 mg, 18.3% yield). mp > 300°C. ^{1}H NMR ($CDCl_3$, 300 MHz): δ = 8.35 (s, 2 H, N-H between 7 and 8), 8.30 (d, J = 1.4 Hz, 2 H, 3), 8.10 (d, J = 8.0 Hz, 2 H, 9), 8.00 (d, J = 7.7 Hz, 2 H, 11), 7.85 (s, 1 H, 1), 7.81 (tr, J = 8.0 Hz, 2 H, 10), 7.63 (s, 2 H, N-H between 12 and 13), 2.39 (t, J = 7.6 Hz, 4 H, 14), 1.75 (quint, J = 7.0 Hz, 4 H, 15), 1.41 (s, 9 H, 6), 1.26 (m, 20 H, 16, 17, 18, 19 & 20). ^{13}C NMR ($CDCl_3$ + 2% MeOH, 300 MHz): δ = 172.25 (13), 165.37 (7), 153.67 (8), 149.87 (12), 149.82 (4), 140.90 (10), 134.04 (2), 129.86 (3), 120.36 (1), 109.82 (9), 109.77 (11), 37.69 (14), 35.20 (5), 31.02 (6), 28.65 (18), 28.45 (19 & 20), 28.27 (17), 28.18 (16), 25.20 (15). Mass spectrum (ES^+): m/z = 677.3789 $\{M + H^+\}$, calculated : 677.3791. . Crystals of the product, of its complex with barbital and its complex with **39** have been obtained. The resulting crystal structure, as determined by X-ray diffraction, are presented in *Appendix 1*.

19 (diethylene glycol ditosylate)[4]

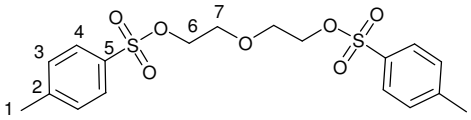

Sodium hydroxide (20 g, 500 mmol) and water (100 mL) were added at 0°C to a solution of diethylene glycol (20 mL, 170 mmol) in THF (200 mL). To this stirred mixture, a solution of *para*-toluenesulphonyl chloride (70 g, 367 mmol) in THF (250 mL) was added drop wise. The mixture was left stirring at room temperature during 2 days. It was then acidified with approx. 7 mL of conc. HCl solution (37% w/w), neutralised with Na_2CO_3 until no bubbling was observed, and extracted with 3 × 75 mL of DCM. The combined organic phase was washed with 75 mL of water, dried with $MgSO_4$, filtered and evaporated, to give 73.5 g of **19** as a yellow oil that slowly crystallised at room temperature into a white solid (97.2% yield). ^{1}H NMR ($CDCl_3$, 300 MHz): δ = 7.77 (d, J = 8.1 Hz, 4 H, 4), 7.34 (d, J = 8.1 Hz, 4 H, 3), 4.09-4.06 (m, 4 H, 6), 3.61-3.58 (m, 4 H, 7), 2.44 (s, 6 H, 1). The analysis is in agreement with the literature data.[4]

19h (Diethylene glycol monotosylate)[5]

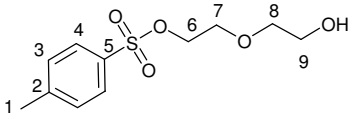

Tosyl chloride (1.25 g, 6.5 mmol) was added to a mixture of sodium hydroxide (0.29 g, 7.2 mmol) and diethylene glycol (0.60 mL, 6.3 mmol) in THF (20 mL) and water (1 mL). The mixture was left stirring at room temperature during 24 hours. Then the THF was evaporated, the crude redissolved in 80 mL of water and extracted with 3 × 35 mL of ethyl acetate. The combined organic phase was dried with $MgSO_4$, filtered and evaporated. The colorless oil that was obtained was separated by flash chromatography (solvent: diethyl ether), affording 0.828 g of **19h** (61% yield). ^{1}H NMR ($CDCl_3$, 300 MHz): δ = 7.79 (d, J = 8.3 Hz, 2 H, 4), 7.34 (d, J = 8.3 Hz, 2 H, 3), 4.20-4.17 (m, 2 H, 6), 3.69-3.64 (m, 4 H, 7 & 8), 3.53-3.51 (m, 2 H, 9), 2.44 (s, 3 H, 1), 2.06 (s, 1 H, OH). The analysis is in agreement with the literature data.[5]

20 (Triethylene glycol ditosylate)[4]

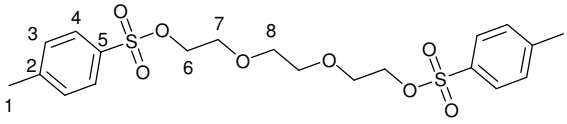

A solution of sodium hydroxide (20 g, 500 mmol) in water (100 mL) was added to a solution of triethylene glycol (22 mL, 171 mmol) in THF (200 mL). To this stirred mixture, a solution of *para*-toluenesulphonyl chloride (70 g, 367 mmol) in THF (250 mL) was added drop wise. The mixture was left stirring at room temperature for 2 days. It was then acidified with approx. 7 mL of conc. HCl solution (37% w/w), neutralised with Na_2CO_3 until no bubbling was observed, and extracted with 3 × 75 mL of DCM. The combined organic phase was washed with 75 mL of water, dried with $MgSO_4$, filtered and evaporated, to give 73.5 g of **20** as a yellow oil that slowly crystallised at room temperature into a white solid (97.2% yield). mp 78°C. ^{1}H NMR ($CDCl_3$, 300 MHz): δ = 7.78 (d, J = 8.1 Hz, 4 H, 4), 7.33 (d, J = 8.1 Hz, 4 H, 3), 4.13 (t, J = 4.8 Hz , 4 H, 6), 3.64 (t, J = 4.8 Hz , 4 H, 7), 3.51 (s, 4 H, 8), 2.43 (s, 6 H, 1). ^{13}C NMR ($CDCl_3$, 300 MHz): δ = 144.81 (2), 132.93 (5), 129.80 (3), 127.90 (4), 70.63 (7), 69.15 (6), 68.69 (5), 21.58 (1). Mass spectrum (ES^+, exact mass): m/z = 481.0962 {M + Na^+}, calculated: 481.0967.

Elemental analysis: found: C, 51.64; H, 5.56; N, 0.00; calculated with 0.25 equiv. water: C, 51.71; H, 5.79; N, 0.00. The analysis is in agreement with the literature data.[4]

21 (Tetraethylene glycol ditosylate)[4]

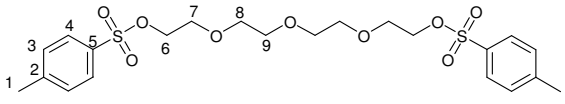

A solution of sodium hydroxide (20 g, 500 mmol) in water (100 mL) was added to a solution of triethylene glycol (28.8 mL 167 mmol) in THF (200 mL). To this stirred mixture, a solution of *para*-toluenesulphonyl chloride (70 g, 367 mmol) in THF (250 mL) was added drop wise. The mixture was left stirring at room temperature for 2 days. It was then acidified with approx. 7 mL of conc. HCl solution (37% w/w), neutralised with Na_2CO_3 until no bubbling was observed, and extracted with 3 × 75 mL of DCM. The combined organic phase was washed with 75 mL of water, dried with $MgSO_4$, filtered and evaporated, to give 62.9 g of **21** as a yellow oil (77% yield). ^{1}H NMR ($CDCl_3$, 300 MHz): δ = 7.78 (d, J = 8.2 Hz, 4 H, 4), 7.33 (d, J = 8.2 Hz, 4 H, 3), 4.14 (t, J = 4.9 Hz , 4 H, 6), 3.67 (t, J = 4.9 Hz , 4 H, 7), 3.55 (s, 8 H, 8 & 9), 2.43 (s, 6 H, 1). The analysis is in agreement with the literature data.[4]

22 (1-Iodo-2-(2-iodo-ethoxy)-ethane)[4]

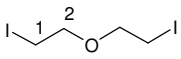

Sodium iodide (56.4 g, 376 mmol) was added to a stirred solution of diethylene glycol ditosylate (30.0 g, 72.3 mmol) in acetone (400 mL) at 0°C. After 24 hours of stirring at room temperature, the mixture was filtered and the acetone solution was evaporated. The orange solid obtained was dissolved in ether (300 mL), washed with water (3 × 100 mL), dried with $MgSO_4$, filtered and evaporated to afford 23.87 g of a red oil, which contains 90% of **22** and 10% of minor impurities according to the NMR, and which was used for the next step without further purification. ^{1}H NMR ($CDCl_3$, 300 MHz): δ = 3.77 (t, J = 6.8 Hz, 4 H, 2), 3.26 (t, J = 6.8 Hz, 4 H, 1). The analysis is in agreement with the literature data.[4]

23 (1-Iodo-2-[2-(2-iodo-ethoxy)-ethoxy]-ethane)[4]

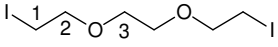

Sodium iodide (67.3 g, 449 mmol) was added to a stirred solution of triethylene glycol ditosylate (40.0 g, 87.2 mmol) in acetone (500 mL) at 0°C. After two days of stirring at room temperature, the mixture was filtered and the acetone solution was evaporated. The yellow solution obtained was dissolved in ether (400 mL), washed with water (2 × 100 mL), dried with $MgSO_4$, filtered and evaporated to give 28 g of **23** as a brown oil (87% yield). ^{1}H NMR ($CDCl_3$, 300 MHz): δ = 3.78 (t, J = 6.8 Hz, 4 H, 2), 3.67 (s, 4 H, 3), 3.27 (t, J = 6.8 Hz, 4 H, 1). The analysis is in agreement with the literature data.[4]

24 (1-Iodo-2-{2-[2-(2-iodo-ethoxy)-ethoxy]-ethoxy}-ethane)[4]

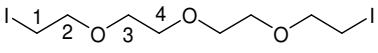

Sodium iodide (67.2 g, 448 mmol) was added to a stirred solution of tetraethylene glycol ditosylate (40.0 g, 79.6 mmol) in acetone (500 mL) at 0°C. After two days of stirring at room temperature, the mixture was filtered and the acetone solution was evaporated. The yellow solution obtained was dissolved in ether (400 mL), washed with 2 × 100 mL, dried with $MgSO_4$ and evaporated to give 31.6 g of **24** as a dark orange oil (96% yield). ^{1}H NMR ($CDCl_3$, 300 MHz): δ = 3.75 (t, J = 6.9 Hz , 4 H, 2), 3.67 (s, 8 H, 3 & 4), 3.26 (t, J = 6.9 Hz , 4 H, 1). The analysis is in agreement with the literature data.[4]

25 (9-{2-[2-(2-Iodo-ethoxy)-ethoxy]-ethoxy}-anthracene)[6]

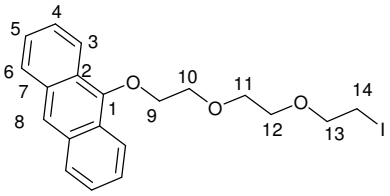

In an apparatus protected from light by a foil cover, a solution of 1-Iodo-2-[2-(2-iodo-ethoxy)-ethoxy]-ethane (20 g, 54 mmol) in THF (200 mL, non distilled) and water (100 mL) was degassed by bubbling nitrogen during 10 minutes. Then potassium hydroxide (6.2 g, 111 mmol) was added and the bubbling of nitrogen was continued during 10 minutes. Then anthrone (3.1 g, 16 mmol) was added and the mixture was heated to reflux under nitrogen, and left at reflux during three days. Then the THF was evaporated. The organic was extracted with 100 mL of dichloromethane, washed with 50 mL of water, dried

with $MgSO_4$, filtered and evaporated. It was then separated by flash chromatography, to give **25** as a white solid (2.96 g, 6.8 mmol, 42.5% yield). ^{1}H NMR ($CDCl_3$, 300 MHz): δ = 8.37-8.40 (m, 2 H, 3), 8.23 (s, 1 H, 8), 7.98-8.01 (m, 2 H, 6), 7.45-7.49 (m, 4 H, 4 & 5), 4.38-4.41 (m, 2 H, 9), 4.00-4.04 (m, 2 H, 10), 3.80-3.87 (m, 6 H, 11, 12 & 13), 3.30 (t, J = 6.7 Hz, 2 H, 14). Mass spectrum (ES^+): m/z = 459.1 {M + Na^+}. The analysis results are consistent with those already reported.[6]

26 (9-(2-{2-[2-(2-Iodo-ethoxy)-ethoxy]-ethoxy}-ethoxy)-anthracene)[6]

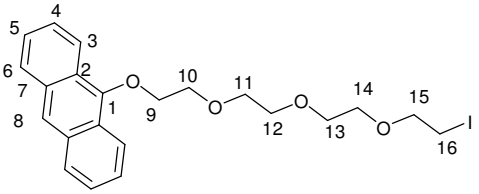

In an apparatus protected from light by a foil cover, a solution of potassium hydroxide (6.3 g, 112 mmol) in water (50 mL) was added to a solution of 1-Iodo-2-{2-[2-(2-iodo-ethoxy)-ethoxy]-ethoxy}-ethane (21 g, 44 mmol) in THF (100 mL). The mixture was degassed by bubbling nitrogen during 20 minutes, then anthrone (3.1 g, 16 mmol) was added and the mixture was heated to reflux and left at reflux during three days. Then the THF was evaporated. The organic was extracted with 3 × 50 mL of dichloromethane and 20 mL of ethyl acetate, the combined organic phase was washed with 50 mL of brine, dried with $MgSO_4$, filtered and evaporated. It was then separated by flash chromatography, to give **26** as an orange oil (2.18 g, 4.5 mmol, 28% yield). ^{1}H NMR ($CDCl_3$, 300 MHz): δ = 8.37-8.41 (m, 2 H, 3), 8.23 (s, 1 H, 8), 7.98-8.01 (m, 2 H, 6), 7.44-7.51 (m, 4 H, 2 H, 4 & 5), 4.38-4.41 (m, 2 H, 9), 3.99-4.02 (m, 2 H, 10), 3.68-3.84 (m, 10 H, 11, 12, 13, 14 & 15), 3.25 (t, J = 7.0 Hz, 2 H, 16). The analysis results are consistent with those already reported.[6]

27 (Tetraethylene glycol mono trityl ether) and **27d** (tetraethylene glycol di trityl ether)

A solution of trityl chloride (6.0 g, 21.5 mmol) in DCM (25 mL) was added drop wise to a solution of tetraethylene glycol (4.0 g, 20.6 mmol) and triethylamine (3.0 mL, 2.2 g, 21.5 mmol) in DCM (50 mL). The mixture was left stirring overnight at room temperature.

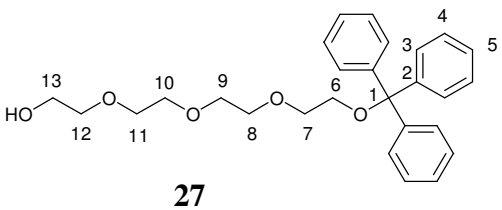

27

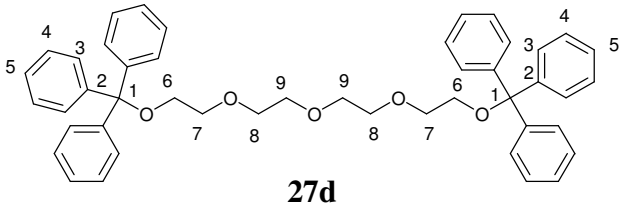

27d

Then 75 mL of DCM were added and this organic solution was washed with water (3 × 120 mL), dried with $MgSO_4$, filtered and evaporated to give a viscous oil which was separated by flash chromatography (eluent: dichloromethane) to give the desired product **27** as a viscous oil (4.74 g, 52.8% yield), and **27d** as a white solid (1.85 g, 13.2% yield). **27**: ^{1}H NMR ($CDCl_3$, 300 MHz): δ = 7.53-7.51 (m, 6 H, 3), 7.37-7.26 (m, 9 H, 4 & 5), 3.75 (m , 10 H, 8, 9, 10, 11, 12), 3.64 (t, J = 4.6 Hz, 2 H, 13), 3.52 (m, 2 H, 7), 3.30 (t, J = 5.1 Hz, 2 H, 6), 2.02 (br. s, 1 H, OH). Mass spectrum (ES^+): m/z = 459.3 $\{M + Na^+\}$. **27d**: ^{1}H NMR: δ 7.49-7.46 (m, 12 H, 3), 7.32-7.20 (m, 18 H, 4 & 5), 3.71-3.67 (m , 12 H, 7, 8 & 9), 3.24 (t, J = 4.6 Hz, 4 H, 6). Mass spectrum (ES^+): m/z = 701.5 $\{M + Na^+\}$.

28 (2-{2-[2-(2-Trityloxy-ethoxy)-ethoxy]-ethoxy}-ethyl tosylate)

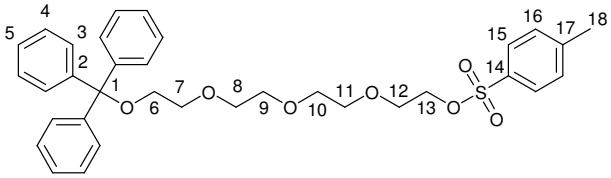

A solution of sodium hydroxide (2.08 g, 52.0 mmol) in water (10 mL) was prepared. 3.3 mL of this solution (containing 17.2 mmol of NaOH) were added to a solution of **27** (4.74 g, 10.9 mmol) and tosyl chloride (2.30 g, 12.1 mmol) in THF (20 mL). The mixture was left stirring overnight at room temperature. Then it was acidified with conc. HCl and neutralised with $NaHCO_3$. The organic phase was extracted with DCM (4 × 100 mL), dried with $MgSO_4$, filtered and evaporated, to give **28** as a yellow oil (5.18 g, 80.7% yield). ^{1}H NMR ($CDCl_3$, 300 MHz): δ = 7.79 (d, J = 8.0 Hz, 2 H, 15), 7.47 (m, 6 H, 3), 7.34-7.21 (m, 11 H, 4, 5 & 16), 4.14 (t, J = 4.8 Hz, 2 H, 13), 3.76-3.60 (m, 12 H, 7, 8, 9, 10, 11 & 12), 3.24 (t, J = 4.8 Hz, 2 H, 6), 2.43 (s, 3 H, 18).

29 (2-{2-[2-(2-Iodo-ethoxy)-ethoxy]-ethoxy}-ethanol trityl ether)

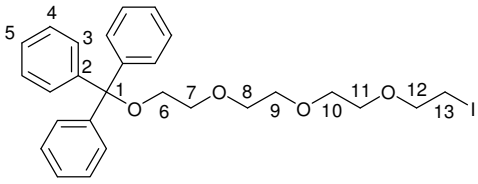

Sodium iodide (3.29 g, 21.9 mmol) was added to a solution of **28** (5.18 g, 9.49 mmol) in acetone (30 mL). The reaction was slightly exothermic and a white solid formed after the rapid dissolution of sodium iodide. It was left stirring at room temperature overnight, then it was filtered and evaporated, giving a yellow solid (7.46 g), insoluble in ether and little soluble in chloroform, but soluble in ethyl acetate when water was added. Thus it was dissolved in ethyl acetate (100 mL) and water (100 mL). The organic phase was separated and washed with water (100 mL again) and brine (100 mL), dried with $MgSO_4$, filtered and evaporated, giving **29** as a yellow solid (4.39 g, 91.7% yield). ^{1}H NMR ($CDCl_3$, 300 MHz): δ = 7.46 (d, J = 7.1 Hz, 6 H, 3), 7.32-7.20 (m, 9 H, 4 & 5), 3.76-3.67 (m, 12 H, 7, 8, 9, 10, 11 & 12), 3.26-3.20 (m, 4 H, 6 & 13).

30 (2,2-Bis-(2-{2-[2-(anthracen-9-yloxy)-ethoxy]-ethoxy}-ethyl)-malonic acid diethyl ester)[6]

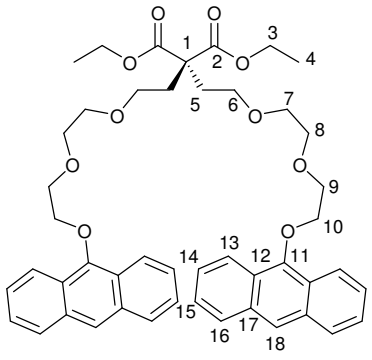

To a suspension of sodium hydride (61 mg, 2.54 mmol) in THF (40 mL), diethyl malonate (190 mg, 1.19 mmol) was added drop wise. After a few minutes, a solution of **25** (1.00 g, 2.29 mmol) in THF (10 mL) was added. The mixture heated to reflux and left stirring 24 hours, then it was cooled to room temperature and 100 mL of water were added. The organic phase was extracted with 4 × 50 mL of ether, dried with $MgSO_4$, filtered and evaporated to give an orange oil, which was separated by flash chromatography on silica gel to give finally 588 mg of **30** as an orange oil (66% yield). ^{1}H NMR ($CDCl_3$, 300 MHz): δ = 8.34-8.41 (m, 4 H, 13), 8.23 (s, 2 H, 18), 7.95-8.00 (m, 4 H, 16), 7.44-7.50 (m, 8 H, 14 & 15), 4.35-4.38 (m, 4 H, 10), 4.13-4.18 (m, 4 H, 3), 3.99-4.10 (m, 4 H, 9), 3.70-3.79 (m, 8 H, 7 & 8), 3.52-3.61 (m, 4 H, 6), 2.03 (t, J = 4.8 Hz, 4 H, 5), 1.24 (t, J = 7.4 Hz, 6 H, 4). The analysis results are consistent

with those already reported but they also contain additional data since some hydrogens in the ^{1}H NMR spectrum had previously not been assigned.[6]

31 (2,2-Bis-[2-(2-{2-[2-(anthracen-9-yloxy)-ethoxy]-ethoxy}-ethoxy)-ethyl]-malonic acid diethyl ester)[6]

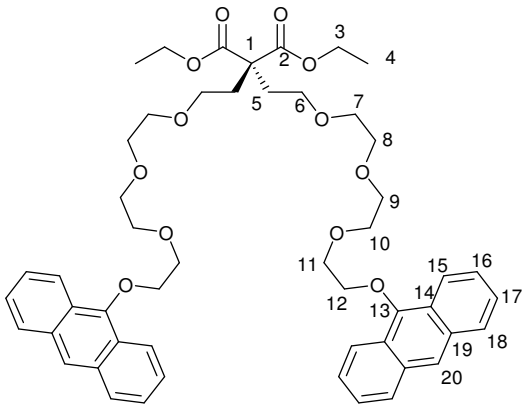

To a suspension of sodium hydride (73 mg, 3.04 mmol) in THF (50 mL), diethyl malonate (221 mg, 1.38 mmol) was added drop wise. After a few minutes, a solution of **26** (1.33 g, 2.77 mmol) in THF (10 mL) was added. The mixture heated to reflux and left stirring at reflux during 24 hours, then it was cooled to room temperature and 100 mL of water were added. The organic phase was extracted with 4 × 50 mL of ether, dried with $MgSO_4$, filtered and evaporated to give an orange oil, which was separated by flash chromatography on silica gel to give finally 752 mg of **31** as an orange oil (63% yield). ^{1}H NMR ($CDCl_3$, 300 MHz): δ = 8.36-8.39 (m, 4 H, 15), 8.22 (s, 2 H, 20), 7.96-7.99 (m, 4 H, 18),7.44-7.48 (m, 8 H, 16 & 17), 4.35-4.39 (m, 4 H, 12), 4.09-4.18 (m, 4 H, 3), 3.96-3.99 (m,4 H, 11), 3.75-3.81 (m, 8 H, 9 & 10), 3.64-3.67 (m, 4 H, 8), 3.47-3.56 (m, 8 H, 6 & 7), 2.26 (t, J = 6.6 Hz, 5), 1.19-1.28 (m, 6 H, 4). The analysis results are consistent with those already reported but they also contain additional data since some hydrogens in the ^{1}H NMR spectrum had previously not been assigned.[6]

32 (2,2-Bis-(2-{2-[2-(2-trityloxy-ethoxy)-ethoxy]-ethoxy}-ethyl)-malonic acid diethyl ester)

Sodium hydride (250 mg of 60% w/w dispersion in mineral oil, 6.25 mmol) was washed with dry hexane and suspended in THF (60 mL). Diethyl malonate (0.48 mL, 0.51 g, 3.16 mmol) was added. After 5 min. of stirring, a solution of **29** (3.0 g, 5.49 mmol) in THF (30 mL) was added. The reaction mixture was left stirring overnight at room temperature. The THF was

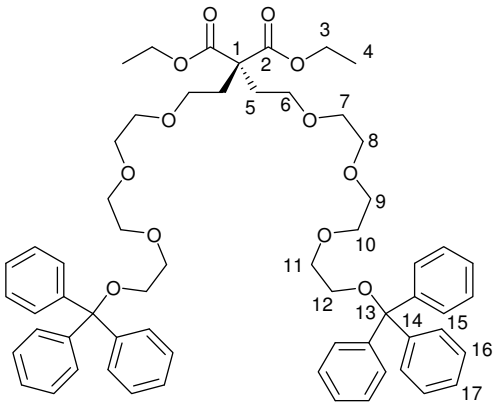

evaporated and the crude re-dissolved in ether (100 mL) and brine (200 mL). The organic phase was separated and the aqueous extracted again with ether(3 x 50 mL). The organic phases were combined, dried with $MgSO_4$, filtered and evaporated. The crude obtained was separated by flash chromatography, giving **32** as a yellow solid (265 mg, 9.3% yield). ^{1}H NMR ($CDCl_3$, 300 MHz): δ = 7.46 (d, J = 7.0 Hz, 12 H, 15), 7.31-7.19 (m, 18 H, 16 & 17), 4.13 (q, J = 7.1 Hz, 4 H, 3), 3.69-3.58 (m, 16 H, 7, 8, 9 & 10), 3.50 (t, J = 5.2 Hz, 4 H, 11), 3.46 (t, J = 6.8 Hz, 4 H, 6), 3.23 (t, J = 5.2 Hz, 4 H, 12), 2.23 (t, J = 6.8 Hz, 4 H, 5), 1.19 (t, J = 7.1 Hz, 6 H, 4). Mass spectrum (ES$^+$): m/z = 1019.5{M + Na$^+$}, 501.2 {loss of 2 EtOH and one CO_2, + Na$^+$}.

33 (2,2-Bis-dec-9-enyl-malonic acid diethyl ester)

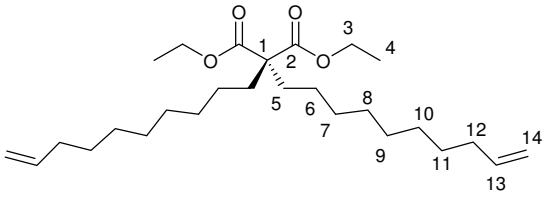

Diethyl malonate (380 µL, 2.5 mmol) and 1-bromodec-9-ene (1.38 mL, 6.9 mmol) were added to a suspension of sodium hydride (260 mg of a 60% w/w dispersion in mineral oil, 6.5 mmol) in THF (100 mL). The mixture was heated to reflux and left stirring at reflux during 2 days, then 2 mL of ethanol were added, and the volatiles were evaporated. The crude was re-dissolved in ethyl acetate (50 mL) and brine + water (50 mL). The two phases were separated and the aqueous was extracted with ethyl acetate (3 × 20 mL). The combined organic phases were dried with magnesium sulphate, filtered and evaporated to afford an colourless oil which was separated by flash chromatography (eluent: hexane / DCM) (176 mg, 16% yield). ^{1}H NMR ($CDCl_3$, 300 MHz): δ = 5.86-5.73 (m, 2 H, 13), 5.01-4.90 (m, 4 H, 14), 4.16 (q, J = 7.1 Hz, 4 H, 3), 2.02 (q, J = 7.4 Hz, 4 H, 5), 1.86-1.81 (m, 4 H, 12), 1.38-1.18 (m, 30 H, 6, 7, 8, 9, 10, 11 & 4). Mass spectrum (ES$^+$): m/z = 459.3 {M + Na$^+$}.

34 (5,5-Bis-(2-{2-[2-(anthracen-9-yloxy)-ethoxy]-ethoxy}-ethyl)-pyrimidine-2,4,6-trione)

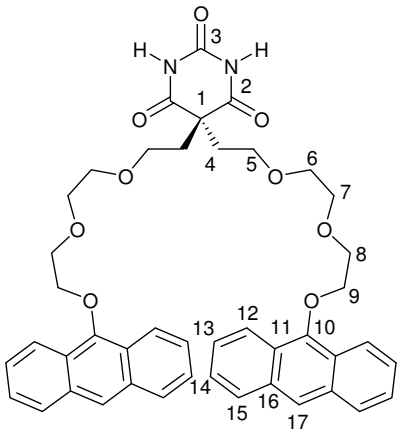

To a solution of urea (1.12 g, 18.6 mmol) in dry DMSO (6 mL), sodium hydride (200 mg, pure, 8.33 mmol) was added. After 30 minutes of stirring at room temperature, **30** (1.44 g,1.85 mmol) was added. The colour of the mixture turned immediately from yellow to red. The reaction mixture was left stirring overnight in the dark (flask covered with foil) at room temperature. Then ice (5 g) was added. The solution was allowed to warm up to room temperature, re-dissolved in water (150 mL) and acidified with concentrated hydrochloric acid until the solution became turbid. Then sodium chloride was added and the organic phase was extracted with ethyl acetate (150 mL), washed with 2×50 mL of water, dried with $MgSO_4$, filtered and evaporated, to give an orange oil which was separated by flash chromatography, giving finally 392 mg of **34** as an orange solid (28% yield). ^{1}H NMR ($CDCl_3$, 300 MHz): δ = 8.78 (s, 2 H, NH), 8.24-8.33 (m, 4 H, 12), 8.09 (s, 2 H, 17), 7.83-7.86 (m, 4 H, 15), 7.32-7.41 (m, 8 H, 13 & 14), 4.15-4.16 (m, 4 H, 9), 3.59-3.62 (m, 4 H, 8), 3.43-3.45 (m, 12 H, 5, 6 & 7), 2.27 (tr, J = 5.7 Hz, 4 H, 4). ^{13}C NMR ($CDCl_3$, 300 MHz): δ = 8174.81 (2), 173.20 (3), 149.43 (10), 132.30 (16), 128.17 (15), 125.29 (14), 125.49 (13), 124.72 (11), 122.66 (12), 122.45 (17), 86.82 (1), 75.10 (9), 70.51 (8), 70.29 (6 & 7), 67.13 (5), 39.39 (4). Mass spectrum (ES$^+$): m/z = 767.2941 {M+H$^+$}, calculated : 767.2945.

35 (5,5-Bis-[2-(2-{2-[2-(anthracen-9-yloxy)-ethoxy]-ethoxy}-ethoxy)-ethyl]-pyrimidine-2,4,6-trione)

To a solution of urea (1.12 g, 18.6 mmol) in dry DMSO (7 mL), sodium hydride (200 mg, pure, 8.33 mmol) was added. After 30 minutes of stirring at room temperature, **31** (1.60 g, 1.85 mmol) was added. The colour of the mixture turned immediately from yellow to red. The

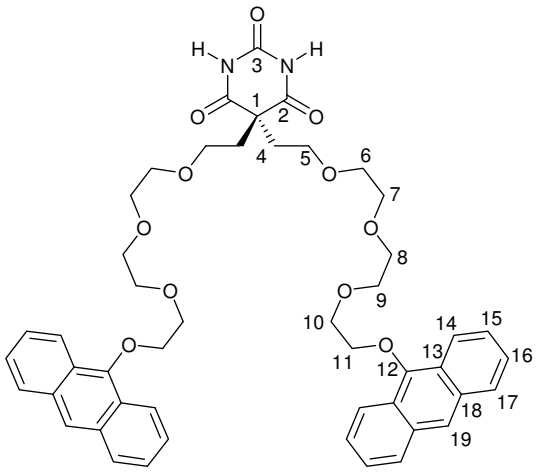

reaction mixture was left stirring overnight in the dark at room temperature. Then ice(5 g) was added. The solution was allowed to warm up to room temperature, re- dissolved in water (150 mL) and acidified with concentrated hydrochloric acid until a persistent white turbidity remains visible. Then sodium chloride was added and the organic phase was extracted with ethyl acetate (150 mL), washed with 2 × 50 mL of water, dried with $MgSO_4$, filtered and evaporated, to give 802 mg of orange oil which was separated by flash chromatography, giving finally 407 mg of **35** as an orange oil (26% yield). ^{1}H NMR ($CDCl_3$, 300 MHz): δ = 9.53 (s, 2 H, NH), 8.38-8.42 (m, 4 H, 14), 8.19 (s, 2 H, 19), 7.94-7.97 (m, 4 H, 17), 7.41-7.51 (m, 8 H, 15 & 16), 4.42-4.46 (m, 4 H, 11), 4.07-4.13 (m, 4 H, 10), 3.85-3.88 (m, 4 H, 9), 3.58-3.61 (m, 4 H, 8), 3.20-3.23 (m, 4 H, 7), 3.11-3.15 (m, 4 H, 6), 2.94-2.97 (m, 4 H, 5), 2.16 (tr, *J* = 5.5 Hz, 4 H, 4).

36 (5,5-Bis-(2-{2-[2-(2-trityloxy-ethoxy)-ethoxy]-ethoxy}-ethyl)-pyrimidine-2,4,6-trione)

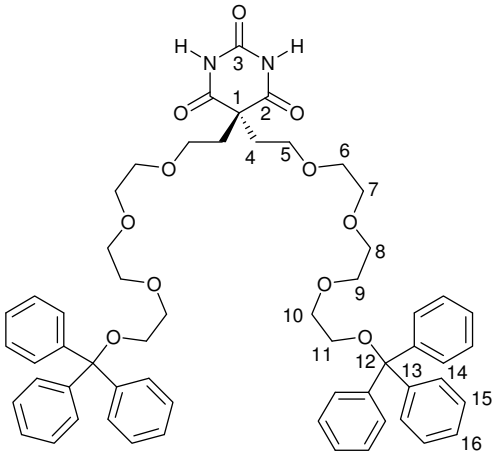

Sodium hydride (90 mg of 60% w/w dispersion in mineral oil, 2.25 mmol) was suspended in DMSO (0.5 mL). To this suspension, urea (170 mg, 2.83 mmol) and a solution of **32** (265 mg, 2.25 mmol) in DMSO (0.5 mL) were added. The colour changed quickly from colourless to beige. It was left stirring overnight at room temperature. Then the solution was dissolved in water (50 mL). $NaHCO_3$ (10 g) was added. The solution was acidified until an important bubbling was observed. Then it was neutralised with more $NaHCO_3$. The organic phase was extracted with

ethyl acetate (3 × 25 mL), washed with brine (2 × 20 mL), dried with $MgSO_4$, filtered and evaporated. The yellow solid obtained (152 mg) was separated by flash chromatography, giving **36** as a colourless viscous oil (67.1 mg, 26.1% yield). ^{1}H NMR ($CDCl_3$, 300 MHz): δ = 9.34 (s, 2 H), 7.45 (d, J = 7.4 Hz, 12 H, 14), 7.30-7.18 (m, 18 H, 15 & 16), 3.80-3.74 (m, 8 H, 8 & 9), 3.70-3.67 (m, 4 H, 7), 3.62-3.59 (m, 4 H, 6), 3.47-3.44 (m, 4 H, 10), 3.38-3.30 (m, 8 H, 11 & 5), 2.25 (t, J = 5.4 Hz, 4 H, 4). Mass spectrum (ES^+): m/z = 987.2{M + Na^+}, 745.2 {loss of 1 trityl, + Na^+}.

37 (5,5-Bis-dec-9-enyl-pyrimidine-2,4,6-trione)

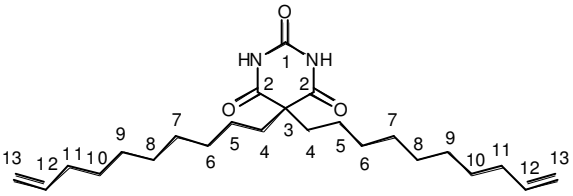

To a solution of **33** (176 mg, 0.4 mmol) in DMSO (2 mL), sodium hydride (50 mg of a 60% w/w dispersion in mineral oil) and urea (50 mg) were added. It was left stirring at room temperature during 20 hours, then a saturated aqueous solution of $NaHCO_3$ (50 mL) was added. The organic phase was extracted with ethyl acetate (2 × 40 mL), dried with $MgSO_4$, filtered and evaporated, affording an orange oil which partly crystallized to a white solid. This solid was washed with hexane, affording **37** (66.7 mg, 41% yield). mp 80°C. ^{1}H NMR ($CDCl_3$, 300 MHz): δ = 7.96 (br. s, 2 H, N-H), 5.80 (ddt, J_t = 6.8 Hz, J_{d1} = 10.2 Hz, J_{d2} = 17.0 Hz, 2 H, 12), 5.02-4.91 (m, 4 H, 13), 2.06-1.94 (m, 8 H, 4 & 11), 1.47-1.02 (m, 24 H, 5, 6, 7, 8, 9 & 10). ^{13}C NMR ($CDCl_3$, 300 MHz): δ 172.57 (2), 148.64 (1), 139.96 (12), 114.17 (13), 56.72 (3), 39.17 (11), 33.73, 29.29, 29.24, 29.07 , 28.96, 28.81 (4, 6, 7, 8, 9 & 10), 25.04 (5). Mass spectrum (ES^-, exact mass): m/z = 403.2950 {M - H^+}, calculated: 403.2961. Elemental analysis: found: C, 71.24; H, 10.12; N, 6.95; calculated: C, 71.25; H, 9.97; N, 6.92.

38 (5,5-Bis-(4-hydroxy-phenyl)-pyrimidine-2,4,6-trione)[7]

Alloxan monohydrate (1.60 g, 10.0 mmol) and phenol (1.90 g, 20.2 mmol) were suspended

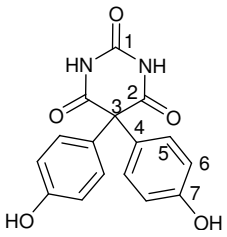

acid (98%, 1.2 mL, 20 mmol) was added, The mixture was heated to 85°C and left stirring in acetic acid (10 mL). Sulfuric at this temperature 2 hours under nitrogen. Then 50 mL of water were added. The organic phase was extracted with chloroform (3 × 50 mL), and the aqueous phase was neutralised with Na_2CO_3 until pH ≈ 7.5 according to pH paper.Then it was extracted with ethyl acetate (3 × 50 mL), dried with $MgSO_4$, filtered and evaporated, to afford 2.61 g of **38** as a white solid (83.6% yield). mp 267°C (lit. 292°C). ^{1}H NMR (d^6-acetone, 300 MHz): δ = 10.38 (br. s, 2 H, NH), 8.57 (s, 2 H, OH), 7.08 (d, *J* = 9.0 Hz, 4 H, 5), 6.83 (d, *J* = 9.0 Hz, 4 H, 6). ^{13}C NMR (d^6-acetone, 300 MHz): δ = 172.96 (2), 159.11 (1), 150.94 (7), 132.29 (5), 131.04 (4), 116.87 (6), 107.52 (3). IR (ν, cm^{-1}): 3388 (s, OH H-bonded), 3198 (m, Csp^2-H), 3110 (m, Csp^2-H), 1746 (s, C=O), 1694 (s, C=O), 1613 (m, C=C aromatic), 1594 (m, C=C aromatic), 1514 (m, C=C aromatic), 1420 (m), 1340 (s), 1217 (m), 1184 (m), 1030 (m), 1016 (m), 832 (m), 816 (m), 772 (m). Mass spectrum (EI): *m/z* = 312 {M$^{\bullet+}$}, 255, 226, 198. Mass spectrum (ES$^-$): 311 {M - H$^+$}, 225; exact mass determination on the {M - H$^+$} peak: *m/z* = 311.0662, calculated: 311.0668. Elemental analysis: found: C, 58.85; H, 3.44; N, 8.72; calculated with 0.14 equiv. sulphuric acid: C, 58.90; H, 3.80; N, 8.59. The NMR spectra are in agreement with the literature data, but not the melting point,[7] which indicates that the product is not pure, as is also indicated by the mass spectra and elemental analysis. Crystals of the product have been obtained. The resulting crystal structure, as determined by X-ray diffraction, is presented in *Appendix 1*.

39 (5,5-Bis-(4-methoxy-phenyl)-pyrimidine-2,4,6-trione)[8a]

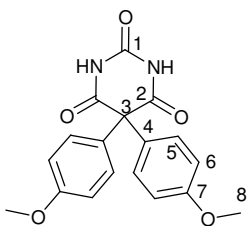

Alloxan monohydrate (0.40 g, 2.5 mmol) and anisole (0.55 mL, 5.05 mmol) were suspended in acetic acid (5 mL). Sulfuric acid (0.28 mL, 20 mmol) was added. The mixture was heated to 85°C and left stirring at this temperature 2 hours under nitrogen. Then

water (20 mL) was added. The solution was poured into a solution of 3.2 mg of sodium hydroxide. Then it was neutralised with a saturated aqueous $NaHCO_3$ solution. The organic phase was extracted with ethyl acetate (3×50 mL), dried with $MgSO_4$, filtered and evaporated, to afford a yellow oil which was separated by column chromatography (eluent: petroleum ether / ethyl acetate) to give **39** as a yellow solid (215 mg, 25% yield). mp 166°C. ^{1}H NMR (d^3-acetonitrile, 300 MHz): δ = 9.23 (br. s, 2 H, NH), 7.07 (d, J = 9.3 Hz, 4 H, 5), 6.91 (d, J = 9.3 Hz, 4 H, 6), 3.79 (s, 6 H, 8). ^{13}C NMR ($CDCl_3$, 300 MHz): δ 171.61 (2), 159.79 (1), 150.82 (7), 130.13 (5), 128.65 (4), 114.19 (6), 70.20 (3), 55.34 (8). IR (ν, cm^{-1}): 3217 (m, NH H-bonded), 3091 (m, Csp^3-H), 2841 (m, O-Me), 1709 (s, C=O), 1608 (m, C=C aromatic), 1584 (m, C=C aromatic), 1510 (m, C=C aromatic), 1439 (s, C-H bending), 1418 (m), 1299 (m), 1249 (w), 1180 (m), 1028 (m), 827 (m), 795 (m), 761 (m), 734 (m). Mass spectrum (ES^+, exact mass): m/z = 363.0952 {M + Na^+}, calculated: 363.0957. Crystals of the product have been obtained. The resulting crystal structure, as determined by X-ray diffraction, is presented in *Appendix 1*.

40 (5,5-Bis-(4-hydroxyphenyl)-1,3-dimethyl-pyrimidine-2,4,6-trione)[8a]

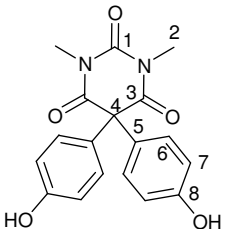

38 (200 mg, 0.64 mmol) was dissolved in acetone (20 mL). Potassium carbonate (0.210 g, 1.52 mmol) was added. The mixture was heated to reflux, then methyl iodide (0.09 mL, 1.5 mmol) was added. The mixture was left stirring overnight at room temperature. Then it was filtered and the solid was washed with acetone. The acetone solution was evaporated, re-dissolved in ethyl acetate (50 mL) and water (100 mL). The organic phase was extracted with 2×50 mL of ethyl acetate, the organic phases were combined, dried with $MgSO_4$, filtered and evaporated, to afford **40** as a beige solid (145 mg, 67% yield). mp 277°C. ^{1}H NMR (d^6-acetone, 300 MHz): δ = 8.58 (br. s, 2 H, OH), 6.99 (d, J = 9.1 Hz, 4 H, 6), 6.80 (d, J = 9.1 Hz, 4 H, 7), 3.27 (s, 6 H, 2). IR (ν, cm^{-1}): 3527 (s, OH free), 3341 (s, OH H-bonded), 1690 (s, C=O), 1666 (s, C=O) 1610 (m, C=C aromatic), 1593 (m, C=C aromatic),

1512 (m, C=C aromatic), 1439 (s, C-H bending), 1419 (m), 1370 (s), 1270 (m), 1225 (w), 1168 (m), 1115 (m), 1101 (m), 834 (m), 825 (m), 807 (m), 753 (m). Mass spectrum (ES^+): *m/z* = 363 $\{M + Na^+\}$. Mass spectrum (ES^-, exact mass): *m/z* = 339.0990 $\{M - H^+\}$, calculated: 339.0981. Elemental analysis: found: C, 63.56; H, 4.54; N, 8.37; calculated: C, 63.52; H, 4.74; N, 8.23.

Other attempts to substitute **38** on the O site with different iodides or under different conditions: see reference below.[8a]

41 (Diethyl 2,2-Bis-(4-hydroxy-phenyl)-malonate)[8b]

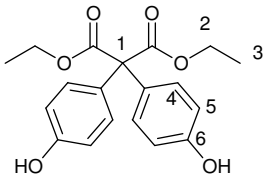

Phenol (1.90 g, 20.2 mmol) was dissolved in acetic acid (10 mL). Diethyl ketomalonate (1.55 mL, 1.77 g, 10.1 mmol) was added. The yellow solution was heated to 50°C, then sulphuric acid (1.12 mL) was added. It was then heated to 80°C. After two hours at reflux, the solution has turned red. It was cooled to 50°C and water (20 mL) was added: the solution turned pale green. After cooling it to room temperature, it was mixed with 50 mL of an aqueous solution of sodium hydroxide (9.4 g). Then sodium hydrogen carbonate was added until the reaction mixture was neutral. The organic phase was extracted with 3 × 30 mL of ethyl acetate, dried with $MgSO_4$, filtered and evaporated. It was then separated by flash chromatography (eluent: petroleum ether / ethyl acetate) and the product was re-crystallised in methanol + petroleum ether, to afford **41** (1.495 g, 42.7% yield) as a yellow solid. ^1H NMR ($CDCl_3$): δ 7.20 (d, *J* = 8.8 Hz, 4 H, 4), 6.70 (d, *J* = 8.8 Hz, 4 H, 5), 5.64 (s, 2 H, OH), 4.24 (q, *J* = 7.1 Hz, 4 H, 2), 1.21 (t, *J* = 7.1 Hz, 6 H, 3).

42 (Diethyl 2,2-Bis-(4-methoxy-phenyl)-malonate)[8b]

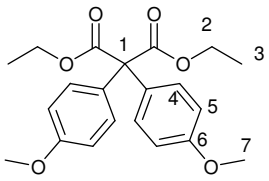

To a solution of Anisole (2.2 mL, 20.2 mmol) in acetic acid (10 mL), diethyl ketomalonate (1.55 mL, 10.1 mmol) was added followed by H_2SO_4 (1.2 mL). The solution was heated to 85ºC

for 3 hours resulting in a red/orange solution, which was then cooled to room temperature. A solution of KOH (9.45 g) in water (50 mL) was added to the solution. It was then neutralised with a saturated solution of sodium hydrogen carbonate and separated using ethyl acetate (3×20 mL). The organic phase was dried with $MgSO_4$, filtered and evaporated to afford a reddish-brown oil, which was purified by column chromatography (eluent: ethyl acetate:hexane 1:1) to give **42** as a yellow oil (0.539 g, 14.3% yield), which later crystallised and was re-crystallised in hexane and chloroform. ^{1}H NMR ($CDCl_3$, 300 MHz): δ = 7.3 (m, 4 H, 4), 6.8 (m, 4 H, 5), 4.1 (q, J = 6.9 Hz, 4 H, 2), 3.8 (s, 6 H, 7), 1.3 (m, 6 H, 3). Mass spectrum (ES^+): m/z = 395.2 $\{M + Na^+\}$. The crystal structure of this compound, as determined by X-ray diffraction, is presented in *Appendix 1*.

42 by substitution of **41**.[8b]

Potassium carbonate (0.706 g, 5.11 mmol) and **41** (0.474 g, 1.38 mmol) were suspended in acetonitrile (30 mL). After 10 minutes of stirring (all **41** was dissolved but not K_2CO_3), methyl iodide (0.26 mL, 4.2 mmol) was added and the solution was left stirring at reflux for 35 hours. The resulting milky white solution was then allowed to cool to room temperature. Water (20 mL) was added, the organic phase was extracted using ethyl acetate (3×15 mL), dried with $MgSO_4$, filtered and evaporated to yield a yellow oil, which crystallized to give **42** (0.3073 g, 59.9% yield).

43 (2,2-Bis-(4-oct-7-enyloxy-phenyl)-malonic acid diethyl ester)

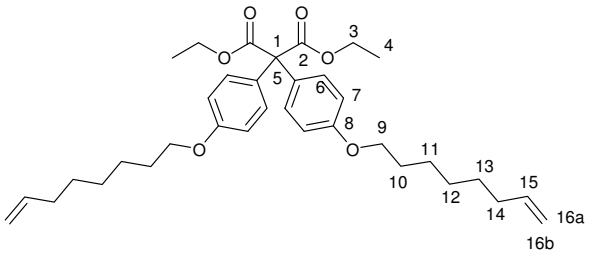

Potassium carbonate (640 mg, 4.63 mmol) and **41** (240 mg, 697 µmol) were suspended in acetonitrile (15 mL). The mixture was heated to reflux during 30 min., then 8-bromo-oct-1-ene (350 µL, 2.09 mmol) was added and the mixture was left stirring at reflux during 2 days. Then the solvent was evaporated and the remaining oily solid

was dissolved in 20 mL of ethyl acetate and 30 mL of water. The two phases were separated and the aqueous was extracted with 2 more times 20 mL of ethyl acetate. The combined organic phase was dried with $MgSO_4$, filtered and evaporated. The resulting brown oil was separated by flash chromatography (eluent: hexane / ethyl acetate), to give **43** as an colourless oil (169 mg, 42.9% yield). ^{1}H NMR ($CDCl_3$, 300 MHz): δ = 7.28 (d, J = 9.1 Hz, 4 H, 6), 6.82 (d, J = 9.1 Hz, 4 H, 7), 5.81 (ddt, J_t = 6.7, J_{d1} = 10.2, J_{d2} = 17.0 Hz, 2 H, 15), 5.00 (br d, J = 17.0 Hz, 2 H, 16a), 4.94 (br d, J = 10.2 Hz, 2 H, 16b), 4.24 (q, J = 7.1 Hz, 4 H, 3), 3.93 (t, J = 6.7 Hz, 4 H, 9), 2.06 (q, J = 6.9 Hz, 4 H, 14), 1.77 (quint, J = 7.0 Hz, 4 H, 10), 1.41 (m, 12 H, 11, 12 & 13), 1.22 (t, J = 7.1 Hz, 6 H, 4). ^{13}C NMR ($CDCl_3$, 300 MHz): δ = 170.24 (2), 158.29 (8), 138.95 (15), 130.63 (6), 130.62 (5), 114.25 (16), 113.70 (7), 67.80 (9), 67.04 (1), 61.61 (3), 33.65 (14), 29.16 (10), 28.79 (12), 28.78 (13), 25.86 (11), 13.87 (4). Mass spectrum of the crude (before column) (ES^+): m/z = 477 {mono + Na^+}, 587 {M + Na^+}, 603 {M + K^+}.

44 (2,2-Bis-(4-dec-9-enyloxy-phenyl)-malonic acid diethyl ester)[8b]

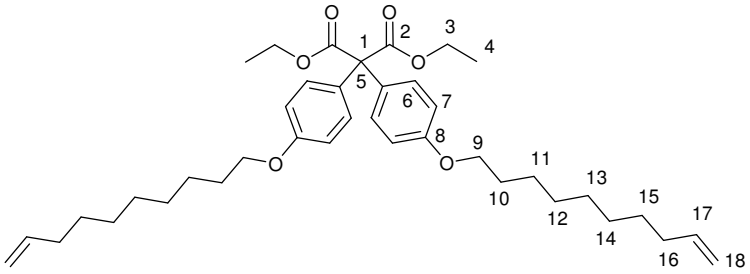

To a solution of 2,2-bis-(4-hydroxyphenyl)malonate (0.240 g, 0.698 mmol) in acetonitrile (15 mL), 10-bromodec-1-ene (360 µL) was added. The solution was heated under reflux at 85ºC for 14 hours. Then it was cooled to room temperature, acidified with HCl and neutralised with a saturated sodium hydrogen carbonate aqueous solution. The organic phase was extracted using ethyl acetate (2 × 10 mL), the combined organic phase was dried over anhydrous magnesium sulphate, filtered and evaporated to give an oil, which was purified by column chromatography on silica (eluent: hexane), to give **44** as a brown oil (0.214 g, 49.5% yield). ^{1}H NMR ($CDCl_3$, 300 MHz): δ = 7.40 (m, 4 H, 7), 6.90 (m, 4 H, 6), 5.90 (m, 2 H, 17), 5.05 (m, 4 H, 18), 4.35 (m, 4 H, 3), 4.05 (t, J = 6.7 Hz, 4 H, 9), 2.10 (q, J = 6.9 Hz, 4 H, 16), 1.20 (m, 30 H, 10, 11, 12, 13, 14, 15 & 4). Mass spectrum (ES^+): m/z = 643.4 {M + Na^+}.

39 by condensation of **42** with urea

To a solution/suspension of urea (0.115 g, 1.92 mmol) and sodium hydride (60% dispersion in mineral oil, 0.0843 g, 1.41 mmol) in dry deuterated DMSO (0.75 mL in capsule), a solution of **42** (0.1553 g, 0.417 mmol) in dry deuterated DMSO (0.75 mL in capsule) was added. After stirring for 15 hours at room temperature, water (10 mL) and saturated potassium chloride solution (20 mL) were added and a white precipitate formed, which dissolved after adding ethyl acetate (20 mL). The organic phase was extracted using ethyl acetate (2 more times 20 mL), dried with $MgSO_4$, filtered and evaporated, yielding an oily solid which was purified by flash chromatography (eluent: 1:1 hexane : ethyl acetate). **39** was obtained as a crystalline white solid (0.0268 g, 18.9% yield).

First Attempt to obtain **45** from **43** using NaH in DMSO

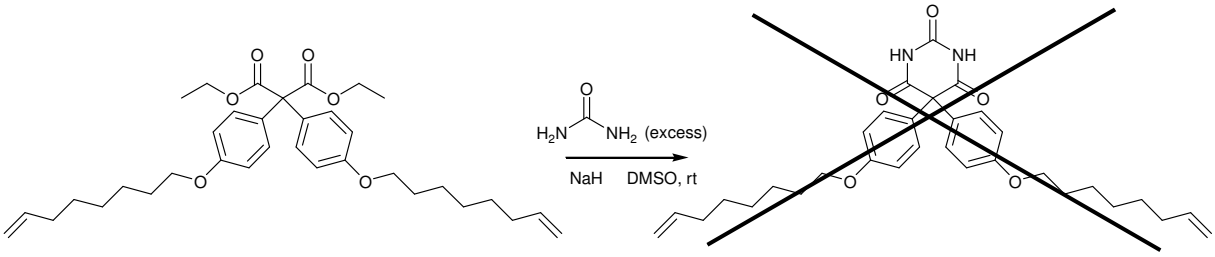

Sodium hydride (55 mg of a 60% w/w dispersion in mineral oil, 1.38 mmol) was washed with dry hexane and added to DMSO (2 mL). After 5 minutes of stirring, urea (167 mg, 2.78 mmol) was added. Then 5 minutes later a solution of **43** (147.0 mg, 0.26 mmol) in DMSO (2 mL) was added. The colour of the solution turned immediately from colourless to dark brown. It was left stirring at room temperature overnight, then water (30 mL) was added. It was mixed with 20 mL of a saturated solution of $NaHCO_3$, then acidified with conc. HCl until the solution was neutral according to pH paper. The organic phase was extracted with 4 × 15 mL of ethyl acetate, dried and evaporated, to afford a dark red oil. After adding 2 mL of ethanol and cooling it to 0°C, a white solid crystallised and was filtered, affording

146.4 mg of product which was proved by NMR and mass spec to be identical to the starting material **43**, recovered in 99.6% ± 0.2% yield.

Second Attempt to obtain **45** from **43** using NaH in DMSO

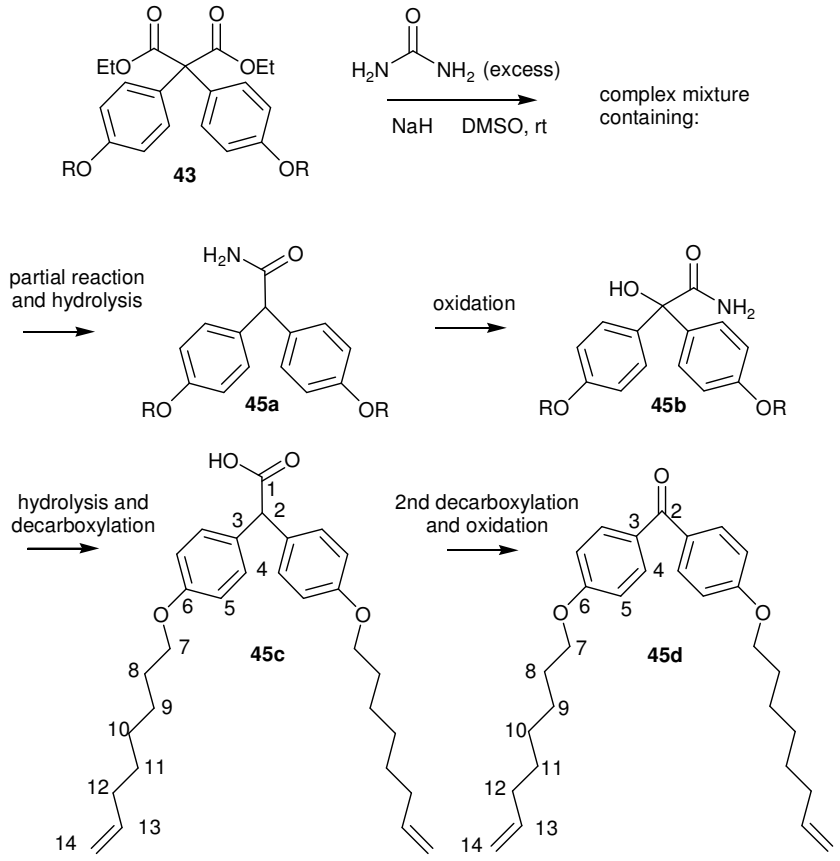

Sodium hydride (141 mg of a 60% w/w dispersion in mineral oil, 3.53 mmol) was washed with dry hexane and added to DMSO (2.5 mL). After 5 minutes of stirring, urea (35 mg, 0.58 mmol) was added. Then 5 minutes later a solution of **43** (169 mg, 0.299 mmol) in DMSO (3 mL) was added. The colour of the solution turned immediately from colourless to red. It was left stirring at room temperature overnight, then a saturated aqueous solution of ammonium chloride (50 mL) was added. The organic phase was extracted with 3 × 25 mL of ethyl acetate, washed with 25 mL of saturated ammonium chloride solution, dried with magnesium sulphate and evaporated, to afford an orange oil. The components of the mixture were separated by chromatography on silica gel, eluent: hexane/ethyl acetate with increasing ratio of ethyl acetate. Three main fractions were collected : the first (10 mg of incolor oil) was identified to the ketone **45d** (Bis-(4-oct-7-enyloxy-phenyl)-methanone). ^{1}H NMR ($CDCl_3$,

300 MHz): δ = 7.77 (d, J = 9.1 Hz, 4 H, 4), 6.94 (d, J = 8.9 Hz, 4 H, 5), 5.81 (ddt, J_t = 6.7, J_{d1} = 10.3, J_{d2} = 17.1 Hz, 2 H, 13), 5.04 (m, 4 H, 14), 4.03 (t, J = 6.7 Hz, 4 H, 7), 2.08-2.04 (m, 4 H, 12), 1.85-1.77 (m, 4 H, 8), 1.57-1.37 (m, 12 H, 9, 10, 11). Mass spectrum (ES^+): m/z = 457 $\{M + Na^+\}$. The second fraction (30 mg of white solid) was identified to the carboxylic acid **45c** (Bis-(4-oct-7-enyloxy-phenyl)-acetic acid). ^1H NMR ($CDCl_3$, 300 MHz): δ = 7.21 (d, J = 8.5 Hz, 4 H, 4), 6.84 (d, J = 8.8 Hz, 4 H, 5), 5.81 (ddt, J_t = 6.7, J_{d1} = 10.3, J_{d2} = 17.1 Hz, 2 H, 13), 5.00 (dq, J_q = 2.2, J_d = 17.2, 2 H, 14a), 4.96-4.89 (m, 3 H, 14b & 2), 3.92 (t, J = 6.6 Hz, 4 H, 7), 2.05 (q, J = 6.6 Hz, 4 H, 12), 1.76 (quint, J = 7.0 Hz, 4 H, 8), 1.50-1.26 (m, 12 H, 9, 10, 11). ^{13}C NMR ($CDCl_3$, 300 MHz): δ = 178.94 (1), 158.39 (6), 138.98 (13), 130.18 (3), 129.59 (4), 114.54 (5), 114.26 (14), 67.91 (7), 55.34 (2), 33.67 (12), 29.17 (8); 28.81 (10 & 11), 25.87 (9). Mass spectrum : ES^+: m/z = 509 $\{M - H^+ + 2\ Na^+\}$, ES^-: m/z = 463 $\{M - H^+\}$, 419 $\{M - CO_2 - H^+\}$. The third fraction (50 mg) is a complex mixture which contains **45a** and **45b**. Mass spectrum : ES^+: m/z = 486 $\{M_{\mathbf{45a}} + Na^+\}$, 502 $\{M_{\mathbf{45b}} + Na^+\}$, 950, 966.

Attempt to obtain **45** from **43** using sodium ethoxide in ethanol

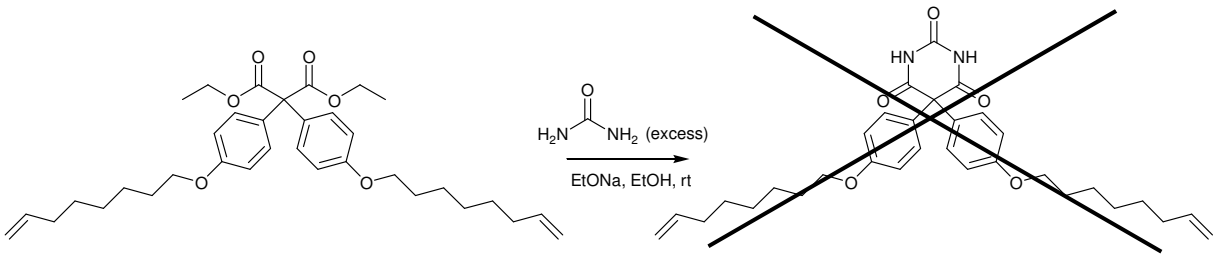

To a solution of urea (167 mg) and sodium ethoxide (100 mg) in ethanol (2 mL), a solution of recuperated **43** (146.4 mg) in hot ethanol (2 mL) was added. The mixture was heated to reflux overnight. Then water (20 mL) was added, the ethanol was evaporated, and the remaining aqueous solution was mixed with 30 mL of $NaHCO_3$ solution and acidified until neutral with conc. HCl. The organic phase was extracted with 2 × 15 mL of ethyl acetate, dried with $MgSO_4$, filtered and evaporated, affording an orange oil (107.3 mg) which was analysed by

^{1}H NMR and mass spec, reavealing only the starting material **43** and its products of hydrolysis.

Attempts to obtain **46** from **44** using NaH in DMSO, using NaH in DMF and using sodium ethoxide in ethanol: see reference below.[8b]

47 (Dec-9-enyloxybenzene)

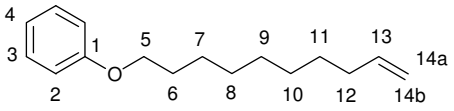

Phenol (0.33 g, 3.5 mmol) was dissolved in acetonitrile (40 mL). Potassium carbonate (1.0 g, 7.2 mmol) was added. The mixture was heated to 40 °C, then 10-bromo-dec-1-ene (0.71 mL, 3.5 mmol) was added. The mixture was heated to reflux and let stirring at reflux over 3 days, then the solvent was evaporated and the crude redissolved in water (50 mL) and ethyl acetate (15 mL). The two phases were separated and the aqueous extracted again with 2 × 15 mL of ethyl acetate. The combined organic phase was washed with 15 mL of conc. $NaHCO_3$ aqueous solution, dried with $MgSO_4$, filtered and evaporated. The oil obtained was separated by flash chromatography (eluent: hexane / DCM) to afford the desired product **43** as an colorless oil (807.7 mg, 99% yield). ^{1}H NMR ($CDCl_3$, 300 MHz): δ = 7.31-7.25 (m, 2 H, 3), 6.96-6.89 (m, 3 H, 2 & 4), 5.82 (ddt, J_t = 6.7, J_{d1} = 10.2, J_{d2} = 17.1 Hz, 1 H, 13), 5.00 (br. d, J = 10.2 Hz, 1 H, 14b), 4.94 (br. d, J = 17.1 Hz, 1 H, 14a), 3.95 (t, J = 6.6 Hz, 2 H, 5), 2.05 (q, J = 7.1 Hz, 2 H, 12), 1.78 (quint., J = 7.2 Hz, 2 H, 6), 1.56-1.25 (m, 10 H, 7, 8, 9, 10 & 11).

Attempt to obtain **46** by Friedel-Crafts reaction from **47** and alloxan

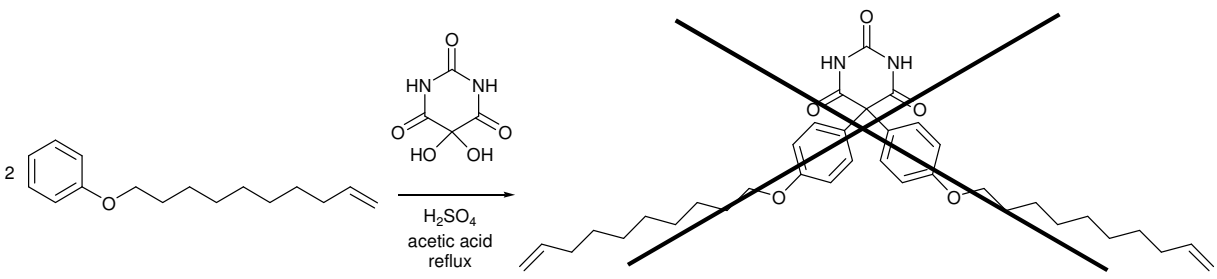

Alloxan monohydrate (281 mg) and **47** (807 mg) were dissolved in acetic acid (4 mL). Sulphuric acid (0.2 mL) was added and the mixture was heated to 90°C during 3 hours. Then the mixture was cooled to room temperature and a solution of sodium hydroxide (2.52 g) in water (50 mL) was added. A solid appeared in suspension. The mixture was cooled to 0°C, then mixed with a saturated solution of $NaHCO_3$ (50 mL). The organic phase was extracted with 3 × 20 mL of ethyl acetate, dried with $MgSO_4$, filtered and evaporated. The crude solid was analysed by ^{1}H NMR and mass spec (ES^+), showing no sign of desired product **46**. The terminal olefin signal, in particular, is absent from the NMR spectrum.

48 (5,5-Bis-[4-(*tert*-butyl-dimethyl-silanyloxy)-phenyl]-pyrimidine-2,4,6-trione)[8a]

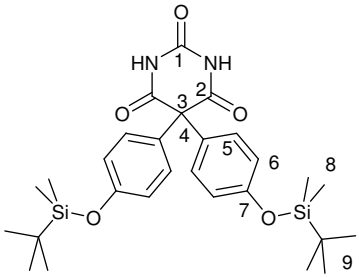

A solution of **38** (325 mg, 1.04 mmol), *tert*-butyl-dimethyl-silyl chloride (350 mg, 2.32 mmol), 4-dimethylaminopyridine (50 mg, 0.41 mg) and triethylamine (330 µL, 2.37 mmol) in acetonitrile (50 mL) was heated to reflux overnight. Then the solvent was evaporated, the crude dissolved in 50 mL of ethyl acetate, washed with 3 × 50 mL of $NaHCO_3$ solution, dried with magnesium sulphate, filtered and evaporated to afford a pink solid. It was then purified by column chromatography (neutral alumina, ethyl acetate / methanol) to afford **48** as a white solid (88 mg, 15.6% yield). ^{1}H NMR ($CDCl_3$ + MeOH, 300 MHz): δ = 7.99 (br. s, 2 H, NH), 7.07 (d, J = 8.9 Hz, 4 H, 5), 6.91 (d, J = 8.9 Hz, 4 H, 6), 0.97 (s, 18 H, 9), 0.20 (s, 12 H, 8). IR (ν, cm^{-1}): 3215 (m, NH H-bonded), 3098 (m, Csp^2-H), 2952 (m, Csp^3-H), 2930 (m, Csp^3-H), 2858 (m, Csp^3-H), 1738 (s, C=O), 1709 (s, C=O), 1608 (m, C=C aromatic), 1509 (m, C=C aromatic), 1471 (w), 1426 (m), 1337 (s, CH bending), 1263 (s), 1221 (m) 1178 (m), 1114 (m), 1014 (w), 913 (m), 870 (m), 831 (m), 778 (m).

49 (5,5-Bis-(4-hydroxy-phenyl)-1,3-di-oct-7-enyl-pyrimidine-2,4,6-trione)

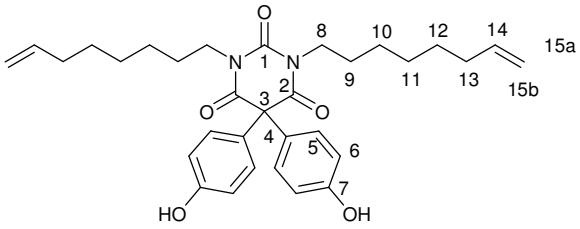

8-bromooct-1-ene (80 µL, 0.48 mmol), was added to a solution of **48** (71.6 mg, 0.132 mmol) in THF (2 mL) at 50°C. The mixture was heated to 64°C, then tetrabutylammonium fluoride (0.30 mL of a 1.0 M solution in THF, 0.30 mmol) was added drop wise. After 16 hours of stirring at reflux, the THF was evaporated. The orange oil obtained was dissolved in 20 mL of ethyl acetate, washed with 2 × 20 mL of water, dried with magnesium sulphate, filtered and evaporated. The orange viscous ail obtained was separated by column chromatography (eluent: pertroleum ether / ethyl acetate) to afford **49** as an colourless oil (49 mg, 69% yield). ^{1}H NMR ($CDCl_3$, 300 MHz): δ = 6.95 (d, J = 8.7 Hz, 4 H, 5), 6.74 (d, J = 8.7 Hz, 4 H, 6), 5.79 (ddt, J_t = 6.7, J_{d1} = 10.2, J_{d2} = 17.1 Hz, 2 H, 14), 5.25 (s, 2 H, 0H), 4.98 (br. d, J = 17.3 Hz, 2 H, 15b), 4.93 (br. d, J = 10.2 Hz, 2 H, 15a), 3.91 (t, J = 7.3 Hz, 4 H, 8), 2.01 (q, J = 6.8 Hz, 4 H, 13), 1.69-1.51 (m, 4 H, 9), 1.38-1.15 (m, 12 H, 10, 11 & 12). IR (ν, cm^{-1}): 3417 (m, OH H-bonded), 2928 (m, Csp^3-H), 2857 (w), 1667 (s, C=O), 1613 (m, C=C aromatic), 1595 (m, C=C aromatic), 1512 (s, C=C aromatic), 1437 (s, CH bending), 1398 (s, CH bending), 1365 (s), 1273 (m), 1217 (s), 1178 (s), 1116 (m), 1032 (w), 1015 (w), 996 (w), 909 (m), 833 (s), 758 (m), 734 (m), 703 (w).

6.2) Titrations and spectrometry

6.2.1) Titrations followed by UV-Vis. spectrometry

The UV spectra were made on a Cary Varian 5000 UV-visible spectrometer.

General procedure for the titrations by UV absorption of the receptors with low UV absorption near 300 nm**: Titration of 18 with barbital**.

A solution of 16.40 mg of **18** in 10 mL analytical grade DCM was prepared. From this first solution, 1.00 mL was transferred to a 100 mL graduated flask and diluted to 100 mL with DCM (stock solution, [**18**] = 2.504×10^{-5} *M*). A second aliquot of 1.00 mL of the first solution was added to another 100 mL graduated flask containing 23.0 mg of barbital, and diluted to 100 mL with DCM (barbital solution, [**18**] = 2.504×10^{-5} *M* and [barbital] = 1.249×10^{-2} *M*). Then a first UV spectrum of the stock solution was made between 200 and 700 nm. Before each new spectrum of the stock solution, a volume V_i was removed from the stock solution and the same volume V_i of barbital solution was added. The volumes V_i are shown **Table 6.1**. Then the spectra were corrected for the baseline deviation by withdrawing the average value of absorption between 600 and 700 nm (supposed to be close to zero) to the whole spectrum (cf. **Figure 6.1**).

Table 6.1. Volumes for the titration of **18** with barbital by absorption.

i	V_i / µL	$n_{eq\ barbital}$
0	0	0
1	20	0.01
2	20	0.02
3	20	0.03
4	20	0.04
5	60	0.07
6	60	0.10
7	100	0.15
8	100	0.20
9	200	0.30
10	195	0.41
11	405	0.61
12	405	0.81
13	395	1.02
14	1020	1.53
15	1020	2.03
16	2070	3.05

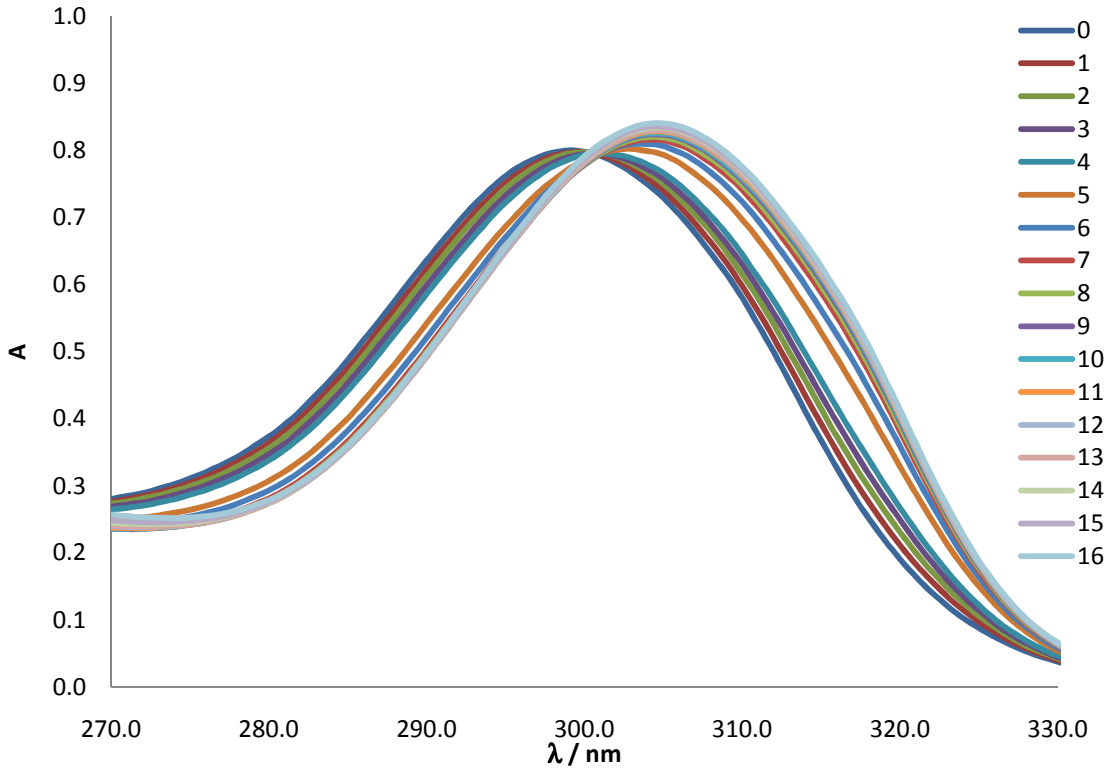

Figure 6.1. Corrected absorption spectra during the titration of **18** (2.5×10^{-5} *M* in DCM) with barbital (see **Table 6.1** for the equivalents), at room temperature.

The exact values of the starting concentration of barbital and **18** were calculated for each spectrum. A matrix was then created with the first two columns containing the calculated values of concentration, and the next fourteen columns the corrected absorption value at 14 wavelengths between 275 and 327 nm. This matrix was submitted to the Letagrop software,[9] with a starting value for the computation chosen by trials and errors in order to minimize the χ^2 value. Result: $log(K) = 5.7886 \pm 0.0271$; $\chi^2 = 10.07$.

A similar procedure was followed for the titrations of all other receptors with barbital, and for the titration of **18** with **36**. Results are given in *Chapter 2* and *Chapter 3*. The spectra of crude and corrected data as well as binding isotherms are given in *Appendix 3*.

Second titration of 17 with barbital by UV absorption

A solution of 2.750 mg of **17** in 10 mL DCM was prepared. From this first solution, 2.61 mL were transferred to a 50 mL graduated flask which was diluted with DCM to 50 mL (stock solution, [**17**] = 2.398×10^{-5} *M*), and 445 µL was transferred to a second 10 mL graduated

flask containing 11.036 mg of barbital, which was diluted to 10 mL with DCM (barbital solution, [**17**] = 2.411×10^{-5} M and [barbital] = 5.992×10^{-3} M). Then a first UV spectrum of the stock solution was made between 200 and 700 nm. Before each new spectrum, a volume V_i was removed from the stock solution and the same volume V_i of barbital solution was then added into it. Then *ca.* 3 mL was taken from the stock solution and added to a cuvette to obtain a reading. The solution was then returned to the stock solution and the procedure repeated with the next V_i value.

The volumes V_i are shown **Table 6.2**. The last spectrum (20) was made by mixing the remaining 1.4 mL of barbital solution with 2.5 mL of the stock solution. Then the spectra were corrected for the baseline deviation by withdrawing the average value of absorption between 600 and 700 nm (supposed to be close to zero) to the whole spectrum (cf. **Figure 6.2**).

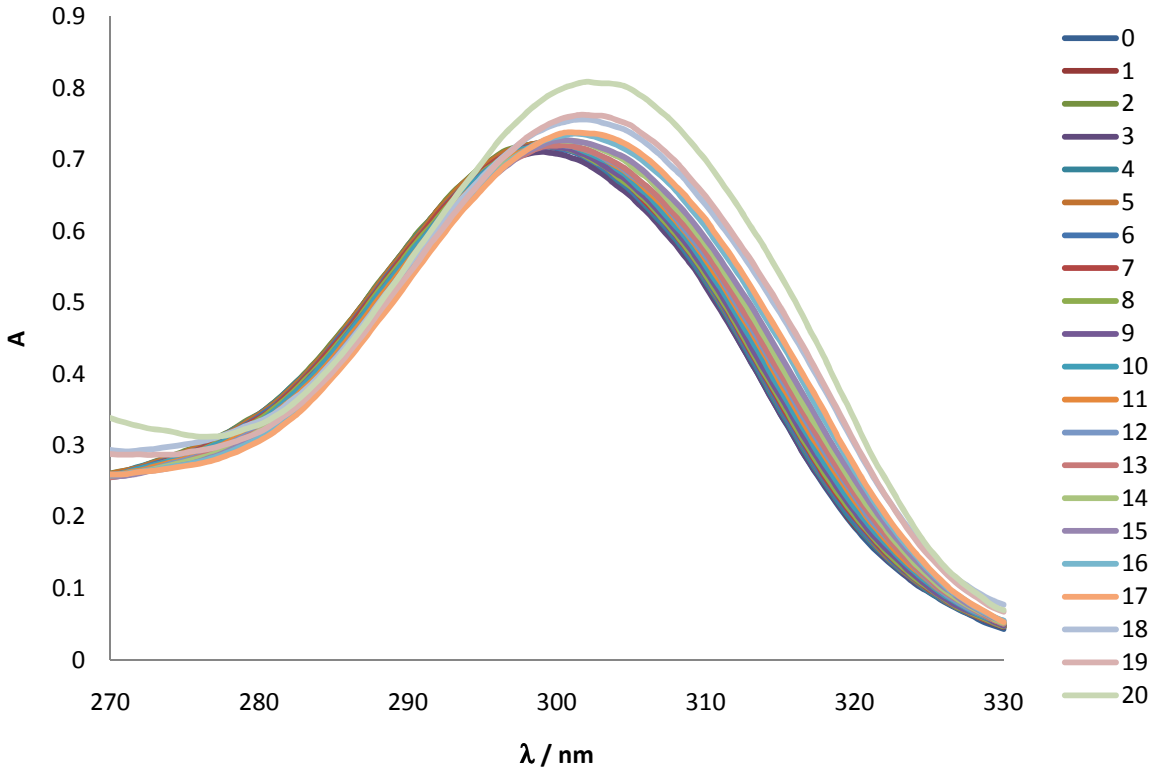

Figure 6.2. Corrected absorption spectra during the titration of **17** (2.4×10^{-5} *M* in DCM) with barbital (see **Table 6.2** for the equivalents), at room temperature.

Table 6.2. Volumes for the second titration of **17** with barbital by absorption.

i	V_i / µL	$n_{eq\ barbital}$
0	0	0
1	10	0.05
2	10	0.10
3	10	0.15
4	10	0.20
5	30	0.35
6	30	0.50
7	50	0.75
8	50	1.00
9	100	1.50
10	100	2.00
11	205	3.01
12	200	4.00
13	205	5.00
14	410	7.01
15	615	10.00
16	1045	15.01
17	1065	20.01
18	2175	30.00
19	2280	40.01
20	X	115.07

The exact values of the starting concentration of barbital and **17** were calculated for each spectrum. A matrix was then created with the first two columns containing the calculated values of concentration, and the 21 next columns the corrected absorption value at 21 wavelengths between 291 and 331 nm. This matrix was submitted to the Letagrop software[9] for fitting with 2 complexes (1:1 and 1:2), with starting values for the computation chosen by trials and errors in order to minimize the χ^2 value. Result: $log(K_1) = 4.226 \pm 0.213$; $log(K_2) = 7.217 \pm 0.288$; $\chi^2 = 11.92$. The spectra of crude and corrected data as well as binding isotherms are given in *Appendix 3*.

General procedure for the titrations by UV absorption of the receptors with significant UV absorption near 300 nm**: titration of 12 with 35**.

A solution of 1.4057 mg of **12** in 100 mL DCM (stock solution, [**12**] = 1.984×10^{-5} *M*) and a solution of 8.2780 mg of **35** in 25 mL DCM ([**35**] = 3.975×10^{-4} *M*) were prepared. Then a first UV spectrum of the stock solution was made between 200 and 700 nm. Before each new spectrum of the stock solution, a volume V_i of **35** solution was added to the stock. The volumes V_i are shown in **Table 6.3**.

The exact values of the starting concentration of **35** and **12** were calculated for each step. Then the spectra were corrected for the baseline deviation by withdrawing the average value of absorption between 600 and 700 nm (supposed to be close to zero) to the whole

spectrum. The proper absorption of **35** was also corrected by withdrawing the spectrum of **35** at its calculated initial concentration from the obtained spectrum. A matrix was then created with the first two columns containing the calculated values of concentration, and the eighteen next columns the corrected absorption at 18 wavelengths between 275 and 326 nm. This matrix was submitted to the Letagrop software,[9] with a starting value for the computation chosen by trials and errors in order to minimize the χ^2 value. Result: *log(K) = 3.7272 ± 0.0332; χ^2 = 11.50.*

Table 6.3. Volumes for the titration of **12** with **35**.

i	V_i / µL	$n_{eq\ 35}$
0	0	0
1	250	0.050
2	250	0.100
3	250	0.150
4	250	0.200
5	250	0.250
6	245	0.300
7	250	0.350
8	250	0.400
9	250	0.450
10	250	0.500
11	500	0.600
12	500	0.700
13	500	0.800
14	500	0.901
15	500	1.001
16	500	1.101
17	495	1.200

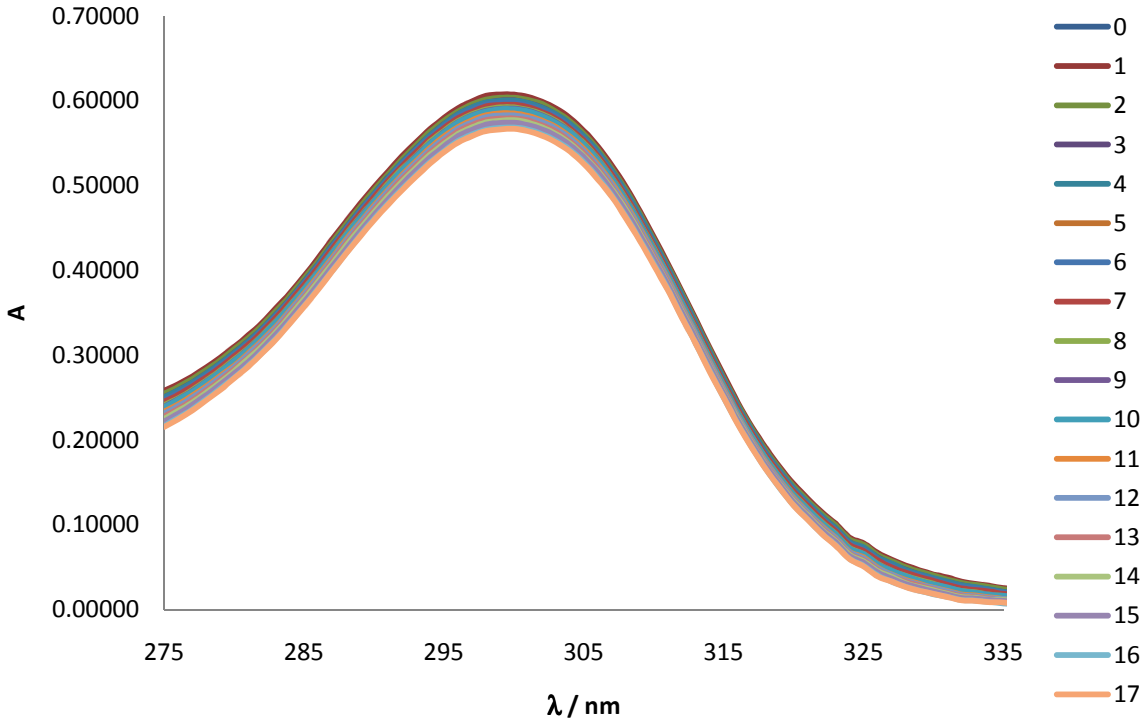

Figure 6.3. Absorption spectra corrected by substracting the absorption due to the anthracene during the titration of **12** (2.0×10^{-5} *M* in DCM) with **35** (see **Table 6.3** for the equivalents)

A similar procedure was followed for the titrations of **16** with **34**, **15** with **35**, **16** with **35**, **17** with **39** and **18** with **39**. Results are given in *Chapter 3* and *Chapter 5*. The spectra of crude and corrected data as well as binding isotherms are given in *Appendix 3*.

6.2.2) Fluorescence experiments

Fluorescence quantum yield of 34

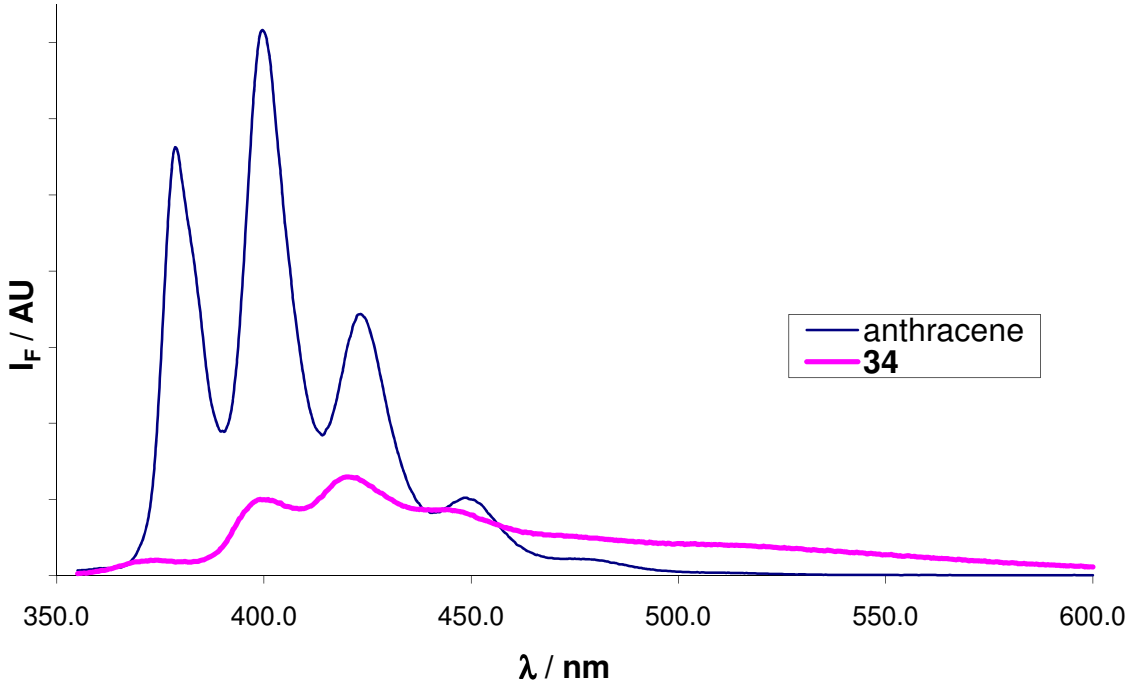

Figure 6.4. Emission spectra of **34** in DCM and anthracene in ethanol for the determination of the quantum yield of fluorescence of **34**.

A solution of **34** in DCM and a solution of anthracene in ethanol were prepared with an approximate maximum absobance close to 0.2 in UV (see absorption spectrum of anthracene in *Chapter 1*, **Figure 1.7**). It was observed that both solutions had the same absorbance at 351 nm. So the fluorescence emission spectra of both solutions were recorded with an excitation at $\lambda_{exc} = 351\ nm$ (cf. **Figure 6.4**). The quantum yield of fluorescence Φ_f was calculated according to the following formula:[10]

$$\Phi_f = 0.270.\frac{I_{\mathbf{34}}}{A_{\mathbf{34}}}.\frac{A_{anthracene}}{I_{anthracene}}.\left(\frac{n_{DCM}}{n_{ethanol}}\right)^2$$

where I_m is the integral of the fluorescence signal of the solution of the compound m between λ_{exc} and $+\infty$, A_m is its absorbance at λ_{exc}, and n_s is the refractive index of the solvent s. Result: $\Phi_f = 0.184$.

Fluorescence quantum yield of 16

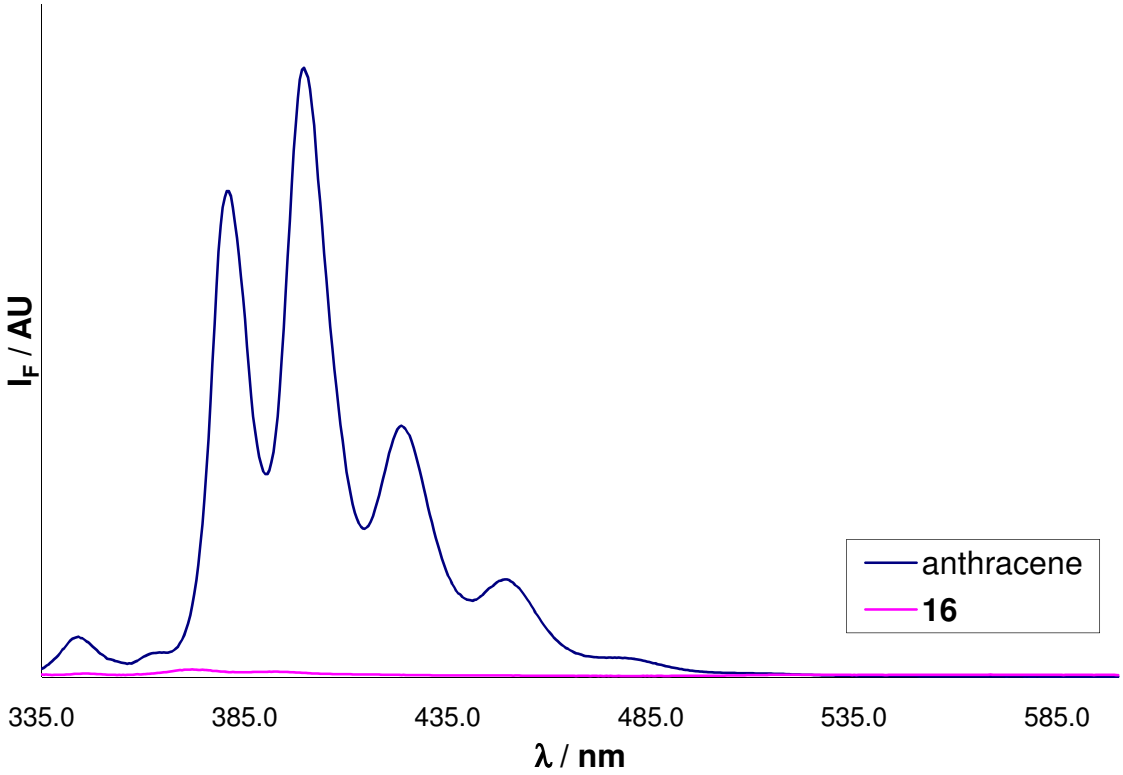

Figure 6.5. Emission spectra of **34** in DCM and anthracene in ethanol for the determination of the quantum yield of fluorescence of **34**.

It was measured by the same method as the fluorescence quantum yield of **34**, but at an excitation wavelength of *314 nm* (**Figure 6.5** for the comparison with anthracene, **Figure 2.5** in *Chapter 2* for a more detailed spectrum). Result: $\Phi_f = 0.00781$. The unexpected shape of this spectrum may indicate that this result is overevaluated because of the possible fluorescence of an impurity in solution.

Lifetimes of fluorescence of 34

The lifetimes of the excited states of **34** was measured by registering the fluorescence decay using a 50 W miniature Arc lamp and Time-Correlated Single-Photon Counting

fluorometer.[11] The decay parameters were determined by a non-linear least squares deconvolution method using the DECAN (1.0) programme.[12] The solutions used for these measures were at a concentration of 2×10^{-5} *M* in DCM, degased by multiple freeze-pump-thaw cycles on a high-vacuum line and sealed under vacuum in a quartz UV cuvette.

The decay was measured at different wavelengths of emission, at *415 nm* (region of the monomer emission) and at *510 nm* (region of the excimer emission). Each time, the best model for the decay was found to be a biexponential model:

$$I_F(t) = A.exp(-t/\tau_a) + B.exp(-t/\tau_b))$$

The results were as follow :

At 415 nm: $A = 1.02$, $\tau_a = 1.38$ *ns*; $B = 0.11$, $\tau_b = 8.60$ *ns*; $\chi^2 = 1.01$.

At 510 nm: $A = 0.061$, $\tau_a = 1.40$ *ns*; $B = 0.583$, $\tau_b = 14.6$ *ns*; $\chi^2 = 1.02$.

Lifetimes of fluorescence of 35

It was also measured by the same method as **34** at *415* and *510 nm*, each time with a biexponential model. The results were as follow:

At 415 nm: $A = 0.16$, $\tau_a = 7.00$ *ns*; $B = 0.68$, $\tau_b = 3.14$ *ns*; $\chi^2 = 1.15$.

At 510 nm: $A = 0.20$, $\tau_a = 7.09$ *ns*; $B = 0.64$, $\tau_b = 3.57$ *ns*; $\chi^2 = 1.04$.

Titration of 34 with 18 by fluorescence excitation and emission

Table 6.6. Volumes for the titration of **18** with **34** by fluorescence.

I	V_i / µL	$n_{eq\ 34}$
0	0	0
1	250	0.05
2	255	0.10
3	250	0.15
4	250	0.20
5	250	0.25
6	255	0.30
7	250	0.35
8	250	0.40
9	255	0.45
10	250	0.50
11	505	0.60
12	500	0.70
13	505	0.80
14	500	0.90
15	505	1.00
16	500	1.10
17	rest	1.99

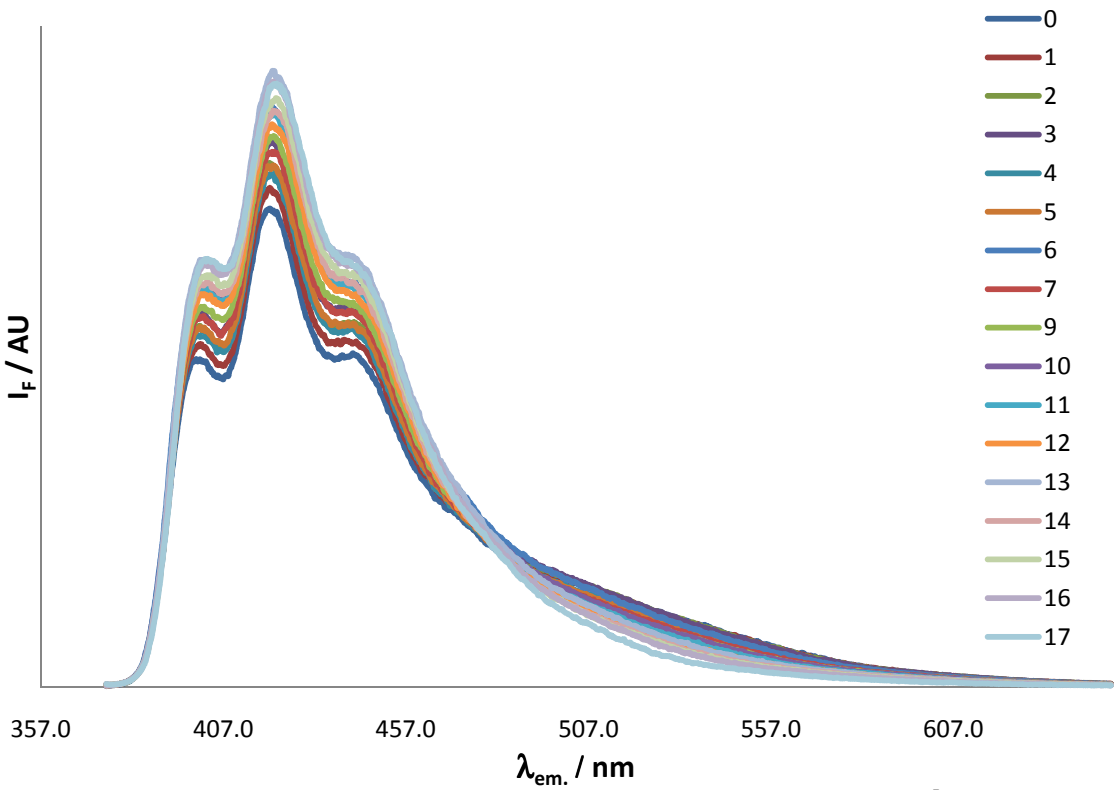

Figure 6.6. Corrected emission spectra during the titration of **34** (2.0×10^{-5} *M* in DCM) with **18** (see **Table 6.6** for the equivalents).

A solution of 1.4976 mg of **34** in 100 mL DCM (stock solution, [**34**] = 2.011×10^{-5} *M*) and a solution of 2.6176 mg of **18** in 10 mL DCM (solution of **18**, [**18**] = 3.997×10^{-4} *M*) were prepared. Then a series of spectra was made, and between each a volume V_i of the solution of **18** was added to the stock solution (see **Table 6.6**). Absorption *A* was measured at 369 nm, emission spectra were recorded between 375 and 650 nm with an excitation wavelength of 369 nm, and excitation spectra were recorded at 420 nm with the excitation wavelength varying from 220 to 400 nm. Then the emission and excitation spectra were corrected by multiplying them by a facto A/A_0, where A_0 is the value of *A* in the spectrum of **34** (i = 0) (cf. **Figures 6.6** and **6.7**). The exact values of the starting concentration of 18 and 34 were calculated for each spectrum. A matrix was then created with the first two columns containing the calculated values of concentration, and the 17 next columns the corrected emission value at 21 wavelengths between 470 and 602 nm. This matrix was submitted to the Letagrop software,[9] with starting value for the computation chosen by trials and errors in order to minimize the χ^2 value. Result: $log(K) = 5.126 \pm 0.177$; $\chi^2 = 23.9$.

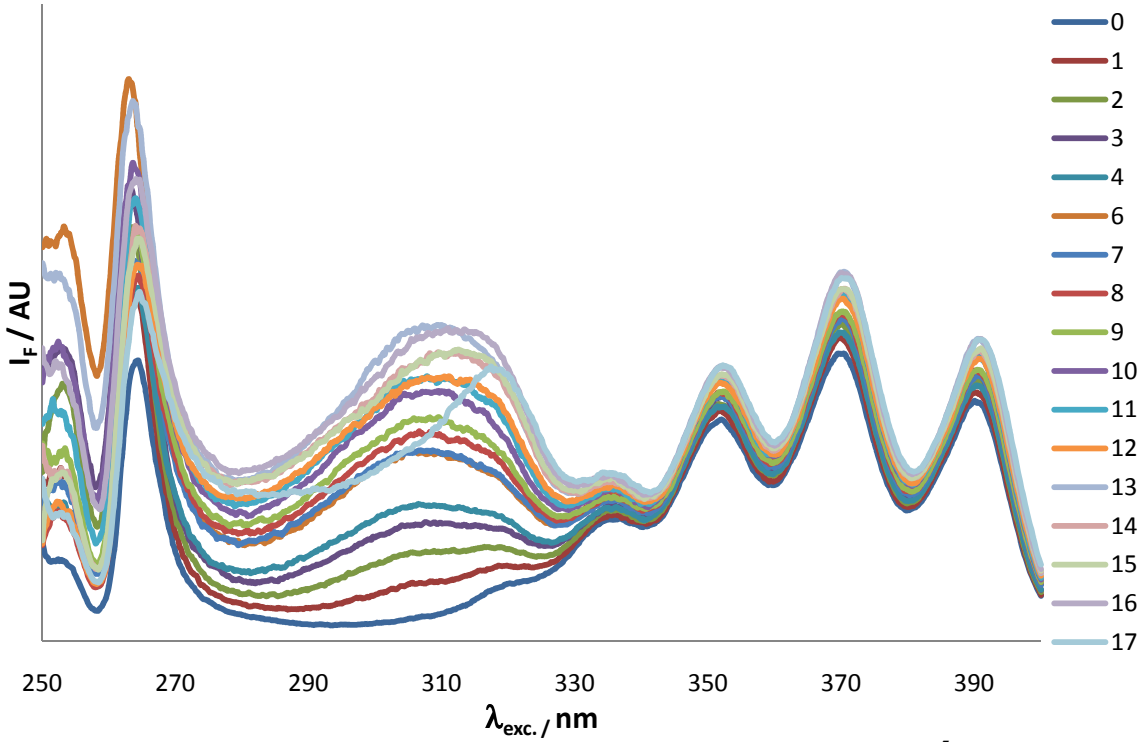

Figure 6.7. Corrected excitation spectra during the titration of **34** (2.0×10^{-5} *M* in DCM) with **18** (see **Table 6.6** for the equivalents).

Another matrix was created with again the concentration values of the 2 first lines and emission value at 420 nm for a range of 21 excitation wavelengths between 277 and 329 nm, without the values of the two last spectra were $n_{eq\ 34} > 1.0$ (also they are shown as well on **Figure 6.7**) This matrix was submitted to the Letagrop software,[9] with starting value for the computation chosen by trials and errors in order to minimize the χ^2 value. Result (average of many fits): $log(K_1) = 5.175 \pm 0.202$.

A similar procedure was followed for **16** with **34**. Result: $log(K_1) = 5.112 \pm 0.328$.

6.2.3) Titrations followed by ITC

General considerations:

The ITC titrations were made with a Microcal © VP-ITC machine, and the data treated with the ORIGIN software provided with the machine. Before each experiment, the injection syringe as well as the reference and sample cells were thoroughly washed with deionised water, then methanol, then DCM, and the reference cell was filled with DCM. After each

experiments, they were washed with DCM, then methanol, then deionised water and the reference-cell was re-filled with deionised water.

General procedure: titration of 18 with barbital by ITC at 0.1 mM

A solution of 3.30 g of **18** in 50 mL DCM ([**18**] = *0.1 mM*) was prepared. It was observed that the dissolution was slow and the solution had to be sonicated for 5 minutes in a ultrasonic bath in order to obtain a complete dissolution (this was observed with all the different receptors). The sample cell was then filled to its exact volume with this solution, by removing the excess with a syringe posed on the margin of the cell. A solution of 11.09 g of barbital in 20 mL DCM ([barbital] = *3.0 mM*) was introduced in the addition syringe. The automatic injection was then started with the following parameters: the cell temperature was *25 °C*, the reference power *15 µcal/s*, the initial delay *60 s*, the stirring speed *307 rpm*, there was *30* injection with a duration of *4.6 s* and a spacing of *210 s*, the 1^{st} *injection* with a volume of *1 µL*, the 2^{nd} *to* 7^{th} *injections* with a volume of *2.5 µL*, and the 8^{th} *to* 30^{th} *injections* with a volume of *5 µL*.

For the data treatment, the first two data points were systematically deleted: the first according to normal practice and the second due to perceived auto-association. The concentration of the starting solution in the cell was adjusted to allow a fit with a value of *n = 1*. Before this correction, the calculated value of *n* typically fell in the range 0.9-1.0, and the values calculated for the thermodynamic parameters did not change after correction of the concentration. The crude data and experimental results are presented in *Appendix 3*.

6.2.4) *Ab-initio* models and comparison with IR in solution

FTIR Measurements

Infrared spectra of **17** (**18**), barbital (**39**), and their 1:1 complexes were recorded with a ThermoNicolet Nexus 670 FTIR spectrometer at a resolution of *4* cm^{-1}, by co-adding 50 scans. Samples were held in a variable path length cell with BaF_2 windows (Eurolabo). IR spectra

were measured in $CDCl_3$ at a concentration of *5 mM* and at a path length of *250 μm*, excepted barbital for which $CDCl_3$ + DMSO-d_6 95:5 mixture was used. All infrared spectra were shown with solvent absorption subtracted out. The results are shown in *Chapters 2* and *5*.

DFT calculations

The geometry optimizations, vibrational frequencies, and absorption intensities were calculated by Gaussian 03 program[13] on a SGI Altix XE 1300 of the Pôle Modélisation of the Institut des Sciences Moléculaires (University Bordeaux I). Calculations of the optimized geometry of **17** (**18**), barbital (**39**), their 1:1 complexes, and the two isomers *cis* and *trans* of the catenane formed with **18** and **37c**, were performed at the density functional theory level using B3PW91 functional and 6-31G* basis set. Vibrational frequencies and IR intensities were calculated at the same level of theory. For comparison to experiment, the calculated frequencies were scaled by *0.964* (*0.95* for calculations in the NH/CH stretching region) and the calculated intensities were converted to Lorentzian bands with a half-width of *7* cm^{-1} (*15* cm^{-1} for calculations in the NH/CH stretching region). A half-width of *100* cm^{-1} has been applied for NH stretching modes of barbital (**39**) involved in strong hydrogen bonds with nitrogen atom of the pyridin groups of **17** (**18**). Pictures of the structure found for the complexes and simulated IR spectra (when applicable) are shown in *Chapters 2*, *4* and *5*.

6.3) Metathesis experiments

6.3.1) General considerations

The NMR spectra were recorded on Bruker AC300 or AV300 spectrometers (300 MHz). The mass spectra were recorded on VG Zabspec mass spectrometer.

6.3.2) Experimental procedures and spectra

General procedure for the cyclisation of receptors with barbital: **cyclisation of 10 with barbital**:

A solution of **10** (40 mg, 64 µmol) and barbital (13 mg, 71 µmol) in DCM (20 mL) was heated to reflux. Then a solution of Grubbs 1st generation catalyst (6.0 mg, 7 µmol) in DCM (2 mL) was added. After 2 hours of stirring at reflux, the solvent was evaporated and the brown solid obtained was analysed by ^{1}H NMR and mass spectrometry (electrospray). The proportion of cyclised vs. non-cyclised receptor obtained was evaluated by comparing the integration of the signals of remaining terminal olefin (5.80 ppm, ddt, 2 H and 5.00 ppm, m, 4 H), with the signal of the new olefinic proton (5.40 ppm, m, 2 H). In this case 10% of cyclised receptor **14** were observed for 90% of starting receptor **10**. In mass spec., both the non-cyclised and the cyclised product were observed (sodium adduct), but no peak for the complex.

General procedure for the cyclisation of receptors with 36: **cyclisation of 12 with 36**:

A solution of **36** (8.9 mg, 9.2 µmol) and **12** (5.2 mg, 7.6 µmol) in $CDCl_3$ (1.5 mL, previously passed on a short column of $MgSO_4$ and basic alumina) was prepared, and a first ^{1}H NMR was made. Then Grubbs 1st generation catalyst (0.8 mg, 1.0 µmol) was added. The reaction mixture was heated to reflux during 30 min. and then cooled to room temperature. A new ^{1}H NMR was made. Then methanol (7 µL) was added and the solution was analysed by ^{1}H NMR and mass spectrometry (electrospray and MALDI). The results of these analysis are given in *Chapter 4*.

Cyclisation of barbiturate 37 in presence and absence of 18:

A solution of **37** (3.05 mg, 7.54 µmol) and **18** (6.33 mg, 8.90 µmol) in $CDCl_3$ (1.5 mL) was analysed by ^{1}H NMR and a few drops were submitted for mass spectrometry (ES^-). Then Grubbs 1st generation catalyst (1 mg, 1.2 µmol) was added and the mixture was heated to reflux during 2 hours, and then cooled to rt. It was analysed again by ^{1}H NMR and mass spec., then an excess of barbital (approx. 15 mg) was added, and it was analysed again.

A solution of **37** (3.10 mg, 7.66 µmol) and Grubbs catalyst (0.8 mg, 1 µmol) was heated to reflux during 2 hours, analysed by ^{1}H NMR and mass spec., then **18** (6 mg) was added, it was analysed again, and finally barbital (approx. 15 mg) was added and it was analysed again.

The NMR spectra are presented in *Chapter 4* and the mass spectra are presented in *Appendix 2*.

6.4) Photodimerisation experiments

6.4.1) General considerations

The NMR spectra were recorded on a Buker AC 250 spectrometer (250 MHz) at the CESAMO (University of Bordeaux, France).

MALDI-MS spectra were performed by the CESAMO on a Voyager mass spectrometer (Applied Biosystems). The instrument is equipped with a pulsed N2 laser (337 nm) and a time-delayed extracted ion source. Spectra were recorded in the positive-ion mode using the reflectron and with an accelerating voltage of 20 kV. Samples were dissolved in CHCl3 at 10 mg/ml. The dithranol matrix solution was prepared by dissolving 10 mg in 1 ml of CHCl3. A MeOH solution of cationisation agent (NaI, 10 mg/ml) was also prepared. The solutions were combined in a 10:1:1 volume ratio of matrix to sample to cationisation agent. One to two microliters of the obtained solution was deposited onto the sample target and vacuum-dried.

6.4.2) Photodimerisation experiments followed by UV

General procedure for quantum yield and thermal return rate measurements: example with **34**

A solution of **34** (1.603 mg) in DCM (100 mL) was prepared: [**34**] = $2.152.10^{-5}$ *M*. 3 mL of this solution were introduced in a fluorescence cuvette, degased by 3 freeze/pump/thaw cycles, and sealed. Absorption spectra of of this solution were taken after different intervals of time of irradiation performed at *365 nm* using a mercury lamp and a monochromator, converting "monomeric" **34** to cyclic **34c**. The concentration of remaining **34** was calculated according to Beer's law.

The photonic flux *P* of the lamp was measured using Parker's actinometry:[14] Three measuring flasks of 25 mL were prepared with in all three 1.5 mL of buffer solution (prepared with 300 mL of sodium acetate 1N + 180 mL of H_2SO_4 1N + 20 mL H_2O) and 2 mL of *o*-phenanthroline solution (0.1% w/w in water), then 3 mL of potassium ferrioxalate solution (0.006 M, kept in the dark) were irradiated during exactly 2 minutes in the same conditions as the solution of **34** and added to the first measuring flask, 3 mL of the ferrioxalate solution, non irradiated, were added to the second flask, and all three were completed to 25 mL with deionised water. They were stirred in the dark during one hour, then the absorbance of both solutions 1 and 2 at *510 nm* was measured, using the 3rd solution for the baseline. The value of *P* was given by the following formula:

$$P = \frac{\mathcal{N}_A . V . \Delta A}{l . \Phi_f . \varepsilon_p}$$

where $\mathcal{N}_A$ is Avogadro constant, *V* is 25 cm^3, ΔA is the difference of absorption between solutions 1 and 2 at *510 nm*, Φ_f is the quantum yield of production of ferrous ions from potassium ferrioxalate at *365 nm* and is equal to *1.21*, and ε_p is the molar extinction coefficient of the complex of ferric ions with phenanthroline at *510 nm*, which is equal to *11100*.

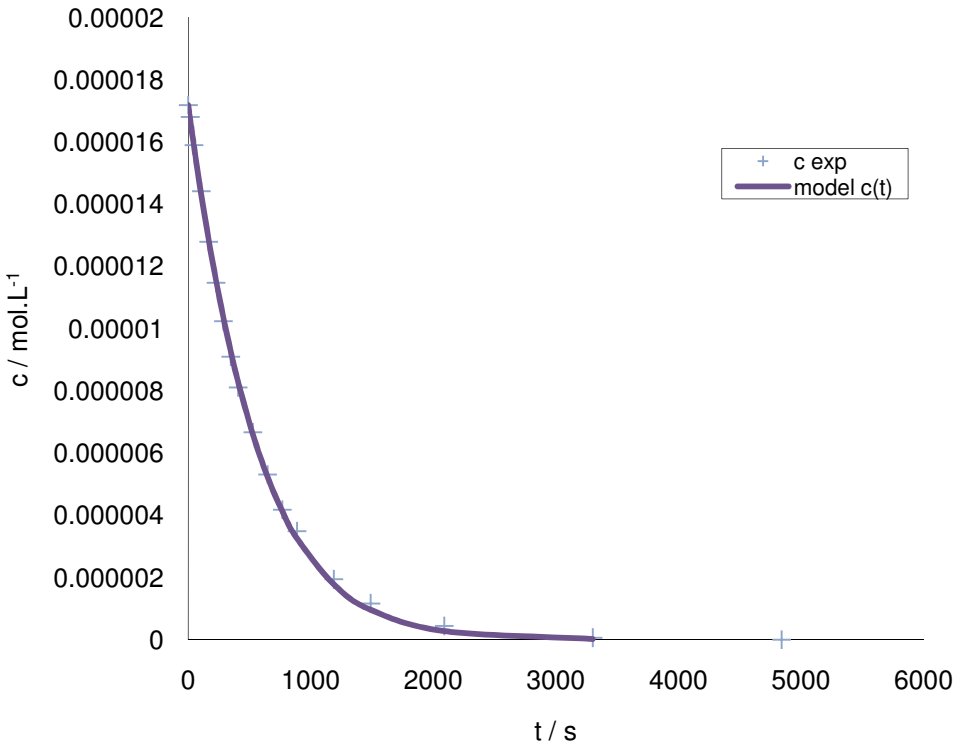

Figure 6.8: Experimental values and model of the concentration of monomeric **34** as a function of the time of irradiation.

A model *c(t)* describing the evolution of the concentration *c* of **34** as a function of the time of irradiation *t* was established, using only the parameters of the problem (molar absorption coefficient ε of **34** in DCM at *365 nm*, initial concentration *c0*, volume *V*, incident photonic flux *P* determined by Parker actinometry, optical path *l*, and the unknown quantum yield Φ):

$$c(t) = \frac{ln\,(1-(1-10^{A_0}).exp\,(-\frac{P.\Phi.\varepsilon.l.ln(10)}{V.\mathcal{N}_A}.t)}{\varepsilon.l.ln\,(10)}$$

Then, for different values of Φ, the values of *c(t)* according to this model were compared to the experimental values of *c* at *t* obtained from the spectra by using Beer's law. The best value of Φ is the one that gives a model that fits the experimental points with the smallest standard deviation. Result: $\Phi = 0.101$ (cf. **Figure 6.8**).

Finally, the cuvette was left at room temperature (25°C) and the absorption at *369 nm* (due to "monomeric" **34** reappearing in solution by conversion of **34c**) was measured. The

value of k_{ret} retained for the rate constant of the reaction **34c** → **34** was the one that gave the best fit with experimental points according to the following law:

$$A(t) = A_{\infty}.(1 - e^{-k_{ret}.t})$$

where A_{∞} is the initial absorbance of the solution of **34** before irradiation (cf. **Figure 6.9**). Result: $k_{ret} = 3.45 \times 10^{-6}\ s^{-1}$.

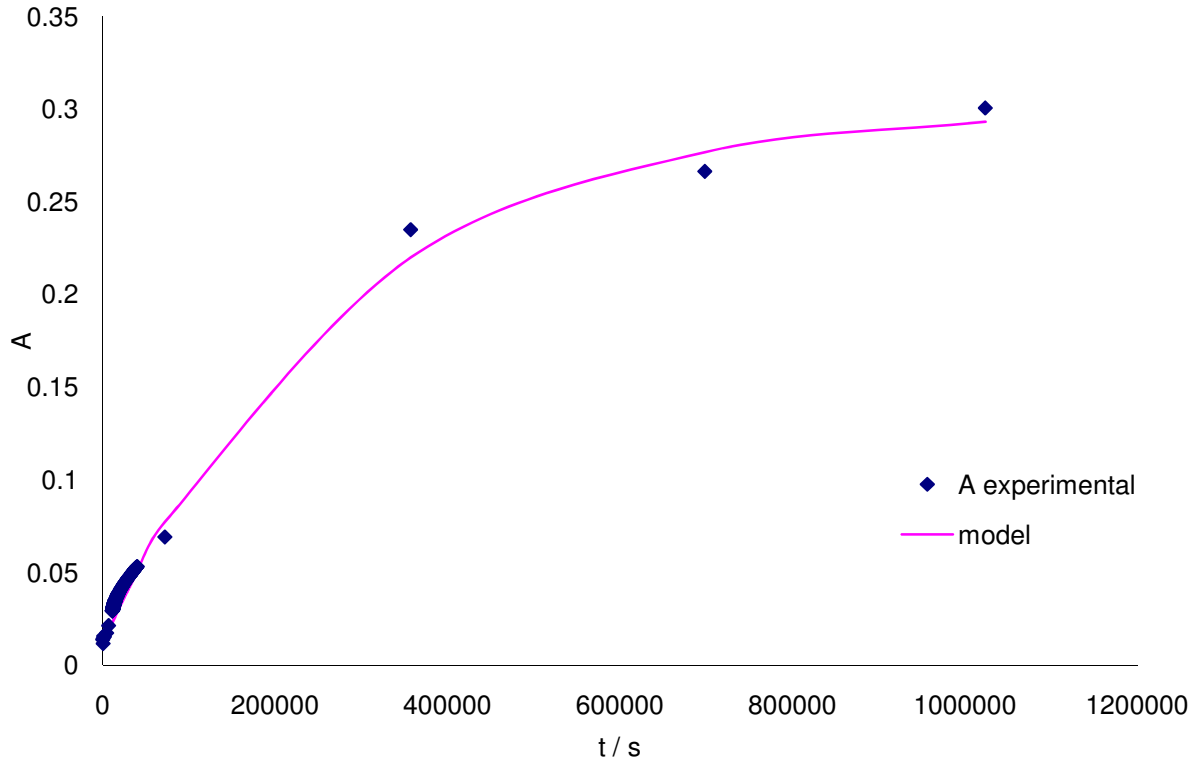

Figure 6.9. Experimental values and model of the absorbance of a solution of **34c** allowed to return to **34** at rt. as a function of time.

A similar procedure was used to measure Φ and k_{ret} for **35** and 1:1 mixtures of **16** with **34** or **35**. Results: **35**: $\Phi = 0.280$, $k_{ret} = 7.62 \times 10^{-4}\ s^{-1}$; **34•16**: $\Phi = 0.00141$, $k_{ret} = 2.30 \times 10^{-4}\ s^{-1}$; **35•16**: $\Phi = 0.00260$, $k_{ret} = 2.70 \times 10^{-4}\ s^{-1}$.

6.4.3) Photodimerisation experiments followed by NMR

Irradiation of 34 and its complexes with 14, 15 and 16 in CD_2Cl_2

A solution of 3.5752 mg of **34** in 1.2 mL of CD_2Cl_2 was prepared. 0.3 mL of this solution was added to 0.3 mL of CD_2Cl_2 and also to the following solutions:

- **14**: 0.7156 mg in 0.3 mL CD_2Cl_2,
- **15**: 0.7834 mg in 0.3 mL CD_2Cl_2,
- **16**: 0.8501 mg in 0.3 mL CD_2Cl_2

Those four solutions (concentration 2 mM) were introduced in NMR tubes that were degassed by 3 freeze/pump/thaw cycles and NMR were taken after different intervals of irradiation using a white lamp with a $Pb(NO_3)_2$ filter.

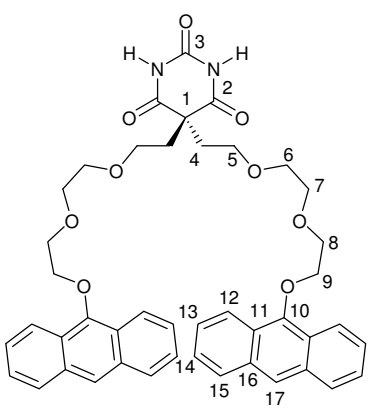

34

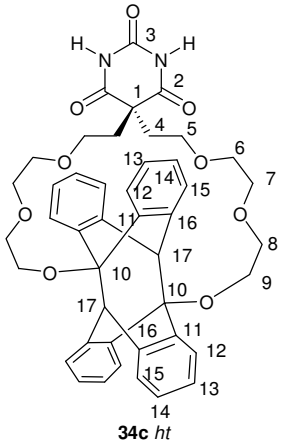

34c *ht*

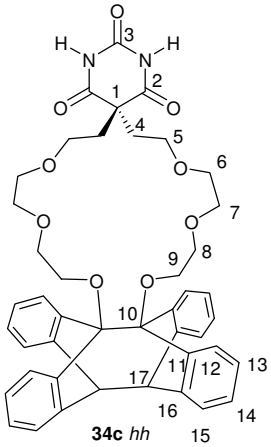

34c *hh*

^{1}H NMR of **34** before irradiation (CD_2Cl_2, 250 MHz): δ = 8.75 (br. s, 2 H, NH), 8.35 (m, 4 H, 12), 8.20 (s, 2 H, 17), 7.80 (m, 4 H, 15), 7.40 (m, 8 H, 13 & 14), 4.25 (m, 4 H, 9), 3.70 (m, 4 H, 8), 3.45 (m, 12 H, 5, 6 & 7), 2.30 (t, J = 5.7 Hz, 4 H, 4).

^{1}H NMR of the solution of **34** after 45 min. of irradiation (identified to **34c** *hh*) (CD_2Cl_2, 250 MHz): δ = 7.30 (m, 6 H, 12 & NH), 6.90-6.85 (m, 12 H, 13, 14 & 15), 4.50 (s, 2 H, 17), 3.85 (br. s, 4 H, 9), 3.70 (m, 4 H, 8), 3.45 (m, 12 H, 5, 6 & 7), 2.40 (t, J = 5.7 Hz, 4 H, 4).

Irradiation of 35 and its complexes with 14, 15 and 16 in CD_2Cl_2

A solution of 4.70 mg of 34 in 1.4 mL of CD_2Cl_2 was prepared. 0.3 mL of this solution was added to 0.3 mL of CD_2Cl_2 and also to the following solutions :

- **14**: 0.720 mg in 0.3 mL CD_2Cl_2,
- **15**: 0.803 mg in 0.3 mL CD_2Cl_2,
- **16**: 0.852 mg in 0.3 mL CD_2Cl_2

Those four solutions (concentration 2 mM) were introduced in NMR tubes that were degassed by three freeze-pump-thaw cycles on a high-vacuum line and sealed under vacuum. ^{1}H NMR spectra were taken after different intervals of irradiation using a 450 W mercury lamp. The NMR tubes were plunged in vials containing the filter solution (saturated solution of lead acetate), placed in a merry-go-round apparatus to ensure their uniform irradiation, and the entire setup was immersed in a water bath, which allowed to filter IR radiation and thermostat the samples.[15]

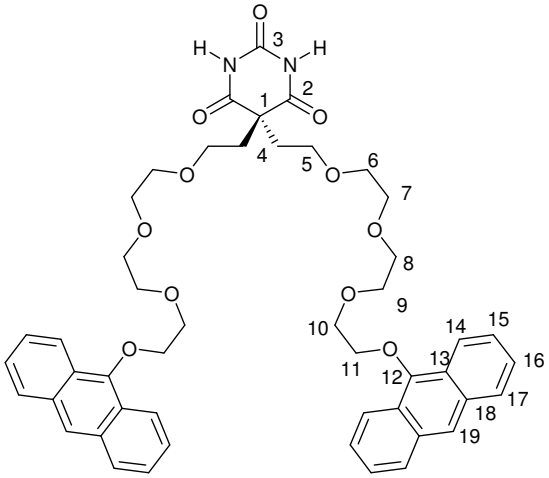

35

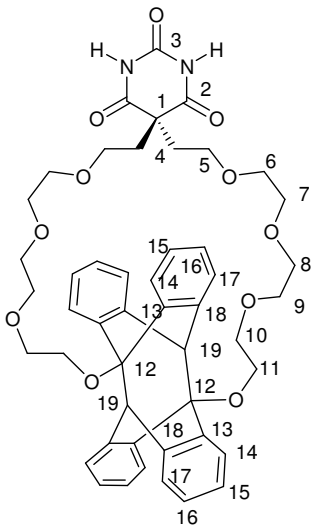

35c *ht*

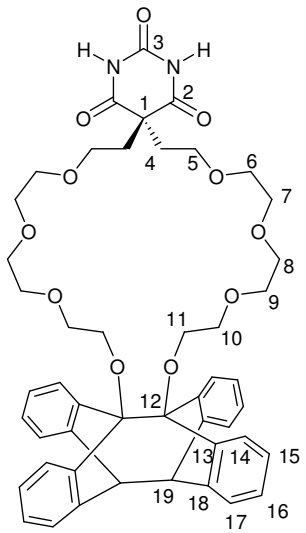

35c *hh*

^{1}H NMR of **35** before irradiation (CD_2Cl_2, 250 MHz): δ = 9.35 (s, 2 H, NH), 8.40 (m, 4 H, 14), 8.20 (s, 2 H, 19), 8.00 (m, 4 H, 17), 7.45 (m, 8 H, 15 & 16), 4.45 (m, 4 H, 11), 4.05 (m, 4 H, 10), 3.80 (m, 4 H, 9), 3.60 (m, 4 H, 8), 3.20 (m, 4 H, 7), 3.15 (m, 4 H, 6), 2.95 (m, 4 H, 5), 2.10 (t, J = 5.5 Hz, 4 H, 4).

^{1}H NMR of **35** after 10 min. of irradiation (CD_2Cl_2, 250 MHz): δ = 9.10 (s, 2 H, NH), 7.25 (d, 4 H, 14), 6.80 (m, 12 H, 15, 16 & 17), 4.45 (s, 2 H, 19), 3.95 (m, 4 H, 11), 3.85 (m, 4 H, 10), 3.65 (m, 8 H, 9 & 8), 3.50 (m, 12 H, 5, 6 & 7), 2.30 (t, J = 5.7 Hz, 4 H, 4).

Test of catenation: 17 + 34

Three solutions were prepared, each one in 0.75 mL $CDCl_3$:

- **17**: 2.233 mg of **17**
- **34**: 2.783 mg of **33**
- **17 + 34**: 2.251 mg of **17** and 2.793 mg of **33**

NMR spectra of each solution was taken, as well as MALDI on a small portion of the solutions. To this small portion of **17** and **17 + 34**, an excess of barbital was then added and another MALDI was performed. Then the rest of the solutions of **34** and **17 + 34** were degassed by freeze/pump/thaw then irradiated over a period of 90 minutes at 4 cm of a medium pressure Hg lamp (400 W) in the presence of a lead nitrate solution as a filter, after what the NMR shown that the cyclisation was complete: the signal of the H in *para* of the O on the anthracene in the NMR at 8.09 ppm has disappeared, and a new peak for the bridgehead proton at 4.5 ppm has appeared. 2.233 mg of **17** were then added to the tube of **34c** (irradiated), and NMR and MALDI were performed as described above, before and after adding an excess of barbital.

The same procedure was followed for the test of catenation of **18 + 34**. The NMR are reproduced in *Chapter 4*. The MALDI spectra are given in *Appendix 2*.

---

[1] Gan, Y.; Wang, P.; Spencer, T. A. *Journal of Organic Chemistry* **2006**, *71*, 9487-9490.

[2] Goudreau, N.; Brochu, C.; Cameron, D. R.; Duceppe, J.-S.; Faucher, A.-M.; Ferland, J.-M.; Grand-Maître, C.; Poirier, M.; Simoneau, B.; Tsantrizos, Y. S. *Journal of Organic Chemistry* **2004**, *69*, 6185-6201.

[3] Bugarin, A.; Connell, B. T. *Organometallics* **2008**, *27*, 4357-4369.

[4] Marquis, D.; Desvergne, J.-P.; Bouas-Laurent, H. *Journal of Organic Chemistry* **1995**, *60*, 7984-7996.

[5] Percec, V.; Peterca, M.; Ducley, A. E.; Imam, M. R.; Hudson, S. D.; Nummelin, S.; Adelman, P.; Helney, P. A. *Journal of the American Chemical Society* **2008**, *130*, 13079-13094.

[6] Lincheneau, C. *Photogénération de Molécules Entrelacées : Photocaténation*, Master report, Université Bordeaux 1, **2006**.

[7] Song, H. N.; Lee, H. J.; Kim, H. R.; Ryu, E. K.; Kim, J. N. *Synthetic Communications* **1999**, *29*, 3303-3311.

[8] (**a**) Manchester, J. *Synthesis of interlocked structures using Barbiturate templates and Anthracene dimerisation*, MSci project report, University of Birmingham - School of Chemistry, **2008**; (**b**) Saraswat, A. *Synthesis of Catenanes Using Hamilton-like Hosts and Barbiturate Guests*, MSci project report, University of Birmingham - School of Chemistry, **2009**.

[9] (**a**) L. G. Sillen, B. Warnqvist, *Arkiv för Kemi* 1968, **31**, 377; (**b**) L. G. Sillen, B. Warnqvist, *Arkiv för Kemi* 1968, **31**, 315; (c) J. Havel, Haltafal-Spefo program; Mazaryle University: Brno, Moravia, Czech Republic

[10] (**a**) Rhys Williams, A. T.; Winfield, S. A.; Miller, J. N. *Analyst* **1983**, *108*, 1067-1071; (**b**) Melhuish, W. H. *Journal of Physical Chemistry* **1961**, *65*, 229-235.

[11] *Jobin Yvon Application Notes F-10 - Which Fluorescence Lifetime System is Best for You?*, URL: http://www.horiba.com/fileadmin/uploads/Scientific/Documents/Fluorescence/F-10.pdf.

[12] T. deRoeck, N. Boens, J. Dockx, DECAN 1.0, K.U. Leuven, Belgium.

[13] M. J. Frisch, G. W. Trucks, H. B. Schlegel, G. E. Scuseria, M. A. Robb, J. R. Cheeseman, J. A. Montgomery, Jr., T. Vreven, K. N. Kudin, J. C. Burant, J. M. Millam, S. S. Iyengar, J. Tomasi, V. Barone, B. Mennucci, M. Cossi, G. Scalmani, N. Rega, G. A. Petersson, H. Nakatsuji, M. Hada, M. Ehara, K. Toyota, R. Fukuda, J. Hasegawa, M. Ishida, T. Nakajima, Y. Honda, O. Kitao, H. Nakai, M. Klene, X. Li, J. E. Knox, H. P. Hratchian, J. B. Cross, C. Adamo, J. Jaramillo, R. Gomperts, R. E. Stratmann, O. Yazyev, A. J. Austin, R. Cammi, C. Pomelli, J. W. Ochterski, P. Y. Ayala, K. Morokuma, G. A. Voth, P. Salvador, J. J. Dannenberg, V. G. Zakrzewski, S. Dapprich, A. D. Daniels, M. C. Strain, O. Farkas, D. K. Malick, A. D. Rabuck, K. Raghavachari, J. B. Foresman, J. V. Ortiz, Q. Cui, A. G. Baboul, S. Clifford, J. Cioslowski, B. B. Stefanov, G. Liu, A. Liashenko, P. Piskorz, I. Komaromi, R. L. Martin, D. J. Fox, T. Keith, M. A. Al-Laham, C. Y. Peng, A. Nanayakkara, M. Challacombe, P. M. W. Gill, B. Johnson, W. Chen, M. W. Wong, C. Gonzalez, and J. A. Pople. *GAUSSIAN 03;* Revision B.04, Gaussian Inc., Pittsburgh, PA, **2003**.

[14] (**a**) Parker, C. A. *Proceedings of the Royal Society A* **1953**, *220*, 104-116; (**b**) Hatchard, C. G.; Parker, C. A. *Proceedings of the Royal Society A* **1956**, *235*, 518-536.

[15] For a similar setup, see: Carteau, D.; Brunerie, P.; Guillemat, B.; Bassani, D. M. *Photochemical and Photobiological Sciences* **2007**, *6*, 423-430.

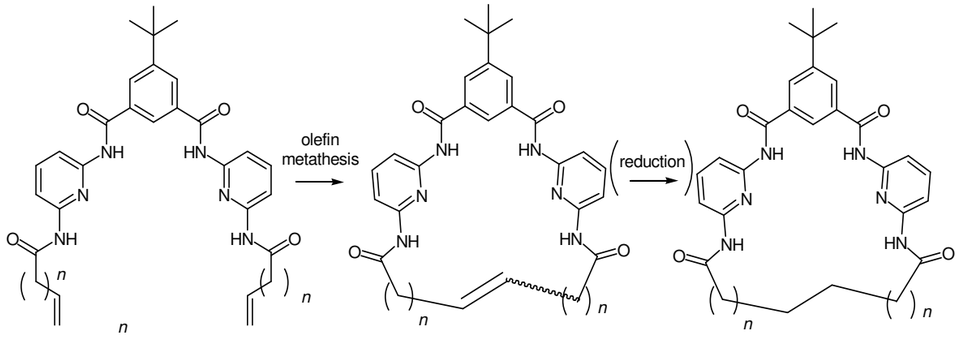

n	
2	**9**
4	**10**
5	**11**
6	**12**
8	**13**

n	
4	**14**
6	**15**
8	**16**

n	
4	**17**
6	**18**

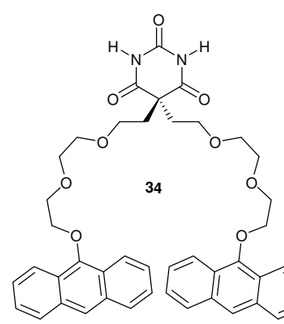

34

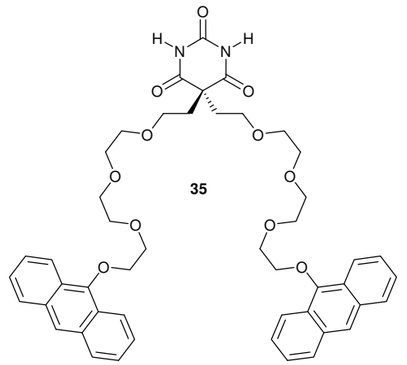

35

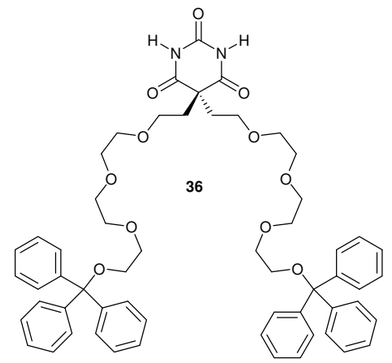

36

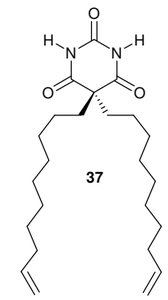

37

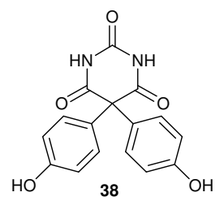

38

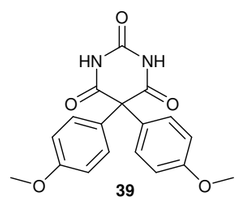

39